# Open Research Online

## The effects of Morris water maze learning on the number, morphology and molecular composition of rat hippocampal dentate gyrus synapses

Thesis

## oro.open.ac.uk

# The effects of Morris water maze learning on the number, morphology and molecular composition of rat hippocampal dentate gyrus synapses.

by

## Mark Eyre

A thesis submitted in partial satisfaction for the degree of
Doctor of Philosophy

Submitted May 2002

Supervised by Professor Michael G. Stewart
Department of Biological Sciences
The Open University
Walton Hall
Milton Keynes
MK7 6AA
England

ProQuest Number: 27532783

ProQuest 27532783

# Disclaimer

All of the work conducted in this thesis was conducted by myself except for the behavioural training of rats in the Morris water maze. Assistance was given with perfusions, embedding and freeze substitution, as well as sectioning and incubation for immunological analysis. Certain images were kindly donated for inclusion, as was advice on statistical methods.

# Acknowledgements

# Abstract

Spatial long-term memory formation is dependent upon the hippocampus and associated brain structures in mammals. Memory storage is believed to involve changes in the way information is exchanged between neurons, and this is principally governed by their synaptic connections. Changes can occur in the functional properties of individual synapses, but evidence suggests that morphological changes may also occur. Research described in this thesis has used the Morris water maze, a behavioural paradigm that requires rodents to form long-term memories about a spatial environment, and this learning task involves the function of the hippocampus. Electron microscopy was used to investigate the ultrastructural morphology and composition of synapses in the hippocampal dentate gyrus in several groups of animals. Three time-points were investigated, 3, 9 and 24 hours after the start of training, which also corresponded to small, intermediate and large amounts of training, as well as two different types of control, naïve and swim-only. Animals investigated 3 hours after the start of training did not show significant long term memory for the task, whereas animals investigated 9 and 24 hours after the start of learning displayed long-term memory recall when measured by the quadrant analysis test (probe trial). Hippocampal dimensions and dentate granule cell densities were similar between all animal groups.

No significant changes to synaptic ultrastructural morphology were evident in the 3 hour group. In the 9 hour group, significant increases in synapse density and synapse to neuron ratio were observed, with a simultaneous decrease in the synapse mean height and average area of PSD (post-synaptic density) per synapse. No significant changes were observed in the exercise-matched swim-only controls, suggesting that the changes were related to long-term memory formation. Morphological changes were not evident in the 24 hour group, despite long term memory recall, suggesting that the morphological changes following spatial learning in the Morris water maze are transient. The total amount of synaptic membrane was not significantly different between any of the groups, suggesting that although new, smaller synapses may be formed as a result of learning, changes also occur to existing synapses, which may result in their re-categorisation or even removal. Analysis of ionotropic glutamate receptors following training proved inconclusive, particularly for NMDA receptors, but did suggest that AMPA receptors are increased in the initial stages of learning, which may be a mechanism of short-term memory storage.

# Table of Contents

# List of Figures and Tables

# List of Equations

# List of Abbreviations

$\pi$ - Pi (3.14159265359........)

$^oC$ - degrees Celsius

[$^3H$]L-glutamate - the L isoform of the ligand glutamate with an attached radioactive hydrogen atom (tritium)

AMPA - $\alpha$-amino-3-hydroxy-5-methyl-4-isoxazole proprionate

ANOVA - Analysis of variance statistical test

Arc - activity-related cytoskeleton-associated protein

CA - *cornu ammonis* (Ammon's horn)

$Ca^{2+}$ - Calcium ions

CaM - calmodulin

CaMK II - Calcium and calmodulin-dependent kinase II

CAMK IV - Calcium and calmodulin-dependent kinase IV

cAMP - cyclic adenosine monophosphate

CBP - calcium binding protein

CNS - central nervous system

CPEB - cytoplasmic polyadenylation element binding protein

CREB - cyclic AMP response element binding protein

CS - conditioned stimulus

D-AP5 - D-2-Amino-5-phosphonovalerate

$ddH_2O$ - double distilled water

DNA - deoxyribonucleic acid

EPSP - excitatory post-synaptic potential

ER - endoplasmic reticulum

ERK - extracellular signal-related kinase

F1 - fast-decaying facilitation

F2 - slow-decaying facilitation

FM 1-43 - Frei Mao 1-43 fluorescent styryl dye

g - gram

G-proteins - guanosine trisphosphate-binding proteins

GABA - $\gamma$-amino-butyric-acid

GFP - green fluorescent protein

GluR - glutamate receptor subunit

GRIP - a PSD protein that binds to AMPA receptors by way of PDZ domains

GTP - Guanosine trisphosphate

GTPase - an enzyme that utilises GTP

HCl - Hydrochloric acid

H.M. - the initials of an oft-studied patient with amnesia

HOMER - a PSD protein that binds to mGluR's

Hz - Hertz (cycles per second)

IgG - Immunoglobulin 'G'

iGluR - ionotropic glutamate receptor

IMHV - intermediate and medial hyperstriatum ventrale (an area of the chick brain)

$IP_3$ - inositol trisphosphate

IUR - isotropic uniform random (i.e. completely random with respect to all possible rotations and orientations in 3-dimensional space)

$K^+$ - Potassium ions

KA - Kainate receptor subunit

L1 - a nerve cell adhesion molecule similar to NCAM

$L_A$ - Length per unit area

LEC - Lateral Entorhinal Cortex

LFS - Low Frequency Stimulation

LSD - Least significant difference post-hoc statistical test

LTD - long-term depression

LTP - long-term potentiation

MAGUK - membrane-associated guanylate kinase

MAP2 - microtubule-associated protein 2

MAPK - mitogen-activated protein kinase

MEC - Medial Entorhinal Cortex

$Mg^{2+}$ - Magnesium ions

mGluR - metabotropic glutamate receptor

ml - millilitre

mm – millimetre; $x10^{-3}$

MRI - magnetic resonance imaging

mRNA - messenger riboxynucleic acid

$Na^+$ - Sodium ions

NaCl - Sodium chloride

NAD - Non-perforated axodendritic (synapse)

NaOH - Sodium hydroxide

NAS - Non-perforated axospinous (synapse)

NCAM - nerve cell adhesion molecule

nm – nanometre; $\times 10^{-9}$

NMDA - n-methyl-d-aspartate

NR - NMDA receptor subunit

NSF - *N*-ethylmaleimide-sensitive factor

$N_V$ - Numerical density (number per unit volume)

PAS - Perforated axospinous (synapse)

PAD - Perforated axodendritic (synapse)

PDZ domain - specific sequence of amino-acids involved in protein-protein interactions named after the proteins it was first categorised in (PSD-95, Discs-large, ZO-1)

pH - a measure of acidity or alkalinity (inverse $\log^{10}$ of hydrogen ions)

PKA - protein kinase A

$P_L$ - Number of points per unit length of line

PP - protein phosphatase

PSA - polysialic acid

PSD - post synaptic density

PTP - post-tetanic potentiation

Rab3 - a small GTP-binding protein

Ras - a small GTP-binding protein

r.t. - room temperature

s.e.m. - standard error of the mean

SHANK - a PSD protein involved in linking glutamate receptors to the cytoskeleton

SI - primary somatosensory cortex

$S_N$ - Surface area per numerical object

SNARE - soluble NSF attachment receptor

STE - short-term enhancement

$S_V$ - Surface area density (units of surface area per unit volume)

synGAP - synaptic Ras-GTPase-activating protein

TE & TEO - anterior & posterior inferotemporal cortex, after von Bonin and Bailey

Tukey's HSD test - honest significant difference post-hoc test

$\mu m$ – micrometer; $\times 10^{-6}$

$\mu m^2$ - square micrometers

$\mu m^3$ - cubic micrometers

US - unconditioned stimulus

# Introduction

The main subject of this thesis concerns the processes of learning and memory. Memory is the name given to the ability of the brain to store information, be it sights, sounds, etc. Learning is the name given to the process of memory formation, the addition of new memories, and is often evident as a change in the way that an animal interacts with its environment. Although some memories may be a part of an organism's genetic inheritance, such as instincts, learning is a more versatile mechanism that allows adaptation to a changing environment, a particularly useful trait for longer-lived organisms. Memories may persist for the entire lifetime of an individual, as do a large proportion of vertebrate neurons, but memories can also be short-lived, or even forgotten, suggesting that neurons store memory information in a variety of ways.

## Memory types and locations

Memory has been classified into several different categories **(Milner *et al.*, 1998)**, but these can be grouped under two main headings. The usual notion of memory is for facts and/or events, and these can be termed *explicit* or *declarative* in nature because they involve conscious thought. The other type of non-conscious, *non-declarative* memory is termed *implicit*, examples of which include procedural skills and habits, classical conditioning and non-associative learning (i.e. reflexes). These different types of memory are shown in Figure 1, along with the specific parts of the central nervous system (CNS) to which they are localised.

Reflexes such as the Patella reflex are controlled by two neurons, connected by a single synapse in the spinal cord, and are a 'built-in' or 'hardwired' behavioural mechanism designed to respond to a particular stimulus **(Nolte, 1993)**. Such reflexes can be lost when the spinal cord is damaged. Withdrawing a hand from a painful stimulus is another such reflex memory, although this differs in that it can be overridden voluntarily. Basic behavioural responses can be utilised to react to, or remember, a particular sensory stimulus or cue. This was shown by the conditioning experiments of Pavlov, in which a dog would salivate when a bell was rung because it had associated the sound of the bell with being given food **(Faneslow, 1998)**.
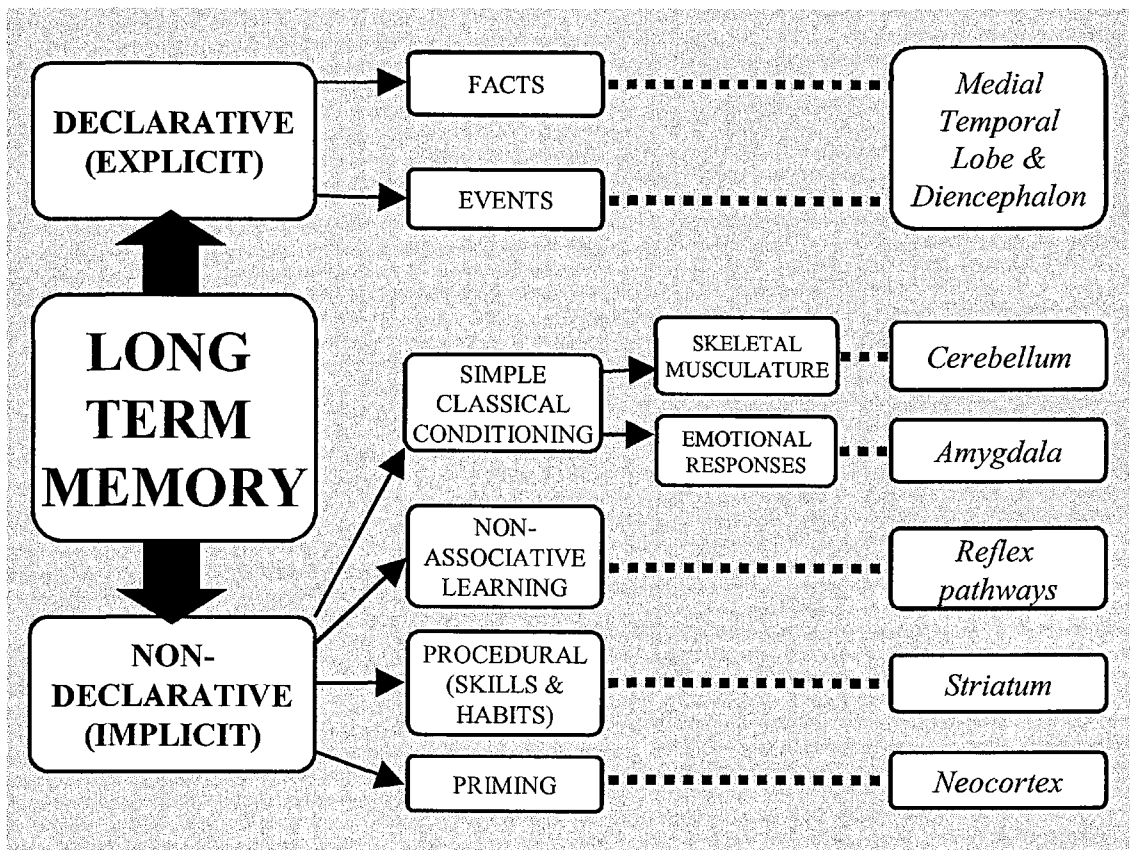
Figure 1 - The broad classification of memory types. Different types of memory are shown, along with their associated anatomical brain regions. Adapted from Milner *et al.*, 1998.

An apparently simple memory is for learnt skills, such as riding a bicycle, and these are sometimes referred to as *how-to* procedural skill memories. Although such skills require conscious input to acquire them, they become 'second nature' i.e. autonomous and reproducible without conscious effort. The reproduction of these learnt procedures are disrupted by damage to the cerebellum **(Nolte, 1993)**, although the striatum may be involved in their initial formation **(Willingham, 1997)**.

When a visual object is viewed, all the components of an object are remembered and associated when first encountered. The information is processed by the visual cortex somewhat automatically, as the eyes scan the object. In addition, other senses feed information into the brain, which is combined in cortical association areas. What an object is and what it does can then be readily recalled upon subsequent encounters, and the associated information will also be accessible. Information can be associated between different times, places, objects, people etc. Such memory for events specific

15

in time and space is called 'episodic' memory. Episodic memory is a type of explicit memory, as is 'semantic' memory, the storage of factual information.

Evidence points to the localisation of different memory functions to particular areas of the CNS, and the cerebral cortex is no exception. Damage to the left prefrontal region will impair verbal memory, whereas non-verbal memory is affected by right prefrontal cortex damage. Interestingly, different areas appear to store subtly different information, and localised damage will affect only specific memories **(Poldrack and Gabrieli, 1998)**. If certain portions of the parietal lobe are damaged, patients can lose much of their spoken language memories. The words have to be re-learnt, and patients explain that they lost the ability to express themselves, although they knew what they wanted to say.

A similar situation is known as aphasia, which means the inability to use language. 'Expressive aphasia' is the inability to express language, whereby all but the most important words are absent from speech, which instead consists of isolated individual words. This condition was studied by Broca, and is caused by damage to part of the anterior temporal lobe known as Broca's area **(Milner _et al._, 1998; Nolte, 1993)**. A second type of aphasia was studied by Wernicke, who observed that damage to the posterior temporal lobe produced a 'receptive aphasia' that rendered patients unable to comprehend language. However, they could still produce language, although their sentences may have been jumbled or contained made-up words.

The transformation of memories from a labile to a stable state is termed memory consolidation. Patients who have damage in their medial temporal lobe show deficits in the ability to form, or 'consolidate', long-lasting memories. One highly studied individual, known by his initials H.M., suffered from global anterograde amnesia after neurosurgery, in which large parts of the temporal lobes including the hippocampus were removed bilaterally to control intractable epilepsy. This meant that he could not remember information about places that he visited, people that he met or events that happened after his surgery, a deficit of explicit memory formation **(Milner _et al._, 1998)**.

However, the short-term or working memory of H.M. was still intact, as well as his ability to recall memories of people and events in his life prior to the surgery. He was

also able to show improvements in other memory tasks, for example mirror drawing. This task is difficult because all the conscious movements must be reversed in order to successfully trace around a picture, but this skill can be learnt over time by normal subjects. H.M. showed improvement in this task upon subsequent trials, despite being convinced that he had never performed the task before.

The Gollin Figures task involves a set of pictures of objects and words that have had most of the contours removed so that their identification is initially difficult. Memory for the actual object or word in each picture makes a second trial of the same pictures easier. This effect is known as priming, and is present in H. M. despite his damaged hippocampus **(Willingham, 1997)**. Other amnesiac patients have slightly different memory deficits to that of H.M., and can remember a vocabulary list for some time if care is taken to use words that are context-free. Such a reduction in associative requirements shows that these patients still retain their semantic memory abilities, although their episodic memory is impaired **(Mishkin *et al.*, 1998)**. Magnetic Resonance Imaging (MRI) scans revealed that these patients had slightly different patterns of damage to the medial temporal lobe than H.M.

## Medial temporal lobe anatomy

On the ventral surface of the brain at the tip of the medial temporal lobe lies the parahippocampal cortex (termed postrhinal cortex in non-primate mammals), and the neighbouring perirhinal and entorhinal cortices. These cortical areas are very similar in structure to other areas of homotypical neocortex, containing various categories of pyramidal and granular neurons which are typically separated into six layers of cells that interconnect with each other. However, they are slightly different to the neighbouring neocortex because they lack a well defined inner layer of granular cells (i.e. layer IV is not well developed). This is in stark contrast to the group of structures that lie deeper in the brain beneath these cortical surfaces, collectively called the hippocampal formation.

The structures that comprise the hippocampal formation are the dentate gyrus, the fields of Ammon's horn, or *Cornu Ammonis*, abbreviated to CA1, CA2 and CA3, and the subiculum, and are termed archicortex because they all contain only three layers **(Witter *et al.*, 2000)**. The boundary between the subiculum and the entorhinal cortex is

occupied by two structures, the presubiculum, which lies next to the subiculum, and the adjoining parasubiculum, which lies next to the entorhinal cortex. These structures have an additional cortical sheet that distinguishes them from the three-layered structures of the hippocampal formation, and are not considered as part of this group. The anatomy of these cortical and sub-cortical structures is shown in Figure 2.
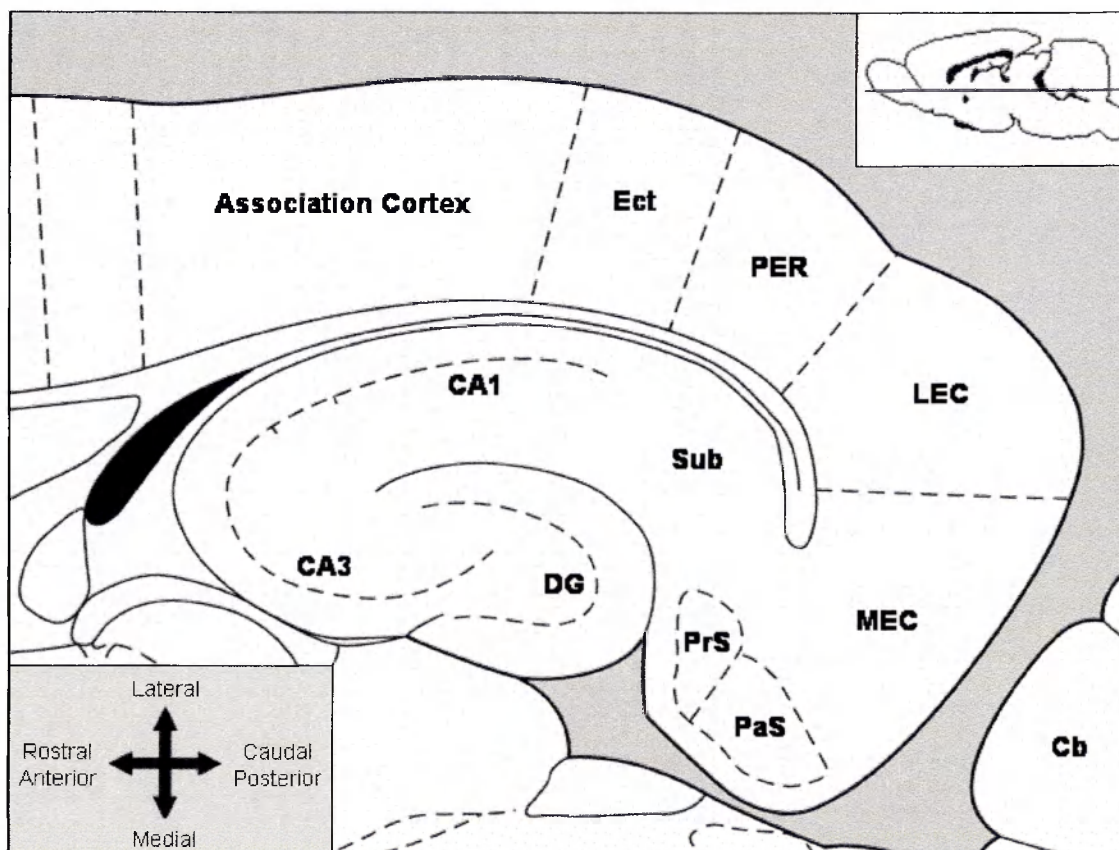


Figure 2 - Horizontal section through the rat brain showing the anatomy of the medial temporal lobe. The slice is at 6.1 mm below the Bregma point, as indicated by the transverse section in the top-right corner of the figure. The location of deep (hippocampal) and surface (cortical) structures are indicated - see text for details. DG - dentate gyrus, CA1 and CA3 - regions of the *Cornu Ammonis*, Sub - subiculum, PrS - Presubiculum, PaS - Parasubiculum, MEC and LEC - Medial and Lateral Entorhinal Cortex, Ect - Ectorhinal Cortex, Association Cortex - in the rat these areas include structures equivalent to areas TE and TEO. Perirhinal and Parahippocampal cortices lie at different horizontal levels and are not shown. Adapted from Paxinos and Watson, 1998.

Brain scans of H.M. indicated that much of his temporal lobe had been damaged, whereas in the patients with intact semantic memory, the damage was limited to the hippocampal formation. The scans of these patients suggest that their lack of episodic but not semantic memory can be explained by the damage of their hippocampal structures but not the surrounding cortical areas. The extra associations of context that are required in order to form episodic memory would appear to occur in the hippocampal formation. Indeed, evidence suggests that the perirhinal and entorhinal cortices have important functions in short-term recognition memory **(Suzuki, 1999)**. Is this functional requirement for more associational processing by the hippocampal formation during episodic memory formation related to the anatomy of the medial temporal lobe?

As explained previously, different areas of the cerebral cortex perform different functions. Anatomically, the cortical areas in the medial temporal lobe are connected with several association areas that integrate information about different aspects of visual objects. The ventral stream inputs are primarily from association cortex such as the cytoarchitectonic areas of the anterior and posterior inferotemporal cortex, which lie adjacent to the entorhinal cortex (see Figure 2). Detailed studies of these areas have been performed in the monkey *Macaca mulatta*, where they are named TE (anterior) and TEO (posterior) **(Suzuki and Amaral, 1994; von Bonin and Bailey, 1947)**. These areas transmit sensory information concerning stimulus quality, and have large reciprocal connections with the perirhinal cortex. The dorsal stream inputs are important for analysing the location of a stimulus, irrespective of the sensory modality. Such areas include the retrosplenial, posterior parietal and dorsolateral prefrontal cortices, which form reciprocal connections with the parahippocampal cortex **(Inausti *et al.*, 1997; Mishkin *et al.*, 1997)**.

Both the perirhinal cortex and the parahippocampal cortex make strong reciprocal connections with the entorhinal cortex. This means the entorhinal cortex is a convergent point for the ventral and dorsal streams of sensory information that flow from primary and association areas. The entorhinal cortex also provides the major input to the hippocampal formation by way of a bundle of axon fibres called the perforant path. However, this pathway is unidirectional, a feature that is common to many of the connections between the structures of the hippocampal formation. These differences in connectivity are mirrored by differences in the cellular anatomy of the

hippocampal formation structures, which differ from the usual layered organisation of cortical areas.

The hippocampal formation consists of two sets of principal neurons, which form two arcs that appear as a pair of interlocking 'C' shapes when viewed in a cross-section perpendicular to the long rostro-caudal axis of the hippocampus **(Amaral and Witter, 1989)**. One of these arcs is called the dentate gyrus because it has a beaded, tooth-like external appearance, and consists of three layers. The deep or polymorphic layer contains various interneurons, and lies on the inside of the arc. Next comes the granule cell layer, which contains the principal excitatory neurons, the granule cells. On the outside of the arc lies the molecular layer, which contains the dendritic fields of the granule cells, and is bordered by the hippocampal fissure.

The other arc is the hippocampus proper, also called the *cornu ammonis* or CA region. The principal cells of the CA region are traditionally divided into three types, named CA1, CA2 and CA3, on the basis of the anatomical descriptions of Lorente de No **(Lorente de No, 1934)**. The CA3 cells lie in the first half of the arc of the CA region, nestled in between the two blades of the dentate gyrus. The other half of the arc contains the CA1 cells, which continue around the outside of the upper, or inner, blade of the dentate gyrus on the far side of the hippocampal fissure. This arc is continuous with the subiculum in one direction and the CA2 and CA3 cells in the other. The CA2 region is quite small, lying between the CA3 and CA1 areas. These cells are only distinguished from CA3 by subtle differences in their connections, often being included as a part of this field in the literature **(Amaral and Witter, 1989)**, and I shall also use this convention unless otherwise stated.

In addition to the layer of pyramidal neurons, the CA fields posses 3 dendritic layers. The first of these is called the *stratum oriens*, which lies on the outside of the pyramidal cell arc, and contains the basal dendrites of the principal cells. The apical dendrites lie on the inside of the arc, and are divided into the *stratum radiatum* and the *stratum lacunosum-moleculare*. This latter area forms a thinner band on the innermost part of the arc close to the hippocampal fissure, and is where the distal dendrites of each cell have a much more widespread extension. In addition, a further distinction is made in the CA3 region so that this area also includes a layer between the *stratum pyramidale* and *stratum radiatum*. This area is termed *stratum lucidum*, and contains 'thorny

excrescences', which are specialised structures that occur on CA3 pyramidal cell proximal dendrites and contain multiple synaptic contacts.

The principle connections between the structures of the hippocampal formation are unidirectional, and link these areas together in a series, like a chain. These connections are shown diagrammatically in Figure 3. This chain begins with the perforant path axons that send inputs to the dentate gyrus from the entorhinal cortex. The cells of the dentate gyrus send their output to the cells of area CA3, which in turn innervates CA1. Axons of CA1 cells then synapse onto cells in the subiculum, which send efferents to
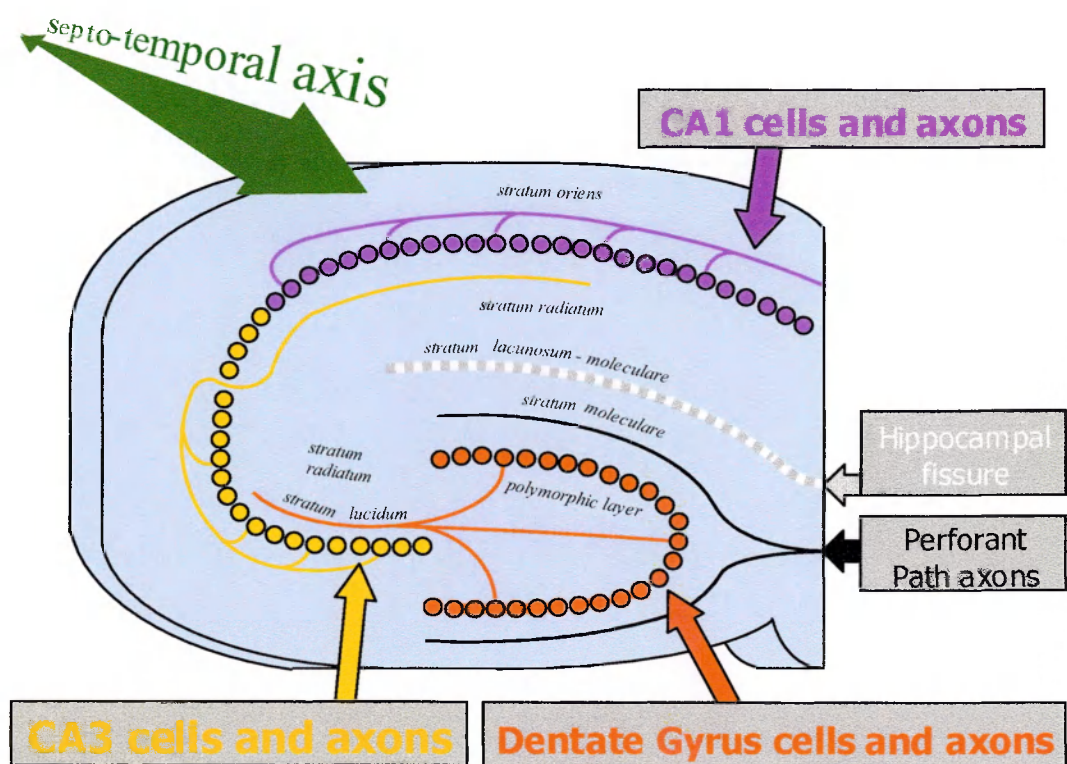


Figure 3 - Illustration of hippocampal 'tri-synaptic loop' anatomy, showing the major efferents of each cell type. A representative section through the hippocampal formation perpendicular to the septo-temporal axis (green arrow and text) is shown. The anatomical arrangement of the three different principal cell types is indicated, and the cells are colour-coded with their primary axonal connections. The different dendritic field *strata* are shown in italics at their respective locations. The hippocampal fissure is indicated by a grey and white striped line, and the perforant path input from the Entorhinal cortex is also shown. Adapted from Amaral and Witter, 1989.

the pre- and parasubiculum. All three of these structures output to the entorhinal cortex, and so the chain of connections actually forms a loop. Also, it was suggested that the hippocampal formation possesses a lamellar structure, such that each layer or slice along the rostro-caudal axis contains a discrete loop of connections. Information entering the dentate gyrus at one point along the septo-temporal axis would be constrained to this lamella at subsequent points along the processing loop (i.e. CA3, CA1 and subiculum) **(Andersen et al., 1971)**.

Although original anatomical investigations have detailed the principal connections of the medial temporal lobe structures **(Lorente de No, 1934)**, more recent examinations have revealed that the situation is more complex, and this is shown diagrammatically in Figure 4. The entorhinal cortex is divided up into two cytoarchitectonic regions, the medial entorhinal cortex (MEC) and the lateral entorhinal cortex (LEC). In the rat, the MEC predominantly receives input from the postrhinal cortex, whereas the LEC receives input from the perirhinal cortex **(Witter et al., 2000)**. These inputs contact cells in the superficial layers of the entorhinal cortex (layers I-III), which contain projection neurons.

Inputs also arise from areas such as the orbital frontal, cingulate, limbic and insular cortices, which constitute one third of the cortical inputs to the entorhinal cortex **(Squire and Zola-Morgan, 1991)**. Axonal connections from olfactory areas (particularly in rodents and cats) are made to superficial layers of both the MEC and LEC, whereas inputs from the limbic cortical areas are non-standard in that they ramify in the deeper cell layers (layers V and VI) of the entorhinal cortex, which then contact the superficial layers **(Witter, 1993)**.

The deep layers of the entorhinal cortex send connections to other cortical areas, such as perirhinal, postrhinal/parahippocampal and association cortex, as well as subcortical structures such as the amygdala, basal ganglia and thalamus **(Inausti et al., 1997)**. The entorhinal cortex also sends axons from cells in the superficial layers to the hippocampus in a bundle known as the 'perforant path'. These axons make connections in the dentate molecular layer with the dendrites of the dentate granule cells, most commonly contacting small projections from the dendrites that are called dendritic spines, and these will be described below. Cells in layer II of the LEC send axons to
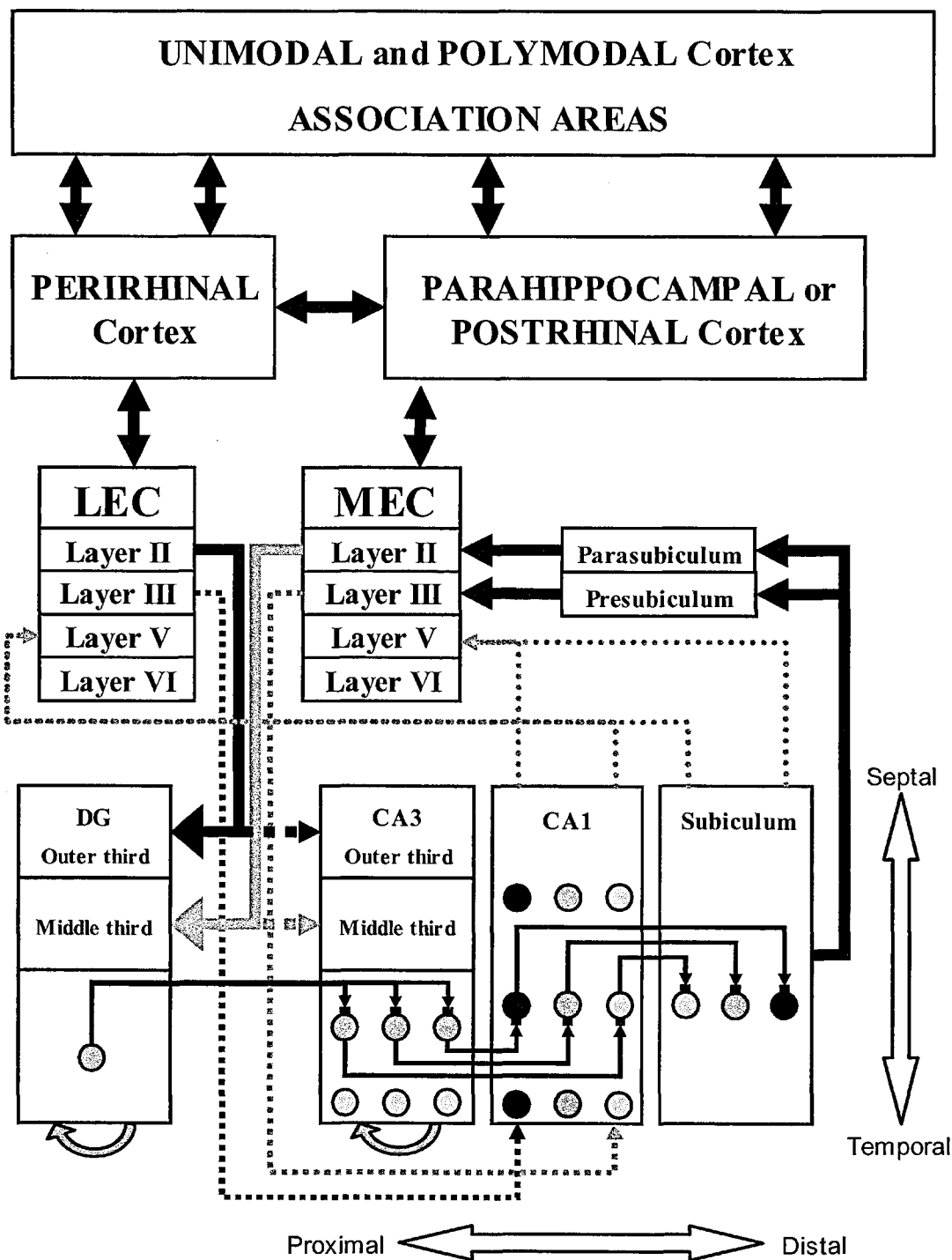
Figure 4 - The anatomy of the medial temporal lobe and hippocampal formation. Principal connections are indicated by large solid arrows, and lesser connections by small dashed arrows. Proximal, Distal, Septal and Temporal directions within the hippocampal regions CA3, CA1 and subiculum are denoted by white, double-ended arrows (see text). Adapted from Alkon *et al.*, 1991, Amaral and Witter, 1989, Witter, 1993 and Witter *et al.*, 2000.

the outer third of the dentate gyrus molecular layer and a smaller projection to the outer third of CA3 *stratum lacunosum-moleculare*, whereas cells in layer II of the MEC send axons to the middle third of the dentate gyrus molecular layer and a smaller projection to the middle third of CA3 *stratum lacunosum-moleculare*. This data relates to the rat and the cat, whereas in the monkey this distinction between the projections of the LEC and MEC is less pronounced **(Witter et al., 2000; Witter, 1993)**.

In both the LEC and MEC, the more lateral parts of these areas project to more septal areas along the septo-temporal axis, and similarly, more medial areas project to more temporal areas of the hippocampal formation. However, both areas form connections in the full extent of the transverse extent of the dentate gyrus and CA3 i.e. all along the arc of cells at a given septo-temporal location. In contrast to neocortical areas, there is also a small projection from cells in layer VI of the entorhinal cortex to both the dentate gyrus and CA3, which may make subtle additions to the information conveyed by the perforant path to the hippocampal structures.

The axons of the dentate gyrus neurons synapse in two main areas. Firstly, they make collateral connections with the interneurons of the polymorphic layer of the dentate gyrus, which are then involved in feedback inhibition of the excitatory granule cells **(Freund and Buzsaki, 1996)**. Secondly, they form the 'mossy fibre' pathway, which terminates onto the dendritic 'thorny excrescence' synapses of CA3 cells in the *stratum lucidum*, along the whole of the transverse axis. The projections from the CA3 cells are twofold, in a similar manner to those of the dentate gyrus. Firstly, they terminate in the *stratum oriens* and *stratum radiatum* of CA3, and form associational feedback connections within the CA3 region. Secondly, they project to the *stratum oriens* and *stratum radiatum* of the CA1 field, and these connections are often called the Schaffer collaterals **(Amaral and Witter, 1989)**.

These Schaffer collateral connections show a distinct pattern of innervation in CA1 along the transverse axis, such that CA3 cells close to the border with CA1 project most heavily to the proximal half of CA1, whereas CA3 cells furthest from the CA3/CA1 border project most heavily to the distal half of CA1 close to the CA1/subiculum border. Furthermore, the Schaffer collaterals also shift their transverse innervation in relation to the location of their origin along the septo-temporal axis i.e. septal CA3 projects more to proximal CA1, whereas temporal CA3 projects to more

distal CA1 (closer to the border with the subiculum) (**Alkon** *et al.*, **1991**). The pattern of transverse specificity is also present in the connections from CA1 to the subiculum, such that proximal CA1 projects to distal subiculum and distal CA1 projects to the adjacent proximal subiculum (**Alkon** *et al.*, **1991; Bartesaghi** *et al.*, **1995**).

In contrast to the simple view of the hippocampal processing loop, the entorhinal cortex also sends projections to CA1 and the subiculum. These axons differ in that they arise from cells in layer III of the entorhinal cortex, and they also differ in their pattern of innervation along the transverse axis. Axons from the LEC innervate the distal part of CA1 (closer to the border with the subiculum) and the proximal part of the subiculum (closer to the border with CA1). Conversely, the MEC axons from layer III innervate the proximal part of CA1 (closer to the border with CA3) and the distal part of the subiculum (closer to the border with the presubiculum). This is shown in Figure 4. Also, there is a small contribution to these projections from cells in layer V of the entorhinal cortex (**Witter, 1993**).

As well as projecting to the LEC, the perirhinal cortex also makes reciprocal connections directly with the same areas of CA1 and the subiculum as the LEC. This is also true of the postrhinal cortex, which makes connections with the same target areas of CA1 and the subiculum as the MEC, as well as directly to the MEC. Functionally, these connections will thus send a copy of information to the hippocampal structures that has not been processed by the entorhinal cortex, just as the projections from layer III send a copy of information to CA1 and the subiculum that has not been processed by the dentate gyrus and CA3. These differing representations of the same sensory information may be important in comparisons, novelty detection, associational computation and temporal coding functions related to memory (**Fuster, 1997; Singer, 1999**).

The cells of CA1 send a projection to layer 5 of the entorhinal cortex, as well as innervating the subiculum. However, unlike the dentate gyrus and CA3, they do not give rise to feedback connections. The major cortical output from the subiculum is to the presubiculum and the parasubiculum, which in turn send connections to layers 3 and 2 of the entorhinal cortex, respectively. The subiculum sends an output back to the cells in layer 5 and to a lesser extent layer 3 of the entorhinal cortex. Interestingly, the direct projections from the subiculum and CA1 target specific areas of the entorhinal

cortex that are in register with the perforant pathway input from these areas. In other words, proximal CA1 (adjacent to CA3) and distal subiculum (adjacent to the presubiculum) project to the MEC, whereas distal CA1 and the adjacent proximal subiculum project to the LEC **(Witter *et al.*, 2000)**. These connections therefore form a loop from and back to the entorhinal cortex that may be important for the comparisons, associational computation and temporal coding mentioned above.

With regards to the lamellar hypothesis, the extent of all projections into and within the hippocampal formation does not appear to be restricted to and organised in a lamellar fashion. Most connections, either from the entorhinal cortex or from one hippocampal structure to another, project along approximately 20-25% of the septo-temporal axis **(Witter *et al.*, 2000)**. The only exceptions to this appear to be the mossy fibre projection from the dentate gyrus to CA3, which does indeed appear to be highly restricted in its divergence along the septo-temporal axis. Interestingly, the inhibitory cells of the dentate polymorphic layer provide feedback inhibition to the inner third of the dentate gyrus molecular layer approximately 1 mm septally and temporally from their level of origin, but do not project to their own septo-temporal level **(Alkon *et al.*, 1991)**. They therefore do not inhibit the granule cells that activate them, but do inhibit other nearby granule cells. The septo-temporal divergence of connections means that information from different areas of the perceptual field is mixed and combined at most levels of hippocampal processing. This adds a further level of interconnections to the anatomy of the medial temporal lobe, indicating that these structures are more than simple loops of connections arranged in a lamellar fashion.

## Synaptic anatomy

The word synapse was first suggested by Sherrington as a name for sites of contact between nerve cells which enabled information transfer **(Sherrington, 1897)**. However, it became increasingly clear that the conduction of information between nerve cells was a complex issue. The mechanisms of synaptic function provided potential opportunities for controlling and modifying the electrical signals of nerve cells **(Shepherd and Erulkar, 1997)**, suggesting that the connections of each neuron were unique. Different patterns of sensory input could mean that individual cells respond to different memories, but it seems unlikely that it is simply a matter of specific, single cells responding to specific, single memories. The divergence of axonal

outputs and the convergence of dendritic inputs suggest that potentially many synapses will be modified by learning. Hence, memory storage has generally come to be considered as being distributed amongst sets of synaptic connections between sets of neurons **(Levy and Steward, 1979; Zigmond *et al.*, 1999)**.

Most of the cells that interconnect different areas of the brain utilise glutamate as their principal neurotransmitter, and this is also true of medial temporal lobe structures. Dentate granule cells and pyramidal cells of the CA regions are glutamatergic, and can be referred to collectively as 'principal cells'. In several brain areas the postsynaptic site of principal cell connections take the form of dendritic spines, as is the case for the majority of synapses in the hippocampus **(Peters *et al.*, 1991)**. Dendritic spines are small projections from the main branches of the dendritic shaft which have a thin neck that ends in a bulbous head, in a similar way to a leaf on the branch of a tree, an example of which is shown in Figure 5. Spines usually have a glutamatergic, excitatory synapse in the bulbous head, and these synapses are called 'type 1' or 'asymmetric' because they contain a specialised area of membrane called the post-synaptic density (PSD). The PSD is a complex made up from a variety of protein molecules including glutamate receptors, anchoring molecules, second messenger proteins, kinases and phosphatases **(Kennedy, 1998; Ziff, 1997)**. The PSD occurs opposite the presynaptic site specialised for vesicle release, which often has clusters of presynaptic vesicles in close proximity. Protein complexes are also present in the presynaptic membrane that are involved with vesicle docking and exocytosis, and are visible in scanning electron micrography of freeze-fracture preparations made in the plane of the synapse **(Peters *et al.*, 1991)**.

The presence of spines on a dendrite means that connections can be made with many more axons in the limited volume of the brain because they increase the available area for synaptic contacts and increase the effective diameter of the dendrite, enabling it to interact with more axons **(Harris and Kater, 1994)**. Type 1 axodendritic synapses do occur in the hippocampus, but they are much less common than axospinous synapses. An example of such a synapse is shown in Figure 6. Inhibitory synapses are termed 'type 2' or 'symmetric' because both pre- and postsynaptic membranes appear similar, and a prominent PSD is lacking (see Figure 17 for examples and a comparison of these
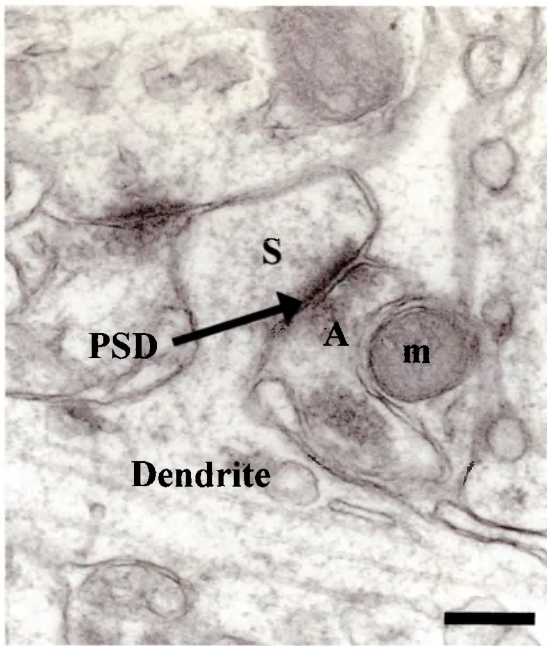
Figure 5

Electron micrograph of a typical type 1 non-perforated axospinous synapse in the middle molecular layer of the dentate gyrus. The postsynaptic membrane of the dendritic spine is continuous with the parent dendrite, and apposed to a presynaptic axon terminal.
PSD; postsynaptic density (indicated by arrow) S; postsynaptic dendritic spine A; axon terminal m; mitochondrion Scale bar = 250 nm.
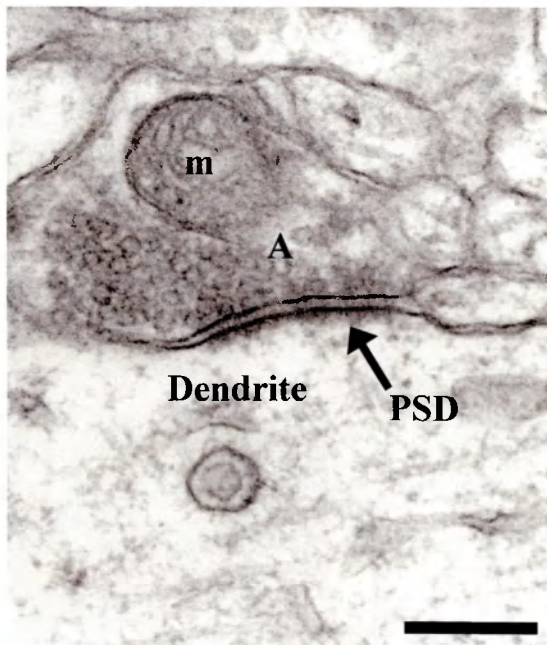


Figure 6

Electron micrograph of a typical type 1 non-perforated axodendritic synapse in the middle molecular layer of the dentate gyrus. The presynaptic axon terminal is apposed to the main trunk of the postsynaptic dendrite.
PSD; postsynaptic density (indicated by arrow), A; axon terminal, m; mitochondrion. Scale bar = 250 nm.
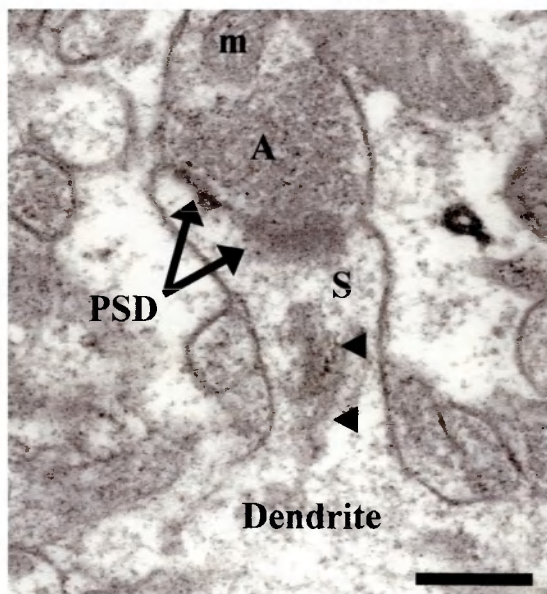


Figure 7

Electron micrograph of a typical type 1 perforated axospinous synapse in the middle molecular layer of the dentate gyrus. The postsynaptic membrane is larger with a cup-like appearance, and the PSD can be seen in two separate locations (branching arrow). The thicker spine neck contains a spine apparatus (arrowheads).
PSD; postsynaptic density, S; postsynaptic dendritic spine, A; axon terminal, m; mitochondrion. Scale bar = 250 nm.

two types of synapse). Inhibitory synapses are usually formed by interneurons, which use the neurotransmitter GABA (γ-amino-butyric-acid). These connections are predominantly located in proximal dendritic segments (the inner third of the molecular layer) in the dentate gyrus, and are also observed on the cell soma and axon hillock. Type 1 and 2 synapses also form onto interneurons, which are non-principal, inhibitory cells that commonly contain GABA. These synapses form either on their cell body or dendrites, as interneurons mostly do not have dendritic spines, and so further discussion will not include these cell types and their inputs unless specifically mentioned.

The physical parameters of dendritic spines can vary in surface area, volume and morphological shape, which can be expressed in terms of parameters such as curvature or tortuosity. In most synapses the PSD forms a discrete, disc-shaped area that follows the contours of the bulbous spine head, be it concave or convex, and can be referred to as 'macular' synapses. Larger spines are frequently termed 'mushroom' spines, because their bulbous head forms a cup that surrounds the presynaptic bouton. These larger spines also may possess a 'complex' synapse, where the PSD is not macular but 'doughnut-shaped', 'horse-shoe-shaped' or even 'perforated' or 'segmented'.

This third type of complex synapse have a PSD that forms two or more completely separated or 'partitioned' discs of PSD that look - and may act like – individual macular synapses within the same dendritic spine. An example of such a spine is shown in Figure 7, which also contains a 'spine apparatus' in the neck of the dendritic spine. This is a specialised portion of the endoplasmic reticulum (ER) that is believed to be of great importance in the regulation of intracellular calcium concentrations within these large dendritic spines **(Spacek and Harris, 1997)**. The classification of dendritic spines will be discussed below - see also Figure 13.

In some cross-sectional images through such large, perforated synapses, the postsynaptic membrane can be seen to form an elaboration in the shape of a spike, which is often termed a 'spinule'. Spinules encroach into the presynaptic axon bouton, but the pre- and postsynaptic membranes remain separated by the synaptic cleft, which has the effect of separating the two areas of PSD by a larger amount of membrane that does not contain the high density of receptors found in the PSD. Spinules may therefore functionally divide the synapse into separate transmission zones **(Jones and Harris, 1995)**.

Sensory events will activate pathways which convey and process information in the brain, and the synapses of these pathways are modified by the information that is encoded into long-term memories. The presence of dendritic spines increases the number of synaptic contacts available to take part in the integration of information by the neuron. This may be particularly relevant in the hippocampus, which is involved in the association of different kinds of input. The number of connections is important for information processing, but not every sensory event is remembered. More important, novel and frequently occurring events are all common subjects of memory, but why are some events stored and some ignored? Associative conditioning has been used to study memory, and involves the pairing of two separate events, a conditioned stimulus (CS) which is rapidly followed by an unconditioned stimulus (US).

If the memory of the association is to be formed, changes must occur in the synaptic circuitry such that information indicating the occurrence of the CS will now also activate synapses and cells that deal with information about the US. The timing of the two stimuli is important for the association to occur, and requires coincident activity in both a pre-synaptic neuron and its post-synaptic counterpart. Donald Hebb proposed an associative learning rule by which such coincident activity would modify the response of synapses between the two cells that are active at or around the same time (**Hebb, 1949**). The short temporal spacing of stimuli means that the US arrives when the postsynaptic cell is still depolarised by the CS. This coincident activity will fulfil the conditions for the Hebbian learning rule, and result in the strengthening of synapses at the convergent point(s) of information flow from the CS and US (**Weinberger, 1995**). However, activity in only one pathway (i.e. only pre- or post-synaptically) would not result in coincident activity or any change to synaptic strength. A summary of the effects of synchronous and non-synchronous pre- and postsynaptic activation on synaptic strength is shown in Table 1.

Table 1 - The rules governing coincident synaptic activity, which strengthen or weaken synaptic responses and result in conditioning or habituation. Adapted from Figure 71.11, p.1086, Weinberger, 1995.

| | | Is the Presynaptic input active? | |
|---|---|---|---|
| | | Yes | No |
| Is the Postsynaptic cell depolarised? | Yes | Strengthen (CS, conditioning) | Weaken (non-CS, conditioning) |
| | No | Weaken (CS, habituation) | No change (non-CS, habituation) |

## Electrophysiology

Experiments by O'Keefe and colleagues indicated that cells in the hippocampus will alter their electrical activity in response to the movement of the animal. Recordings from individual cells showed that different locations promoted different patterns of activity, such that each cell had a *firing field* of locations where it would be active. Cells would be maximally activated by specific locations and orientations of the animal, with other locations evoking less firing, and these cells were described as *place cells* for this reason (**O'Keefe and Dostrovsky, 1971; Rotenberg *et al.*, 1996; Taube, 1995**). This evidence suggested that the hippocampus is involved in forming an internal representation of the external environment.

Whole ensembles of cells are activated by each location, and if the location changes, such as when an animal moves, the pattern of activity in the hippocampus also changes (**Wilson and McNaughton, 1993**). This change is apparent in many cells, such that some may increase their activity, whereas others may simultaneously decrease their activity. Also, different cells may be recruited into the ensemble, whereas other cells may cease activity altogether in the new location (**Best *et al.*, 2001**). Animals placed in a novel environment will rapidly form new firing fields for that particular location, suggesting that changes in cell activity result from the sensory information produced by this novel experience. Interestingly, antagonists to the NDMA (N-methyl-D-aspartate) type of glutamate receptor will block the long term stability of new firing fields, even though they do form and persist in the short term (**Kentros *et al.*, 1998**), and this issue will be discussed below.

In primary sensory cortex, input is represented as a topographical map, with adjacent sensory field areas being represented in physically adjacent cells. However, the hippocampus seems to form a more abstract 'cognitive' map, such that when the animal moves into an adjacent location, the anatomically adjacent cells in the hippocampus are not necessarily activated **(Stevens, 1996)**. The organisational principles underlying these ensemble changes are not yet understood, and are complicated by the possibility of differences between species, strains and even individuals. Such a dynamic method of representation may be necessary for the encoding of novel locations, but also implies that particular locations are not represented by particular cells. New locations are encoded by some of the same cells that encode familiar locations, and the addition or removal of sensory cues, particularly visual ones, will change the pattern of cells responding to the same environment **(Best *et al.*, 2001)**. The difference between particular representations is a result of the activity of the cells involved in the representation, which is defined by their synaptic connections **(Bartesaghi *et al.*, 1995; Skelton *et al.*, 1987; Wilson and McNaughton, 1993)**.

Instead of changing the sensory input from the external environment, an alternative approach is to manipulate the activity of the cells directly. Work by Bliss and Lømo in the hippocampus pioneered the investigation of a phenomenon that has been named long-term potentiation, or LTP **(Bliss and Lømo, 1973)**. This technique involves using a stimulating electrode to depolarise axonal fibres, and a recording electrode to monitor the electrical responses in the post-synaptic cells. The highly ordered anatomy of the hippocampus facilitates the precise activation of presynaptic axons in the perforant path, and the simultaneous recording from the cells of the dentate gyrus. If a number of pulses (50-100), are applied to the axons in very rapid succession, called a tetanus, typically at 100 Hz, subsequent single pulses will produce an enhanced response from the dentate granule cells compared to the response before the tetanus was applied. This potentiation is due to changes in the synapses between the perforant path axons and the dendrites of the granule cells.

LTP can be induced in all the excitatory connections of the hippocampus **(Bliss and Collingridge, 1993)**, as well as various specific areas and layers of neocortex, such as layer III of the visual cortex **(Kirkwood and Bear, 1994)** and layer II/III of the somatosensory cortex **(Castro-Alamancos *et al.*, 1995)**. Different stimulation protocols are capable of causing LTP, such as 'theta burst stimulation' and 'primed-

burst stimulation'. Theta burst stimulation mimics the pattern of discharges seen in the rodent hippocampus during locomotion, which occurs at about 4-5 Hz, and this is also important for spatial memory functions **(Winson, 1978)**. The stimulation protocol typically consists of a small number of shocks given in at high frequency, such as a 'burst' of 4 shocks at 100 Hz, which are repeatedly given many times at an interval of two hundred milliseconds, which corresponds to between 4 and 5 'bursts' per second (i.e. 4-5 Hz) **(Larson et al., 1986)**. Primed-burst stimulation involves a single stimulus, which is then followed by a high frequency burst of several stimuli after an interval of 200 milliseconds **(Rose and Dunwiddie, 1986)**.

One common factor between these protocols is the need for synchronised patterns of impulses, and this underlies the three basic properties of LTP. Only activated fibres have the opportunity to potentiate (input specificity), and only sufficiently active or synchronised activity will produce LTP (cooperativity), although less stimulated fibres may be potentiated if they are activated at the same time as a strong, convergent input (associativity) **(Bliss and Collingridge, 1993)**. The processes that initially produce LTP, termed *induction of LTP*, in many cases require the activation of NMDA receptors. These have been proposed to act as a molecular switch that is capable of detecting simultaneous pre- and post-synaptic activity, and signalling this occurrence by allowing postsynaptic $Ca^{2+}$ influx. The processes that cause LTP to persist for hours or even days, termed *maintenance of LTP*, are dependent upon several mechanisms, particularly protein kinases and the translation of mRNA (messenger riboxynucleic acid). These molecular aspects will be discussed in more detail below.

Other types of protocol were found to reduce the level of response in the post-synaptic cells, rather than enhance them, and this was named long-term depression (LTD). The first example of LTD was demonstrated to occur in connection with LTP formation **(Lynch et al., 1977)**, and was termed 'heterosynaptic' LTD because it occurred at inactive synapses when another afferent pathway was stimulated. This change in synaptic strength without association or activity was the opposite of Hebb's proposal concerning synaptic modifications, but activity-dependent forms of LTD have also been demonstrated **(Stanton and Sejnowski, 1989; Kerr and Abraham, 1993)**.

Protocols to induce so-called 'homosynaptic' activity-dependent LTD typically employ relatively low level frequency of stimulation (1-3 Hz), but it can also be produced after

short bursts of higher frequency stimulation if they are timed to coincide with the negative phase of the theta brain rhythm. Although some problems arose concerning the reproducibility of LTD, it has been demonstrated in various areas of the hippocampus *in vitro* and *in vivo* **(Thiels et al., 1996)**, both in young and adult animals **(Dudek and Bear, 1993; Henyen et al., 1996)**, and in the cerebellum, where it plays an important role in modulating the responses of Purkinje cells **(Lisberger, 1998; Mauk et al., 1998)**. One common feature of many different types of LTD is the requirement for NMDA receptor activation, and subsequent postsynaptic $Ca^{2+}$ influx **(Thiels et al., 1996)**.

Research suggested that potentiated synapses, i.e. those that had undergone LTP, could then be de-potentiated by applying low frequency stimulation (LFS) protocols **(Barrionuevo et al., 1980)**. Work in the hippocampus *in vitro* has indicated that LTP can be reversed by LFS, and that reversal of LTD by tetanic stimulation was also possible **(Dudek and Bear, 1993)**. However, this may not be the case in all pathways, as the hippocampal afferents to the prefrontal cortex show depotentiation of LTP by LFS, but not LTD when LFS was applied without prior LTP **(Burette et al., 1997)**. In spite of this, in the hippocampus the reversal of LTP by protocols that normally produce LTD suggested that LTP was dynamic and readily modified, which has led to the use of the term 'synaptic plasticity'. Indeed, because LTP and LTD are both induced by activity, the term synaptic plasticity is used to describe general changes in activity-driven synaptic strength, be they LTP, LTD or even the reduction of LTP (depotentiation). Another common feature of both LTP and LTD is their requirement for NMDA receptor activation, and this will be discussed below.

Instead of being separate, co-existing processes, it was suggested that LTP, LTD and depotentiation might be the net result of changes in synaptic responses on a continuum of change. The activity of the synapse would allow for either an increase or a decrease in function, according to the stimuli applied, which would be evident as potentiation or depression. A 'sliding threshold' mechanism was suggested as one possible explanation that would enable synapses to recalibrate themselves **(Malenka, 1994; Stanton, 1996)**. This would be essential if synapses were to be capable of storing information by responding to stimuli, but also to adapt to new information without reaching a saturation point **(Turrigiano et al., 1998)**. Research has suggested that synapses exhibit a phenomenon termed 'metaplasticity', which is intended to define the rate at

which changes in activity occur at synapses, rather than the size of the change **(Abraham and Bear, 1996; Tompa and Friedrich, 1998)**. If a particular amount of activity will potentiate a synapse by a given percentage, then metaplastic changes to that synapse will alter how much activity is required for that percentage of potentiation to occur.

In other words, metaplasticity will alter the range of activity that a synapse responds to, so that it can be sensitive enough to detect very small changes in activity, but also represent large amounts of activity. This also means that a particular level of metaplasticity will modulate the way in which a particular amount of activity will affect the synapse. Metaplasticity will determine the outcome on the synapse (strengthening or weakening) by altering the threshold at which activity will produce potentiation in favour of depression. This is shown diagrammatically in Figure 8. Such metaplastic changes have been proposed to occur as a result of activity, but this activity does not necessarily have to induce any changes in the functioning, or efficacy, of a synapse.

The recent history of activity at a synapse is believed to influence the ability of subsequent activity to produce changes in efficacy (synaptic plasticity) **(Li *et al.*, 2000; Markram and Tsodyks, 1996)**. This would imply that synapses are capable of integrating information over time from a record or memory of prior activity. Favourable activity would promote plasticity by coincident activity at particular synapses, an action that would decrease the potential of plasticity at synapses of the same cells where there is not coincident activity. Such a dynamic, interactive and competitive system would promote the facilitation of relevant connections, highlighting important coincident information and ensuring that the pathways processing the information are suitably modified, such that subsequent reactivation will produce a different response.

The requirement of coincident activity for LTP induction mirrors the simultaneous activity suggested by Hebb to be necessary for the formation of associations. Although there is no direct proof that LTP is the mechanism by which learning occurs, there are parallels between the processes of LTP & LTD and the alterations in synaptic function that are thought to underlie the formation of memory. Increases in evoked potentials have been observed in the dentate gyrus of rats trained in an operant conditioning paradigm. The increases remain for many days after training, and are comparable to
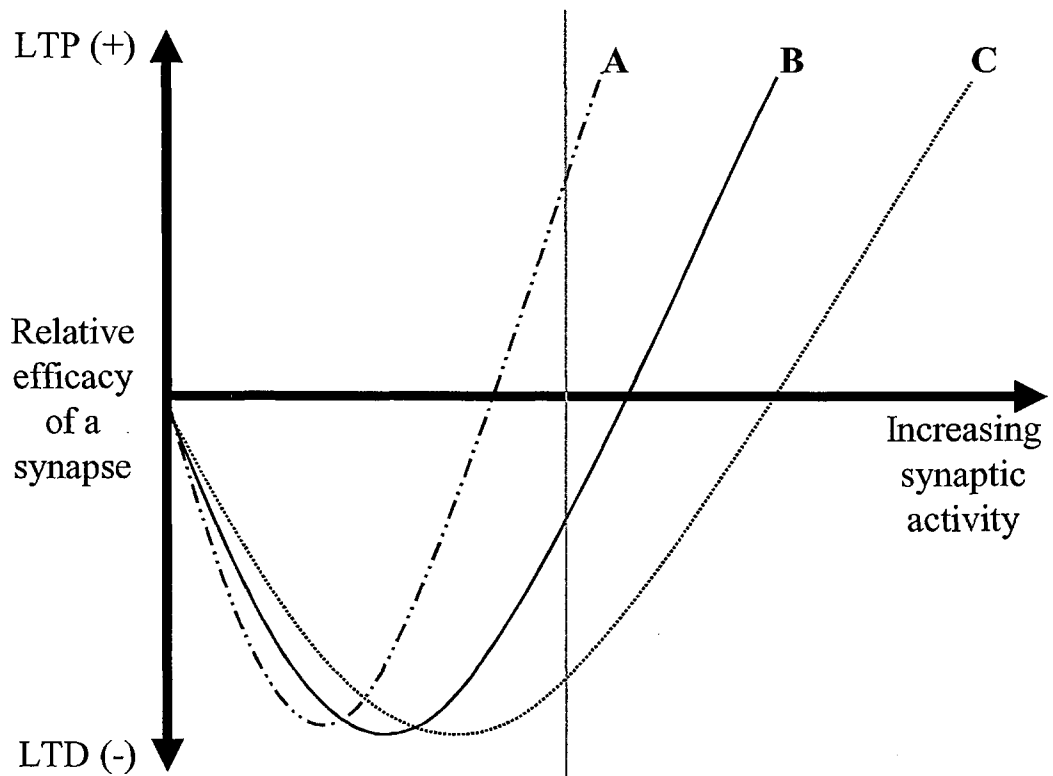
Figure 8 - The sliding scale threshold of plasticity, termed 'metaplasticity'. Different levels of activity will alter synaptic efficacy, producing either LTP or LTD, as shown by trace B. Metaplastic changes shift this trace and alter the amount of activity required to produce either of these modifications, so that the same level of activity (indicated by the vertical grey line) now produces either LTP (trace A) or more LTD (trace C).

those resulting from LTP, which was also inducible in the same animals (**Skelton** *et al.*, **1987**). Work in the sea snail *Aplysia Californica* has demonstrated that conditioning produces changes in the synapses involved in a reflex action which are similar to those seen in LTP, and that if stimuli that produce LTP are applied to these synapses, it will affect the reflex action (**Lechner and Byrne, 1998; Martin** *et al.*, **1997; Murphy and Glanzman, 1997**). Also, work has recently been shown whereby LTP can interfere with learning (**Brun** *et al.*, **2001; Doyère** *et al.*, **1995; Moser and Moser, 1999**), suggesting that LTP and memory formation may share common mechanisms.

## Molecular mechanisms of memory - presynaptic events

With modern advances in experimental techniques, neuroscientists have been able to examine the mechanisms of synaptic function at the cellular and molecular level, and to investigate the changes to these mechanisms that may underlie phenomena such as LTP and memory formation. The fusing of synaptic vesicles with the presynaptic membrane can occasionally be seen in electron microscopy images, and this indicates that they release neurotransmitter, which can then diffuse across the synaptic cleft (**Alberts *et al.*, 1989**). This process has been confirmed by the use of fluorescent dyes such as FM 1-43, which are taken up into synaptic vesicles and show a decrease in fluorescence in proportion to the amount of nerve terminal stimulation and postsynaptic response (**Betz and Bewick, 1993**).

It was observed that postsynaptic responses to axonal stimulation occurred in a stepwise fashion, rather than in a linear manner, and the idea of vesicles as quantal packets of information, each producing one step of the response, was suggested. If more vesicles were released then there would be an increase in postsynaptic receptor activation, and the enhanced response could be considered a form of synaptic plasticity. Synaptic vesicles are thought to undergo a cycle of production and filling, followed by several stages of docking and membrane fusion, before being recycled to produce new vesicles once again (**Südhof, 1995**), and this is shown in Figure 9.

With the discovery of several proteins involved in the molecular mechanics of vesicle fusion and neurotransmitter release, the important stages in this process are now more clearly understood. Important components in the processes of vesicle docking, priming and the eventual membrane fusion that leads to neurotransmitter release include molecules such as SNARE (soluble NSF attachment receptor) proteins (**Bajjalieh, 1999**) and the two proteins Rab3 and synaptotagmin (**Geppert and Südhof, 1998**). Rab3 and synaptotagmin are proposed to play antagonistic roles, a situation that allows tight control of vesicle exocytosis.

However, the initiation of the final stage of neurotransmitter release requires a relatively high concentration of $Ca^{2+}$ ions at the release machinery. Such ions are allowed to enter the presynaptic nerve terminal via voltage-gated $Ca^{2+}$ channels, which are activated when an action potential depolarises the axon terminal. The number of action potentials required to produce exocytosis can vary from one to many, indicating

**Synaptic cleft**

**Presynaptic bouton**

9 - Translocation

1 - Docking

2 - Priming

$Ca^{2+}$

3 - Exocytosis

4 - Endocytosis

5 - Translocation

8 -Transmitter uptake

7 - Budding

*Early endosome*

6 - Fusion with endosome
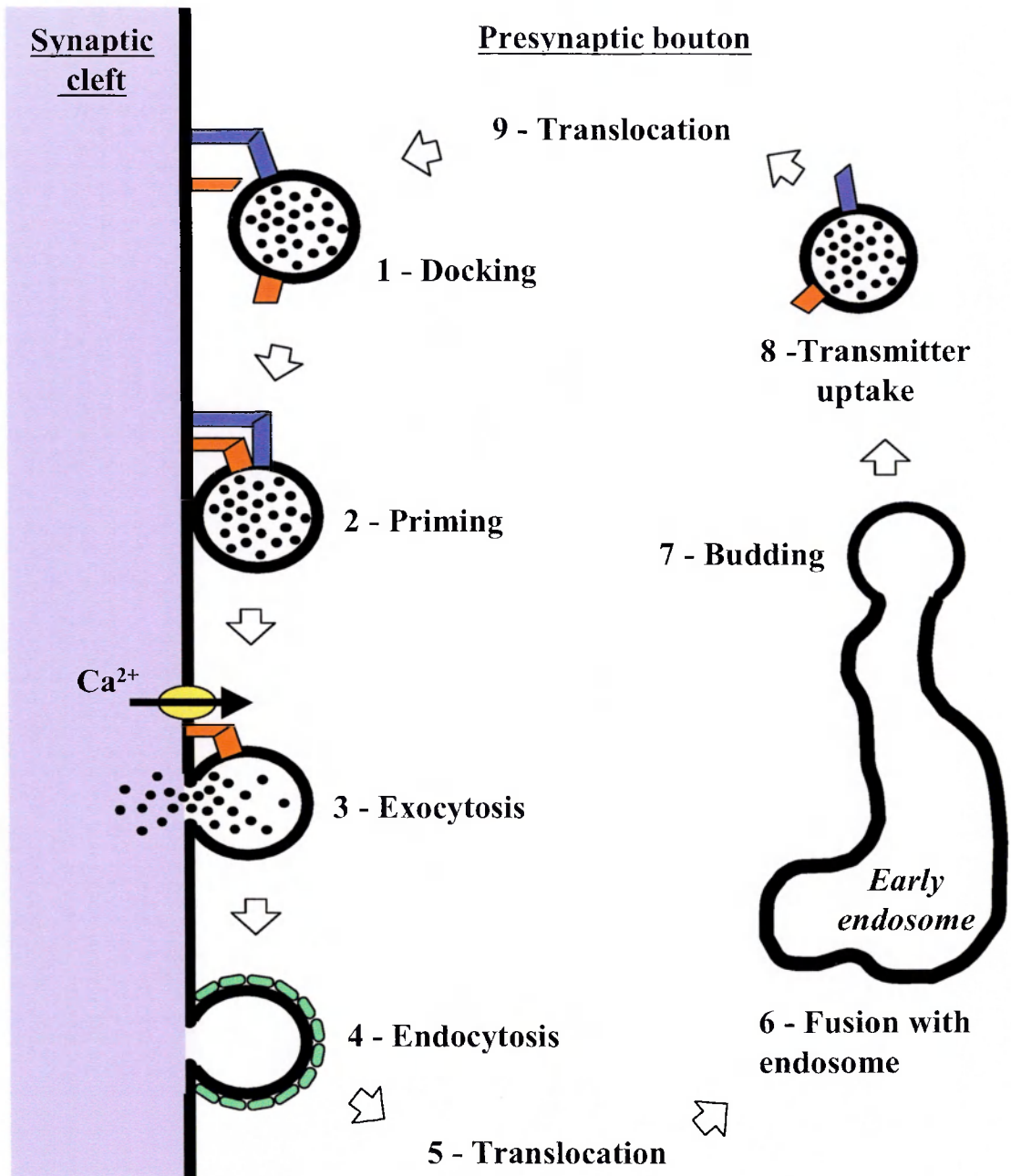
Figure 9 - The synaptic vesicle cycle. 1) Docking proteins (blue) attach the vesicle to the synaptic membrane, and unlock SNARE proteins. 2) SNARE proteins (red) form the fusion core complex. This primes the vesicle for rapid exocytosis. 3) Voltage-gated calcium channels (yellow) located close to the fusion core complex are opened by a presynaptic action potential, allowing an influx of $Ca^{2+}$. Synaptotagmin may act as a calcium detector, and responds to elevated calcium levels by triggering complete membrane fusion of docked and primed vesicles. 4) Empty vesicles coated with clathrin (green) undergo endocytosis from clathrin pits. 5) The clathrin coats are then removed and vesicles are moved to away from the membrane surface. 6) When they arrive at the early endosome, they fuse with it. 7) New vesicles are formed by budding from the endosome. 8) Transmitter is actively uptaken by these new vesicles. 9) Full vesicles are then translocated along cytoskeletal elements to the synaptic membrane, where they are available for docking (step 1). Rab3 is thought to influence the transport and availability of vesicles for docking. Adapted from (S_dhof, 1995) and (Thompson, 2000).

that this final step in the process of neurotransmitter release is highly regulated (**Thompson, 2000**).

The build-up of $Ca^{2+}$ ions is regulated by passive diffusion, active exchange and sequestration pumps, as well as cytoplasmic buffering molecules, all of which act to limit concentration increases. Evidence of the highly regulated nature of calcium influx has promoted models favouring exocytotic mechanisms involving localised regions of increased $Ca^{2+}$ ion concentration, rather than global calcium changes inside the nerve terminal (**Neher, 1998**). Exocytosis requires ion concentrations that are only present very close to $Ca^{2+}$ channels, and evidence suggests that successful triggering may be produced by channels that are actually bound to the molecule complex of the release machinery (**Stanley, 1997**). Changes to these presynaptic release mechanisms, such as the amount of $Ca^{2+}$ influx through ion channels or the sensitivity of the release machinery to $Ca^{2+}$, will influence neurotransmitter release, and are considered to be a type of synaptic plasticity even though such phenomena are only maintained for short periods of time.

Recent studies suggest that such short-term plasticity, or short-term enhancement (STE) of synapses has several different components, and that these can be distinguished kinetically and pharmacologically (**Fisher *et al.*, 1997**). Fast-decaying facilitation (F1) and slow-decaying facilitation (F2) are short-lived events, typically lasting for tens and hundreds of milliseconds, respectively. Both are thought to be governed by the concentration of $Ca^{2+}$ ions that are not bound to buffering molecules, which fluctuates on a similar time-course to the increase and decline of F1 and F2. Augmentation and post-tetanic potentiation (PTP) last for seconds and are though to be governed by more than one process. Both require a build-up of $Ca^{2+}$ ions in the presynaptic terminal, and this can occur after a series of action potentials, each of which will enhance the effect of the next (**Thompson, 2000**). Various diffusion and buffering mechanisms play a role in this situation, with mitochondrial uptake and increased concentrations of $Na^+$ ions being important for PTP. Because membrane pumps exchange intracellular $Na^+$ for extracellular $Ca^{2+}$ after an action potential, nerve terminal $Ca^{2+}$ levels will be reduced more slowly, and this will increase the probability of vesicle fusion, producing PTP.

## Postsynaptic calcium influx mechanisms

Calcium is a very common intracellular second messenger, and it plays significant roles in the events that occur in the postsynaptic compartment. Presynaptic depolarisation results in neurotransmitter release, which will open ionotropic receptors located on the postsynaptic side of the synapse (Craig *et al.*, 1994). This will produce a postsynaptic depolarisation that may be further enhanced by the activation of voltage gated ion channels. Calcium will enter via ligand-gated and voltage-gated channels, and will then be able to initiate second messenger cascades, which can influence a range of processes at the synapse and in the nucleus.

The postsynaptic signalling activity at glutamatergic synapses is mediated by the action of the ligand on specific neurotransmitter receptors. For glutamatergic synapses, these are found in two main forms; channel-forming ionotropic receptors and intracellular-messenger-coupled metabotropic receptors. These receptors are summarised diagrammatically in Figure 10. Metabotropic glutamate receptors (mGluRs) do not form ion channels, instead activating a range of intracellular signalling cascades that involve cAMP (cyclic adenosine monophosphate) or IP$_3$ (inositol trisphosphate). At least eight different mGluR types have been identified, each of which interact with a range of small G-proteins (guanosine trisphosphate-binding proteins) in order to mediate intracellular signalling.

Ionotropic glutamate receptors (iGluRs) are classified into three main categories based on the specific chemical compounds that inhibit them, as well as the electrical conductance of the channels that they form (Hollmann and Heinemann, 1994). The AMPA (α-amino-3-hydroxy-5-methyl-4-isoxazole proprionate) receptor has fast kinetics, opening and closing rapidly, and is only permeable to $Na^+$ or $K^+$ ions. A second category of receptor similar to the AMPA receptor is called the Kainate receptor, and also has fast kinetics, but is not expressed at all synapses (Mulle *et al.*, 2000). The third category are called NMDA (N-methyl-D-aspartate) receptors, and have slower kinetics. They also differ from the other receptors in that they are permeable to $Ca^{2+}$ ions, as well as $Na^+$ and $K^+$. However, they are unusual in that under normal resting membrane conditions they are subject to voltage-dependent blockade by $Mg^{2+}$ ions. All iGluRs are formed from a range of protein subunits that are specific to each receptor category, and these assemble in specific ways to form several different types of ligand-gated ion channel (Hollmann and Heinemann, 1994). Four

subunits assemble to form functional NMDA receptors, and these occur in several variants, known as NR1 type and NR2 type.

The NR1 subunit may be an essential component of functional NMDA receptors because normal ion channel currents are evident in NR1-NR2 heteromers, but not in NR2 homomeric receptors **(Monyer *et al.*, 1992)**. Different combinations of different subunit variants influence the conductance properties of NMDA receptors, and hence $Ca^{2+}$ influx. Because the $Mg^{2+}$-dependent blockade of NMDA receptors is only removed by postsynaptic depolarisation, the channel will only allow $Ca^{2+}$ to flow when this is accompanied by the binding of released glutamate. Only this coincident pre- and postsynaptic activity will allow $Ca^{2+}$ signalling, a necessary event in the formation of LTP **(Bliss and Collingridge, 1993)**. The NMDA receptor of the glutamatergic synapse is an ideal candidate for a molecule that could act as a coincidence detector, of the type proposed by Donald Hebb (see Table 1).

The formation of LTP can be prevented by pharmacological application of NMDA receptor antagonists such as D-AP5 *in vitro* **(Collingridge *et al.*, 1983)**. This is also the case *in vivo*, where it will block LTP, and will cause an impairment of spatial place learning **(Morris *et al.*, 1986)**. NMDA receptor antagonists will also prevent the long-term retention of a new place cell spatial map, although interestingly they do not interfere with the formation of new maps or their short-term retention **(Kentros *et al.*, 1998)**. The formation of all types of NMDA receptor requires the presence of the NR1 subunit. A specific knockout of the gene that encodes this subunit, restricted to the CA1 cells of the hippocampus, was produced in mice. The CA1 cells of these animals do not have NMDA receptor-mediated synaptic currents and LTP cannot be produced at synapses onto CA1 cells. Also, these animals showed deficits in spatial learning, but not other types of non-spatial memory **(Tsien *et al.*, 1996)**.

The inclusion of one NR2B subunit into an NMDA receptor increases the permeability of the ion channel, but the expression of this subunit decreases as the animal matures. Knockout of this gene resulted in impaired LTP and spatial learning **(Sakimura *et al.*, 1995)** whereas over-expression caused enhanced LTP, similar to that seen in juvenile animals. NR2B over-expressing animals also showed improved spatial learning, a greater response to fear conditioning and faster dissociation of this fear when exposed to unpaired stimuli **(Tang *et al.*, 1999)**.
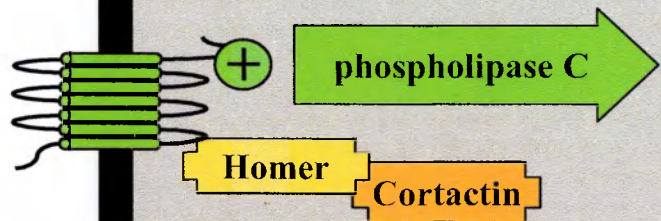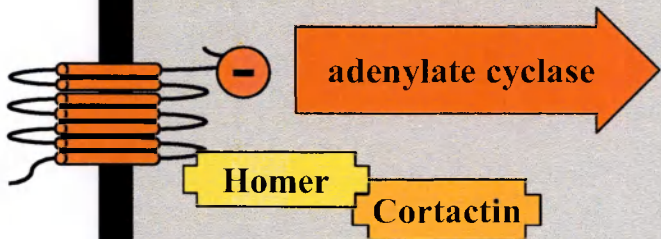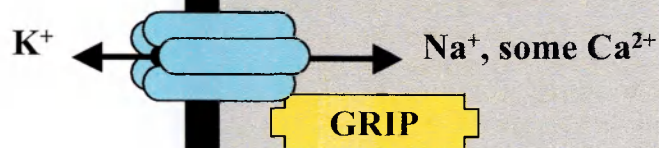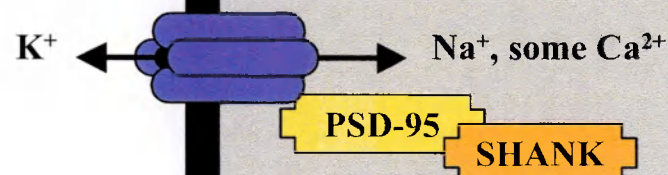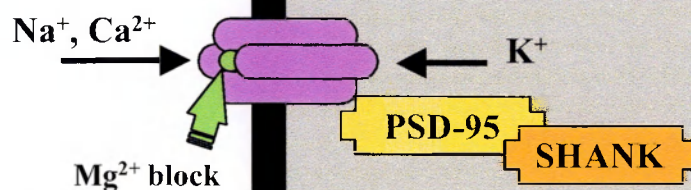
Figure 10 - The structure and function of glutamatergic receptors. Metabotropic receptors (mGluRs) are seven-span transmembrane proteins that activate G-proteins. Types 1 and 5 activate phospholipase C (green), whereas the other types inhibit adenylate cyclase (red). AMPA receptors (light blue) are (probably) pentameric combinations of four subunit types, GluR1-4. Various heteromeric compositions form functional receptors *in vivo*. Kainate receptors (dark blue) are functionally similar, but are (probably) tetrameric and are formed from GluR5-7 or KA 1 & 2 subunits. NMDA receptors (purple) are tetrameric combinations that contain NR1 subunits, and may also include one or more of the four NR2 subunit types, A-D. Also shown are the types of ions potentially conducted by each channel, and several associated proteins (yellow & orange, see text for details).

Synaptic plasticity and learning mechanisms that result from synaptic activation involve the summation of many electrical depolarisations (excitatory post-synaptic potentials - EPSPs), and each one of these will result in postsynaptic $Ca^{2+}$ influx. Work using fluorescent dyes that respond to $Ca^{2+}$, such as Fura-2, can be used to image the response of individual dendritic spines in the hippocampus *in vitro*. Weak stimulation of inputs to these dendritic spines results in fluorescence increases ($Ca^{2+}$ influx) only in the dendritic spine and only strong stimulation affected the $Ca^{2+}$ concentration in the main dendrite, indicating that spines can act as individual calcium compartments **(Müller and Connor, 1991)**. In addition, the fluorescent changes indicating $Ca^{2+}$ influx into dendritic spines were dependent upon NMDA receptors, as D-AP5 was able to block this. Furthermore, manipulation of dendritic $Ca^{2+}$ concentrations did not affect dendritic spines **(Guthrie *et al.*, 1991)**, suggesting that they act as individual integrative units for postsynaptic calcium signalling, in addition to their important role in the filtering of electrical signals **(Rose and Call, 1992)**.

One function of $Ca^{2+}$ signalling may be to influence the efficacy of the synapse during behavioural learning, either strengthening or weakening the effect of the synapse on, and ultimately the electrical activity of, the postsynaptic neuron. Investigations indicate that an increase in postsynaptic $Ca^{2+}$ levels is necessary for the induction of LTP **(Lynch *et al.*, 1983)**, LTD **(Otani and Connor, 1995)** and certain types of long term memory **(Silva *et al.*, 1998a; Tully, 1998; Wong *et al.*, 1999)**. Compared with LTP, lower frequency stimuli and smaller $Ca^{2+}$ increases are associated with LTD **(Lisman, 1989)**, suggesting that activity-related $Ca^{2+}$ influx determines the degree and type of synaptic plasticity.

## Intracellular calcium stores

The endoplasmic reticulum (ER) is an intracellular calcium compartment, and ryanodine receptors on the ER surface will bind $Ca^{2+}$ ions, opening the channel and releasing calcium from the ER. This mechanism of calcium-induced calcium release will produce areas of increased and maintained $Ca^{2+}$ concentrations, and may result in waves of calcium signalling **(Mattson *et al.*, 2000)**. These waves indicate that the ER acts like a neuron within a neuron, summating synaptically induced calcium increases and signalling to the transcription machinery in the nucleus **(Berridge, 1998)**. Some dendritic spines, particularly the larger, perforated type contain a spine apparatus,

which are structures thought to be part of the ER **(Spacek and Harris, 1997)**, as described earlier (see Figure 7). This link between $Ca^{2+}$ influx at synapses and summation of calcium signals throughout the entire neuron indicate that the postsynaptic calcium signalling produced by activity is important for neuronal computation. However, dendritic spines are thought to act as calcium compartments, such that the elevation of calcium concentration is confined to the dendritic spine by regulatory mechanisms **(Guthrie et al., 1991; Müller and Connor, 1991)**. The $Ca^{2+}$ concentration of the parent dendrite will be affected only by spine activation large enough to overcome these compartmentalisation effects.

Calcium-induced calcium release may also occur at $IP_3$ receptors on the ER, although this type of receptor is usually gated by $IP_3$. This ligand is the product of the inositol phospholipid pathway, a signalling mechanism common to many cell types that involves the activation of G-protein-coupled receptors **(Alberts et al., 1989)**. In neurons this includes mGluRs, and their activation and subsequent effect on intracellular $Ca^{2+}$ release is strongly implicated in LTP and LTD **(Anwyl, 1999; Bortolotto et al., 1999; Manahan-Vaughan et al., 1998)**. The PSD in excitatory hippocampal synapses contain two main types of mGluR, which are located on the edge of the synaptic contact area **(Somogyi et al., 1998)**. Positively coupled types activate the enzyme phospholipase C, which generates $IP_3$. Such calcium signalling mechanisms are evident in dendritic spines **(Takechi et al., 1998)**, and blockade of this type of mGluR interferes with long term memory **(Riedel, 1996)**.

Negatively coupled mGluR's do not use calcium as a second messenger. Instead they activate adenylate cyclase, which produces another important second messenger, cyclic adenosine monophosphate (cAMP). Increased levels of cAMP will activate protein kinase A (PKA), which signals to the nucleus, activating DNA binding proteins such as CREB (cAMP response element binding protein) **(Paolillo et al., 1999)**. These in turn promote the transcription of immediate-early genes such as *zif268* **(Jones et al., 2001)** and *cre* (cAMP response element) which have been shown in various animals to be important for learning and memory **(Silva et al., 1998b)**. This evidence suggests gene activation occurs via second messenger signalling pathways, many of which involve changes in postsynaptic calcium **(Guthrie et al., 1991; Helmchen and al, 1999; Yuste et al., 2000)**. The activation of nuclear gene transcription by different mechanisms of calcium signalling is shown in Figure 11.
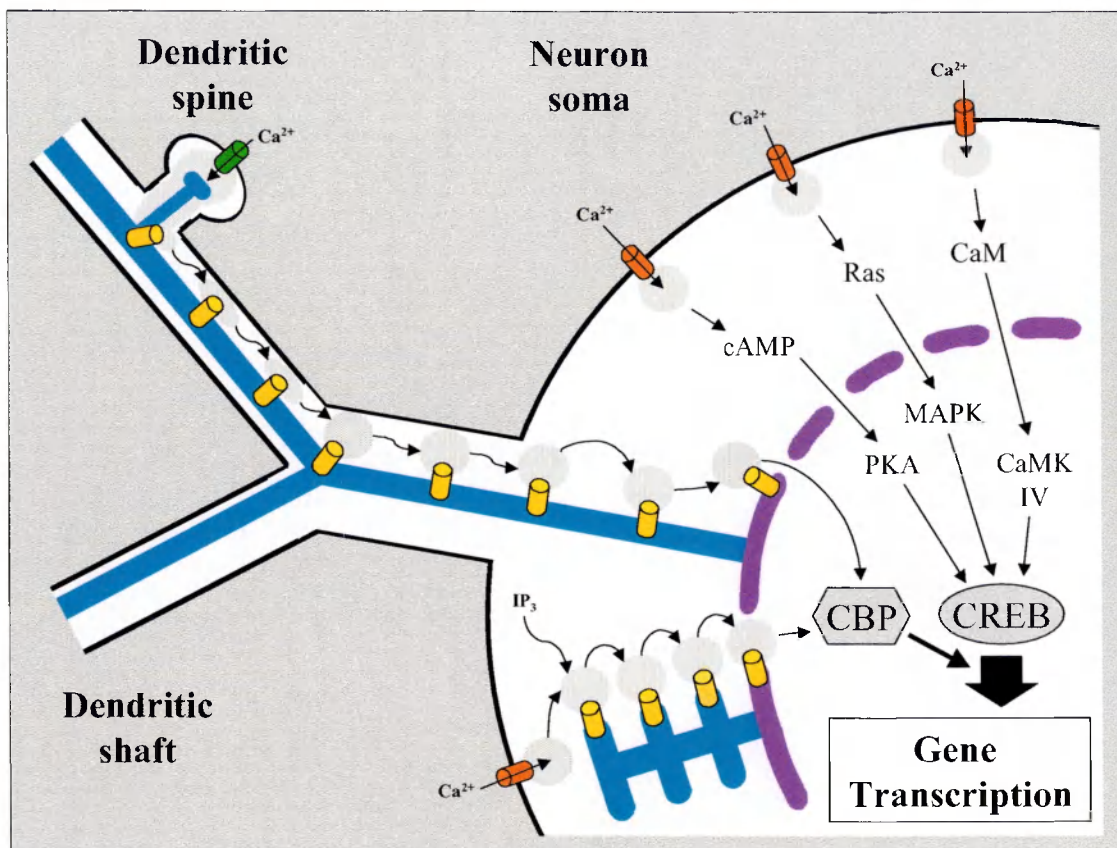
Figure 11 - Mechanisms of calcium signalling to the nucleus. Calcium influx at synapses on dendritic spines occurs mainly through NMDA receptors (green). This activates calcium-induced calcium release from the endoplasmic reticulum (ER, blue) through Ryanodine and $IP_3$ receptors (yellow), which can propagate as a wave of activation along the ER to the nuclear membrane (purple). $IP_3$, produced by activation of type 1 & 5 metabotropic glutamate receptors (not shown), can also initiate such calcium waves. Cell membrane depolarisation will open voltage-operated calcium channels (red), which can activate several signalling cascades (see text for details). These processes activate CREB (cyclic AMP response element binding protein) and CBP (calcium binding protein), which activate gene transcription. Adapted from Berridge, 1998.

## $Ca^{2+}$ binding proteins and kinases

A large number of calcium binding proteins exist in neurons, and their activation can trigger a variety of different effects (**Baimbridge *et al.*, 1992**). Activity-generated postsynaptic calcium increases are capable of activating immediate-early gene expression, and at least two signalling pathways are known that activate CRE in

hippocampal cells **(Hardingham *et al.*, 2001)**. One activates the extracellular signal-related kinase (ERK) cascade, also known as the mitogen-activated protein kinase (MAPK) pathway, and the other involves the calcium-binding protein calmodulin (CaM), which activates CaM kinase IV (see Figure 11). Another calcium-binding protein, calexcitin, can modulate the release of calcium from the ER stores by interacting with ryanodine receptors. Calexcitin, MAPK and the protein kinases A and C can also increase membrane excitability by inhibiting $K^+$ ion channels **(Alkon *et al.*, 1998; Johnston *et al.*, 1999)**. These channels are important in determining the electrical depolarisation of dendrites and the back-propagation of action potentials, both of which are important in regulating the calcium dynamics of dendritic spines **(Koester and Sakmann, 1998)**.

The enzyme $Ca^{2+}$/Calmodulin dependent kinase II (CaMK II) was found to be the major protein component of the PSD of excitatory synapses **(Kelly *et al.*, 1984; Kennedy *et al.*, 1983)**. When activated, CaMK II will phosphorylate itself, but this will be counteracted by phosphatases, such as calcineurin, once $Ca^{2+}$ concentrations return to baseline. However, if a certain threshold of phosphorylation occurs, CaMK II no longer requires $Ca^{2+}$/Calmodulin for autophosphorylation, and will be able to maintain a phosphorylated state despite the return of calcium concentrations to baseline. A mechanism by which this persistence of phosphorylation acts as a molecular site for LTP and memory storage was proposed **(Lisman, 1994)**, but experiments confirmed only the role of CaMK II in short term information storage. The short term retention of information by CaMK II may be explained by its role in phosphorylating a type of glutamate receptor called AMPA receptors. These ionotropic receptors contain an intrinsic $Na^+$ channel, and act to depolarise the postsynaptic membrane. CaMK II phosphorylation would alter their kinetics, and such changes could be maintained by persistent CaMK II autophosphorylation activity.

Mutant mice lacking CaMK II show normal behaviour but do not show hippocampal LTP **(Silva *et al.*, 1992b)**, and show deficits in two spatial memory tasks **(Silva *et al.*, 1992a)**. Partial gene knockouts show abnormal consolidation of fear conditioning after long delays, and abnormal LTP in the cortex, but not in the hippocampus **(Frankland *et al.*, 2001)**. This issue was complicated by reports that only certain types of memory and LTP were affected by mutations to the CaMK II molecule that rendered it independent of calcium **(Bach *et al.*, 1995)**. Such mice also have abnormal place cell

fields **(Cho *et al.*, 1998; Rotenberg *et al.*, 1996)** indicating that CaMK II malfunction impairs the formation of hippocampal spatial representations. The lack of normal spatial representations indicates that both a knockout of CaMK II and permanently active CaMK II disturb spatial representations, and hence the memories that are formed from these representations are impaired.

Other evidence suggests that CaMK II has subtle effects on postsynaptic function so that constitutively active forms of the molecule promote LTD rather than LTP. A resolution to the contradiction between activity enhancing synaptic responses and the same activity promoting a reduction in responses has been suggested. CaMK II autophosphorylation generates a charge effect in the kinase molecules which acts to reduce ion flow and counter the $Ca^{2+}$ influx induced by subsequent synapse activity. This mechanism allows for a reduction in responses after a large $Ca^{2+}$ influx by negative charge build-up. Conversely, the lack of autophosphorylation and inhibiting charge after small $Ca^{2+}$ influx will allow greater activation upon subsequent synaptic activity **(Tompa and Friedrich, 1998)**. The outcome of this charge build-up will be that the recent pattern of activity at a synapse is stored for some time, and will influence the effect of subsequent synaptic activity. This effect may be similar to the phenomenon of metaplasticity described previously.

Protein kinase C is a calcium-dependent enzyme, and as with other kinases found at the PSD, is capable of phosphorylating other proteins. Several types of ionotropic receptors, including glutamate receptors, contain amino-acid sequences that are potential sites for such phosphorylation. Such phosphorylating activity will change the conductance properties of ion channels **(Lieberman and Mody, 1999)**, and is implicated in plastic changes at synapses resulting from LTP **(Kleschevnikov and Routtenberg, 2001; Raymond *et al.*, 1993)**. Several dephosphorylating protein phosphatases (PP's) are also found associated with the PSD. PP1 has multiple functions, being involved in interactions with $Na^+$ channels, $Ca^{2+}$ channels and glutamate receptors, as well as the dephosphorylation of CaMK II **(Price and Mumby, 1999)**. PP2A selectively dephosphorylates soluble CaMK II, and also regulates the stability of neurofilaments and microtubules.

PP2B, also called Calcineurin, has been implicated in regulating presynaptic glutamate release, as well as the negative feedback process that regulates the agonist-induced

desensitisation of NMDA receptors (**Yakel, 1997**). Furthermore, one action of calcineurin is to inactivate inhibitor-1, which would normally inhibit PP1 activity. This action of calcineurin increases PP1 activity, and has been proposed to facilitate the generation of LTD (**Mulkey et al., 1994**). The ability of these processes to alter the effect of receptors on postsynaptic depolarisation adds another mechanism by which the conduction of information by synapses can be modified.

## Receptor population changes

As well as the NMDA receptor, glutamatergic synapses contain AMPA receptors. These are made up of four subunit types that are only found in AMPA receptors, and the channels show faster kinetics than NMDA receptors, but much reduced permeability to divalent cations, such as $Ca^{2+}$. During development, the proportion of excitatory synapses that contain AMPA receptors increases, whereas the number of NMDA receptors remains relatively stable (**Liao et al., 1999; Petralia et al., 1999**). Synapses that do not appear to contain AMPA receptors have been termed 'silent' synapses, because under normal activation conditions the NMDA receptors do not allow any current to flow due to their $Mg^{2+}$ block. However, it was discovered that if stimuli are applied that produce LTP, these silent synapses acquire electrical responses that are attributable to AMPA receptors. These responses may be due to the modification of AMPA receptors present at these synapses, enabling the receptors to function (**Isaac et al., 1995; Liao et al., 1995**).

Synapses do not contain functional AMPA receptors at the initial stages of development, and the inhibitory transmitter GABA (γ-aminobutyric acid) plays an excitatory role (**Ben-Ari et al., 1997**). However, as the brain matures, the role of GABA changes, and activity plays a prominent role in increasing the number of AMPA receptors present at synapses (**Pickard et al., 2000**). Studies have shown that changes to AMPA receptor currents in non-silent synapses are due to the insertion of new receptors into the membrane at the PSD (**Lissen et al., 1998**). When LTD is induced in the synapses of cultured hippocampal cells, the number of AMPA receptors clustered at synapses has been found to decrease (**Carroll et al., 1999**). Other work has found alterations to AMPA receptor distribution as a result of changes in activity (**Lissen et al., 1998; O'Brien et al., 1998; Turrigiano et al., 1998**). The number of AMPA receptors varies considerably from synapse to synapse in mature animals (**Nusser et al.,**

1998), and this has lead to the view that the plasticity of responses at mature synapses may be governed, at least in part, by the number of functional AMPA receptors present in the PSD (Craig, 1998).

NMDA receptor activation is required for the insertion of AMPA receptors into the synaptic membrane (Shi et al., 1999), which are delivered to the cell surface at extra-synaptic sites by the fusion of receptor-containing Golgi vesicles (Lu et al., 2001). AMPA receptors are removed from the synaptic membrane by endocytosis, and this process is regulated by synaptic activity. Activity induced changes are mediated by $Ca^{2+}$ influx through the NMDA receptor, which raises the proportion of AMPA receptors that are rapidly recycled back into the synaptic membrane (Ehlers, 2000). Synaptic transmission that activates AMPA, but not NMDA receptors, stimulates a $Ca^{2+}$-independent mechanism which increases the proportion of AMPA receptors that undergo degradation.

The population of NMDA receptors at synapses can be reversibly increased by the application of NMDA receptor antagonists (Rao and Craig, 1997). Receptor populations can be altered in the intact hippocampus by the application of electrical stimuli, and these changes are influenced by previous induction of LTD (Heynen et al., 2000). Metabotropic glutamate receptors may also have a role in regulating NMDA receptor numbers at synapses, as has been observed during development (Gomperts et al., 2000), although in mature animals, the number of NMDA receptors present at hippocampal synapses varies much less than AMPA receptors (Racca et al., 2000).

An important issue concerns the nature of the subunits present in neurotransmitter receptors, with different subunit types affecting the final conductance properties of the ion channel. Mice with the gene for the GluR-A (GluR-1) subunit of AMPA receptors knocked out do not show AMPA receptor-related currents or LTP, but are still capable of spatial learning in the Morris water maze (Zamanillo et al., 1999). This is in contrast to mice made to over-express the NR2B subunit of the NMDA receptor, which show increases in both LTP and memory capabilities (Tang et al., 1999). NMDA receptors which contain NR2B subunits have greater ion permeability, and are thought to be important for synapse development because their expression is down-regulated as a synapse matures (Tovar and Westbrook, 1999). Visual experience has been reported to influence the composition of receptors, changing within hours the

proportion of receptors that contain particular subunits present at the synaptic membrane **(Philpot *et al.*, 2001)**. Because NR2B-containing NMDA receptors have a greater permeability to $Ca^{2+}$ ions, such experience-dependent decreases in the proportion of NR2B-containing receptors at a synapse will cause a relative decrease in $Ca^{2+}$ signalling. This indicates that activity-induced changes to receptor composition will affect ion channel conductance, and hence synaptic function.


## The PSD and PDZ domains

Because of the dynamic nature of receptor populations at synapses, the PSD is not a rigidly fixed structure, but instead is in a constant state of change. Different sizes of synapse exist in the mature hippocampus, and the ratio of NMDA to AMPA receptors is linearly correlated with PSD size, except in the smallest of synapses which contain no AMPA receptors **(Takumi *et al.*, 1999)**. The PSD contains a wide variety of different proteins in addition to neurotransmitter receptors and CaMK II **(Kennedy, 1998; Ziff, 1997)**, and their characterisation has revealed several that have the potential to influence the flux of neurotransmitter receptors **(Scannevin and Huganir, 2000)**.

One family of proteins contain sequences known as PDZ domains, which are involved in protein-protein interactions. One group of PDZ-containing molecules are the MAGUK (membrane-associated guanylate kinase) proteins, which include PSD-95, a protein so-named because it is found in the PSD and has a molecular weight of 95 kilodaltons. PSD-95 interacts with the cytoplasmic tail of NMDA receptor subunits and is involved with receptor clustering **(Kornau *et al.*, 1995)**. Indeed, different MAGUK proteins are specifically involved in the expression of particular NMDA receptor subunits during development **(Sans *et al.*, 2000)**, and may control the insertion and removal of different receptor subtypes.

Several different kinases and phosphatases are attached to the PSD by special class of anchoring proteins, as is the case for protein kinase A **(Ziff, 1997)**. The protein synGAP is a Ras-GTPase-activating protein that binds to PSD-95, suggesting that NMDA receptors may be positioned to directly influence the $Ca^{2+}$-dependent activation of the Ras signalling pathway. Other unrelated proteins, such as GRIP, found in the PSD have been shown to interact with AMPA receptors **(Dong *et al.*, 1997)**. GRIP is thought to influence AMPA receptor clustering, and because particular proteins are

subunit specific, the presence of AMPA receptor subtypes at a synapse may also be differentially regulated **(Scannevin and Huganir, 2000)**. GRIP also contains PDZ domains, and these are important in the protein-protein interactions that organise the PSD.

Homer is a protein which is different again from MAGUK and GRIP types, and specifically binds to metabotropic glutamate receptors **(Brakeman *et al.*, 1997)**. Expression of Homer is regulated as an immediate early gene, and can therefore be controlled by synaptic activity. NMDA receptors can be coupled to metabotropic receptors through a protein called SHANK, which binds to both PSD-95 and Homer. SHANK also binds to cortactin, a protein which functions as a regulator of the cytoskeleton.

NMDA receptors may be even more directly linked to the cytoskeleton by several proteins, including α-actinin-2. This protein is found associated with the cytoskeleton at the PSD, the spine apparatus and the microtubules of dendritic spines, and is particularly abundant in the hippocampal dentate gyrus **(Wyszynski *et al.*, 1998)**. Interference with actin filament binding in the cytoskeleton does not perturb the clustering of NMDA receptors by PSD-95, but does disrupt the localisation of these NMDA receptor clusters to synapses **(Allison *et al.*, 1998)**. Protein phosphatases are found associated with neurofilaments, and may control their phosphorylation-dependent assembly or interactions with other cytoskeletal components. Phosphatases are also implicated in controlling MAPs (microtubule-associated proteins), which dissociate from the cytoskeleton and destabilise it when phosphorylated **(Price and Mumby, 1999)**. Therefore, protein interactions in the PSD are important for associating molecules involved in synaptic signalling and plasticity, as well as influencing the cytoskeletal components that govern the morphology of dendritic spines.

## The role of gene transcription in LTP and learning

Calcium signalling is important in both learning and LTP, both of which have been shown to involve gene expression activated by the $Ca^{2+}$-dependent CREB pathway, which is one of the main mechanisms for gene activation by neuronal activity **(Impey *et al.*, 1996; Impey *et al.*, 1998)**. The importance of gene activation and protein

synthesis in the process of memory formation can be confirmed by infusion of the protein synthesis inhibitor anisomycin *in vivo*, which will block the formation of memories for an inhibitory avoidance task when applied just prior to, or 3 hours after, training **(Quevedo et al., 1999)**. One gene that is involved in learning is c-*fos*, which shows increased activation in the hippocampus upon exposure to a novel environment **(Zhu et al., 1997)**. Indeed, the hippocampal expression of this immediate-early gene is also increased in spatial working memory tasks, especially when they require novelty detection **(Vann et al., 2000)**.

The permeability of NMDA receptors to $Ca^{2+}$ ions is important for synaptic plasticity and learning, as this route of $Ca^{2+}$ influx has been shown to stimulate the synthesis of CaMK II **(Scheetz et al., 2000)**. Calcium signalling to the nucleus, and the subsequent mRNA transcription and translation raises the problem of how the newly synthesised proteins are then transported specifically to the synapses which were initially stimulated. One possibility could be that specific, targeted transport of these molecules occurs, although little is currently known about how this could be accomplished. An alternative model was suggested where synapses are marked in some way by stimulating activity, and the newly synthesised proteins are incorporated into the required synaptic sites because they have been marked, or tagged **(Frey and Morris, 1997)**. Thus, widespread distribution of newly synthesised proteins could occur. It has been demonstrated that this could also lead to enhancement at synapses subsequently stimulated and tagged but insufficiently activated to normally produce potentiation **(Schuman, 1997)**.

Long term enhancement of synapses in the marine mollusc *Aplysia californica* can be elicited either pharmacologically or electrically, but both methods activate the CREB system and require presynaptic protein synthesis **(Martin et al., 1997)**. This presynaptic synthesis produces a widespread distribution of protein, but is only thought to occur in invertebrate species. However, work in vertebrates has indicated that messenger riboxynucleic acid (mRNA) is not confined to the cell nucleus. The presence of mRNAs that encode a variety of proteins have been discovered in the dendrites of vertebrate CNS neurons. These mRNA's differ between cell type and show different individual patterns of localisation **(Steward, 1997)**. Recently it was demonstrated that isolated dendrites from hippocampal cells could be transfected with glutamate receptor mRNA, and then induced to synthesise glutamate receptors and

express them on the cell surface (**Kacharmina** *et al.*, **2000**). Such results indicated that translation machinery is present in dendrites, and that the transcription of endogenous dendritic mRNA is also feasible.

Local synthesis and rapid protein product delivery may thus explain certain types of potentiation, such as that induced by neurotrophins, which requires new protein synthesis within minutes (**Okuno** *et al.*, **1999**). However, other changes to synaptic functioning occur over a longer time-course, one that fits better with signalling to, and transport of proteins from, the nucleus (**Schuman, 1999**). Only certain mRNAs have been found in dendrites so far, and particular signals are required to transport this mRNA into dendrites. For MAP2 (microtubule-associated protein 2) the important signal for translocation of the mRNA into dendrites appears to be a 640 nucleotide sequence in the untranslated end (3' region) of the mRNA (**Blichenberg** *et al.*, **1999**). Only the addition of this particular sequence of amino acids to other mRNA's will result in the transportation of these 'chimeric' mRNA's into dendrites. If other parts of the MAP2 mRNA are used, the chimeras are retained in the cell soma.

The local synthesis of MAP2 in dendrites may be important for stabilising the cytoskeleton and promoting neurite outgrowth in (e.g.) LTP, where relatively rapid filopodial extension is observed, as explained above. Similarly, CaMK II mRNA is present in dendrites, and this dendritic localisation is also dependent upon the 3' untranslated region (**Martin** *et al.*, **2000a**). The transcription of this CaMK II mRNA is dependent upon the cytoplasmic polyadenylation element binding protein (CPEB), a component of the PSD. CPEB binds to the 3' untranslated region of CaMK II, and acts to repress protein synthesis until the mRNA has been polyadenylated, a process that can be triggered by the phosphorylation of CPEB (**Wells** *et al.*, **2000**).

In the hippocampal dentate gyrus, the translation of *Arc* mRNA, an immediate-early gene, can be induced in dendrites by NMDA receptor activation. The protein 'Arc' (activity-related cytoskeleton-associated protein) contains regions homologous to α-spectrin, and interacts with cytoskeletal proteins such as F-actin (**Lyford** *et al.*, **1995**), although its function is unclear. Stimulation of specific parts of the perforant path axons activates synapses at particular locations on the dendritic tree of dentate gyrus granule cells. This stimulation also causes the specific localisation of *Arc* mRNA at the same set of activated synapses, and was not disrupted by the local inhibition of protein

synthesis (**Steward** *et al.*, **1998**). Low frequency stimulation and the induction of seizures both resulted in widespread, not localised, *Arc* mRNA and a lack of Arc protein synthesis. The function of the Arc protein is not known, but it is crucial for embryonic development, as mice with the Arc gene deleted or 'knocked out' die before the completion of embryogenesis (**Liu** *et al.*, **2000**).

Work by Guzowski *et al.* has indicated that this activity-induced localisation of *Arc* occurs in the same set of hippocampal CA1 cells which encode 'place fields', suggesting that the synaptic localisation of *Arc* mRNA is somehow involved in the behavioural process of neural encoding (**Guzowski** *et al.*, **1999**). Furthermore, injection of *Arc* antisense mRNA, which binds to and prevents normal mRNA from being transcribed, impairs the maintenance (but not induction) of LTP and also impairs long-term consolidation (but not short term memory and acquisition) of a spatial water maze task (**Guzowski** *et al.*, **2000**). The Arc protein, and the targeted localisation of *Arc* mRNA into dendrites in response to synaptic activity, appears to be an important process in development, synaptic plasticity and learning. To summarise, as well as controlling dendritic (local) and nuclear (global) protein synthesis, neurons are able to direct the delivery of (at least one) mRNA to synapses in response to particular types of activation relevant to learning and memory.

## Modifications to cortical connections

One feature of primary sensory cortical areas is that they contain maps of particular sensory modalities. These maps are representations of a particular set of sensory receptors, for example different parts of primary visual cortex contain neurons that respond to input from particular parts of the retina (**Hubel and Wiesel, 1968**). Far from being fixed, static representations, sensory maps in cortical areas have dynamic properties that enable them to be modified. Work on the development of the visual cortex in kittens indicated that sensory maps could be manipulated and altered. If one eye was deprived of visual stimulation during development, the pattern of retinal representation in the primary visual cortex was very different to that seen in normal animals. Instead of being equally responsive to both eyes, the non-deprived eye dominated the visual cortex and was represented by a much greater portion of the cortex than in normal, binocular animals (**Wiesel and Hubel, 1965**).

Changes to sensory representations are not just apparent during development however, as demonstrated by experiments with adult Owl and Squirrel monkeys. The median nerve relays sensory information from the hands and fingers in these monkeys, with different digits having separate, adjacent areas of representation in the primary sensory cortex (areas 3b and 1). Transection of a limited part of the median nerve resulted in changes to these representations when investigated several months later, and it was found that the area of cortex representing the sensory information from the part of the hand innervated by the transected nerve had been invaded by representations in the surrounding areas of cortex, and that these remaining, surrounding representations had become enlarged **(Merzenich *et al.*, 1983)**. The role of activity in maintaining cortical representations, even during adult life, has been further examined in adult owl monkeys, who were given behavioural training to increase the use of their manual dexterity and tactile sensitivity. Microelectrode maps of their primary sensory cortical representations of their hands (area 3b) taken before training were compared to maps made during and several weeks after training, and it was concluded that the cortical representations of the sensory areas of their hands were increased after training, expanding into adjacent cortical areas, for example area 3a **(Jenkins *et al.*, 1990)**.

Recordings from single neurons in cortex have also been used to investigate changes to neuronal connections. Visual discrimination learning is a type of behavioural training used to familiarise primates with complex pictures and real objects, and requires then to distinguish between familiar and unfamiliar stimuli. Such training was performed in *macaca mullata* monkeys, in conjunction with simultaneous recordings from visually responsive neurons in medial temporal lobe cortex (perirhinal and entorhinal areas). Responses in a fraction of all cells recorded were significantly smaller upon the second presentation of an object, compared to the first presentation, and this reduced response was still present upon further presentation of the same object, even when other, novel objects had been displayed in between presentations of the repeated object. Other neurons became more responsive when novel objects were presented.

The activity of a third category of neuron appeared to be related to how recently a familiar object had been presented, and a few neurons showed a change in response upon presentation of a familiar object that lasted for more than 24 hours **(Fahy *et al.*, 1993)**. Similar object (picture) recognition learning in rats has been shown to preferentially activate the perirhinal cortex, as indicated by an increase in the

55

expression of the immediate-early gene c-fos (**Zhu et al., 1997**). Interestingly, the pattern of c-fos expression was observed to be increased in the hippocampus in animals that had no prior experience of the learning environment, indicating that the hippocampus responds to the situation in which the learning takes place, rather than the aspects of the presented object, which agrees with the theory that the hippocampus is involved in the formation of episodic memories.

Visual learning in chicks activates cells in the IMHV (intermediate and medial hyperstriatum ventrale), a region of the forebrain. Young chicks can be taught to recognise and respond to a particular visual object, a process called imprinting, which can be considered as a form of recognition memory. Imprinting increases the electrical responsiveness of individual hyperstriatal neurons in the chick brain (**Brown and Horn, 1979**). Also, significantly more cells of the IMHV respond to a visual image once it has been imprinted. The increase in response is seen after 1 hour and after 21.5 hours, but not after 4.5 hours, suggesting that the learning is not represented simply by increases in the firing of cells (**Horn et al., 2001**). Further to this, imprinting has been used to investigate changes to synapses in the chick brain, and it was concluded that imprinting increased average dendritic spine volume by 19%, although unbiased stereological techniques were not used for this calculation (**Bradley and Horn, 1979**).

One-trial passive avoidance training can also be used to cause long term memory formation in chicks. Training increases the levels of $[^3H]$L-glutamate binding in the IMHV when measured 30 minutes afterwards, but this does not occur in untrained chicks, or chicks made 'amnestic' (to forget) by trans-cranial electric shock (**Steele et al., 1995**). This increase in NMDA receptors is also accompanied by an increase in the density of dendritic spines in the IMHV when measured 24-26 hours after training, but other measured parameters of dendritic spine morphology were not significantly altered (**Patel et al., 1988**). Comparisons of vertical and horizontal pathways within sensory-deprived cortex indicate a reduction in electrical responses, indicating that a lack of activity will reduce synaptic connections, possibly as a result of a competitive mechanism between the synapses (**Finnerty and Connors, 2000**).

In addition to research in monkeys, cats and chickens, similar investigations have also been performed in rodents. Representations of cutaneous sensations from the forepaws of rats exist in their primary somatosensory cortex, an area called SI. Forepaw

immobilisation will reduce the sensory input and physical use of that particular limb, resulting in a form of sensory deprivation. If one forepaw is immobilised for several days, the area of SI primary cortex that represents the immobilised limb will become reduced in size, and the cortical area that once completely represented that limb will now be shared by other representations from adjacent areas **(Coq, 1999)**. However, once the forepaw is released from immobilisation, the representation recovers, and the cortical area representing the immobilised limb enlarges.

Rat barrel cortex is the name given to the area of somatosensory cortex that contains a representation of the mechanosensory input from the large facial whiskers (vibrissae). These whiskers are clearly distinct from each other, and the cortical representations are similarly identifiable as separate areas of cortex. Removal of individual vibrissae at birth produces changes to the sensory cortex maps, such that the cortex that normally represents the removed whisker(s) is invaded by adjacent vibrissae representations, which are larger than normal **(Kaas *et al.*, 1983)**. Whisker removal in this way has also been reported to cause a significant decrease in the dendritic spine density of layer V cortical pyramidal cells, as measured by counting the number of dendritic spines per µm of dendritic length **(Ryugo *et al.*, 1975)**. Recent work using an *in vitro* preparation of the rat barrel cortex has investigated the role of experience on the plasticity of dendritic spines **(Lendvai *et al.*, 2000)**. This study indicates that experience-derived activity plays a large role in producing plastic changes that take place during development. In summary, experiments indicate that cortical changes in neuronal connections (i.e. cortical plasticity) can occur during development and also in adult animals, that these changes may take several days or weeks to occur, and that they are governed by levels of sensory input.

## Morphological plasticity of dendritic spines

Green fluorescent protein (GFP) occurs naturally in particular species of jellyfish, and has been adapted to many biological imaging applications by the use of molecular biology and transfection techniques. The dendritic processes of living neurons transfected with a GFP-protein construct can be imaged *in vitro* with high spatial and temporal accuracy using confocal microscopy, and an example of such images is shown in Figure 12. Work with GFP linked to actin has shown that dendritic spines are capable of a high degree of motility, which is regulated by the cytoskeletal assembly
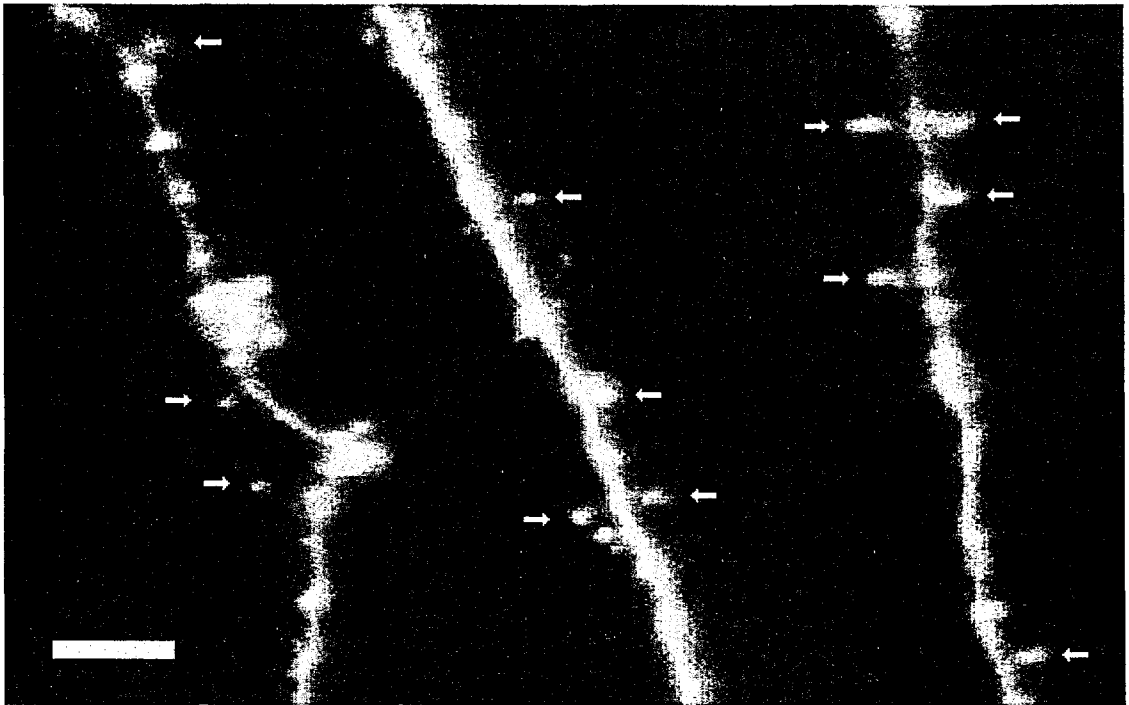
Figure 12 - Fluorescent light micrograph of a rat hippocampus organotypic culture transfected with GFP-Sindbis virus. Individual dendritic spines, indicated by small white arrows, can be seen projecting from the three *stratum radiatum* dendrites, which belong to the same CA1 pyramidal neuron. Scale bar = 5μm. Image courtesy of Dr. R. Schoepfer.

**(Fischer *et al.*, 1998)**. Further work by Fischer *et al.* has shown that such motility is functionally relevant, because activity stabilises the morphological plasticity of dendritic spines and gives them a more regular appearance. This process is due to $Ca^{2+}$ influx through voltage-gated calcium channels, a process that requires the membrane depolarisation produced by AMPA receptor activation **(Fischer *et al.*, 2000)**.

When GFP is used to visualise the location of microtubule-binding proteins MAP2 and tau, they are found to associate with and stabilise microtubules, although these microtubule structures are still dynamic and capable of producing neurite outgrowth **(Kaech *et al.*, 1996)**. Cytoskeletal organisation is important for neurite outgrowth during development and also for processes critical to neuronal survival such as microtubule transport **(Yang *et al.*, 1999)**. Using neurons filled with a cytoplasmic form of GFP, filopodia-like extensions have been observed to extend from dendrites that are in close proximity to a high frequency stimulating electrode. These filopodia-like processes were often seen to develop a bulbous head similar to those observed in

mature dendritic spines, an indication that functional synapses were formed. The extension of these processes is not seen after low frequency stimulation, nor are they seen when LTP stimulation is induced in the presence of NMDA receptor-specific antagonists **(Maletic-Savatic et al., 1999)**. Similar findings were reported by Engert and Bonhoeffer, who used a more localised method of stimulation to show that the projection of filopodia-like extensions from dendrites commenced 30 minutes after the long term, but not short term, enhancement of synaptic responses **(Engert and Bonhoeffer, 1999)**.

This evidence indicates that dendritic spines are motile structures which are capable of altering their morphology, and may be newly created by electrical stimulation. At excitatory synapses in the hippocampus, this plasticity is thought to depend upon the activation of glutamate receptors, which have the ability to interact with the cytoskeleton through $Ca^{2+}$-activated second messenger systems and a host of protein-protein interactions **(van Rossum and Hanisch, 1999)**. NMDA receptors are proposed to initiate the formation of new filopodial extensions, which are then stabilised and converted into mature spines by the insertion and subsequent activity of AMPA receptors **(Matus, 1999)**. Although direct evidence for this process is lacking *in vivo*, the observed plasticity of dendritic spine morphology *in vitro* parallels the variety of morphologies observed by electron microscopy of the *ex vivo* brain.

Parameters of spine size and morphology are highly varied, both between cells of different brain regions and of spines onto dendrites of the same cell type, and even the same individual cell. The diameter, volume and surface area of a spine's bulbous head, and the length and diameter of the spine neck are all variable between individual spines **(Harris and Kater, 1994)**. They have therefore been classified into three broad descriptive types; thin, stubby and mushroom, and these are shown in Figure 13. However, such classification may be inappropriate because of the heterogeneity of these structures, and variation in the PSD of the associated synapses. This has led to the suggestion of a continuum of interchangeable morphologies between perforated and non-perforated synapses **(Geinisman, 1993; Geinisman et al., 1996)**. As such, the three different types of spines and their synapse mentioned above may represent stages in the maturation of dendritic spines **(V. Popov, personal communication)**.

**Thin**

a) non-perforated or macular PSD

**Stubby**

g) fenestrated PSD

b) fenestrated PSD with spinule

**Mushroom**

f) horseshoe PSD

c) horseshoe PSD with spinule

e) segmented PSD

d) segmented PSD with spinule partition
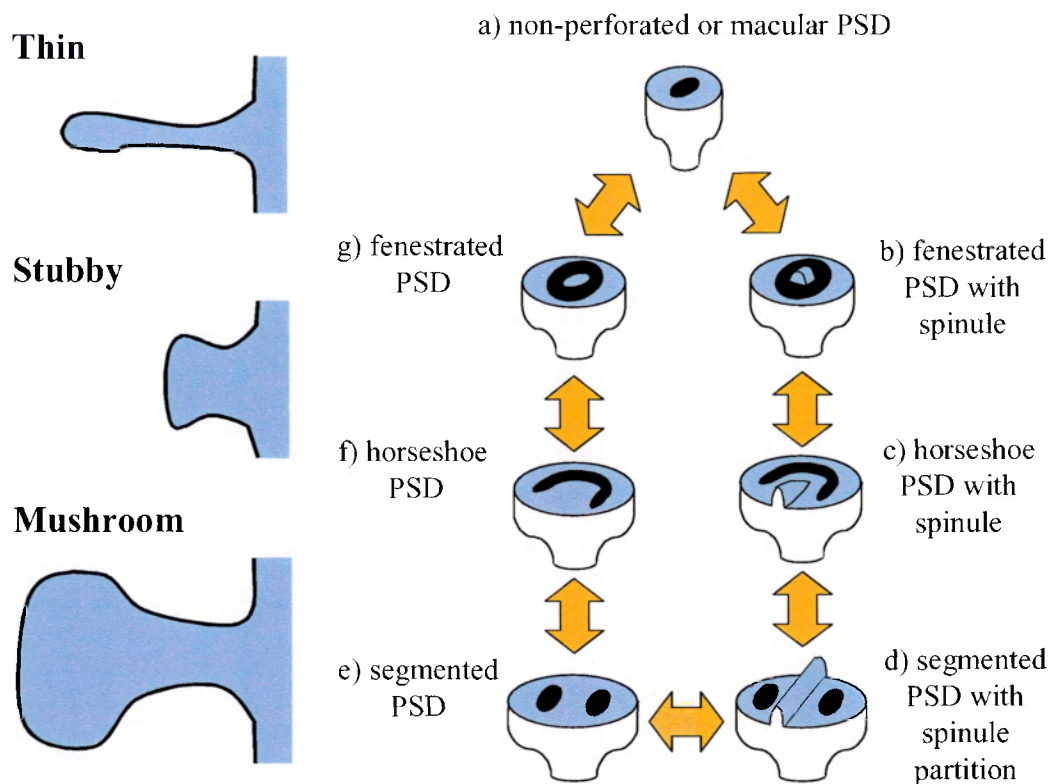
Figure 13 - The classification of dendritic spines and their synapses. The morphology of the three proposed types of dendritic spine, thin, stubby and mushroom, are shown on the left. On the right is a proposed scheme of interchangeable morphologies after Geinisman, 1993. These vary from the simple, non-perforated synapses shown in a to several perforated types that include synapses with completely seperate areas of PSD, shown in d and e.

The structural differences may have subtle effects on the electrical properties of the individual spine, but this is not strongly supported by comparisons with morphological data. However, the length of the spine neck may be particularly important in the $Ca^{2+}$ dynamics of dendritic spines, such that longer spine necks effectively isolate the spine head from the dendrite and stop or delay elevated spine $Ca^{2+}$ from affecting the parent dendrite **(Majewska *et al.*, 2000; Segal, 2001)**. Moderate calcium fluctuations cause novel spine formation and the elongation of existing spines, which are thought to result from central (dendrite) and local (spine) calcium increases respectively. Conversely, high calcium concentrations that persist over time cause shrinkage and elimination of spines, although this may be a result of excitotoxicity rather than a normal activity-related process **(Harris and Kater, 1994)**.

During development, filopodial extensions from dendrites are thought to seek out axons, in addition to the well-documented process of axonal target selection (**Alberts *et al.*, 1989**). Developing synapses can be observed on dendritic shafts, at the base of filopodia and on filopodial extensions, and are thought to be stabilised initially by cell adhesion molecules prior to the addition of neurotransmitter receptors (**Harris, 1999; Zhang and Benson, 2000**). Dendritic filopodia may well be the immature precursors of dendritic spines, which are observed after the process of synapse formation. Consistent with this is the observation that the dynamic nature of neuronal morphology reduces as development progresses (**Dunaevsky *et al.*, 1999; Lendvai *et al.*, 2000**). However, although mature (3 week old) neuronal cultures normally show a stable morphology, application of compounds such as caffeine, that elicits the release of $Ca^{2+}$ from intracellular stores, will rapidly alter the morphology and size of dendritic spines (**Korkotian and Segal, 1999**).

## Morphological changes induced by electrical stimulation

Mature neurons are therefore theoretically capable of morphological changes, and there is some evidence to support this. The total area of 'concave' synapse PSD in the dentate gyrus has been shown to increase in response to LTP, and persist for at least 60 minutes (**Desmond and Levy, 1986b**). A study investigating the numerical density of synapses in the dentate gyrus indicated increases in the density of 'concave' synapses following LTP (**Desmond and Levy, 1986a**). However, it is unclear in these studies whether 'concave' equates to 'perforated' synapses or mushroom type synapses (see Figures 7 and 13), and as only single sections were analysed the results may be subject to experimental bias.

This is because approaches such as these have relied on traditional assumptions about the morphology of the objects investigated, which can lead to inaccurate, or biased, results (**Howard and Reed, 1998**). For example, the calculation of synapse area was based on the assumption that each synapse forms a perfectly circular disk, whereas 3-dimensional reconstruction reveals that this is a simplification of the actual structure of synapses, which are often not circular. Similar assumptions have also been made concerning the counting of objects, a process which is complicated by the variability in the size of objects. The disector technique avoids making assumptions about the homogeneity of structures by counting objects irrespective of size (see Methods).

By adhering to the methodology of unbiased stereological approaches, assumptions do not need to be made, making these mathematically and statistically designed techniques better at producing reliable data **(Benes and Lange, 2001; Guena, 2000; West, 1999; West, 2001)**. The application of stereological techniques establishes mathematically comparable measures of (for example) the morphological parameters of synapses, and is therefore very important for the meaningful interpretation and comparison of such data **(Coggeshall and Lekan, 1996; Mayhew, 1996)**.

Unbiased stereological techniques have been used to investigate the induction of LTP. Potentiation of the perforant path increased the density of perforated synapses in the dentate gyrus 1 hour after the last stimulation selectively in the middle but not the inner molecular layer of the dentate gyrus **(Geinisman et al., 1991)**. Conversely, a study using stereological analysis and 3-dimensional reconstruction failed to show any changes in density or size 2 hours after the induction of LTP *in vitro* **(Sorra and Harris, 1998)**. However, of note is the fact that this investigation was performed in the CA1 area of the hippocampus, rather than the dentate gyrus.

Longer delays after the induction of LTP have also been used to investigate the morphology of synapses at timepoints that correspond to the maintenance of LTP. Two studies have analysed synapse morphology 24 hours after the induction of LTP in the dentate gyrus and the results are in agreement. Significant increases in the density of non-perforated axospinous synapses have been observed 24 hours after LTP induction **(Stewart et al., 2000)**. The second study suggests that the observed increases in synapse density after LTP are correlated with the degree of potentiation, suggesting that the increased electrical responses are a result of more synapses being formed **(Weeks et al., 1998)**. Analysis of dentate gyrus middle molecular layer synapses 13 days after LTP induction indicated that the density of perforated synapses was not increased, but that the density of axodendritic synapses was increased **(Geinisman et al., 1996)**. These results suggest that considerable changes to synaptic morphology take place during the induction and subsequent long term maintenance of LTP. The occurrence of perforated synapses is linked with the initial induction phases of LTP, whereas the maintenance of this phenomenon is governed by the formation of new axospinous and axodendritic synapses.

Complete 3-dimensional reconstruction of perforated synapses allows a clearer understanding of these complicated structures, suggesting that these synapses may be functionally compartmentalised by the occurrence of spinules **(Geinisman, 1993)**. The many different morphologies observed in such temporally restricted electron micrographs suggested that a continuum of changes might occur during normal synaptic function. This, and evidence of increases in synapse size after stimulation, lent support to the theory that synapses may increase in size, develop a perforation, and then divide or split in two **(Carlin and Siekevitz, 1983)**. The conversion of axospinous synapses into axodendritic synapses would potentially alter the postsynaptic effect of that synapse, particularly in terms of the calcium signalling, which would directly affect the dendrite. Indeed, the increase in PSD size could conceivably be a result of increased numbers of receptors, the (synthesis and) insertion of which occurs after LTP.

Perforations in a PSD, and the presence of a spinule, have been proposed to increase the available sites for neurotransmission, a process which will increase the efficiency with which a presynaptic depolarisation results in a postsynaptic response **(Jones and Harris, 1995)**. Because neurotransmitter release is probabilistic, the presence of more than one release site will increase the likelihood of release, and hence synaptic efficacy **(Lisman and Harris, 1993)**. In the rat neocortex, both non-perforated and perforated synapses are observed from early in development, and the increase in number and size of each type follows a different temporal profile. This, and the fact that perforated synapses are generally larger, led to the alternative theory that perforated synapses form a separate population from non-perforated synapses, and that inter-conversion does not occur **(Itarat and Jones, 1993)**.

The activation of cultured hippocampal cells for several days by reducing inhibitory neurotransmission produced an increase in perforated synapses that was blocked by inhibition of NMDA receptors **(Neuhoff et al., 1999)**. By using a method of calcium precipitation to detect activated synapses, Buchs and Muller showed that three times as many perforated synapses contained precipitate than did non-perforated synapses 35 minutes after LTP induction, and that this was dependent upon NMDA receptors **(Buchs and Muller, 1996)**. This further supports the idea that activity-mediated postsynaptic calcium signalling has important effects upon synaptic morphology, as indicated by the localised application of LTP described previously **(Engert and**

**Bonhoeffer, 1999; Maletic-Savatic *et al.*, 1999)**. These *in vitro* studies have demonstrated the induction of morphological changes that involve filopodial extension, a process that results in the formation of new dendritic spines during development. An increase in the density of dendritic spines has been shown after *in vivo* potentiation of the perforant path, with an increase in bifurcating spines that contain two spine heads, but no increase in the size of the spines **(Trommald *et al.*, 1996)**.

One strong argument against the occurrence of synapse splitting during normal synaptic function is the observed lack of more than one connection between the same axon and spines on the same dendrite. As a spine splits, it should produce two smaller spines that will still be in contact with the same axonal bouton. In a 3-dimensional reconstruction analysis of 91 bifurcating spines, Sorra *et al.* concluded that the different branches of such a spine always connected to different axons **(Sorra *et al.*, 1998)**. Bifurcating spines were very infrequently seen in 15 day old animals, suggesting that they are not involved in development. Spines in the process of splitting were never observed, and the spinules of perforated synapses were not large enough to completely partition the spine. Furthermore, spinules were observed to extend from spine necks as often as the PSD, and some projected into axonal boutons that did not form a synapse with that spine. These results point away from the likelihood of synapse splitting towards novel spinogenesis that originates by filopodial extension from spine necks and/or dendritic shafts.

The transient nature of perforated synapses has been suggested to account for the rapid enlargement and perforation of PSDs seen when the recycling of presynaptic vesicles is blocked. A similar process may underlie the increase in spinules 1 minute after stimulation, and suggests that the presence of perforations and spinules is related to the activity at a synapse **(Sorra *et al.*, 1998)**. A transient increase in perforated synapses lasting less than one hour has been reported after induction of LTP, which is followed by a three-fold increase in axonal boutons contacted by two or more dendritic spines **(Toni *et al.*, 1999)**. This report prompted Geinisman and colleagues to re-examine their study investigating trace eyeblink conditioning, a task that is dependent upon the function of the hippocampus. In the first study, animals given eyeblink conditioning showed an increase in the PSD area of CA1 non-perforated axospinous synapses 24 hours afterwards **(Geinisman *et al.*, 2000)**. Further assessment of the same data set

indicated that the conditioning had also caused an increase in the occurrence of multiple synapse boutons **(Geinisman *et al.*, 2001)**.

## Activity-related morphological changes

An increase in multiple synaptic contacts is evident in the visual cortex of mature rats after extended exposure to complex and novel environments **(Jones *et al.*, 1997)**. Exposure of rats to an enriched environment has been shown to improve spatial learning, as measured by acquisition speed of the Morris water maze. These animals also show an increase in the frequency of dendritic spines in area CA1 of the hippocampus. However, these measurements were made using confocal microscopy, a technique that does not posses the resolving power to identify synaptic contacts, and may be subject to errors that arise by the masking of dendritic spines behind other spines and/or the parent dendrite **(Moser *et al.*, 1994)**. Increases in the occurrence of dendritic spines have been detected by electron microscopy in the dentate gyrus of animals given passive avoidance training, another task that is hippocampus-dependent **(O'Malley *et al.*, 1998)**. This study, like the work of Geinisman & co-workers and Jones *et al.*, used unbiased stereological approaches to quantitatively assess the occurrence of synapses.

Studies on morphological changes after learning have been few, involving conditioning paradigms as well as exposure to novel environments. Many of these approaches have relied on traditional assumptions about the morphology of the objects investigated, which can lead to inaccurate, or biased results, as discussed above. However, Regan and co-workers have applied the stereological disector technique to study the effects of avoidance conditioning on synaptic morphology of the hippocampal dentate gyrus **(O'Malley *et al.*, 1998)**.

Rats were familiarised with a partitioned box, which was divided into a dark area and a brightly lit area. Training consisted of placing the animals into the light area of this box, and they were given a mild electric foot shock shortly after they entered the dark area. Upon testing, animals were placed back into the light area, and only animals that avoided the dark area for longer than 300 seconds were considered to have remembered to avoid the dark area. The results indicate that animals examined 6 hours after training and testing had a significantly greater density of dendritic spines than either naïve or

passive control groups. Other time-points after training were also examined (3 hours and 72 hours), but these did not differ significantly from the naïve control, suggesting that morphological changes occur within a restricted time-frame.

Other training protocols have also been used to investigate these morphological changes. The Morris water maze is a spatial memory task for rodents which requires the functioning of the hippocampus **(Morris, 1984)**. For rats, the task involves a pool of water (up to two metres wide), rendered opaque by agents such as milk powder, into which the animal is placed and allowed to swim. By using a platform that is slightly submerged below the surface of the water, the rat cannot directly see the platform. Instead, the animal must rely upon previous memories of the location of the platform in relation to distal visual cues, such as pictures on the walls of the test room. From this information, the rat must estimate its current location in relation to the platform in order to navigate to the platform goal.

This task is computationally intensive, and such associative activity has been shown to require the activation of the hippocampus, as lesions impair the ability to learn this task **(Morris *et al.*, 1982; Moser *et al.*, 1993; Wincour *et al.*, 2001)**. As a behavioural paradigm, the water maze has certain advantages over 'dry' spatial tasks in that it removes the possibility of confounding olfactory cues, which rodents could otherwise rely upon, and is not motivated by food reward, thus excluding any appetite-related changes in motivation to complete the task.

Hence, the Morris water maze has been used in several studies to examine the role of behavioural learning on the morphology of hippocampal synapses. Using stereological approaches, ultrastructural examination of dentate gyrus and CA1 synapses 6 days after water maze training indicated no change in synapse density or size **(Rusakov *et al.*, 1997)**. However, the distribution of synapses in the CA1 area did show a significant decrease in the average distance between synapses, suggesting that synaptic clustering results from morphological alterations induced by learning.

Morris water maze training has been shown to increase the density of synaptic profiles in the dentate gyrus of the hippocampus 6 hours after training **(O'Malley *et al.*, 2000)**. However, the increase was not observed 1 or 72 hours after training, nor in untrained controls. A drawback in the latter study was that although it used unbiased

stereological techniques, dendritic spine profiles were quantified, rather than synapses. The assumption made is that one spine equates to one synapse, but this is not necessarily correct **(V. Popov and M.G. Stewart, personal communication)**.

## Cell surface adhesion molecules

The Neural cell adhesion molecules (N-CAMs) are members of a family of structurally related proteins that contain immunoglobulin domains. These molecules are commonly involved in binding interactions between different cells and different cell types in the nervous system. The expression of many cell adhesion molecules is regulated by developmental genes **(Edelman and Jones, 1998)** and they influence axonal growth & guidance and synaptic plasticity during development, as well as activating signalling mechanisms **(Walsh and Doherty, 1997)**. Facilitation of AMPA receptor responses produced by spontaneous activity in the hippocampus will increase the synthesis of N-CAMs **(Holst _et al._, 1998)**.

N-CAMs can have one of three molecular types, each named after the molecular weight of the molecule. N-CAM 120 is usually found on glial cells, whereas N-CAM 140 is more often found throughout the membranes of immature neurons, particularly at growth cones, which may be related to its lateral mobility in cell membranes. Clustering of N-CAM 140 activates the MAPK pathway and CREB activation, which is important for axonal growth and synaptic plasticity **(Schmid _et al._, 1999)**. N-CAM 180 is much less mobile and is found in mature neurons. The association of N-CAM 180 with spectrin, a cytoskeleton-associated protein, as well as its presence in the PSD of synapses, has prompted the suggestion that it has a role in synapse stability **(Persohn _et al._, 1989)**.

Work by Lüthi _et al._ using antibodies against N-CAM and the adhesion molecule L1 indicated that blocking the formation of N-CAM/L1 complexes will reduce the ability of electrical stimuli to produce LTP in the hippocampus **(Lüthi _et al._, 1994)**. Induction of LTP _in vivo_ increases the presence of N-CAM 180 molecules at rat dentate gyrus synapses after 24 hours **(Schuster _et al._, 1998)**. Increases in N-CAM 180 at synapses are also seen 5-6 hours after passive avoidance training in chicks **(Skibo _et al._, 1998)**.

The carbohydrate molecule polysialic acid (PSA) is a major component of vertebrate brains which is exclusively attached to the N-CAM molecule (Rutishauser and Landmesser, 1996). Selective removal of PSA from the N-CAM molecule will prevent both LTP and LTD, and will impair acquisition and retention of spatial memory (Becker *et al.*, 1996; Muller *et al.*, 1996). This removal of PSA is thought to increase the adhesive functions of N-CAM, indicating that changes to the adhesion between cell membranes is involved in learning processes (Fields and Itoh, 1996). Other important adhesion molecules that may be important in memory include the cadherins, a large family of $Ca^{2+}$-dependent adhesion molecules which play a role in LTP (Serafini, 1999; Tang *et al.*, 1998). Thus the anchoring molecules that hold synapses together appear to be highly flexible and capable of fluidity, suggesting that synaptic contacts can be readily reshaped, and even formed and broken within a relatively short timeframe.

## Aims of the thesis

Evidence indicates that the hippocampus is critically involved in the formation of new episodic memories in humans, and that hippocampal lesions interfere with particular behavioural learning paradigms in a variety of animal species. Such learning is considered to involve changes to the synaptic connections of neurons in brain regions involved in memory encoding. The elucidation of the mechanisms that produce these changes has been rapidly advanced by the use of model systems (Burgess *et al.*, 2001; Foster *et al.*, 2000; LeMasson *et al.*, 1993; Rusakov *et al.*, 1996), which have indicated that such changes may involve the modification of the properties and numbers of neurotransmitter receptors present at synaptic sites, and alterations in synapse number and connectivity. However, the occurrence of morphological changes must first be observed in intact, behaving animals before any definite conclusions can be made about their involvement in normal learning processes.

Hence the work described here aimed to examine aspects of the morphological restructuring that may occur at the dendritic spines and changes in neurotransmitter receptors of synapses in the hippocampal dentate gyrus after behavioural learning in the Morris water maze. Previous work from our laboratory indicated that synapse restructuring and changes to the interconnections of synapses had taken place 6 days

after training in the Morris water maze **(Rusakov *et al.*, 1997)**, and so earlier timepoints were decided upon, focusing on the initial 24 hour period after learning.

This was based on the experiments described previously involving the maintenance of LTP, which suggested that morphology changes within the initial 24 hours **(Weeks *et al.*, 1998; Stewart *et al.*, 2000)**. Additionally, this was supported by the results of O'Malley *et al.*, who indicated that changes are occurring in the initial six hours after learning **(O'Malley *et al.*, 1998; O'Malley *et al.*, 2000)**, as well as the results from other paradigms such as avoidance learning in chicks **(Patel *et al.*, 1988)**. The action of protein synthesis inhibitors is crucial for long-term memory storage during this time **(Bourtchouladze *et al.*, 1998; Martin *et al.*, 1997; Nader *et al.*, 2000)**, and so particular time-points were investigated that were also important for this aspect of long-term memory formation.

The Morris water maze is a complex learning task that involves neuronal information processing by the hippocampal formation. This link allows the investigation of potential changes in this brain structure to be assessed after training. Previous publications have indicated that structural changes are apparent in the middle molecular layer of the dentate gyrus after both LTP and learning paradigms, and so this was selected as the area of interest for the present study. Because of the limitations in resolution of light microscopy, transmission electron microscopy was used to visualise synapses in this brain region. In addition to being able to quantify anatomical parameters, immunogold labelling of sections prepared for electron microscopy enabled the identification of specific individual molecules. Although such techniques do not allow for these parameters to be monitored continuously, this can be overcome by using statistical analysis to compare several different time-points.

In addition to the three groups of trained animals investigated each at a different timepoint, two controls were used. Naïve animals without any experience of the water maze were used as a negative control for the trained groups to provide baseline values for the parameters investigated. As a positive control, a group of animals were exposed to the water maze to provide them with similar physical exercise, and experience of swimming in a pool of water in a novel room different to that used for their normal housing. A second possibility for a type of positive control, the visible maze, was considered. Instead of the platform being slightly submerged, in this task it is raised

above the surface of the water and is clearly visible to the swimming animal. Therefore it provides a direct visual guide for the animal, which does not need to rely on the extramaze cues to escape from the water. Although the task is less demanding than the hidden platform task, it will give the animal in the pool an immediate goal that will reduce the stress to the animal. However, this control was not used.

# Methods

## Spatial memory training

Adult male Sprague-Dawley rats, typically 3 months old and weighing approximately 300 grammes were housed in standard conditions, in groups of 4 or 5 per cage, with *ad libitum* access to food and water.  All water maze training was carried out in the Department of Psychology at the University of Haifa in Israel in two experiments, conducted one year apart, using the same training protocols (see below).  Three groups of animals were trained in the hidden platform version of the Morris water maze **(Morris, 1984)**, and two control groups were also used.  Rats are able to swim, but prefer to spend as little time in water as possible.  The apparatus consisted of a matt black cylindrical container 170 cm in diameter and 50 cm deep, filled to about half depth with water at room temperature (about $^+$23°C).  Located in the pool was a cylindrical platform (12 cm in diameter and 23 cm tall), also matt black in colour, which prevented it from being directly visible to a rat swimming in the pool.  On the wall were pictures of large geometrical shapes and colourful posters, which could be seen by rats swimming in the pool and acted as allocentric visual cues.  This is shown schematically in Figure 14.

In this task, the subject rat was placed into the pool of water at a random starting location around the edge of the pool.  From here it was free to swim around the entire pool until it found the slightly submerged platform, whereupon it would climb out of the water, completing the task.  After a further 15 seconds on the platform, the trial would then end, and the animal would be placed into the home cage for 5 minutes of rest until the next trial.  Trials were conducted in groups of four, which was termed a session.  Upon first experience of the pool, each animal was given 60 seconds to find the platform.  This occurred by the animal bumping into the platform as it swam, but if this did not happen after 60 seconds of searching, the animal was placed onto the platform by the experimenter and allowed to remain there for 15 seconds before the 5 minute rest period in the home cage.
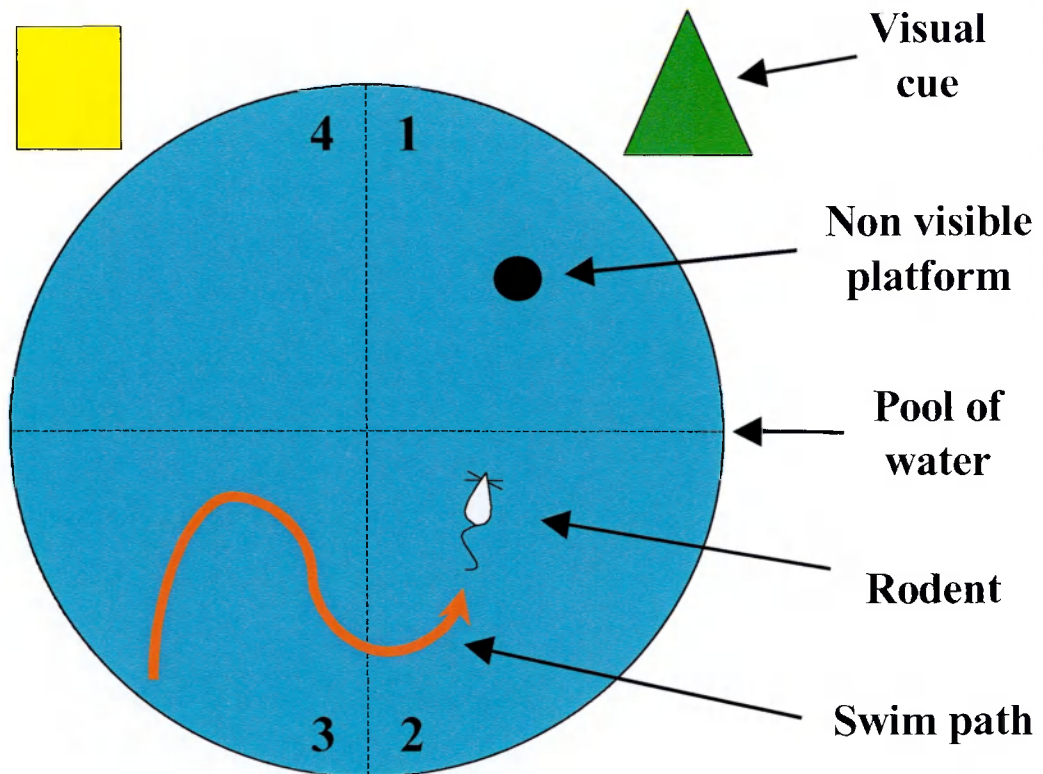
Figure 14 - Schematic representation of the Morris water maze, as viewed from above. The pool is divided into four quadrants, as shown by the dashed lines, and are numbered from 1 to 4 , as indicated at the top and bottom. The red line represents the swim path, a trace of the location of the subject animal from a random start quadrant (in this case quadrant 3). Visual cues, represented by the square and triangle, are provided as allocentric distal visual objects to aid navigation.

Upon subsequent trials, the platform remained in the same position, but the starting position did not. Therefore a simple directional swimming approach would not allow the animal to readily find the platform. Instead each individual had to use memory for the location of the platform with respect to the allocentric visual cues, and calculate its own location with respect to the same cues. It would then be able to calculate the correct direction of swimming in order to find the platform within the 60 seconds allowed for the trial. If the 60 seconds were exceeded, the animal was again placed on the platform for 15 seconds to familiarise it with the arrangement of allocentric cues as seen from the platform, before the next 5 minutes of rest.

### 3 hour group



| | |
|---|---|
| ↑ | ↑ |
| 4 trials | Quadrant test followed by perfusion |

### 9 hour group



↑      ↑      ↑      ↑

4 trials    4 trials    4 trials    Quadrant test followed by perfusion

### 24 hour group



↑    ↑    ↑    ↑         ↑    ↑

4 trials    4 trials    4 trials    4 trials        4 trials

Quadrant test followed by perfusion

### Swim only group



↑    ↑    ↑    ↑

Swimming paired with 9 hour group     Perfusion only
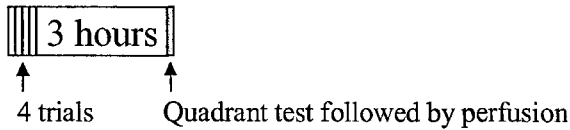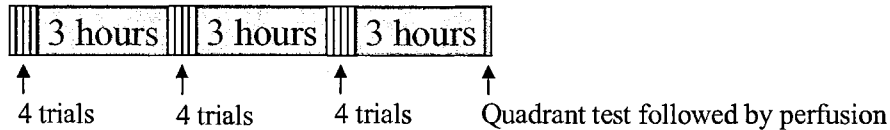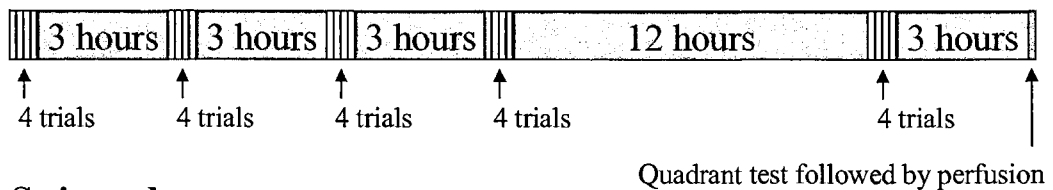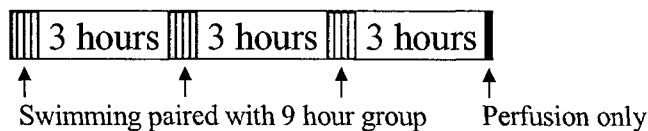
Figure 15 - Schematic of the training protocols used. Each training session consisted of four training trials, shown in white. These were followed by a period spent in the home cage, as indicated by the coloured sections. Each group protocol was completed by conducting a quadrant test (probe trial) shortly followed by perfusion, as indicated in grey. The time spent in the pool by the swim only group was identical to the average latency of the 9 hour group on the same, paired trial. The swim only group animals were not given a quadrant test prior to perfusion.

Three protocols, shown in Figure 15, were used to train separate groups of animals involving increasing numbers of training sessions. The first protocol (3 hour group) involved one training session (4 trials total), the second protocol (9 hour group) involved three training sessions (12 trials total) with a three hour gap between each session. The third protocol (24 hour group) involved five training sessions (20 trials total) with different duration gaps between each session to accommodate the normal sleep-wake cycle of the rats. For each training trial for each animal, the time taken by the animal to find the platform was recorded, as well as a graphical depiction of the route that the animal swam in order to reach the platform. Three hours after the

training had been completed, a probe trial or transfer test (**Morris, 1984**), here called a quadrant analysis test, was conducted. The platform was removed, and the pool was divided into four equal quadrants, one of which used to contain the platform, and as the animal swam around the pool, the time spent in each quadrant was recorded.

In addition to the trained animals, two control groups were used. The first was termed a naïve control because the rats did not have any experience of the room containing the water maze. The second was termed a 'swim-only' control that mirrored the second training protocol, and consisted of three training sessions, each session interspersed by a three hour gap. However, for each trial, the animal was placed into the pool without the platform present, and was allowed to swim for the same duration as the average time taken to find the platform by the 9 hour group. Thus, the swim only group were exposed to the same stimuli and amount of exercise, but not the task of learning the platform location. This group was not given a quadrant analysis test.

## Perfusion fixation

For the three trained groups, each animal was given an intraperitoneal injection of 1ml Urethal/Chloral hydrate anaesthetic (40 g Urethal + 5 g Chloral hydrate in 100 ml of 0.9% NaCl solution) immediately after the quadrant analysis test was completed, and then perfused transcardially. The swim only group animals were perfused three hours after the end of the final swim session. Each animal was perfused with 5 ml of normal saline followed by 200 ml of fixative solution, delivered at a rate of 7 ml per minute by a peristaltic perfusion pump (Watson Marlow, type 505s). Fixative was used that contained a high concentration of glutaraldehyde to cross-link the structural components of the brain tissue, which would preserve the tissue ultrastructure and was suitable for subsequent Epon processing. After perfusion each brain was carefully removed from the skull and kept moist with fixative solution during dissection.

Using a single edged razor blade, the cerebellum was cut from the brain in the transverse plane, and the brain was hemisected along the midline rostro-caudal axis. For both hemispheres, central thalamic and striatal structures were removed with the aid of a small metal spatula to reveal the hippocampal formation beneath, which was then carefully peeled from the overlying cortical structures. Several thin slices approximately 1 mm thick were cut from the intact hippocampus manually with a

Coronal view showing subsequent stages of dissection

Septal portion

Slice taken for investigation

Temporal portion

Initial dissection

Dorsal surface

Coronal view

Dorsal view
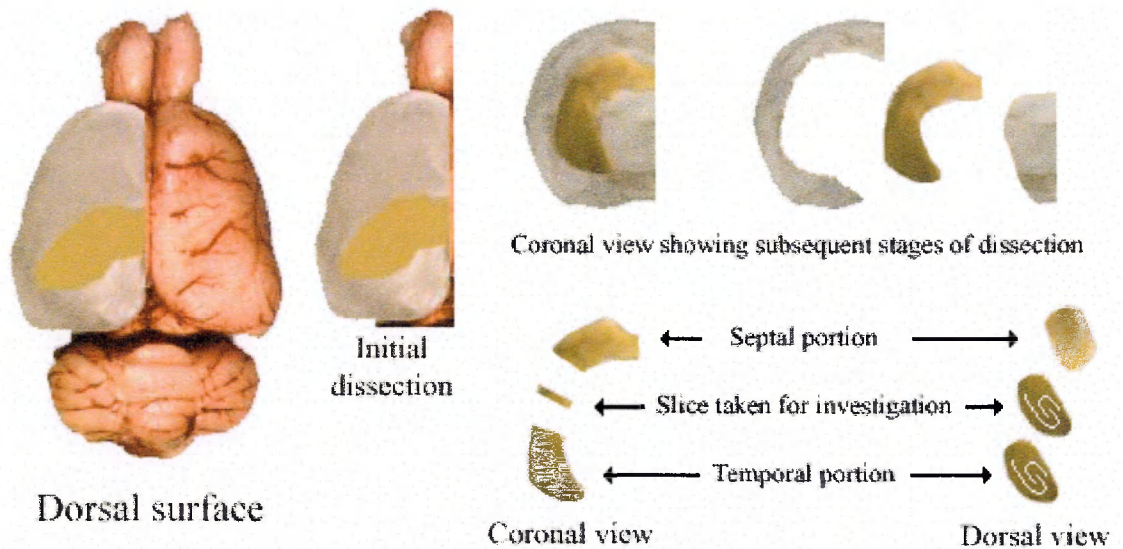
Figure 16 - The dissection of the hippocampus. The left hemisphere of the brain is represented in semi-transparent grey to show the location of the hippocampus, which is shown in yellow. Images from left to right represent stages of dissection, as described in the text. Also shown is the location of slices, which were taken from the middle of the hippocampal septo-temporal axis. The dorsal view shows the orientation of the principal cells arcs, which are indicated as white lines (only one slice is shown for simplicity).

scalpel. These slices were made in the middle of the long septo-temporal axis of the hippocampus, and were orientated perpendicular to this axis so as to include all parts of the hippocampal formation at the same septo-temporal level, as shown in Figure 16. For both hippocampi of each animal, three slices were reacted with a 1% solution of Osmium, dehydrated in a graded series of acetone concentrations and embedded in Epon resin (see Appendix A for electron microscopy protocols).

Some animals were perfused with Lowicryl processing fixative, which contained a low concentration of glutaraldehyde that preferentially preserves antigenicity. These brains were similarly removed and dissected, whereupon two or three of the slices were transferred to Epon processing fixative for 1 hour before being reacted with Osmium and Epon-embedded for morphological analysis. Two or three remaining slices from these animals were placed into graded solutions of glycerol to protect the tissue from damage during freezing. Sections were then rapidly frozen by being slammed into a copper 'mirror' pre-cooled with liquid nitrogen using a Reichert MM80E impact

freezer to control the freezing process. Frozen sections were then transferred into a Reichert/Leica AFS freeze substitution machine pre-cooled to -80°C, dehydrated in methanol and then embedded in Lowicryl resin at this temperature. Once the resin had been polymerised with ultraviolet light, sections were slowly warmed to room temperature, ready for post-embedding immunogold labelling microscopy, as described below (see Appendix A).

## Light microscopy

Epon resin-embedded tissue was prepared and cut using a Reichert-Jung OMUE ultramicrotome or a Leica UCT ultracut ultramicrotome. Serial semithin sections (2 μm thick) were cut for animals in each group on the ultramicrotome in the same plane as the tissue samples, so that all parts of the hippocampal formation at the same septo-temporal level were present. The sections were mounted on glass slides and stained with toluidine blue dye (1% toluidine blue in 5% borax solution), dried and viewed under a Zeiss Axiophot light microscope. Images of the upper blade of the dentate gyrus encompassing the granule cell layer, the molecular layer and the hippocampal fissure were taken using a x5 objective lens, and were digitised using a black and white digital camera linked to Microsoft Windows-based MCID image acquisition software (Applied Imaging Inc.). A graticule image, also taken with a x5 objective lens, was used to calibrate the images, which were then analysed on an Apple Macintosh Quadra computer using the public domain NIH Image program developed at the U.S. National Institutes of Health (this program is available on the Internet at http://rsb.info.nih.gov/nih-image/). Separate measurements of the neuropil thickness and granule cell layer thickness were taken from these images at three points along the upper blade of the molecular layer, as indicated in Figure 17.

Images of the dentate gyrus granule cell layer upper blade were taken from several serial sections with an x40 objective lens, and were digitised to form sets of images for each tissue block. A graticule image (taken with an x40 objective lens) was used to calibrate the sets of serial images, which were then analysed with NIH image software, as above. Bounded areas along the length of the cell layer and restricted to the width of the blade were drawn onto the serial images in corresponding locations. These measured areas were used as counting frames of known size on neighbouring sections, and also for higher magnification measurements of the blade width (see Figure 21).
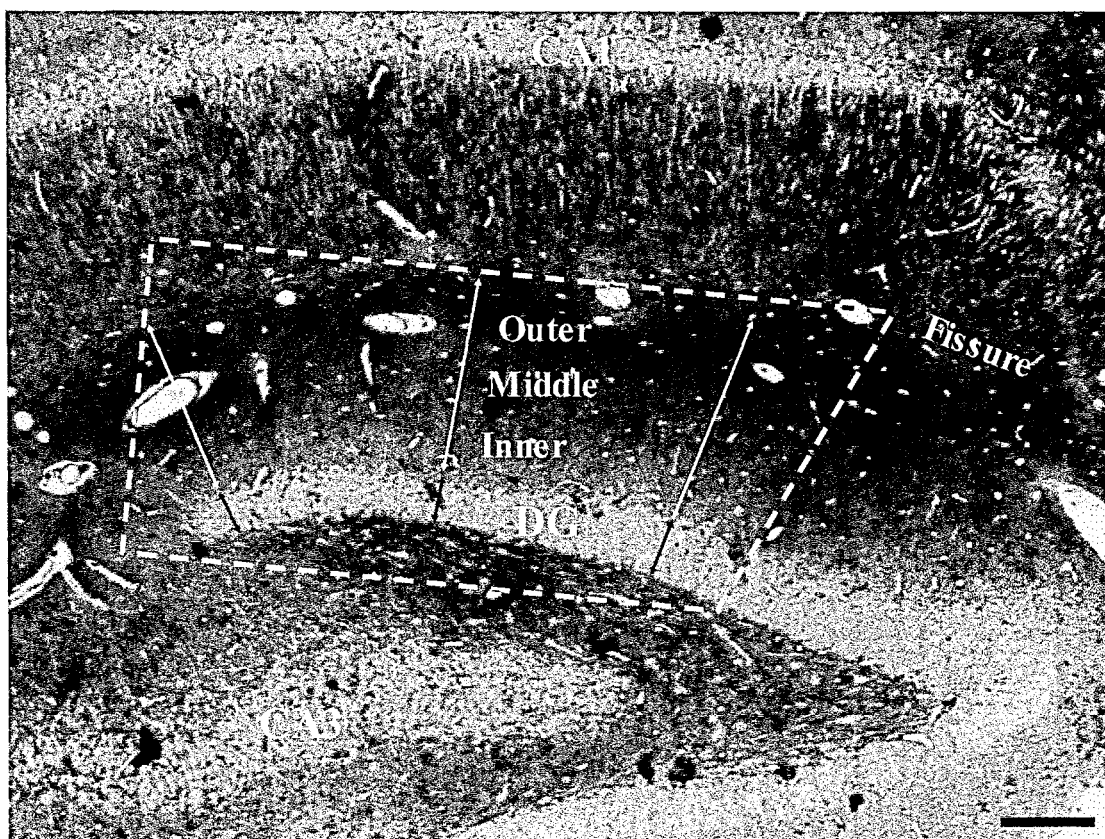
Figure 17 - Light microscope image of the upper limb of the dentate gyrus, indicating the locations of thickness measurements for the neuropil of the molecular layer (yellow arrows) and the cell layer (blue arrows). The red dashed lines indicate the typical size of trapezoid section examined by electron microscopy. The molecular layer is shown divided into outer, middle and inner thirds. DG - dentate gyrus cell layer, CA3 and CA1 - principal cell layers of the hippocampal *cornu ammonis* subregions, Fissure - hippocampal fissure. Scale bar = 100mm.

## Electron microscopy

Ultrathin sections of silver-grey interference colour, typically 70 nm thick, were cut from an area of the upper blade of the hippocampal dentate gyrus using an ultramicrotome in the same plane as the semithin sections. The blocks used were the same as for light microscopy. A 'mesa' technique was used to trim each block and leave a defined area raised above the surrounding tissue so that only this portion of each block would be present in the ultrathin sections. The area of each mesa is shown by the red dashed lines in Figure 17, and encompassed a region that stretched from the blade tip 600 µm toward the hilus region in one dimension, and included the dentate

gyrus cell layer, the molecular layer of the granule cell dendrites, and the hippocampal fissure in the other dimension.

Copper slot grids (3.05 mm, Agar scientific) were washed with chloroform and dried before being placed onto a pioloform support film floated on water. These were made by immersing a glass slide in a solution of 1.5% pioloform in chloroform and then allowing to air dry. A rectangular area was then scored on the slide, and this was then carefully floated off from the slide onto the surface of water in a dish. Once collected onto paper and dried, the films holding the slots were given a coating of vaporised carbon to strengthen the support film and make it more resistant to energy damage caused by the electron beam of the microscope.

Not less than four sequential serial ultrathin sections were mounted onto an individual copper slot, which were then stained with uranyl acetate and lead citrate to enhance the contrast of the cell membranes. Sections were visualised using a Jeol 1010 transmission electron microscope at 80kV acceleration voltage. The thickness of each ultrathin section was calculated by making use of the electron scattering method and the small fold technique **(De Groot, 1988)**. Standard electron microscope operating parameters, such as aperture size, were decided upon and adhered to for all thickness measurements, as these factors influence beam current density **(H. A. Davies, personal communication)**. Ultrathin sections with a range of different individual thickness were cut on an ultramicrotome, and small folds were deliberately introduced into them as they were collected. The microscope current densiometer was set to a predetermined value. The microscope stage was then moved to various unexposed locations on the support film and each ultrathin section, and beam current readings were taken from the current densiometer at each location. The relative electron thickness (RET%) was calculated for each section by using Equation 1;

**Equation 1 - RET% calculation.**

$$\text{RET\%} = \frac{\text{Average beam current reading for ultrathin section}}{\text{Average beam current reading for pioloform film alone}} \times 100$$

Once this was done, digital images of several folds per section were taken, calibrated and the thickness of each fold measured from the image. The RET% value for each section was then plotted against the section thickness measured by the small fold technique, in order to create a standard curve (see Appendix A, Figure 48). Small folds were not introduced into experimental sections because they might have interfered with image analysis. Instead, only beam current readings were taken from experimental sections, which were converted into RET% by using the equation of the standard curve, as shown in Equation 2;

**Equation 2 - Section thickness calculation.**

$$\text{Thickness} = (-4.563 \times \text{RET}\%) + 385.49$$

The dentate gyrus granule cells and the hippocampal fissure were used to determine the middle of the dentate gyrus cell molecular layer dendritic field. A random starting location was chosen at the edge of the granule cell layer near the tip of the upper blade of cells, and the field of view was moved to the middle of the dendritic molecular layer perpendicular to the upper blade. A series of digital images were taken (x12,000 column magnification) systematically at regular intervals along the middle of the molecular layer, parallel to the upper blade, using a Gatan CCD digital camera linked to the electron microscope and an Apple Macintosh G3 computer running Digital Micrograph 3.3.1 acquisition software. At least twelve images were taken, each one being given a nominal identifier. Sketches of the areas on the first section (section A) were used to find and image the corresponding areas on three more successive serial sections (B, C and D) (see Figure 20). Finally, a low magnification image (x120 column magnification) was taken of the sections to show where the set of images had been taken. These areas could be easily seen due to the large degree of thinning that occurs when tissue is exposed to high current densities during the microscope focusing procedure, as shown in Figure 18.
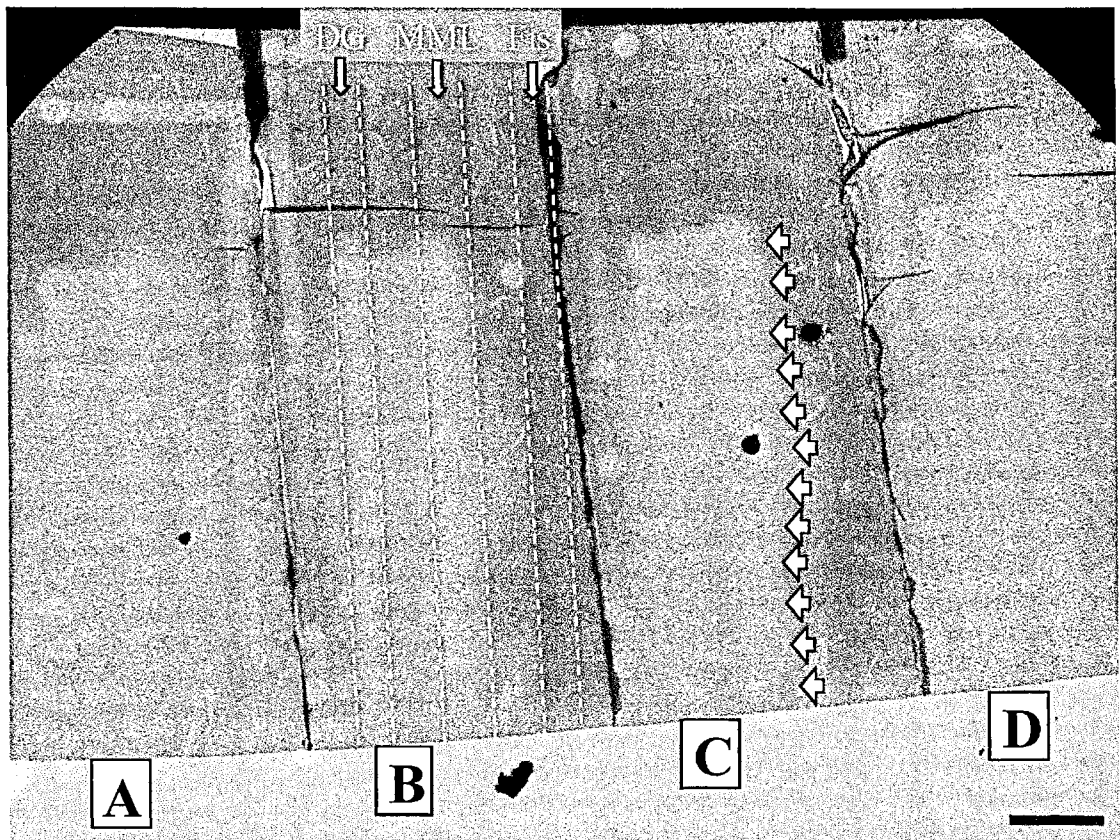
Figure 18 - Low magnification electron micrograph of four serial ultrathin sections, A, B, C and D, corresponding to the mesa area outlined in Figure 17. The location of electron thinning 'burn' marks in the cell layer and the corresponding area of dendrites in the middle of the molecular layer that were imaged can be seen as pale circles. One set of imaging locations are indicated by red arrows. DG - dentate gyrus granule cell layer, MML - middle molecular layer, Fis - hippocampal fissure. Scale bar = 100μm.

Images were stored on high capacity magneto-optical disks, and were analysed using NIH image software, as above. An image of a calibration slot grid, also taken at x12,000 magnification, was used to calculate a scale factor, which was applied to each set of images. A frame with a smaller area of known dimensions (8,000 x 5,000 nm) was placed onto the first image in each series (image A) using a pre-defined macro function of the NIH image software created 'in-house'. This frame placing was done in a random manner, but care was taken that the frame lay entirely inside the original image. This frame was then saved as a separate image (frame a, distinguished from the original image by the use of a lower case letter). The frame was then applied to the remaining original images (B, C and D), but in such a way that they encompassed the same portion of the original images as in frame a. Each of these frames were then also

saved as separate images, to give four sequential, aligned frames having the same known dimensions, to which stereological techniques could be applied.

## Stereological image analysis

Each data set of frames was analysed for synaptic contacts. Type 1 asymmetric synaptic contacts were identified by the presence of a dark area of Post Synaptic Density (PSD) and the presence of vesicles in the corresponding presynaptic structure, as shown in Figure 19. Type 1 synapses are generally excitatory in nature, and differ from type 2 symmetric synapses (Figure 19), which do not contain a PSD, have ovoid-shape vesicles and are considered to be inhibitory. Synapses were distinguished as being either axodendritic or axospinous. In addition, a synapse was regarded as being perforated if the PSD was separated into two or more distinct areas by intervening membrane that did not contain PSD in at least one section.

Excitatory synapses were distinguished into four types on the basis of their structure; non-perforated axospinous (NAS), non-perforated axodendritic (NAD), perforated axospinous (PAS) and perforated axodendritic (PAD). This was done because of the possibility that the differences in the structure of these synapses underlie functional differences. Axodendritic synapses have a potentially greater effect on their postsynaptic target compared to axospinous synapses. Similarly, perforated synapses are believed to have multiple transmission zones, meaning that they can exert a greater postsynaptic effect than non-perforated synapses. Furthermore, only the NAS type of synapse was frequently observed, the other types being considerably less common (see Figure 29).

The disector technique **(Sterio, 1984)** was applied to all twelve pairs of b and c frames in each data set with sections a and d being used to aid the identification of different synapse types, which were labelled with small different coloured dots according to their type (NAS, PAS, NAD or PAD). For each set of images, frame b was identified as the 'look-up' frame, and all synapses were labelled if they lay within the frame area, or touched the inclusion edges of the frame (upper and right-side edges). Synapses were excluded if their PSD touched the exclusion edges of the frame (lower and left-side edges), or the extension of the exclusion boundaries, and the original images were used
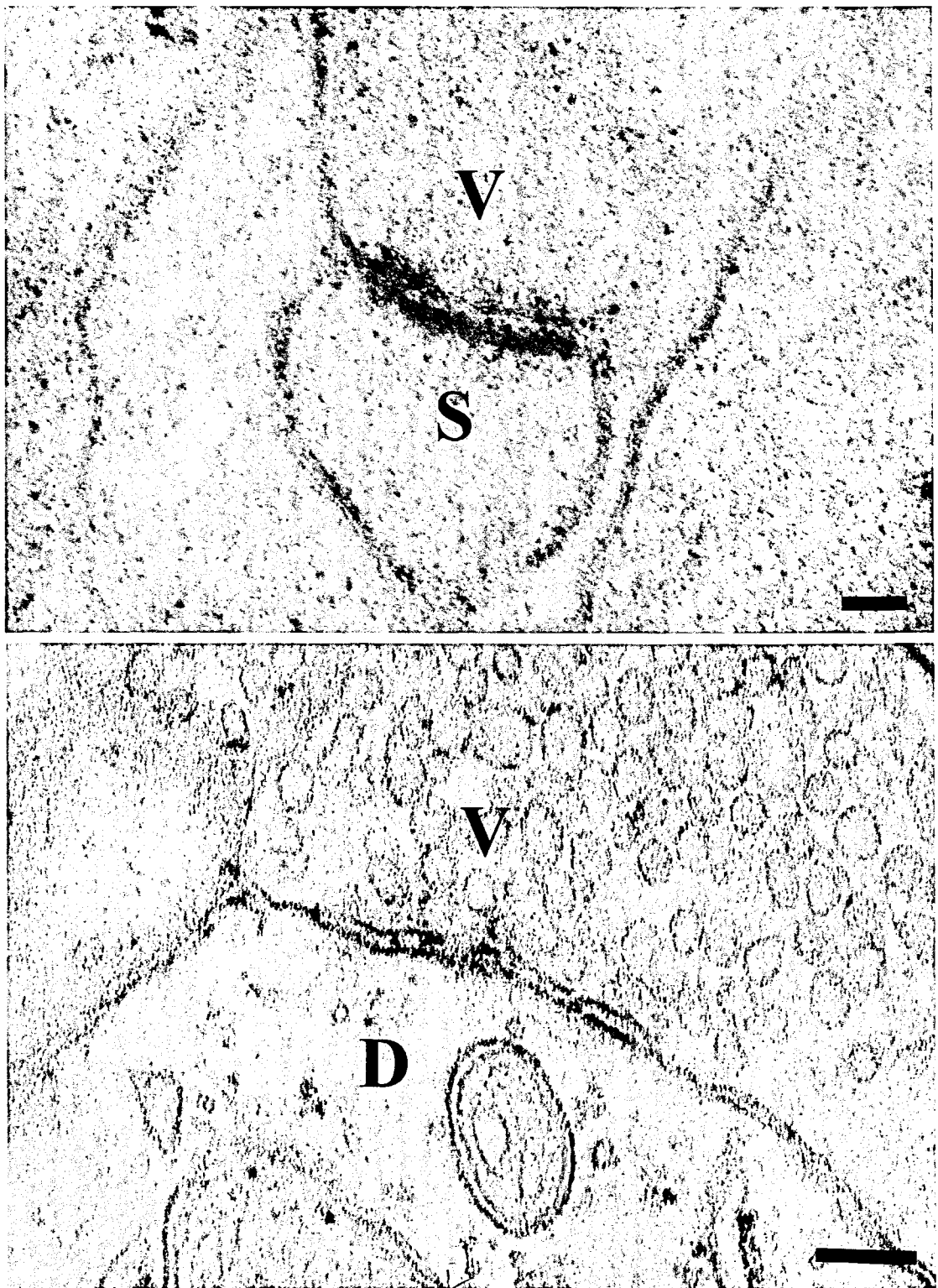
Figure 19 - The two types of synapse, asymmetric, type 1 and symmetric, type 2. Upper image; electron micrograph of an asymmetric, type 1 synapse. V - presynaptic axon terminal, containing spherical vesicles that appear as circles in this cross-sectional image. S - postsynaptic dendritic spine. Note the dark line of PSD between these two structures. Lower image; electron micrograph of a symmetric, type 2 synapse (from Peters, Palay and Webster, 1991). V - presynaptic axon terminal, containing aspherical vesicles that appear as ovals in this cross-sectional image. D - postsynaptic dendrite. Note the absence of PSD, but a similar thickening of both pre- and post-synaptic membranes. Scale bars = 100nm.

to aid the identification of such synapses. This same process was then applied to frame c, which was termed the 'reference' frame.

Large structures present in a brain area are more likely to be present in a slice through that brain area than small structures, which will bias any count of numbers in favour of the larger objects. However, each object has one start and one end, irrespective of size, and the disector technique uses this fact to count objects based on their start- or end-point. Hence, synapses are only counted (termed specific) if their PSD was present in the look-up section (frame b) but <u>not</u> present in the reference section (frame c). Synapses with PSD present in both frames are counted as non-specific, as it is not possible to tell where they begin or end. Synapses with PSD present only in the reference section were ignored. Non-specific synapses were also tabulated and their number counted, as this allows other stereological values to be calculated. The total number of specific synapses was then used to calculate the synaptic density (Synapse $N_V$), the number of synapses per $\mu m^3$ of dendritic field, using Equation 3;

**Equation 3 - Disector $N_V$ (density) calculation.**

$$N_V = \frac{\textbf{Sum of specific objects counted}}{\textbf{Total counting frame area } (\mu m^2) * \textbf{ Look-up section thickness } (\mu m)}$$

The total counting frame area is the area of one frame multiplied by the number of frames counted. The distance between the two counting planes is the same as the thickness of the 'look-up' section, and was calculated as described above. The process was also applied in the reverse direction, using frame c as the look-up section and frame b as the reference section, as different synapses may start/end in frame c. An example of the application of the disector technique is shown in Figure 20. However, the coloured dots represent specific, non-specific and excluded synapses, rather than different categories of morphology in this example for the sake of clarity between specific and non-specific.

The disector technique was similarly applied to the measured counting frames added to the digital images of serial semithin sections. The 'specific' cells were labelled with coloured dots in a similar manner to the electron micrographs of synapses described

83
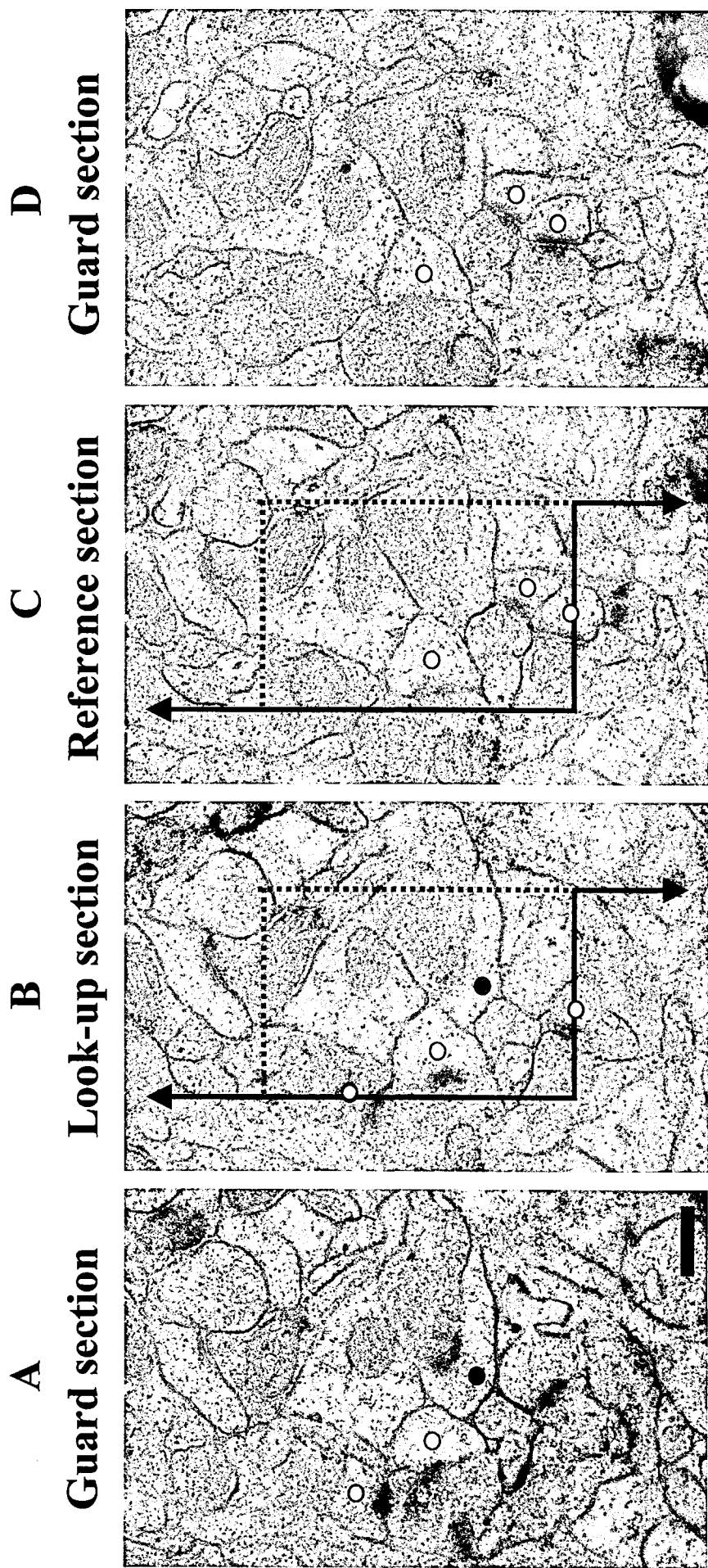
Figure 20 - Representative electron micrographs taken from four sequential sections, A, B, C and D. Synapses were counted (specific) if PSD was present opposite vesicles in the Look-up section (B) but not the Reference section (C), as indicated by the blue circles. Synapses present in both Look-up and Reference sections were not counted, nor were synapses present only in the Reference section, as indicated by the yellow circles. Also, synapses that intersected the solid black exclusion lines were not counted, as indicated by the red circles, whereas synapses intersecting the dashed black inclusion lines were counted. Two Guard sections, A & D were used to confirm the presence and identity of synapses. Scale bar = 500nm.

# A - Look-up section
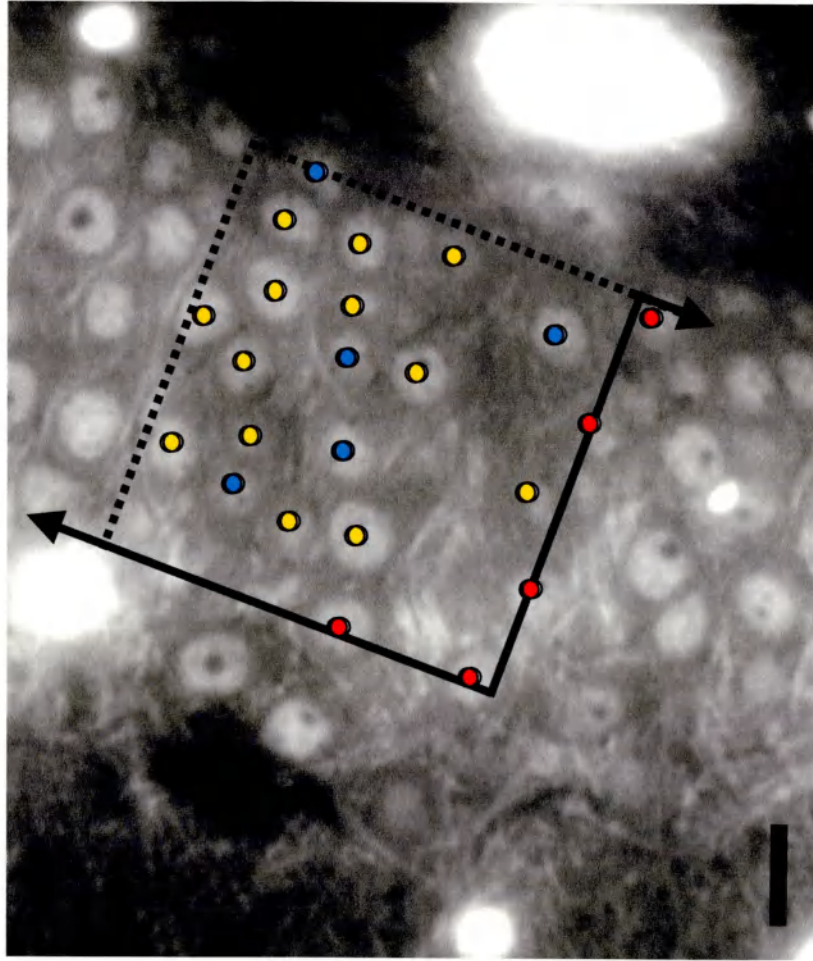
# B - Reference section
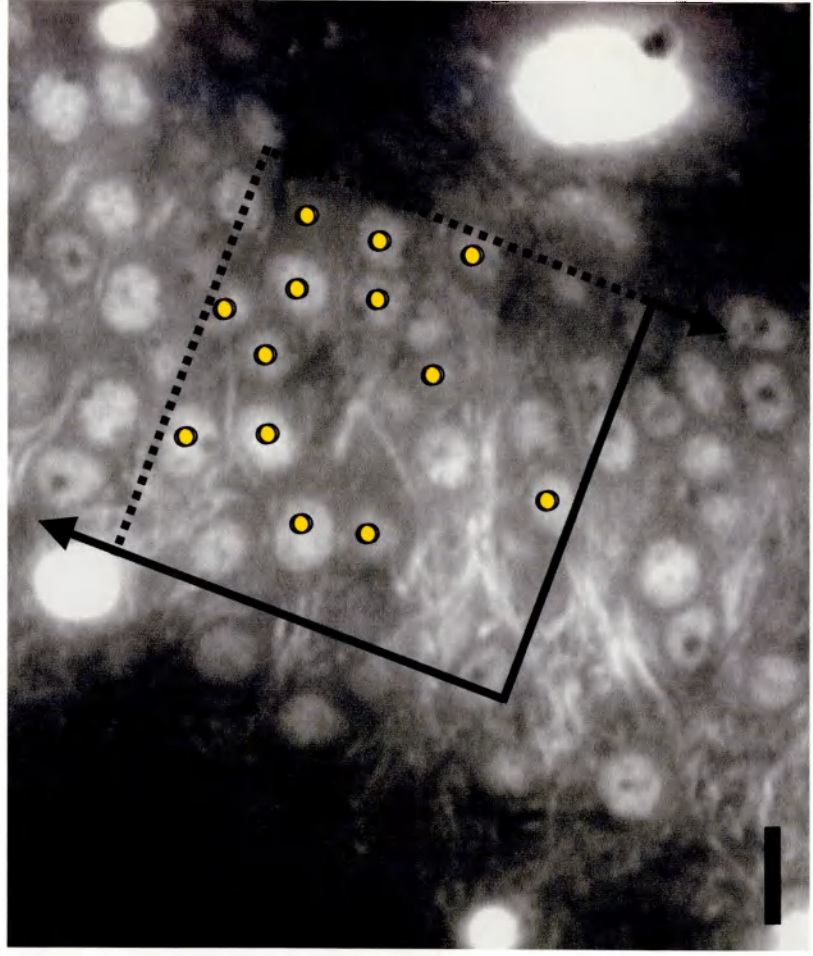


Figure 21 - Representative light micrographs of sequential semithin sections stained with Toluidine blue. Cells were counted (specific) if the cell body profile was present in the Look-up section but not the Reference section, as indicated by blue circles. Profiles intersecting the dashed black inclusion lines were also counted, but those intersecting the solid black exclusion lines were not, as indicated by red circles. Profiles present in both sections (yellow circles) were not counted. Scale bars = 10μm.

above, and the total numbers were used to calculate the cell density (cell $N_V$) using Equation 3. An example of how the disector technique was applied to light microscopic images is shown in Figure 21. The colours represent specific, non-specific and excluded cells. Each section was assumed to be exactly 2 μm thick.

Due to the way in which the hippocampus was dissected, it was not possible to calculate the hippocampal volume, and in consequence either total synapse numbers or total cell numbers. However, instead of using total synapse number and total cell number, the synapse to neuron ratio can be calculated from estimates of synapse density and cell density, as shown in Equation 4;

**Equation 4 - Synapse to neuron ratio calculation.**

$$\text{NAS synapse to neuron ratio} = \text{NAS synapse } N_V / \text{cell } N_V$$

Mean height, an arbitrary measure of synapse size, was calculated for NAS synapses by using Equation 5;

**Equation 5 - Mean height calculation.**

$$\text{Mean height of NAS synapses} = \frac{\text{Sum of all synaptic profiles} \times \text{section thickness}}{\text{Sum of specific synaptic profiles}}$$

For a structure to be sampled in a completely unbiased manner, all possible planes of sectioning must be given an equal chance of being used. This is termed isotropic uniform random (IUR) sampling **(Howard and Reed, 1998)**. Such sampling is used to prevent bias that may result from the three-dimensional shape or regular arrangement of objects within a sample volume. As it is often not possible to determine if structures within a volume have a common orientation, and structures are seldom spherical (which would ensure IUR sampling from any direction), the orientation of sampling must be randomised instead to avoid these biases. In this study, each sample was cut only in the orientation perpendicular to the septo-temporal axis of the hippocampus, as this facilitated the identification of different structures within the hippocampal

formation. Unfortunately, this meant that the samples were not sampled in an IUR manner, and this may have introduced a bias into the estimate of NAS synapse size.

Apposition zone size is a good indicator of synaptic size and hence functional effect on a postsynaptic cell, and can be measured as the size of the PSD present at a synaptic contact. $S_N$, the average surface area of PSD per synapse, can be calculated by way of the intermediate quantities $S_V$ (surface area per unit volume) and $L_A$ (length of line per unit area). The total length of PSD present in all the synaptic profiles was measured for one section in each data set (i.e. all twelve frames from section b) by an in-house macro for NIH image. The value of $L_A$ was then calculated by using Equation 6;

**Equation 6 - $L_A$ calculation.**

$$L_A = \text{Total length of line (μm) / Total frame area containing lines (μm}^2)$$

Equation 7 relates $L_A$ to $P_L$ and Equation 8 relates $P_L$ to $S_V$ **(Underwood, 1970)**. $P_L$ is another stereological quantity, and is defined as the number of points on a line of unit length. This is particularly related to the intersections between two lines, or the intersection of a line with a surface, but can be used in terms of volumes, and provides a useful intermediate for mathematical manipulations that allow the calculation of $S_V$.

**Equation 7 - Relationship between $L_A$ and $P_L$**

$$L_A = (\pi / 2) \times P_L$$

and

**Equation 8 - Relationship between $S_V$ and $P_L$**

$$S_V = 2 \times P_L$$

Equation 7, when rearranged to make $P_L$ the subject, will substitute into Equation 8 to give Equation 9. This was used to calculate the value of $S_V$, which is in itself a useful parameter;

**Equation 9 – Relationship between $S_V$ and $L_A$**

$$S_V = (4 / \pi) \times L_A$$

In a similar way to Equation 4, the values of NAS synapse $S_V$ and cell $N_V$ can be combined to produce the ratio of total NAS synapse area per neuron. This ratio controls for possible differences between individuals and groups, and is calculated in Equation 10;

**Equation 10 – $S_V$ to neuron ratio calculation.**

**NAS synapse PSD area to neuron ratio = NAS synapse $S_V$ / cell $N_V$**

Equation 11 was used to calculate $S_N$, the mean area of PSD per synapse, from the unbiased estimates of $N_V$ and $S_V$ for the same set of NAS synapses;

**Equation 11 – $S_N$ calculation.**

$$S_N = S_V / N_V$$

which has units of $\mu m^2$ per (NAS) synapse.

## Immunogold labelling

In order to identify the different molecular components present at the synapses of the dentate molecular layer, antibodies were used to probe for individual molecules and were identified by conjugated spherical gold labels that are distinguishable in the electron microscope. Post-embedding immunogold labelling was performed on freeze substituted tissue because this technique greatly preserves the antigenicity of the samples and does not suffer from problems concerning tissue penetration by the antibodies used. As described in the above, some animals were perfused with Immuno-electron microscopy fixative, and tissue samples were cryo-protected and impact frozen. These samples were then freeze substituted using a Leica AFS, which involved

dehydrating and embedding the tissue in Lowicryl resin cooled with liquid nitrogen, as described above (see Appendix A for low temperature embedding protocols).

Ultrathin sections approximately 90 nm thick were cut from the blocks using an ultramicrotome and collected onto nickel slots. Sections were cut parallel to the septo-temporal axis of the hippocampus, perpendicular to the previous plane of sectioning used for stereological image analysis. This was done so that sampling could be performed throughout the entire thickness of the lowicryl block, because the impact freezing procedure may damage the ultrastructure of the block close to the surface, whereas the antigenicity may not be so well preserved towards the centre of the block. A similar vertical orientation was used so as to include the main blades of cells in the dentate gyrus and CA regions (see Figure 16). Each block was trimmed in this plane until a point towards the tip of the upper blade of the dentate gyrus.

This meant that sections contained the upper blade of the dentate granule cell layer, the dentate molecular layer, the hippocampal fissure, the *stratum radiatum*, the CA1 cell layer, the *stratum oriens* and the *stratum lacunosum-moleculare*. In addition, most sections also contained the lower blade of the dentate granule cell layer, and the cells and dendritic layers of the CA3 region when this extended between the blades of the dentate gyrus. Semithin sections were used to confirm the presence of these structures in the sections, as shown in Figure 22, at which point ultrathin sections were cut. Ultrathin sections were used to check the ultrastructure of each tissue block, and for experiments to optimise the labelling reaction.

Lowicryl resin used for low temperature embedding absorbs water vapour from the atmosphere, an effect that decreases the efficiency of immunogold labelling. Sections were therefore reacted with antibodies as soon after sectioning as possible. Because sectioning requires time to complete, and to make numbers manageable, the set of analysed samples was restricted to the right hemisphere of individual animals. The sample size was also limited by unsuitable preservation in a few samples, and the lack of any samples from the swim only group of animals. All experiments were performed using a method published previously **(Schuster *et al.*, 1998)**. Each slot was placed section-side down onto a 20µl droplet of diluted antibody or wash solution, as required. As each slot was transferred from one solution to the next using a pair of tweezers, excess liquid was carefully removed with blotting paper.
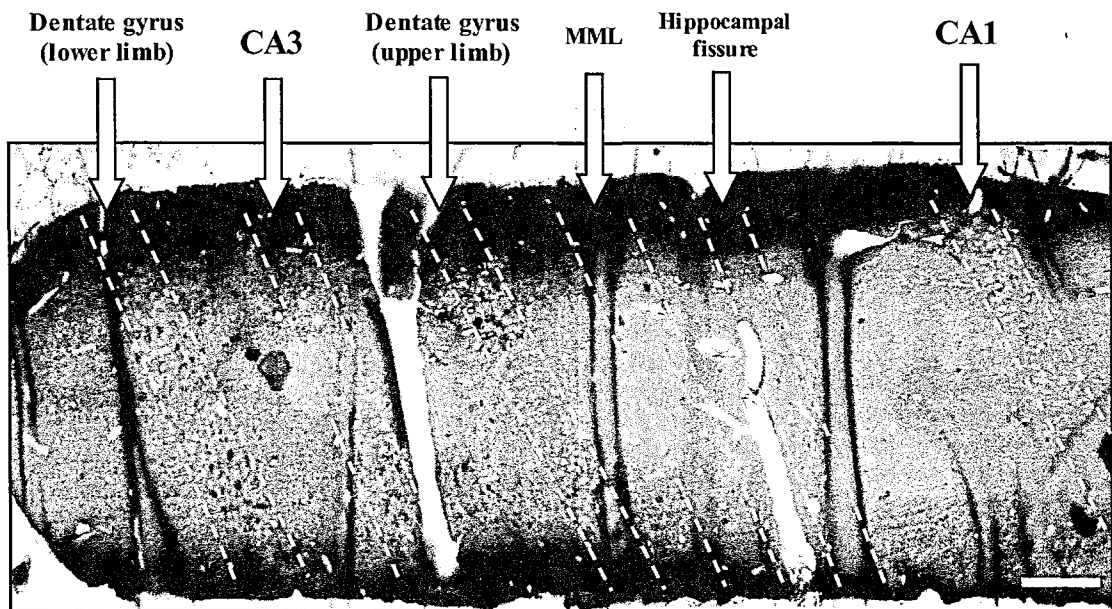
Figure 22 - Light microscope montage image of a Lowicryl-embedded section, showing the various layers of the hippocampal formation. MML - middle molecular layer of the dentate gyrus. Scale bar = 100μm

Preliminary experiments were used to attain optimal conditions for temperature and buffer content, and to titrate the optimal antibody concentration to be used in the final experiment. This was done to minimise the need for non-specific blocking agents, which would maximise specific signal but minimise residual non-specific binding. These experiments were also used to test for the specificity of the relevant secondary gold conjugates for the primary antibody and identify any non-specific secondary binding. Due to the nature of primary and secondary antibodies available it was not possible to use certain antibodies simultaneously, and so labelling of different receptor types was performed on separate sections on separate slots. All preliminary experiments were performed on sections from a single naïve group animal.

## Antibody selection for AMPA and NMDA receptor subunits

Primary antibodies were chosen that recognised several different target sequences present in different principal ionotropic neurotransmitter receptor subtypes. Three primary antibodies were used to identify AMPA receptors. These were raised in rabbit and were directed towards sequences in the GluR 1 subunit, the GluR 2 and 3 subunits and the GluR 4 subunit of rat AMPA type receptors respectively. All three antibodies

were applied as a cocktail, and were labelled by 15 nm gold spheres conjugated to an antibody that recognised the anti-rabbit IgG (Immunoglobulin G) sequence raised in goat.

An antibody that recognised four of the major splice variants of the rat NR1 subunit was chosen as a marker for NMDA receptors. This antibody was raised in rabbit, and thus required a secondary antibody that recognised rabbit IgG, which was conjugated to 15 nm gold spheres. Once all antibody reactions had taken place, sections were reacted with a solution of glutaraldehyde to prevent gold particles being washed off during subsequent contrast staining (see Appendix B for immunolabelling protocols).

Immunogold labelled sections were imaged at x 30,000 magnification using a Gatan CCD camera linked to a Jeol 1010 electron microscope, in a similar way to that described above for the acquisition of images for stereological analysis. Using the hippocampal cell layers and the hippocampal fissure as anatomical landmarks for reference, micrographs were imaged from 20 areas, in a similar manner to the sampling for stereological analysis. Once the middle molecular layer of the dentate gyrus was located, the first image location was randomly selected in this area, and the subsequent images were acquired at a similar distance from the dentate granule cell layer in a systematic manner, as shown in Figure 23. This was performed on single sections that were immunolabelled for either AMPA or NMDA receptors.

The number of NAS synapses present in each of the imaged areas was calculated, as was the number of labelled NAS synapses. Synaptic profiles associated with one or more gold particle were expressed as a percentage of total synapses labelled, both for the AMPA and NMDA labelling experiments. The number of gold particles associated with synaptic PSD was also calculated, and expressed as the number of gold particles per synapse. The total length of PSD present in all examined sections was measured and used to calculate the number of gold particles present per $\mu$m of total NAS synapse PSD. The PSD length of all labelled synapses was also measured and used to calculate the number of gold particles per $\mu$m of PSD in the labelled synapses. The length of PSD for all labelled synapses was also used to calculate a stereologically unbiased estimate of the total PSD area of labelled synapses, $S_V$, using Equation 9.
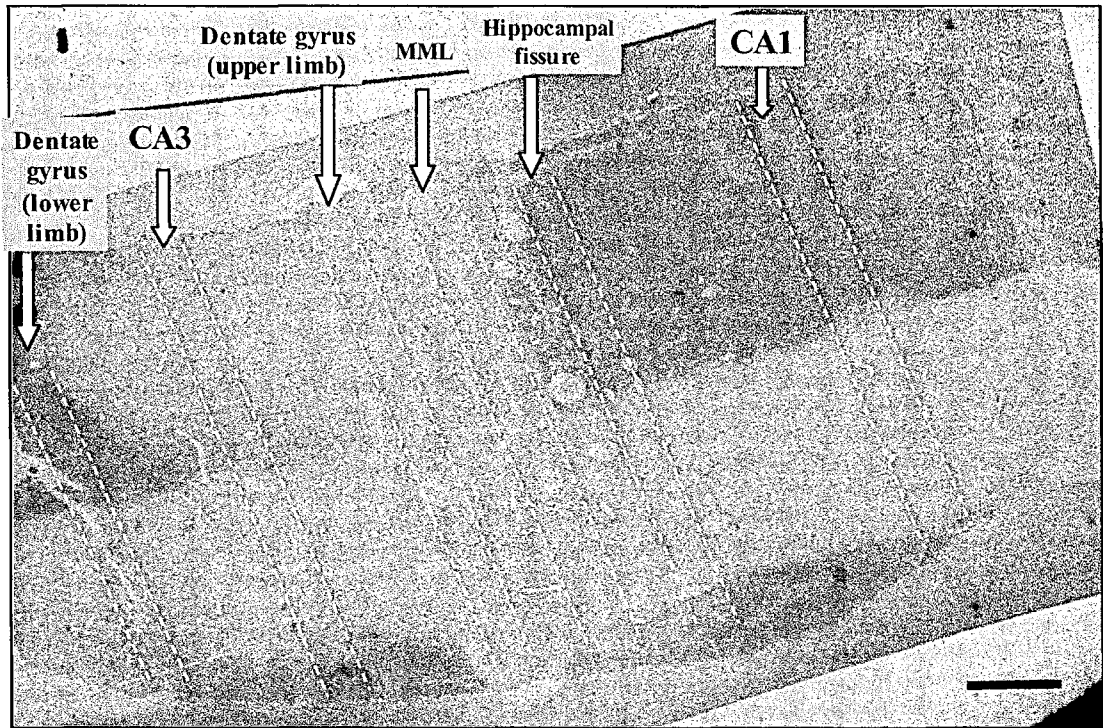
Figure 23 - Low magnification electron micrograph of a Lowicryl-embedded section, showing the areas of section that were imaged for immunolabelling analysis (pale grey, overlapping circles). MML - middle molecular layer of the dentate gyrus. Scale bar = 100μm.

$S_V$ calculations were combined with calculations of $S_N$ derived from morphological data to calculate labelled $N_V$, the number of labelled synapses per $\mu m^3$ of tissue (density). This was achieved by rearrangement of Equation 11 to give Equation 12;

**Equation 12 - Calculation of the density of labelled synapses.**

$$N_V = S_V / S_N$$

Where values of both AMPA receptor labelling and NMDA receptor labelling were available from the same animal, the values were used to calculate a ratio of AMPA to NMDA labelling for each parameter mentioned above. The ratio values for individual animals were then used to calculate averages for each group.

## Statistical analysis

Each block was given a numerical code identifier, and the order of animals and groups was randomised with respect to this code. This was done so that when counts were made from each data set, be it for stereological or immunological analysis, it was not apparent to which experimental group or hemisphere the dataset belonged until decoding after analysis. Data were analysed with SPSS 10.0 (www.spss.com) and Statistica 6.0 (www.statsoft.com) statistical software. Repeated measures ANOVA was used to analyse escape latency data because the performance of each animal was repeatedly measured over several trials. Quadrant test data were analysed using the Chi-squared test to compare expected (random chance 25%) time in each quadrant with observed values as animals searched for the platform.

To assess the effects of the different training protocols on each group, the effect of brain hemisphere and the effect of experiments performed at different times, a General Linear Model incorporating analysis of variance (ANOVA) with a nested design of hemisphere within group was used. This is necessary because the two hemispheres within each animal must be considered separately when comparing groups, so that differences can be investigated. A standard ANOVA was used to compare data from immunolabelling experiments, as only one hemisphere was investigated. Tukey's HSD (honest significant difference) post-hoc test was used to evaluate the contribution of the different group factors to the overall interactions, and the LSD (least significant difference) post-hoc test was also used. Differences were considered to be significant at $p < 0.05$.

# Results

## Behavioural analysis of training effects

Three different trained groups of animals were used to establish a time-course of memory for location of the platform, and two additional groups were included to control for concomitants of the training process. These were i) completely naïve controls which experienced only the home cage environment, so that the effects of a change in environment could be observed, and ii) a 'swim-only' control that had visual experience of the water maze environment, as well as physical exertion from swimming, but was not trained to find the hidden platform. The duration of each swim-only trial was matched to the mean escape latency (group average of time taken to find the platform) of the 9 hour group, ensuring that the swim-only controls and the 9 hour group swam for a similar duration. A quadrant analysis test was not performed because the swim-paths of these animals were random in nature.

A record of the animals trained and perfused in each group is shown in Table 2. Also indicated are the number of animals not perfused and the samples excluded from morphological analysis. For the 3 hour group, analysis was not conducted on one of the perfused animals, and a second animal was discounted because of poor tissue ultrastructure. For the 9 hour group, analysis was not conducted on two of the perfused animals. However, the individual behavioural data was similar for animals that were perfused and those that were not perfused.

Table 2 - Record of animals trained and perfused.

|  | Naïve | Swim-only | 3 hour | 9 hour | 24 hour |
|---|---|---|---|---|---|
| Total in group | 8 | 6 | 9 | 10 | 8 |
| Perfused | 8 | 6 | 8 | 10 | 6 |
| Excluded | 0 | 0 | 2 | 2 | 0 |
| Analysed | 8 | 6 | 6 | 8 | 6 |
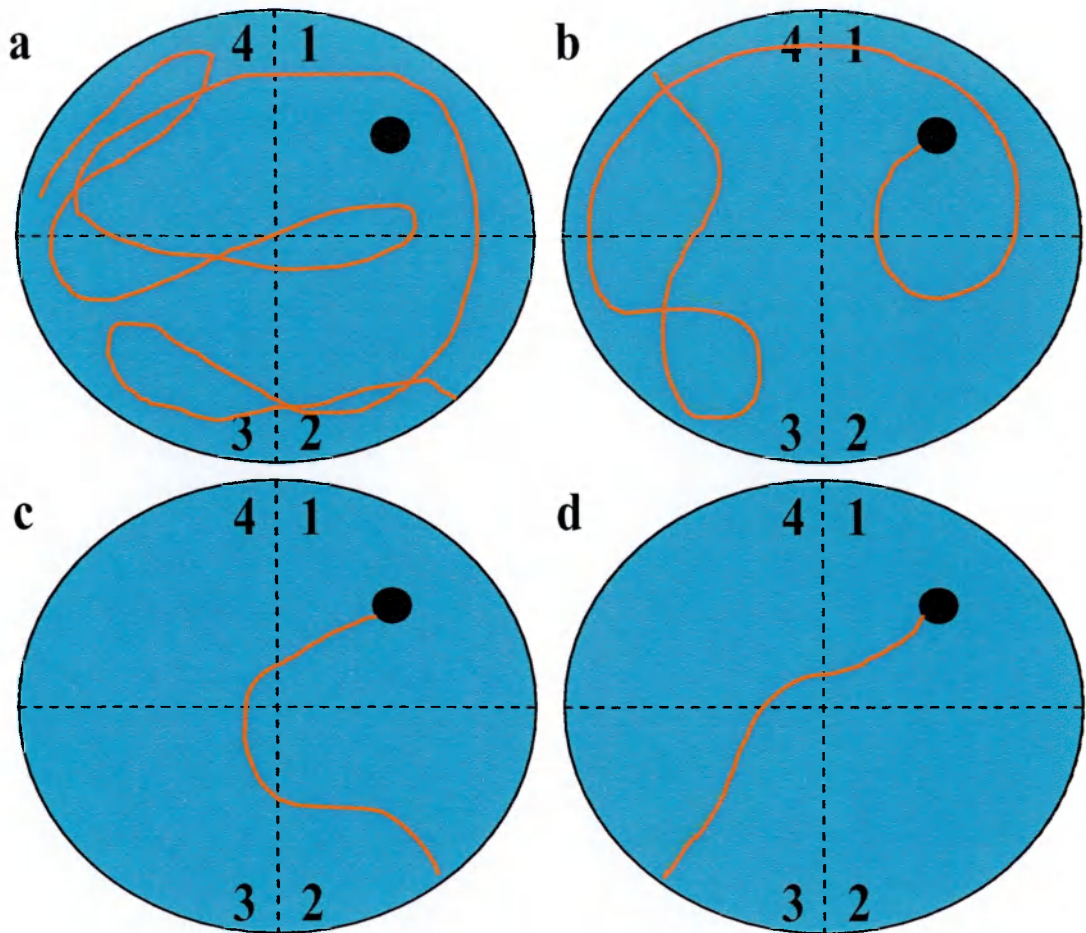
Figure 24 - Example swim paths typically taken by animals during training. Each schematic diagram shows the pool of water from above, and typical paths taken by the rats are indicated by red lines (see Figure 14). a) typical path for a novice rat upon first training session – swimming was random in nature and thigmotaxis (swimming next to the walls of the pool) also common. b) typical path for rats in the 3 hour group upon 4th (final) training trial – however, not all animals found the platform on the 4th trial, an aspect that was also seen in the other groups at this stage of training. c) typical path for animals in the 9 hour group upon 12th (final) training trial, indicating that animals had learnt the location of the platform. d) typical path for animals in the 24 hour group upon 20th (final) training trial. During training, the platform remained in quadrant 1 and visual cue were unchanged, whereas the start location for each trial was varied amongst all four quadrants, indicated by numbers.

## Escape Latency

The escape latencies to find the hidden platform are shown in Figure 25. The average latency to find the platform for the 3 hour group reduced over the four trials of their one and only training session from 57.2 seconds to 30.3 seconds, suggesting that they were developing some knowledge of where the platform was. The 9 hour group received three training sessions spread out over several hours, and showed a progressively shorter average latency as the trials are completed. The latency reduced from 60 seconds on trial number one to 7.8 seconds for trial number twelve, and this data strongly suggests that the animals were utilising memory to find the location of the platform. For the 24 hour group, five training sessions were spread out over a large period of time, including the normal 12 hour sleep period of the animals, and the average latency dropped from 49.8 seconds on trial one to 5.3 seconds on trial twenty.

Statistical analysis by ANOVA with repeated measures indicated that average latency between trials was not the same for the 3 hour group (F $_{[3,8]}$ = 4.612; p = 0.011), and post-hoc testing indicated that this was due to the difference between the first and last swimming trial (p = 0.012). For the 9 hour group, a significant reduction in escape latency was also seen (F $_{[11,9]}$ = 12.092; p < 0.001), and post-hoc analysis indicated trials four to twelve were all significantly reduced when compared with the first trial (p = 0.022 or less in all cases). A significant reduction in escape latency was also seen in the 24 hour group (F $_{[19,7]}$ = 6.407; p < 0.001). Tukey's post-hoc test indicated that trials twelve through twenty were significantly different to the first trial, where p = 0.003 or less for all cases.

It can also be observed that the latency for the first trial of the first training session is much higher than the first trial of the last training session, both in the 9 hour and the 24 hour groups, and the times are either statistically significant (9 hour group, p = 0.013), or close to being so (24 hour group, p = 0.080). This indicates that the animals were forming longer term memories, because the gap between each training session would not allow them to use recent, working memory of the previous trial.

Use of a visible platform control may have been useful in making a comparison between escape latencies, as it would have provided useful information concerning the swimming behaviour of the animals when directed towards a visible goal. As well as a comparison for swimming speed and direction taken, motivational aspects of the
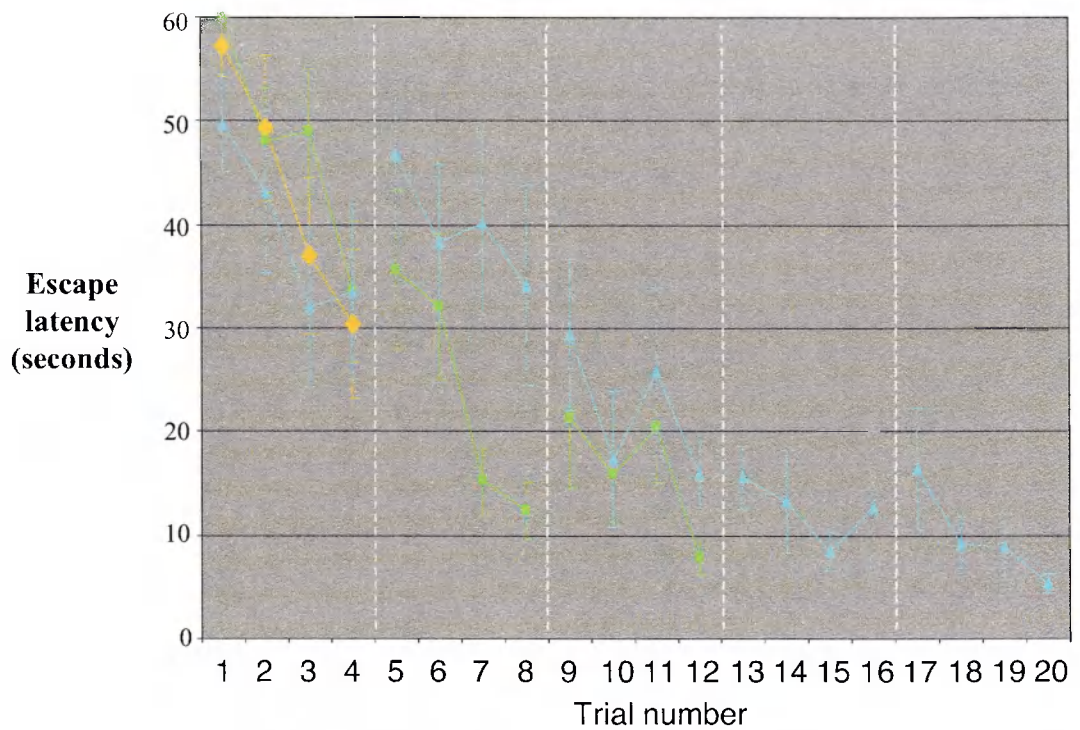
Figure 25 - Escape latency averages for the trained groups. The y axis shows escape latency, the time taken to reach the platform, in seconds. Training trials are shown as groups of four, each of which constitutes a training session. Sessions are seperated by white dashed vertical lines. The same colour-code is used as shown in Figure 15. ◆ - 3 hour group; ▦ - 9 hour group; ▲ - 24 hour group. Error bars indicate standard errors of the mean.
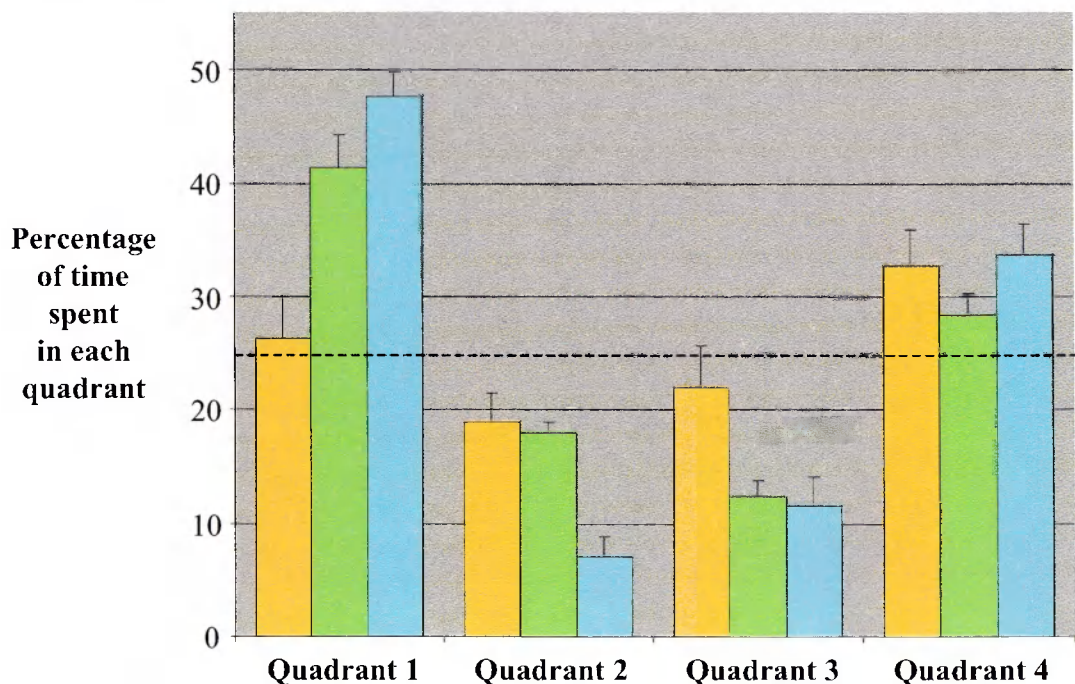


Figure 26 - Quadrant analysis test data for the trained groups. The y axis shows the percentage of time spent in the quadrant. The dashed line indicates the chance level of being in one of four quadrants (25%). The same colour-code is used as shown in Figure 15. ▦ - 3 hour group; ▦ - 9 hour group; ▦ - 24 hour group. Error bars indicate standard errors of the mean.

97

animals could also be qualitatively compared, for example would the animals always swim directly to the visible platform, or would they explore the pool first? Because a visible target would give the animal an objective in order to escape from the water, such a control may also have provided useful information concerning the degree of stress suffered by animals placed in the pool environment.

## Quadrant analysis

In addition to the measurement of escape latency, each animal was given a quadrant analysis (probe trial) test three hours after the end of the final training trial. This test was given immediately before anaesthetisation and perfusion, as described in the methods. The quadrant test was conducted by dividing the pool into 4 arbitrary but fixed quadrants, the hidden platform being in the centre of quadrant 1 (see Figure 14). The platform was then removed from the pool. Each animal was then placed into the pool at the same point in quadrant 4 and allowed to swim in the pool for 60 seconds. As the animal searched for the platform, the duration spent swimming in each quadrant was recorded. The average time spent in each quadrant for the trained groups is shown in Figure 26, expressed as a percentage of the test time (60 seconds).

A random searching behaviour in the pool would predict that animals would spend 25% of the total time, on average, swimming in each quadrant. This kind of random searching would be expected from animals that had not formed a memory for the location of the platform, whereas those that had learnt the location of the platform would be predicted to spend longer searching the correct quadrant (number 1) where they had learnt to find the platform. Compared to chance, for a Chi-squared test with three degrees of freedom, a value of 7.81 would indicate a significance of $p = 0.05$, and a Chi-squared value of 11.35 would indicate significance at the $p = 0.01$ level. Animals in the 3 hour group spent 26.3% of the test time quadrant 1, which was similar to the time spent in quadrants 2, 3 and 4 (18.9%, 22.0% and 32.8% respectively). Compared to chance (25%), there was no statistical difference in the time spent in any of the four quadrants, with Chi-squared values of 0.07, 1.47, 0.36 and 2.41 for quadrants 1-4 respectively.

The results of the 9 hour group indicate that the percentage of time spent in quadrant 1 was greater than time spent in quadrants 2, 3 or 4 (41.4% compared to 17.9%, 12.3% or

28.3% respectively). Statistically, this is significantly greater than chance (Chi-squared value = 10.78, $p < 0.05$), whereas the time spent in quadrants 2, 3 and 4 were not significantly greater than chance (Chi-squared values of 2.01, 6.42 and 0.44 respectively, $p > 0.05$ in all cases). Similarly, the results of the quadrant test for the 24 hour group indicate that quadrant 1 was searched for longer than quadrants 2, 3 or 4 (47.7% compared to 7.0%, 11.6% and 33.7% respectively). Statistically, this is significantly greater than chance (Chi-squared value = 20.57, $p < 0.01$), showing an even greater preference for the correct quadrant that the 9 hour group. The time spent in quadrants 3 and 4 were not significantly greater than chance (Chi-squared values of 7.22 and 3.05 respectively, $p > 0.05$ in both cases). Interestingly, the average time spent by the 24 hour group in quadrant 2 was significantly less than chance (Chi-squared value = 12.92, $p < 0.01$). This indicated that the animals in this group were neglecting to search this quadrant, adding further support to the idea that they were preferentially searching in quadrant 1 for the platform.

## Morphological analysis of the dentate gyrus

The Cavalieri method can be used to estimate the volume of the hippocampus from serial vibratome sections **(Howard and Reed, 1998)**. However, the necessity of sample transportation from Haifa meant that this method was not adopted because tissue was required for ultrastructural preservation and low temperature embedding. Biological variation between individual animals results in possible differences in the volume of brain structures, and such differences potentially influence measurements that are related to the sampling volume, such as density measurements. In order to evaluate this variation, neuropil and cell blade thickness measurements were made from low magnification (x5 objective) images of semithin, toluidine blue-stained sections.

Overall, nested ANOVA used indicated that neuropil thickness did not differ significantly between groups ($F_{[4,44]} = 1,757$ ; $p = 0.150$) or hemispheres ($F_{[5,44]} = 1.096$; $p = 0.373$). However, the neuropil was significantly thicker in the second experiment (305.8 μm) than the first (292.0 μm; $F_{[3,44]} = 7.597$; $p < 0.001$). This is shown in Figure 27. Examination of the dentate granule cell layer thickness also indicated that the blade width was significantly less in the second experiment (56.5 μm) compared to the first (63.8 μm; $F_{[3,44]} = 5.459$; $p = 0.002$), and this is shown in Figure
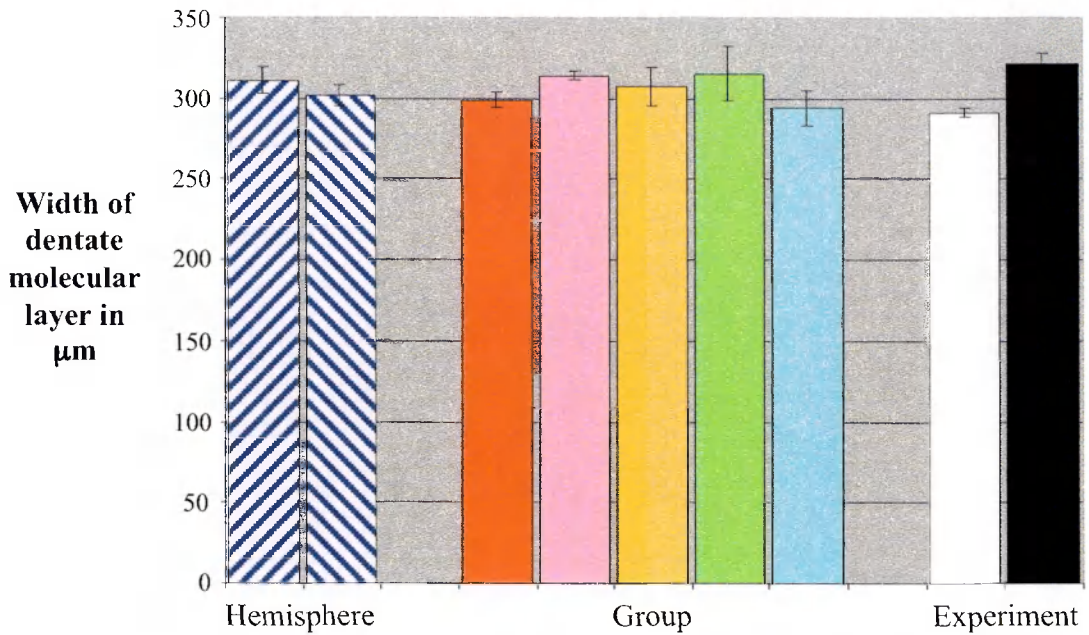
Figure 27 - Neuropil thickness displayed in terms of the statistical analysis, showing averages of all the data from a particular category. Data averaged according to left and right hemispheres is shown as left- and right-sloping hatched bars respectively ⊘ , ◨). Data averaged according to all samples in each group are shown as colour-coded bars; ■ naive group, ▨ - swim only group, ▨ - 3 hour group, ▨ - 9 hour group, ▨ 24 hour group. The white bar ( ☐ ) represents the average of all data in the first experiment, whilst the black bar ( ■ ) represents the average of all data from the second experiment. Error bars indicate standard error of the mean.
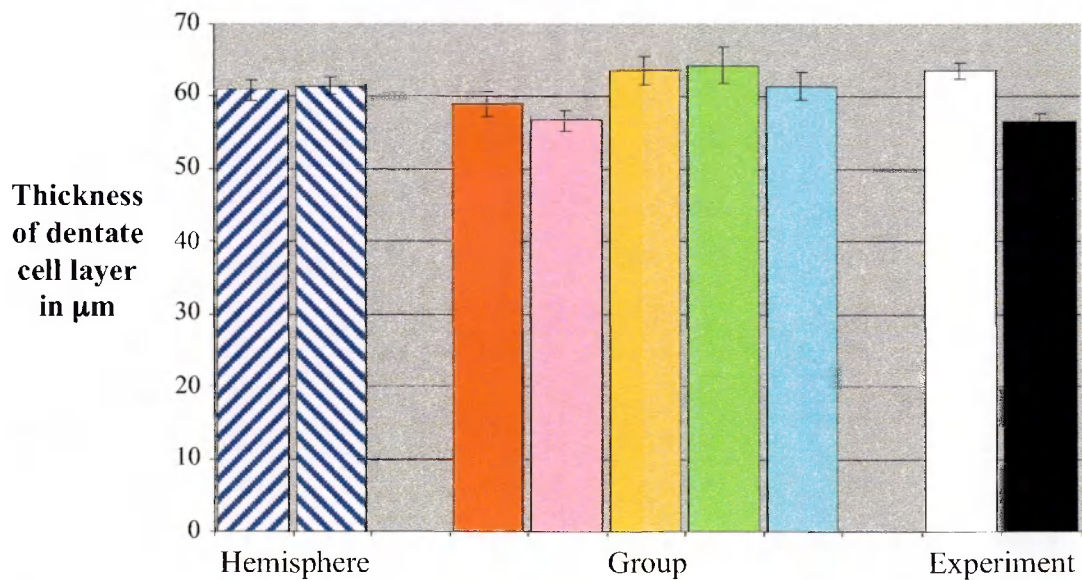


Figure 28 - Cell blade thickness displayed in terms of the statistical analysis, showing averages of all the data from a particular category. Data averaged according to left and right hemispheres is shown as left- and right-sloping hatched bars respectively ⊘ , ◨ ). Data averaged according to all samples in each group are shown as colour-coded bars; ▨ naive group, ▨ - swim only group, ▨ - 3 hour group, ▨ - 9 hour group, ☐ - 24 hour group. The white bar ( ☐ ) represents the average of all data in the first experiment, whilst the black bar ( ■ ) represents the average of all data from the second experiment. Error bars indicate standard error of the mean.

100

28. No significant differences were observed between groups ($F_{[4,44]}$ = 1.222; p = 0.312) or between hemispheres ($F_{[5,44]}$ = 1.270; p = 0.289).

Although no statistical differences were observed between experimental groups or between brain hemisphere, the significant difference between experiment indicated general morphological differences. In order to control for these indicated differences, calibration factors were calculated to normalise the ultrastructural measurements of one experiment with respect to the other. A cell blade width calibration factor was calculated by dividing the average cell blade thickness of naïve animals in the second experiment by the average cell blade thickness of naïve animals in the first experiment. This value was then cubed because the tissue samples were three-dimensional, which resulted in a cell blade correction factor of 0.9076. Cell density measurements (cell $N_V$) of animals in the second experiment were then multiplied by this correction factor.

Similarly, the average thickness of the neuropil in naïve group samples from the second experiment was divided by the average thickness in the first experiment, and cubed, resulting in a neuropil correction factor of 1.1487. Subsequent analysis of middle molecular layer synapses (e.g. NAS synapse $N_V$) was normalised by multiplying this correction factor by the results obtained from samples in the second experiment. The use of these correction factors was considered justified because of the morphological differences between the experimental phases. Incidentally, the correction factors had little effect on the overall results of the data, as analysis of the data before and after the application of the correction factors produced very similar statistical results in all cases.

## Dentate gyrus granule cell density

Estimates for cell density (cell $N_V$) were made from serial semithin section digital images using the disector method. The hippocampi in left and right hemispheres were analysed separately for each animal. Because cell blade thickness was significantly different between experimental years, cell density for the second experiment was normalised with respect to the first by application of the cell blade thickness correction factor. Statistical analysis of the raw granule cell density data indicated a significant difference that was attributable to a difference between experiments ($F_{[4,44]}$ = 3.459; p = 0.013), but not between groups ($F_{[5,44]}$ = 1.018; p = 0.416) or hemispheres ($F_{[3,44]}$ = 2.389; p = 0.078), indicating that the correction factor should be used. ANOVA

analysis of the normalised data showed no interactions between the groups ($F_{[4,44]}$ = 1.359; p = 0.260), hemispheres ($F_{[5,44]}$ = 1.042; p = 0.402) or the two experiments ($F_{[3,44]}$ = 0.127; p = 0.944), and the results are shown in Figure 29.

## Ultrastructural analysis of training effects

Published work indicating physiological changes in synaptic ensembles of the hippocampus after learning prompted investigation of the morphological parameters of synapses during memory formation. Various changes have been observed involving synapse number, synapse size and synaptic morphology after a variety of learning paradigms, indicating that all of these parameters may be affected by memory formation. Most of the synaptic contacts onto dentate gyrus granule cells are in the form of type 1 excitatory glutamatergic synapses that occur between presynaptic axon boutons and small postsynaptic dendritic spines. The morphology of synapses has important implications for synaptic function, and has been used to group them into various subpopulations (see Figure 13). In this analysis, thin, stubby and mushroom spine profiles were all considered as part of the same group termed non-perforated axospinous (NAS) synapses.

Spines exhibit a variety of different PSD morphologies, which is sometimes evident as complex shaped or completely segmented areas of PSD. These synapses are described as being 'perforated', and may also contain a spine apparatus. Perforated axospinous (PAS) synapses were distinguished from NAS synapses by the presence of separate portions of PSD at the same synapse i.e. adjacent to, but not in contact with, each other on the same dendritic spine membrane profile. The use of two additional serial sections on either side of the disector pair facilitated the detection of perforations in the profile images of synapses, and aided confirmation of synapse categorisation. In the set of four serial sections examined for each area, any dendritic spine profile containing a synapse with such a gap in the PSD in any of the four sections was considered to be a perforated synapse. This distinction was made even if the PSD was seen to be continuous in other sections, because the PSD would therefore form a horseshoe shape in three dimensions, and such synapses should be classified as perforated (see Figure 13). Because of their larger size, PAS synapses are less frequently sampled by the disector, which was optimised for the relatively more abundant and smaller NAS synapses. The disector requires approximately 100 specific synapse counts in order to

Figure 29 - Dentate gyrus granule cell density ($N_V$), shown as calculations of averages for left and right hemispheres of animals in each group. Naïve group - red bars, n=8; Swim only group - pink bars, n=6; 3 hour group - orange bars, n=6; 9 hour group - green bars, n=8; 24 hour group - blue bars, n=6. Error bars indicate standard error of the mean.

produce a reliable estimate of number density, and only a fraction of this number was obtained from the procedure used to sample the NAS synapses. Therefore disector estimates of PAS synapses were subject to much higher variation between animals.

Type 1 excitatory synapses that occur between a presynaptic bouton and a dendritic shaft (axodendritic) are also larger and much less abundant than NAS synapses. Very occasionally, perforations in the PSD of axodendritic synapses were seen, and this led to classification of non-perforated axodendritic (NAD) and perforated axodendritic (PAD) synapse types. Because such structural differences may underlie functional differences between these types of synapse, they were distinguished from each other during image analysis. Similar problems in analysing these synapses were also encountered, as explained above for PAS synapses. These difficulties were particularly acute for the PAD synapse category, which were so infrequently observed that many samples contained zero values, which confounded analysis. However, several of this type of synapse were detected, and so their occurrence was not ruled out as being an artefact of some kind. Examples of each category are shown in Figure 30, with the density $^+/_-$ s.e.m. (standard error of the mean) in naïve animals indicated for each type.

## Non-perforated axospinous (NAS) synapse density

The density of NAS synapses (NAS synapse $N_V$) was calculated using the disector counting method from sets of serial images. Two sets of images were acquired from each animal in the middle molecular layer of the upper blade of the dentate gyrus, one from each hemisphere. The synapse densities for each hemisphere were calculated separately, and at least six animals were analysed in each group (see Table 2). When compared statistically, no significant hemispheric differences were found, but there were significant differences between groups. Perfusions at different times of the year were also significantly different, but if these two sets of data are analysed separately, the values and statistical differences between the groups are similar. This indicates that although the numerical values differ, there is reproducibility of the data between experimental data sets with respect to the differences between groups.

**NAS**

Non-perforated
axospinous

$N_V = 2.063$
+/- 0.0874

**PAS**
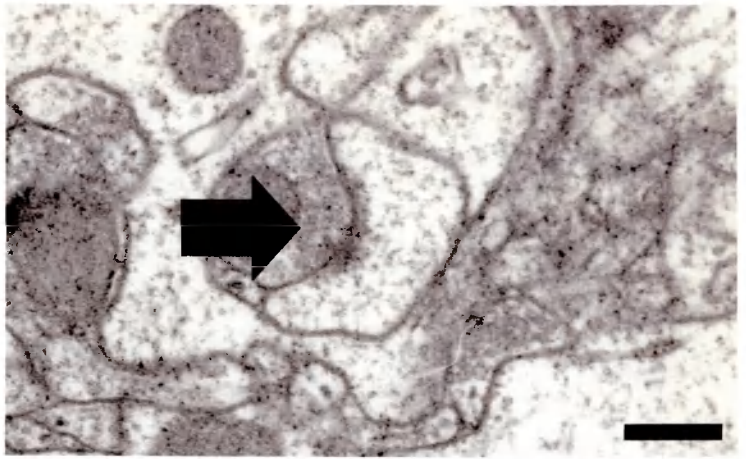
Perforated
axospinous

$N_V = 0.093$
+/- 0.0150

**NAD**
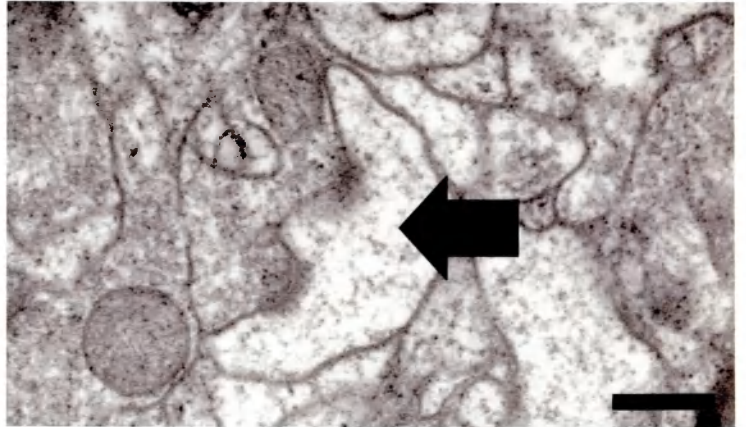
Non-perforated
axodendritic

$N_V = 0.075$
+/- 0.0037

**PAD**
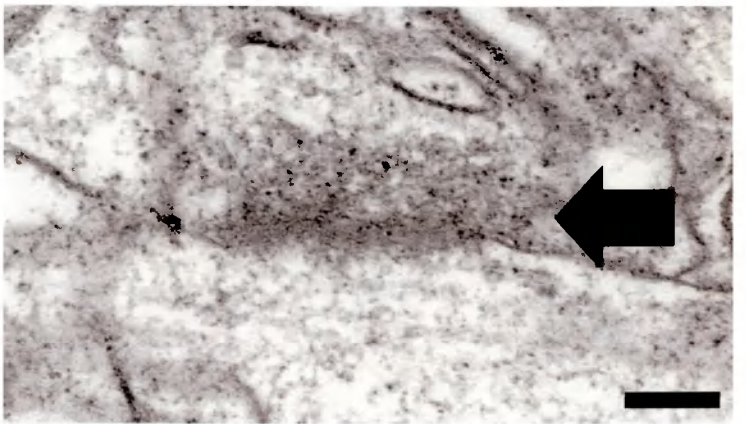
Perforated
axodendritic

$N_V = 0.0022$
+/- 0.00135
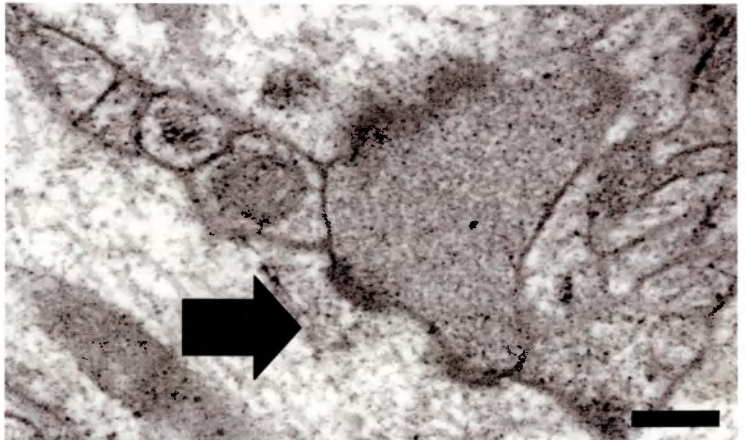
Figure 30 - Electron micrographs showing examples of different synapse categories. Also indicated are estimates of the synapse density ($N_V$) for each particular category of synapse, as present in naïve animals ($^+/_-$ s.e.m.). All scale bars = 200 nm.

However, because the neuropil thickness was significantly different between the two experiments (see Figure 27), a neuropil thickness correction factor was used to normalise the results of the second experiment with respect to the first, and the normalised results are shown in Figure 31. Overall analysis by ANOVA indicated a significant difference between groups ($F_{[4,44]}$ = 6.775; p < 0.001). No significant difference between the left and right hemisphere hippocampi ($F_{[5,44]}$ = 0.212; p = 0.956) or experiment ($F_{[3,44]}$ = 1.848; p = 0.149) was apparent. The synapse density of the 9 hour group was 2.691 synapses per $\mu m^3$, and as can be seen from Figure 27 this is greater than any of the other groups (naïve group = 2.063; swim-only control group = 2.193; 3 hour group = 1.948; 24 hour group = 2.187). Post-hoc analysis indicated that this was the explanation for the significant difference seen in the ANOVA group result, because comparisons of the 9 hour group with all other groups indicated a significant difference (p < 0.007 in all cases), whereas comparisons among any of the other groups were not significant (p > 0.4 in all cases).

## Synapse to neuron ratio

Because of the nature of the methods used to preserve samples for structural and immunological examination, it was not possible to measure the volume of the hippocampus (see above - Morphological analysis of the dentate gyrus). Thus it was not possible to calculate the total number of synapses in each hippocampus of each animal. In order to compensate for possible differences in hippocampal dimensions between animals, the ratio of synapses to neurons was calculated for each hemisphere of each animal. The NAS synapse $N_V$ was divided by the dentate gyrus cell $N_V$ to obtain a ratio. Because both of the density estimates were expressed as number per $um^3$, the units cancel each other out to leave a ratio that effectively normalises the synapse density with respect to the neuron density. Statistical analysis by ANOVA showed that there was a significant difference between groups ($F_{[4,44]}$ = 5.124; p = 0.001), but that there was no significant effect of lateralisation ($F_{[5,44]}$ = 0.476; p = 0.792) or experimental year ($F_{[3,44]}$ = 0.737; p = 0.534; normalised data). The data are shown in Figure 32, averaged across hemispheres in each group. Post-hoc analysis indicates that the difference between groups is due to the 9 hour group (3860:1), this being statistically greater than the naive naïve group (3114:1, p = 0.011), the swim only control (2896:1, p = 0.002), the 3 hour group (2704:1, p < 0.001) and the 24 hour group
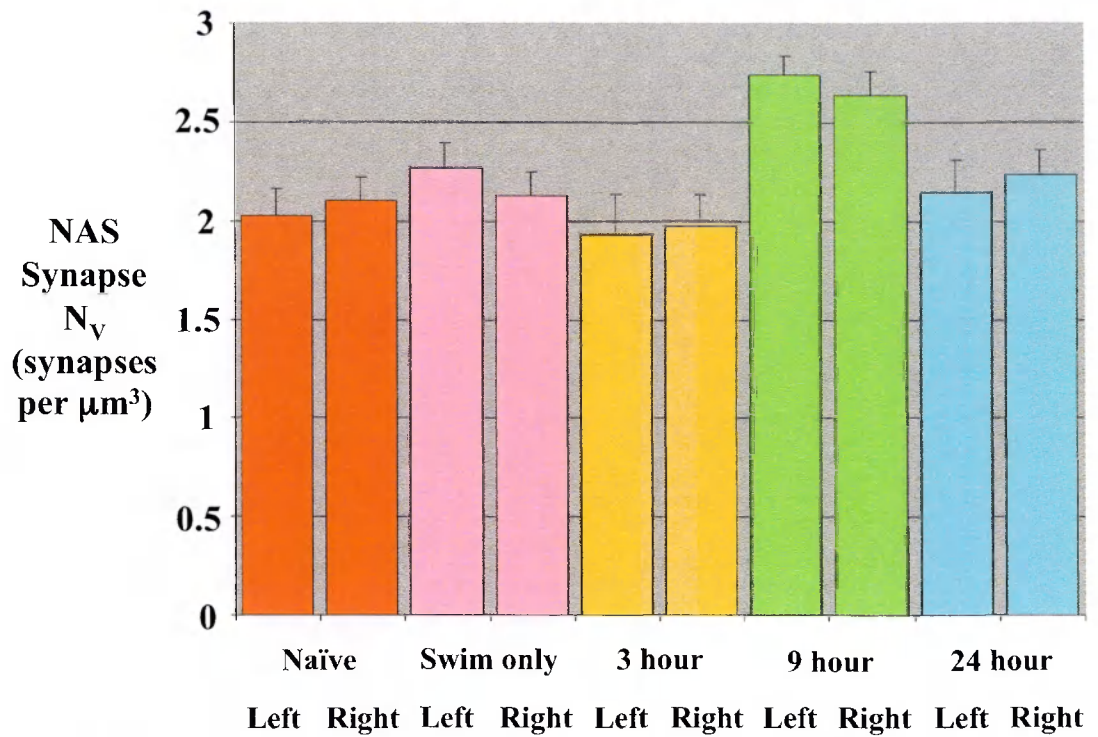
Figure 31 - Non-perforated axospinous synapse density - NAS synapse $N_V$. Bars indicate calculations of averages for left and right hemispheres of animals in each group. Naïve group - red bars, n=8; Swim only group - pink bars, n=6; 3 hour group - orange bars, n=6; 9 hour group - green bars, n=8; 24 hour group - blue bars, n=6. Error bars indicate standard error of the mean.
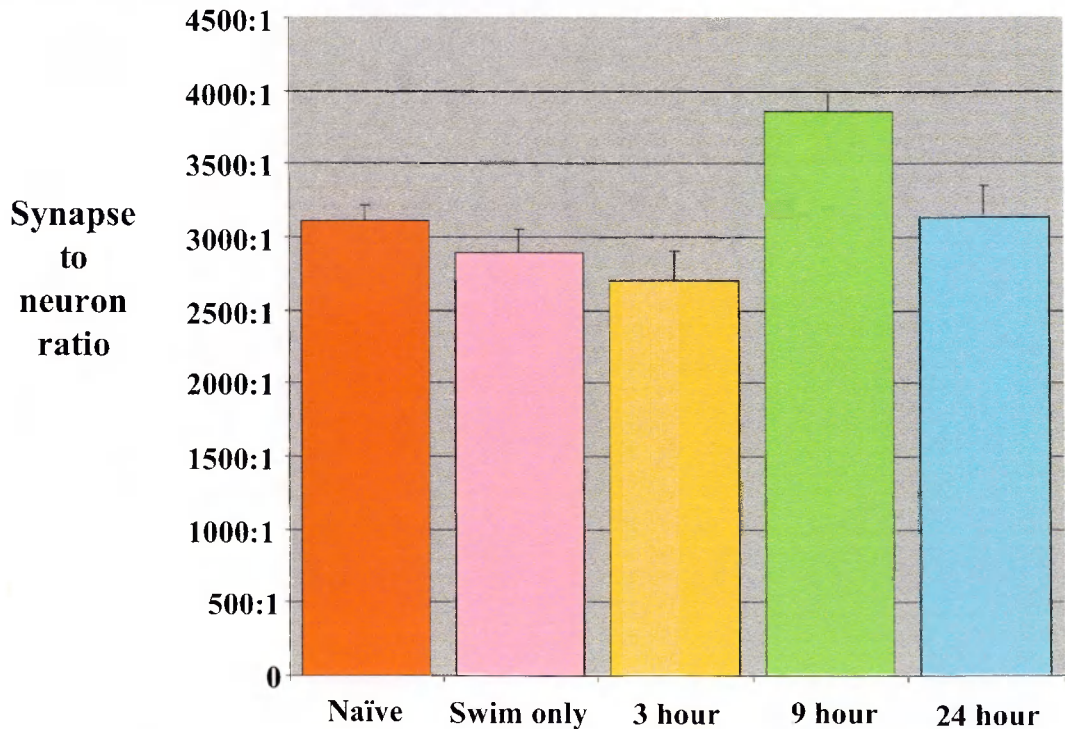


Figure 32 - Synapse to neuron ratio for NAS synapses. Bars indicate calculations of averages for animals in each group. Naïve group - red bar, n=8; Swim only group - pink bar, n=6; 3 hour group - orange bar, n=6; 9 hour group - green bar, n=8; 24 hour group - blue bar, n=6. Error bars indicate standard error of the mean.

(3136:1, p = 0.028). No other differences between any of the groups were statistically significant at the p = 0.05 level or greater.

## Mean height of NAS synapses

Mean height is a quantity that can be calculated from information obtained via the disector method, and is a representation of object size, rather than an estimate of actual object dimensions. Mean height has units that are the same as those of the distance between the two disector planes, and compares the number of specific objects counted with the total number of specific and non-specific object profiles that can be seen in the look-up section frame area. Figure 33 shows the mean height of NAS synapses. The data has been normalised between experiments and combined. Statistical analysis of the data indicated that there was no difference between experimental year ($F_{[3,44]}$ = 1.478; p = 0.230) or hemispheres ($F_{[5,44]}$ = 2.114; p = 0.076), and so the data is shown as an average for animals and hemispheres in each group. There was a significant difference between experimental groups ($F_{[4,44]}$ = 6.371; p < 0.001).

The mean height of synapses in the 9 hour group (174.6) is significantly lower than the mean height of synapses in the naïve group (214.4, p = 0.002) and the 24 hour group (227.0, p < 0.001), but not the 3 hour group (196.8, p = 0.235) or the swim only group (205.2, p = 0.055). To ensure that the estimate of mean height is stereologically unbiased, the orientation of the disector planes must be IUR (isotropic uniform random), i.e. the planes must have a random orientation in three dimensions **(Howard and Reed, 1998)**. This is not the case for the images that comprise each data set, and so the estimates of mean height may be subject to bias, as explained in the methods section above.

## PSD surface area density of NAS synapses

$S_V$, the surface area (of PSD) per unit volume, was calculated for each data set. The results are shown in Figure 34, and indicate that the area of PSD per $\mu m^3$ was similar for each hemisphere ($F_{[5,44]}$ = 1.443; p = 0.223) and experiment ($F_{[3,44]}$ = 0.479; p = 0.698; normalised data). However, there was a difference in the group interaction ($F_{[4,44]}$ = 5.357; p < 0.001). Statistical post-hoc analysis revealed particular interactions between groups, only some of which were significantly different. The naïve control
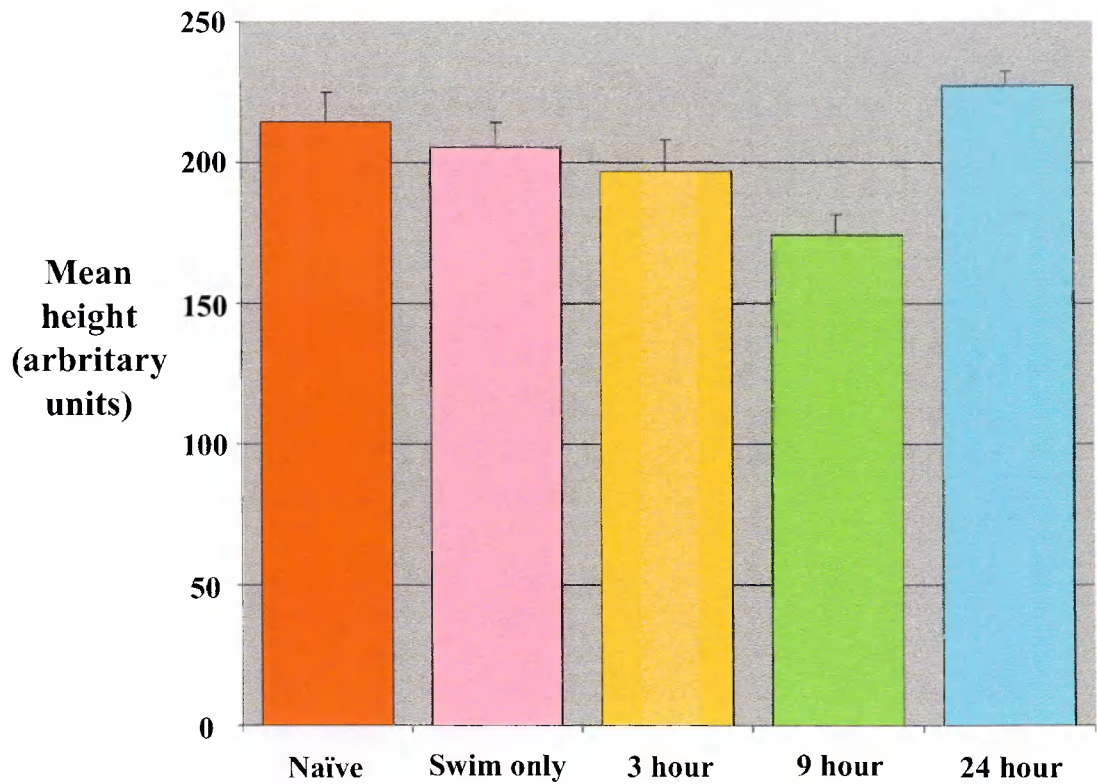
Figure 33 - Mean height of NAS synapses. Bars indicate calculations of averages for animals in each group. Naïve group - red bar, n=8; Swim only group - pink bar, n=6; 3 hour group - orange bar, n=6; 9 hour group - green bar, n=8; 24 hour group - blue bar, n=6. Error bars indicate standard error of the mean.
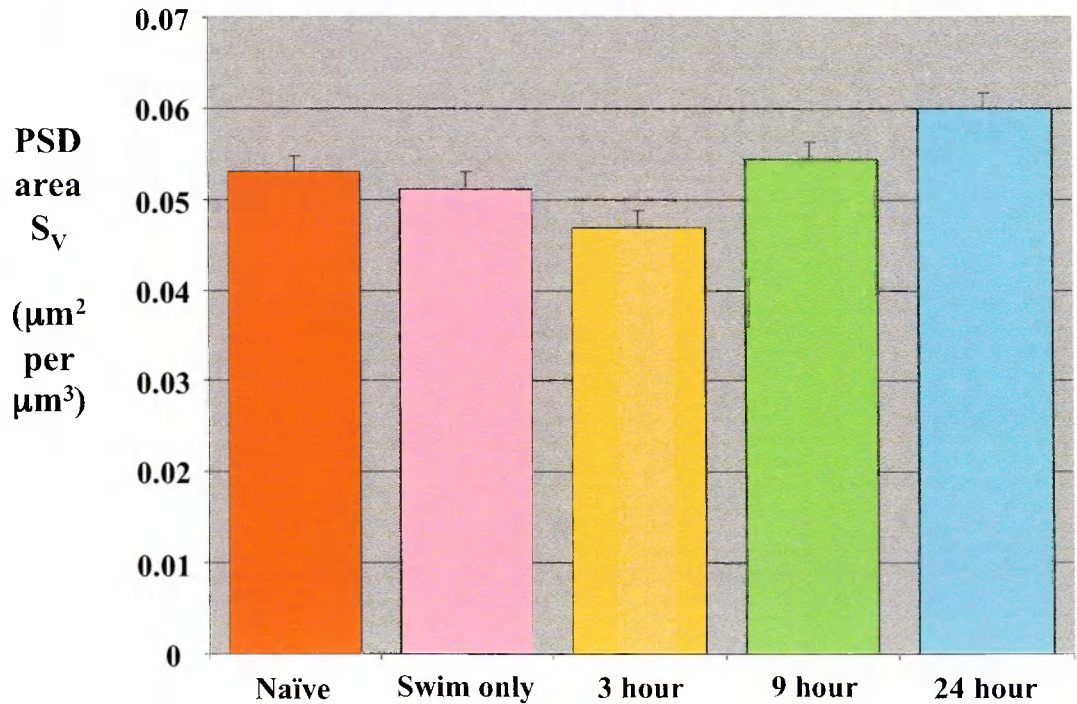


Figure 34 - PSD surface area density for NAS synapses - NAS synapse PSD $S_V$. Bars indicate calculations of averages animals in each group. Naïve group - red bar, n=8; Swim only group - pink bar, n=6; 3 hour group - orange bar, n=6; 9 hour group - green bar, n=8; 24 hour group - blue bar, n=6. Error bars indicate standard error of the mean.

(0.053 $\mu m^2$ per $\mu m^3$) was not significantly different from any of the other groups. However, there was a significant difference between the 3 hour group and the 9 hour group (p = 0.043). There was also a significant difference between the 24 hour group and both the swim-only and 3 hour groups (p = 0.025 and p < 0.001 respectively). These differences between the groups indicated that there was a subtle effect of training on average total synaptic contact area, which was slightly less that both controls in the 3 hour group after a small amount of training (0.047 $\mu m^2$ per $\mu m^3$), but slightly more in the 24 hour group after the most training (0.060 $\mu m^2$ per $\mu m^3$).

## PSD area to neuron ratio

Because the methods used to determine synaptic parameters made calculation of total hippocampal volume difficult, calculations of total populations were not possible. In a similar way to the synapse to neuron ratio mentioned above, the density of PSD surface area, $S_V$, can be converted into a ratio with respect to the density of neurons, giving a PSD area to Neuron ratio. This value was calculated for each hemisphere of each animal, and is shown in Figure 35. Analysis by ANOVA indicated an interaction between the different groups ($F_{[4,44]}$ = 3.603; p = 0.011), but showed no significant difference between hemisphere ($F_{[5,44]}$ = 1.336; p = 0.262) or experiment ($F_{[3,44]}$ = 0.583; p = 0.628). Compared with naïve control, none of the other groups were significantly different. A trend is apparent, with a decrease in the 3 hour group compared to the naïve control group, and a similar decrease is also seen in the swim only control. In contrast, trained animals in the 9 hour group have a PSD area to neuron ratio very similar to that of naïve animals. The value of the 24 hour group shows an increase in ratio above that of the naïve control. Statistical post-hoc analysis revealed particular interactions between groups, but only two differences were statistically significant. These were the difference between the swim-only control and the 24 hour group (p = 0.037), and the 3 hour group and the 24 hour group (p = 0.016).

## Mean PSD area per NAS synapse

$S_N$, the mean area of PSD per NAS synapse, was then calculated. This provided an unbiased estimate of synapse contact area, which was statistically different between groups ($F_{[4,44]}$ = 5.091; p = 0.001), but not between hemispheres ($F_{[5,44]}$ = 1.304; p = 0.275) or experimental year ($F_{[3,44]}$ = 2.578; p = 0.063). The PSD area per synapse was
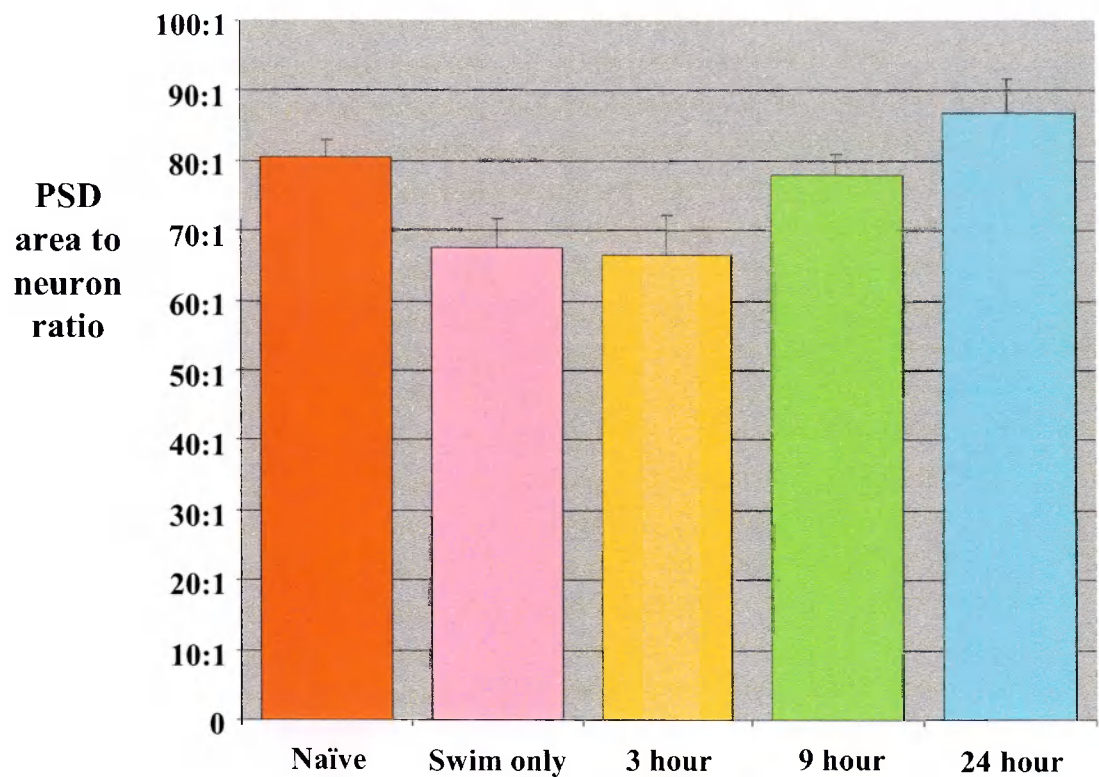
Figure 35 - PSD area to neuron ratio for NAS synapses. Bars indicate calculations of averages for animals in each group. Naïve group - red bar, n=8; Swim only group - pink bar, n=6; 3 hour group - orange bar, n=6; 9 hour group - green bar, n=8; 24 hour group - blue bar, n=6. Error bars indicate standard error of the mean.
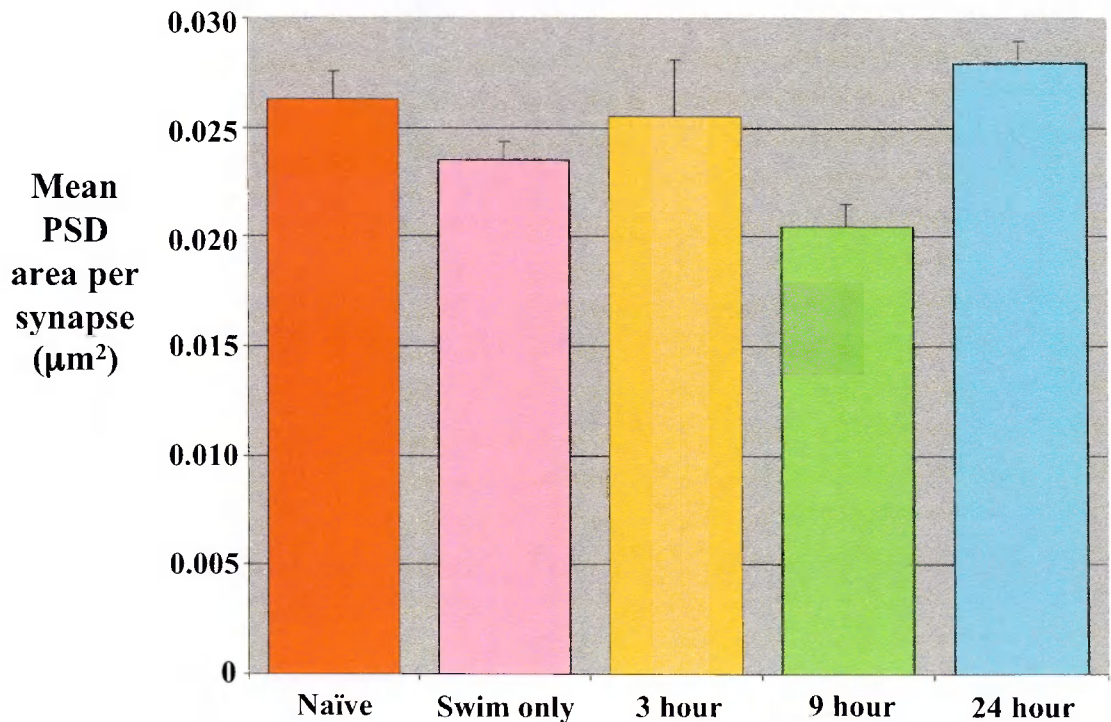


Figure 36 - Mean PSD area per NAS synapse - $S_N$. Bars indicate calculations of averages for animals in each group. Naïve group - red bar, n=8; Swim only group - pink bar, n=6; 3 hour group - orange bar, n=6; 9 hour group - green bar, n=8; 24 hour group - blue bar, n=6. Error bars indicate standard error of the mean.

111

calculated for each animal, and the average results for each group are shown in Figure 36. Statistical analysis showed that the 9 hour group (0.020 $\mu m^2$ per synapse) was significantly smaller than the naïve group (0.026 $\mu m^2$ per synapse; $p = 0.008$), the 3 hour group (0.026 $\mu m^2$ per synapse, $p = 0.037$) and the 24 hour group (0.028 $\mu m^2$ per synapse, $p = 0.001$), but not the swim-only control (0.024 $\mu m^2$ per synapse, $p = 0.441$). However, no other differences were statistically different, suggesting that because the average area of PSD per NAS synapse in the 9 hour group was different to other groups, morphological changes were evident solely at this timepoint.

## Immunogold labelling analysis of training effects

The influence of synaptic structure, and changes thereof, on synaptic function is not limited to the level of morphology. Both LTP and learning modify the production and expression of neurotransmitter receptors present at synapses, and this will have functional consequences on the transmission of information at synapses. It was therefore considered important to investigate the temporal dynamics of receptor population changes at synapses involved in memory formation. Glutamate is the predominant excitatory neurotransmitter in the CNS, and is used by the principal neurons of the hippocampus and the neurons of the entorhinal cortex, which give rise to the input at the axospinous synapses of dentate gyrus granule cell dendrites. Both AMPA and NMDA receptor types are involved in the excitatory neurotransmission of information, and are present at hippocampal synapses (see introduction).

Commercial primary antibodies were used that recognised individual amino acid sequences from a variety of protein molecules that have been described as subunits of neurotransmitter receptors. AMPA receptors are heteromeric complexes of five subunits, each of which may be a different type. Because it is not clear which, if any of the four types of AMPA subunit are essential for the formation of functional receptors, a cocktail of antibodies was used that recognised each of the four AMPA subunit types. NMDA receptors consist of four or five subunits, of which there are two main types. However, an antibody was used that was specific for the major splice variants of the NR1 subunit because this may be an essential component of functional NMDA receptors.

Table 3 shows a record of the number of samples from each group prepared by freeze-substitution, and the number of samples used for immunogold labelling of AMPA or NMDA receptors. Some samples were discounted because of poor structure, poor labelling or because intact slots were not available. This also influenced the number of animals for which both AMPA-labelled and NMDA-labelled sections were available, as shown on the last row of the table. The data from these animals was used to calculate the AMPA to NMDA labelling ratio. So that experimental numbers were practicable, samples from left hemisphere hippocampi were not reacted.

Table 3 - Record of samples used for immunogold labelling.

|  | Naïve | Swim-only | 3 hour | 9 hour | 24 hour |
|---|---|---|---|---|---|
| Total samples | 6 | 0 | 5 | 6 | 6 |
| AMPA | 3 | 0 | 4 | 4 | 4 |
| NMDA | 4 | 0 | 5 | 5 | 4 |
| Ratio | 3 | 0 | 4 | 3 | 4 |

Synaptic profiles were distinguished as either axospinous or axodendritic, and as either perforated or non-perforated, as was done for morphological analysis. The number of synaptic profiles that had at least one gold particle associated with them was calculated as a percentage of the total number of synaptic profiles observed. Because of the lower abundance of PAS, NAD and PAD synapses, the labelling of these synapse types was infrequently observed. For both the AMPA and the NMDA labelling experiments, most labelled NAS profiles had one gold particle associated with them. For the NMDA receptor labelling experiment, two gold particles closely associated with a single synaptic profile was rarely seen, and three or more particles per profile were never observed. The presence of two gold particles per profile was slightly more common in the AMPA receptor labelling experiment, and three gold particles per profile was seen very occasionally.

These levels of post-embedding immunogold labelling were very low compared to published work by several different authors, and may reflect a lack of antigenicity in the tissue due to fixation and processing, despite the methods used. Coupled with the

relatively small number of animals in each group, the low intensity of labelling resulted in small differences between each group of animals. The statistical analysis that was conducted did not indicate any evidence of differences between any of the groups, and most of the comparisons that were conducted by one-way ANOVA produced small F values and levels of significance much greater than 0.05. Some labelling was observed and there were some differences between the groups, and the results can be discussed in terms of general trends, but the general conclusions must be treated with caution, as it was difficult to distinguish the reason for the lack of differences. This may be due to a 'true' lack of difference between the groups, or that there was a difference but it was not detectable in this experiment and the null hypothesis was not rejected. The failure to detect a 'true' difference in this way leads to a type II or $\beta$ statistical error, which can easily be caused by a sample size that is too small.

The results of the immunolabelling experiments will be described in detail below. Examples of sections immunolabelled for AMPA receptor subunits are shown in Figure 37. Also shown are images of typical control sections from which primary antibodies were omitted. Figure 38 shows examples of sections immunolabelled for NMDA receptor subunit NR1, as well as primary antibody-omitted controls.

## Percentage of labelled NAS synapses

The percentage of labelled NAS synapses was calculated for the two single labelling experiments performed for AMPA and NMDA receptors. The results are shown in Figure 39, and represent the percentage of total labelling for the NAS synapses, irrespective of how many gold particles were present at each profile. Also shown is the ratio of AMPA to NMDA labelling. For the AMPA receptor labelling experiment, percentage of synapses labelled increased in the 3 hour group (6.38%), and even more in the 9 hour group (6.96%) compared to the naïve control (5.75%), whereas the value for the 24 hour group (6.08%) was only marginally higher than the naïve control. However, statistical analysis by ANOVA indicated that none of these differences were significant ($F_{[3,7]} = 0.185$ ; p = 0.904). The percentage labelling values for the NMDA receptor shows that there are different effects on NMDA receptor labelling at different time-points after training. Labelling in the naïve group was 3.15%, a value that was higher than the 3 hour group (1.54%), the 9 hour group (2.87%) and the 24 hour group (1.28%), but there was no significant difference between the groups upon statistical
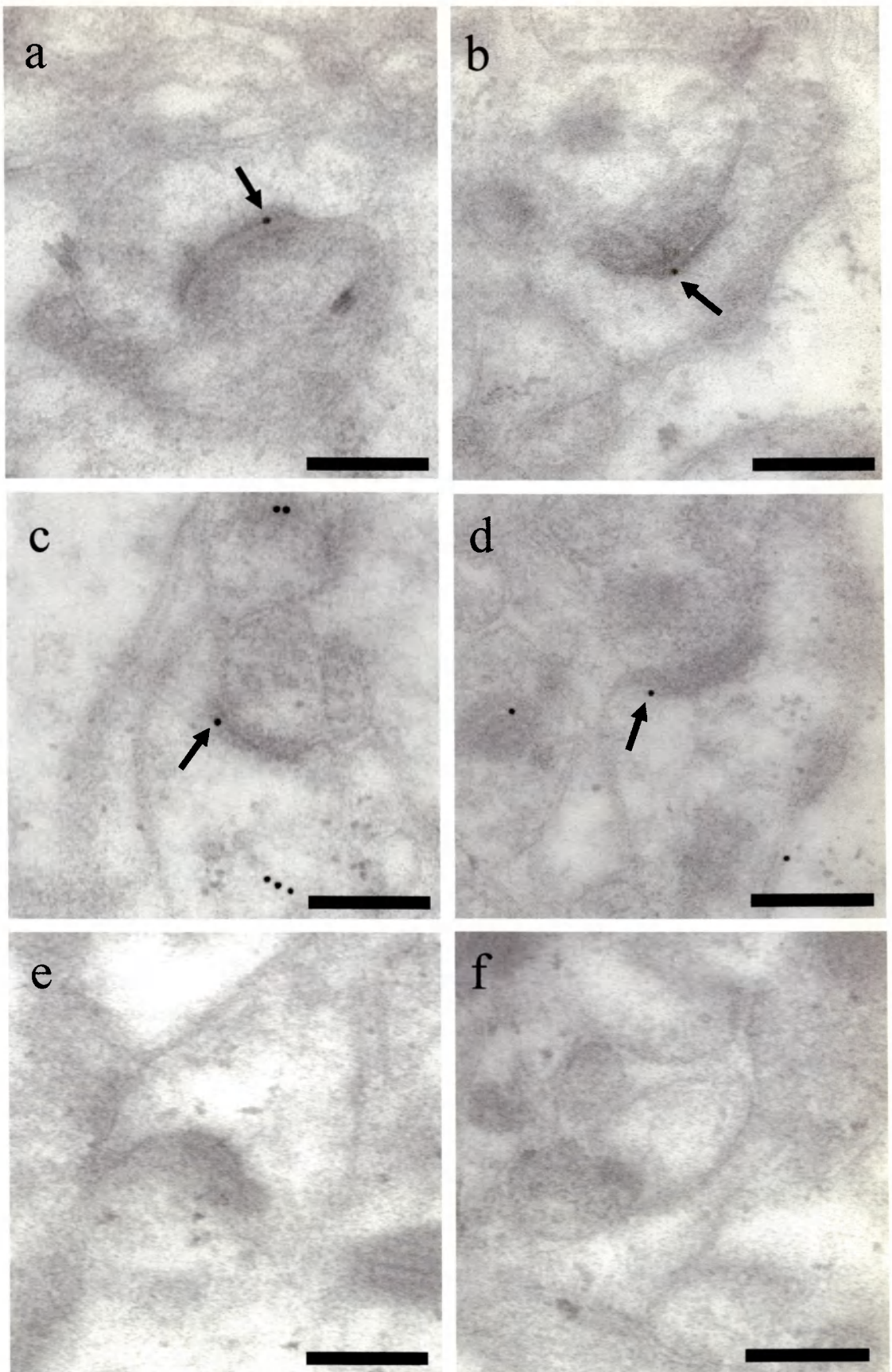
Figure 37 - Micrographs of NAS synapses reacted with a cocktail of antibodies directed against AMPA subunits GluR1, GluR2/3 and GluR4 (a, b, c, d), and corresponding control without primary antibodies (e, f). Electron dense (black) immunogold particles at synapses are indicated by arrows. Scale bars = 200 nm.
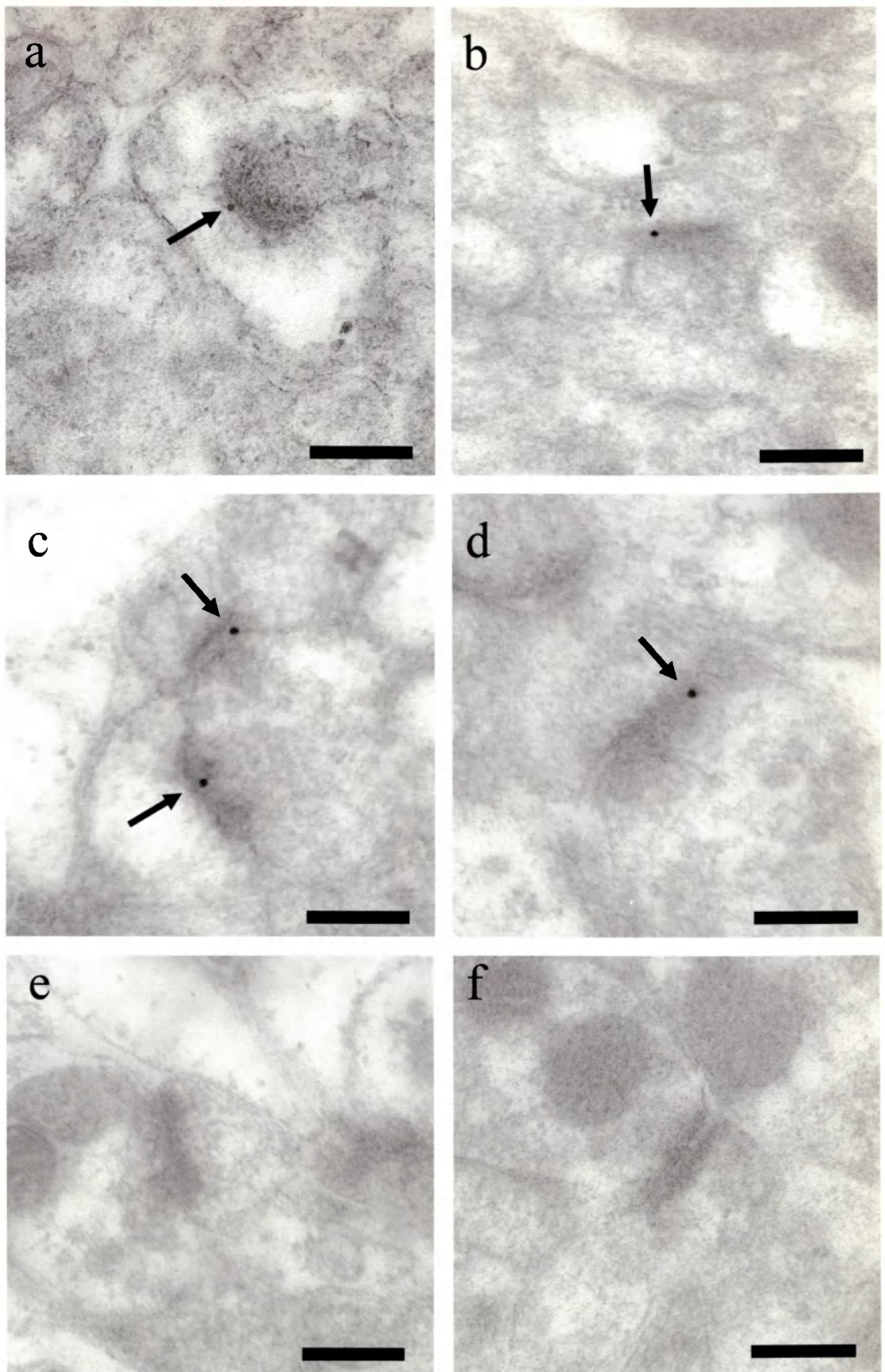
Figure 38 - Micrographs of NAS synapses reacted with an antibody recognising the NR1 subunit of the NMDA receptor (a, b, c, d), as well as control sections from which primary antibody was omitted (e, f). Electron dense (black) immunogold particles at synapses are indicated by arrows. Scale bars = 200 nm.

Figure 39 - Percentage labelling of NAS synapses. Bars indicate calculations of averages for animals in each group. Left-hand side y axis - AMPA receptor subunit labelling - blue bars ☐ , and NMDA receptor NR1 subunit labelling - red bars ◼ . Right-hand side y axis - AMPA to NMDA ratio - yellow bars ☐ . See Table 3 for the number of replicates in each group. Error bars indicate standard error of the mean.
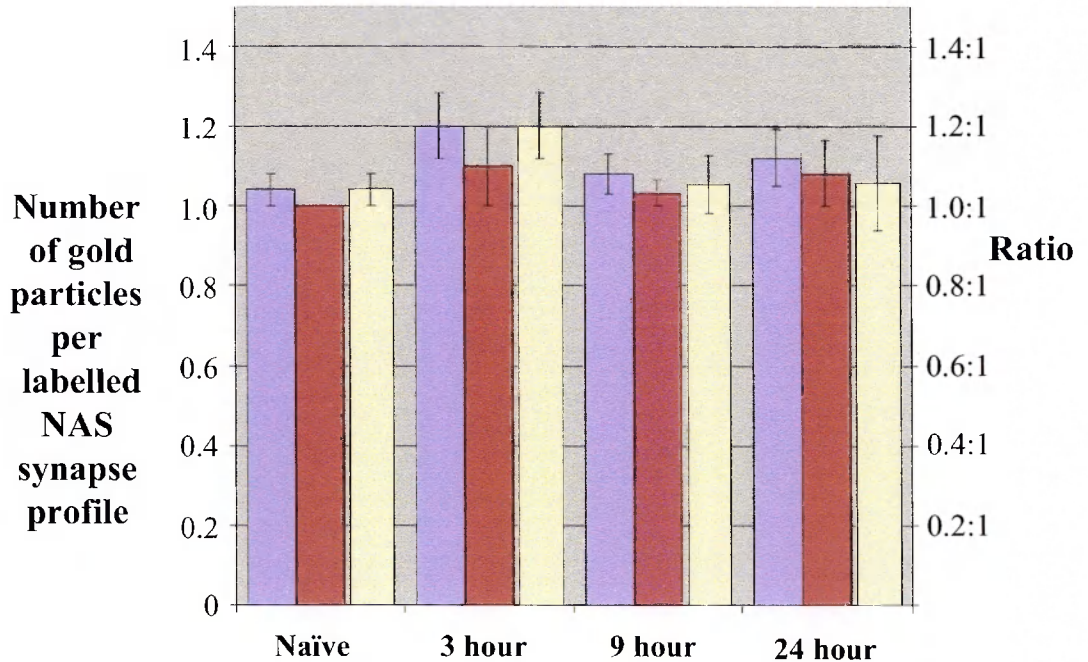


Figure 40 - Number of gold particles per labelled NAS synapse profile. Bars indicate calculations of averages for animals in each group. Left-hand side y axis - AMPA receptor subunit labelling - blue bars ☐ , and NMDA receptor NR1 subunit labelling - red bars ◼ . Right-hand side y axis - AMPA to NMDA ratio - yellow bars ☐ . See Table 3 for the number of replicates in each group. Error bars indicate standard error of the mean.

analysis ($F_{[3,10]} = 0.1.876$ ; p = 0.180). The ratio of AMPA to NMDA labelling in the naïve group (1.61:1) was lower than the 3 hour group (6.69:1), the 9 hour group (2.63:1) and the 24 hour group (8.03:1), but these differences were not statistically significant ($F_{[3,7]} = 2.073$ ; p = 0.162).

## Number of gold particles per synapse

The number of gold particles bound to a synapse is representative of the total number of antigens, in this case glutamate receptors, that were present at the synapse *in vivo*, and this is shown in Figure 40. For AMPA receptors, the number of gold particles per labelled synaptic profile is fairly constant, but shows an increase in the 3 hour group (1.202) and a smaller increase in the 9 hour group (1.094) and 24 hour group (1.122), compared to naïve control (1.042). For NMDA receptors there is also consistency in the number of gold particles per labelled synapse, with a small increase in the 9 hour group (1.033) compared to naïve control (1.000). Slightly larger increases are seen in the 3 hour group (1.100) and the 24 hour group (1.083), but there is also more variance in these groups. The ratio of AMPA to NMDA gold per synapse is smallest in the naïve control (1.042:1) and largest in the 3 hour group (1.202:1), whereas the values of the 9 hour group (1.055:1) and the 24 hour group (1.059:1) are slightly greater than the naïve group. Statistically, there were no significant differences between any of the groups, either for AMPA gold per synapse ($F_{[3,7]} = 0.917$ ; p = 0.464), NMDA gold per synapse ($F_{[3,10]} = 0.424$ ; p = 0.739) or the AMPA to NMDA ratio ($F_{[3,7]} = 0.786$ ; p = 0.526).

## Gold particles per $\mu$m of PSD in all NAS synapses

Because immunogold labelling was performed on single sections, the counting of synaptic profiles will be subject to bias. This is because transected synapses that are larger (with respect to a plane perpendicular to the section) will be more likely to be observed in the section **(Howard and Reed, 1998)**, meaning that synapses will not be sampled irrespective of size. Although calculations of the density of labelled synapses would require serial sections, stereologically unbiased estimates of surface area density ($S_V$) can be made from single sections. Synapse PSD surface area per unit volume is directly proportional to the length of PSD profiles in a given area of section, as can be seen from Equations 6 and 9.

Synapses were not serially sectioned, and only antigens on the surface of the sections could be labelled by gold particles. The total number of gold particles was divided by the total length of NAS synapse PSD profiles, which calculates the gold per μm PSD of all NAS synapses in the examined section area exposed to antibody. This is representative of the abundance of receptors in the total synaptic population. Figure 41 shows the number of gold particles per μm of total PSD length for sections labelled for AMPA receptors, NMDA receptors and the ratio of AMPA to NMDA labelling.

The total length of PSD profile, and hence $S_V$, was very similar between groups, which agrees with the morphological data (Figure 34). For AMPA receptors, the number of gold particles per μm of PSD was increased in all groups compared to naïve control (0.375), but this increase was greater in the 3 hour group (0.462) than in the 9 hour (0.436) or 24 hour (0.432) groups. These differences were not significant ($F_{[3,7]}$ = 0.175 ; p = 0.911). The situation was different for NMDA receptors, with a decrease in value, albeit non-significant, compared to the naïve group (0.180) in both the 3 hour (0.095) and the 24 hour (0.086) groups. The value of the 9 hour group (0.166) was very similar to the naïve group, being only slightly reduced. Statistics indicated that none of the differences were significant ($F_{[3,10]}$ = 1.924 ; p = 0.172).

Less stringent post-hoc analysis using the LSD test indicated that the difference between the naïve group and the 24 hour group was approaching significance (p = 0.062), although this is not the case when Tukey's HSD test is used (p = 0.23). The ratio of AMPA to NMDA gold particles per μm of total PSD was different for each group, the naïve group (1.733:1) being less than the 3 hour group (8.500:1), the 9 hour group (3.179:1) and the 24 hour group (9.250:1), and these values were not significantly different overall ($F_{[3,7]}$ = 1.563 ; p = 0.254. The LSD test indicated that the difference between the naïve group and the 24 hour group was close to significance (p = 0.077), although this is not the case with Tukey's HSD test (p = 0.26).

## Number of gold particles per μm of labelled synapse PSD

The number of gold particles can also be expressed per μm of PSD length for labelled synapses. This is representative of the abundance of receptors at individual synapses because it is directly related to their density, and the data is shown in Figure 42. The number of gold particles per μm of PSD is similar for all groups in the AMPA
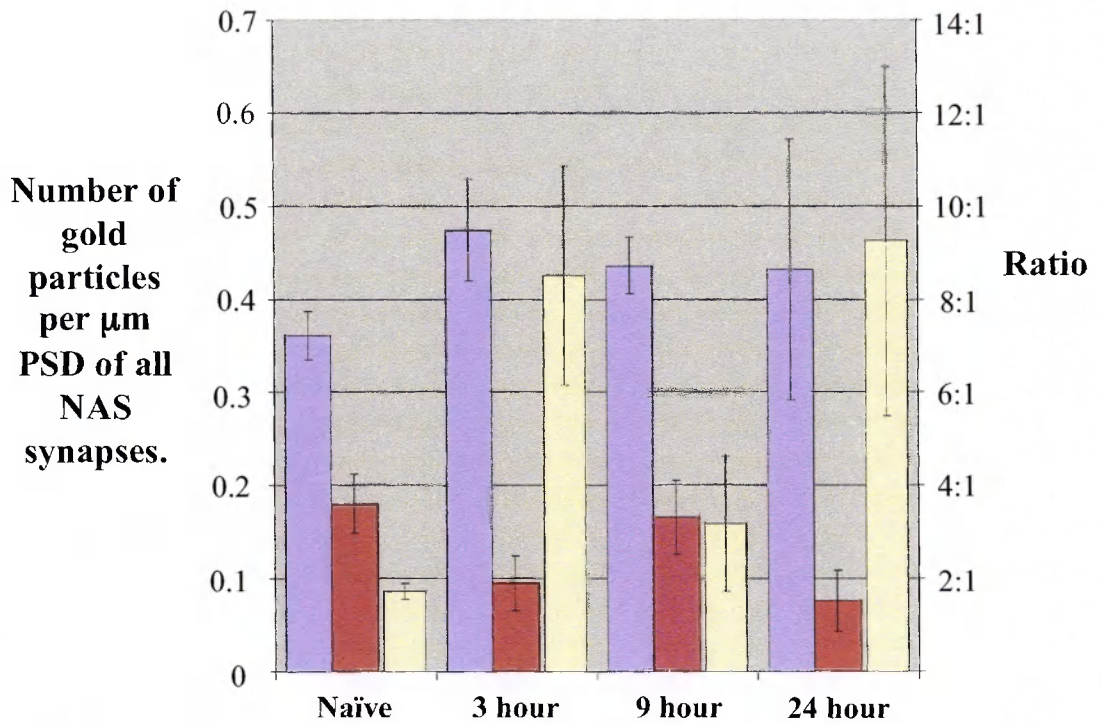
Figure 41 - Number of gold particles per μm PSD of all NAS synapses. Bars indicate calculations of averages for animals in each group. Left-hand side y axis - AMPA receptor subunit labelling - blue bars ☐, and NMDA receptor NR1 subunit labelling - red bars ■. Right-hand side y axis - AMPA to NMDA ratio - yellow bars ☐ . See Table 3 for the number of replicates in each group. Error bars indicate standard error of the mean.
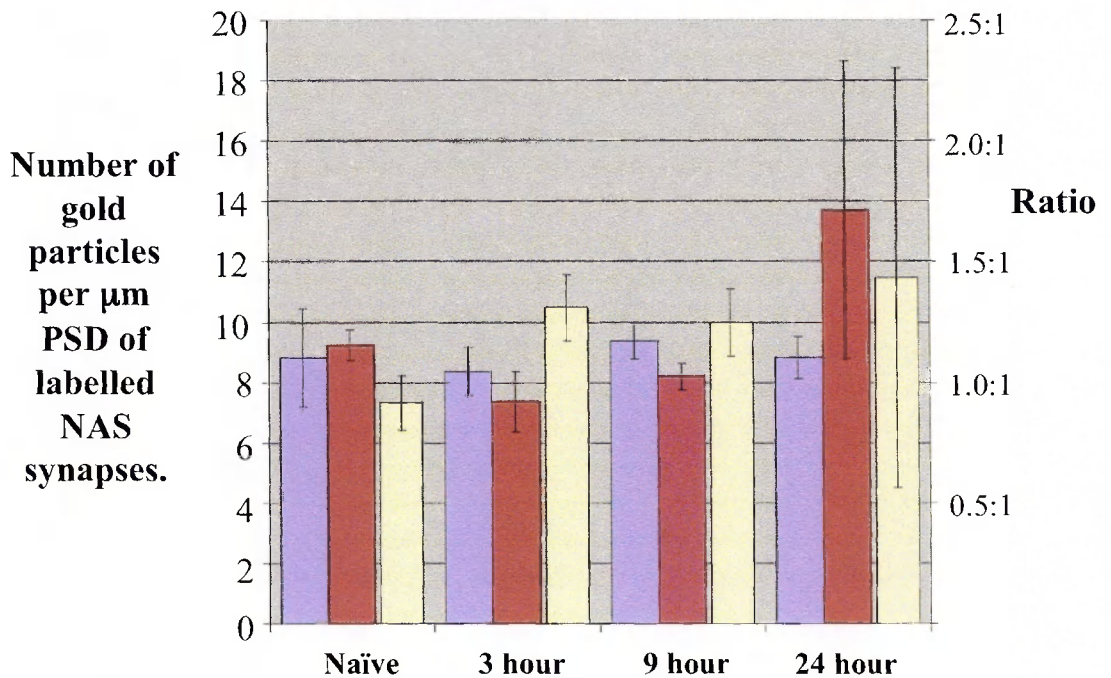


Figure 42 - Number of gold particles per μm PSD of labelled NAS synapses. Bars indicate calculations of averages for animals in each group. Left-hand side y axis - AMPA receptor subunit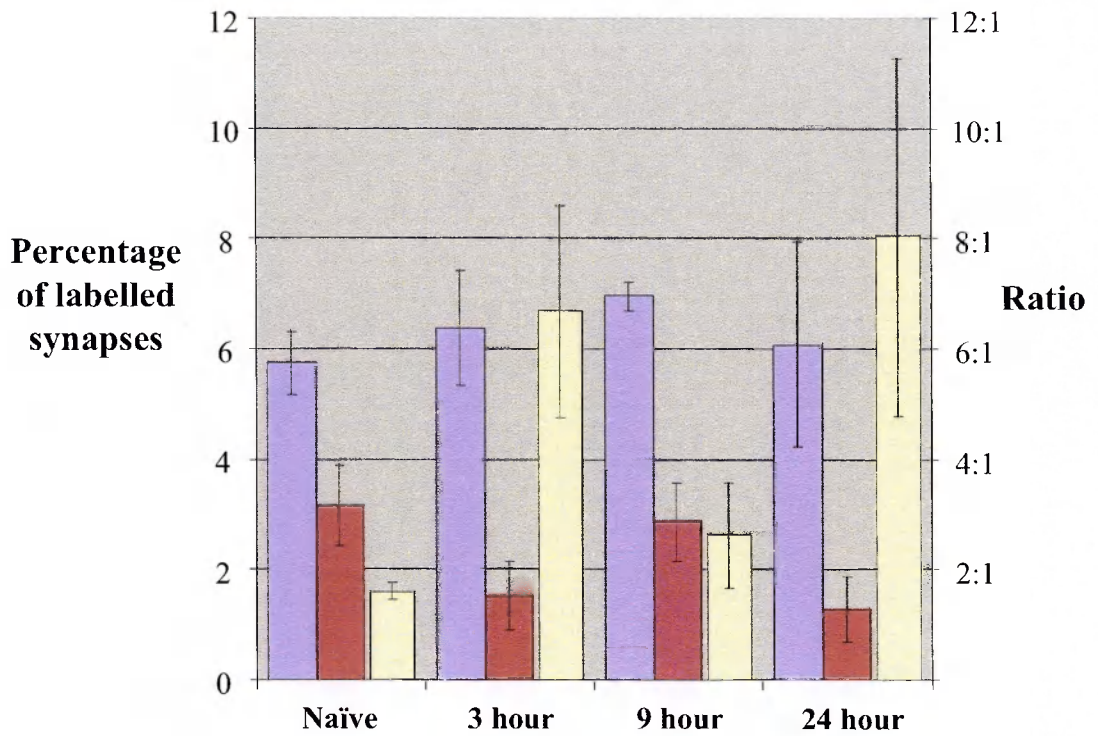 labelling - blue bars ☐ , and NMDA receptor NR1 subunit labelling - red bars ■ . Right-hand side y axis - AMPA to NMDA ratio - yellow bars ☐ . See Table 3 for the number of replicates in each group. Error bars indicate standard error of the mean.

labelling experiment, and the groups do not differ significantly ($F_{[3,7]}$ = 0.236 ; p = 0.869). The 3 hour group value (8.34) is lower than the naïve group (8.83), whereas the 9 hour group (9.37) is higher than naïve. The 24 hour group (8.81) is similar to naive. The NMDA receptor labelling experiment shows much more variability, with the naïve group value (9.24) being greater than both the 3 hour group (7.37) and the 9 hour group (8.20). The 24 hour group shows a much higher value (13.71), and the high variance means that differences between groups are not significant ($F_{[3,10]}$ = 1.459 ; p = 0.269). The LSD post-hoc test suggests that the difference between the 3 hour and the 24 hour group is approaching significance (p = 0.068), but this is not supported by Tukey's HSD test (p = 0.24). The ratio of AMPA to NMDA gold particles per μm of labelled PSD for the naïve group (0.914:1) highlights that there are less AMPA than NMDA receptors present at labelled synapses in this group. The ratio in the 3 hour group (1.308:1), the 9 hour group (1.248:1) and the 24 hour group (1.433:1) are all greater than the naïve group, but these differences are not significant ($F_{[3,7]}$ = 0.200 ; p = 0.894).

## PSD surface area density of labelled synapses

Synaptic size is important because it may be related to functionality, and so PSD area may be representative of receptor number at the synapse. Therefore the area of PSD per unit volume of labelled synapses was calculated by using Equation 9, and these results are shown in Figure 43. For the AMPA receptors, the area of labelled PSD is 0.0028 $μm^2$ per $μm^3$ in the naïve group. This value is increased in the 3 hour group (0.0036), but then reduces slightly in the 9 hour group (0.0032) and the 24 hour group (0.0032). However, these groups are not significantly different ($F_{[3,7]}$ = 0.329 ; p = 0.805). The area of PSD labelled for NMDA receptors shows a different pattern, decreasing from the naïve value (0.0013) in the 3 hour group (0.0008) and the 24 hour group (0.0006), but being similar to naïve in the 9 hour group (0.0014). Again, these groups are not significantly different ($F_{[3,10]}$ = 1.748 ; p = 0.203).

Calculation of the surface area density ratio between AMPA and NMDA receptors indicated that the naïve group had the smallest value (1.928:1). The 3 hour group value (6.117:1) and the 24 hour group value (10.683:1) were greater, and to a lesser extent so was the 9 hour group value (2.879:1). No significant difference was detectible between groups ($F_{[3,7]}$ = 2.283 ; p = 0.136). The difference between the AMPA to NMDA ratio

121
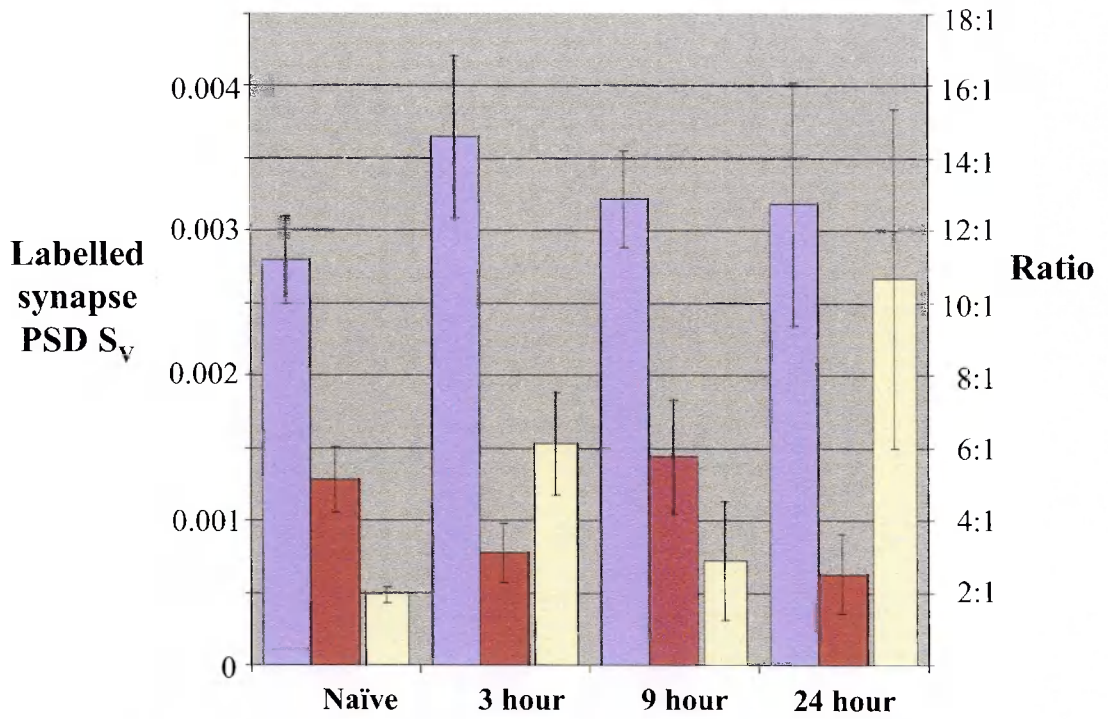
Figure 43 - PSD surface area density of labelled NAS synapses - Labelled synapse PSD $S_V$. Bars indicate calculations of averages for animals in each group. Left-hand side y axis - AMPA receptor subunit labelling - blue bars ☐ , and NMDA receptor NR1 subunit labelling - red bars ■ . Right-hand side y axis - AMPA to NMDA ratio - yellow bars ☐ . See Table 3 for the number of replicates in each group. Error bars indicate standard error of the mean.
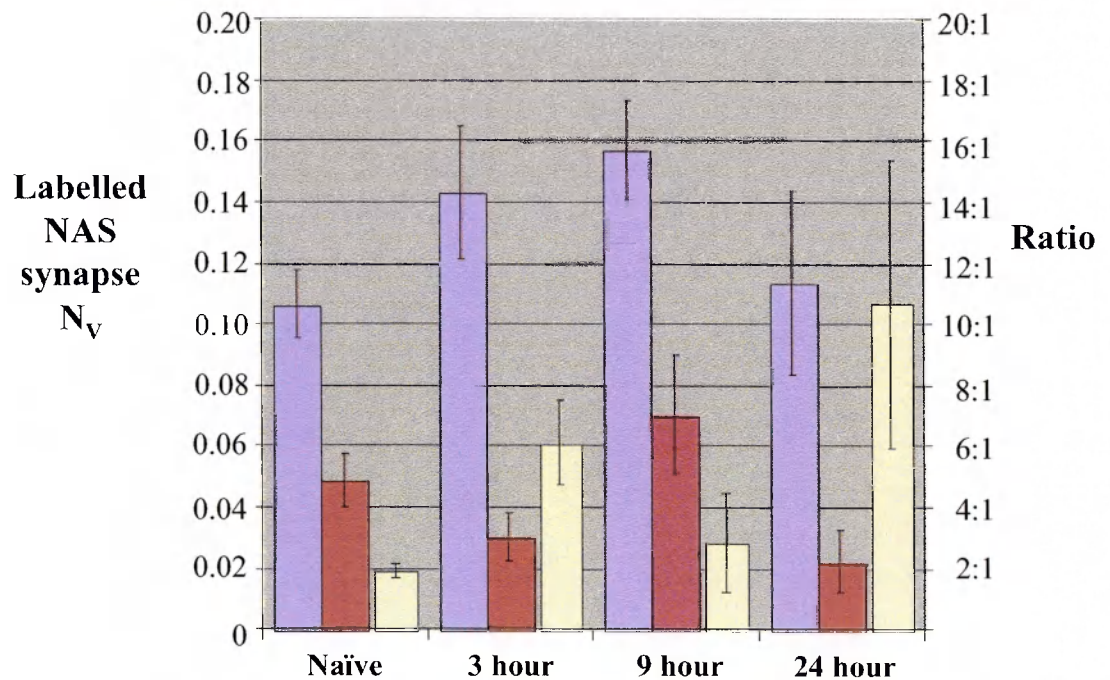


Figure 44 - Density of immunolabelled NAS synapses - Labelled NAS synapse $N_V$. Bars indicate calculations of averages for animals in each group. Left-hand side y axis - AMPA receptor subunit labelling - blue bars ☐ , and NMDA receptor NR1 subunit labelling - red bars ■ . Right-hand side y axis - AMPA to NMDA ratio - yellow bars ☐ . See Table 3 for the number of replicates in each group. Error bars indicate standard error of the mean.

for the naïve group and the 24 hour group was close to significance when analysed with the LSD post-hoc test (p = 0.064), but this was not supported by Tukey's HSD test (p = 0.22).

## Numerical density of labelled synapses

The values of average PSD surface area per synapse, $S_N$, that were calculated from morphological data are independent of any reference area or volume. Because samples used for morphology and immunolabelling were taken from the same animals, the synapses can be considered to be part of the same population. Therefore, the density of immunolabelled synapses ($N_V$) can be calculated from the value of $S_V$ for labelled synapses and $S_N$ by rearranging Equation 11 to make $N_V$ the subject. This calculation was performed for all the groups in both the AMPA and NMDA immunolabelling experiments, and the results are shown in Figure 44. The density of AMPA-labelled synapses is 0.107 synapses per $\mu m^3$ of tissue in the naïve group. The 3 hour group (0.143) and the 9 hour group (0.157) both have a higher density of synapses than the naive group, as does the 24 hour group (0.114), but this value is only slightly higher than naïve. None of these differences were statistically significant ($F_{[3,7]} = 1.129$ ; p = 0.380).

The density of NMDA-labelled synapses shows a different pattern of changes, being reduced at 3 hours (0.030) and at 24 hours (0.022), but increased at 9 hours (0.070) with respect to naïve group values (0.049). Although ANOVA analysis indicated that these were non-significant differences ($F_{[3,10]} = 2.733$ ; p = 0.083), the value is approaching significance. As conducted before, the LSD post-hoc test indicates that the 9 hour group is significantly different to both the 3 hour group (p = 0.039) and the 24 hour group (p = 0.022), and the values obtained by using Tukey's HSD test are close to significance (p = 0.15 and p = 0.09 respectively). The ratio of AMPA-labelled synapse density to NMDA-labelled synapse density is smallest in the naïve group (1.928:1), greatest in the 24 hour group (10.683:1) and intermediate in the 3 hour group (6.117:1) and 9 hour group (2.879:1), but statistically, the groups are not significantly different ($F_{[3,7]} = 2.283$ ; p = 0.136). The LSD post-hoc test indicated that the difference between the naïve group and the 24 hour group was close to significance (p = 0.064), but Tukey's post-hoc test suggests that this is not the case (p = 0.22).

123

# Discussion

## Did learning occur after water maze training?

That memory formation in the adult brain involves changes to the synaptic connections of neurons is a well-established phenomenon **(Bailey and Kandel, 1993)**. Donald Hebb's theory that this involves alterations to synaptic efficacy is accepted as a probable way for learning-induced changes to occur **(Bi and Poo, 2001; Martin *et al.*, 2000b; Weinberger, 1995)**. The convergence of temporally similar inputs can be associated and assimilated by neurons, such that the pattern of neuronal activity, and hence behaviour, is adapted. Hippocampal activity is important for learning strategies to complete the Morris water maze, as demonstrated by lesion studies **(Morris *et al.*, 1982; Moser *et al.*, 1995)**. The activation of NMDA receptors is also reported to be involved in aspects of particular types of learning, because pharmacological NMDA receptor blockade with D-2-Amino-5-phosphonovalerate (D-AP-5) impairs recall of a matching-to-place task **(Steele and Morris, 1999)**.

With regard to the Morris water maze paradigm, D-AP-5 also impairs learning and successful performance. However, experiments by Bannerman *et al.* and Saucier and Cain indicate that only certain aspects of learning in the Morris water maze that relate to particular components of the strategy used to solve the task are susceptible to D-AP-5 treatment. Non-spatial pre-training using a visible platform was used to familiarise animals with the general water maze environment and the process of finding a platform in the pool to treat as a refuge of escape from the water, and it was found that subsequent learning of the task to find the hidden platform would not be impaired by D-AP-5 treatment **(Saucier and Cain, 1995)**. Similarly, pre-training using a hidden platform, but in a visually different spatial environment (downstairs water maze) meant that rats also learnt to find the hidden platform in the original spatial environment (upstairs water maze), despite D-AP-5 treatment **(Bannerman *et al.*, 1995)**. The 'pre-training' effect indicates that learning the strategy to find the platform is NMDA receptor dependent, but not the mechanism to remember the platform location.

Bannerman *et al.* also investigated non-spatial pretraining (downstairs) using a randomly varying hidden platform location, so that no preference for any particular quadrant was learnt by the rats, and this also enabled the animals to learn the water

maze task (upstairs), again despite D-AP-5 treatment, whereas cytotoxic hippocampal lesions did prevent water maze learning (upstairs) despite spatial pretraining. These results indicate that the water maze task is solved by rats using several behavioural components, such as knowing what to do and how to do it, as well as where to go to find the platform. Also, although the specific learning for the location of the platform is not dependent upon NMDA receptor activation, functioning activity of the hippocampus is involved in this process. It would be interesting to know what effect purely spatial training would have on subsequent learning (i.e. passive familiarisation with the learning environment by placing the animal onto the submerged platform and only allowing it to sit and observe it's spatial location, rather than acquire any experience about swimming), and whether this would result in learning of the task despite D-AP-5 treatment. This component of the learning must also be turned into a long-term memory in order for the animals to show improved performance from one day (trial) to the next, but this obviously occurs via a mechanism other than NMDA receptor-mediated $Ca^{2+}$ influx.

The results conflict with other learning studies **(Caramanos and Shapiro, 1994)**, but this discrepancy may be due to differences between working and reference memory. Working memory rapidly stores information and the changes at synapses which encode this information must therefore also be very rapid. Such changes may involve short-term modification of neurotransmitter release and the activity of receptors, as well as the synchronous rates of electrical activity that these processes will influence **(Singer, 1999)**. Analysis of the morphological and molecular aspects of the synaptic connections of neurons involved in the acquisition of a hippocampus-dependant reference memory task would therefore enable us to evaluate the effects of this learning on synapses. Of note is the fact that LTP induction in the same animals was blocked by the D-AP-5 treatment in all experiments, despite the fact that learning had occurred, suggesting that LTP is not related to these spatial aspects of learning, but it cannot be concluded that LTP is related to the acquisition of the swimming strategy components.

The transfer of information into long-term memories does not occur instantly, instead taking several hours, and is dependent upon calcium signals to the nucleus which initiates gene transcription and protein synthesis **(Bernabeu et al., 1997; Nader et al., 2000)**. Such events typically take place within 3 to 6 hours after learning **(Bourtchouladze et al., 1998; Quevedo et al., 1999; Scheetz et al., 2000)**, and so it is

pertinent to investigate time-points after learning that reflect whether or not the results of such events will be apparent. The groups investigated in this thesis reflect short (3 hour group), medium (9 hour group) and longer (24 hour group) durations after the start of training that relate to timepoints prior to (3 hour group), shortly after (9 hour group) and a longer delay after (24 hour group) the occurrence of these protein synthesis events. These groups would therefore allow the investigation of whether the effects of learning-induced protein synthesis on morphological changes possessed a temporal gradient.

The groups also relate to small (3 hour group), medium (9 hour group) and large (24 hour group) amounts of training, and it could be argued that the groups are not equivalent in terms of the amount of protein synthesis induced by training. This problem was not addressed in this thesis, but could have been investigated by the use of immunohistochemical techniques such as *in situ* hybridisation or autoradiographic detection of particular gene transcripts or proteins relevant to learning (e.g. *c-fos*, *cre* and the CREB protein, *arc* and the Arc protein) to determine possible differences between groups in the degree or amount of transcription and/or protein synthesis.

In terms of memory formation, the significant preference for quadrant 1 observed in the 9 and 24 hour groups upon quadrant test is likely to have been reinforced by the greater number of training trials when compared to the 3 hour group. Completion of consolidation processes may require several hours, and may thus only have a significant effect on performance at longer intervals after the start of training, such as in the 9 hour and 24 hour groups. Learning may also have been facilitated by the spaced nature of the training sessions in these groups, as is suggested by work using *in vitro* preparations of hippocampal neurons **(Wu et al., 2001)**. However, it is still possible to form long-term memories using a massed training protocol **(Akirav et al., 2001)**, and it is highly probable that such memories were in the process of being formed in the 3 hour group, despite only one session of massed trials. This conclusion is supported by evidence of long-term memory storage after a five-water-maze-trial training session procedure used in previously published work **(O'Malley et al., 2000)**, as well as manuscript comments of other authors, who indicate that rats learn very rapidly, and that the results of this can often be seen after only four learning trials **(Bannerman et al., 1995; Steele and Morris, 1999)**.

Analysis of the quadrant test data indicated that animals in the 3 hour group did not perform as well as the other groups in learning the location of the platform, because they did not spend a statistically longer time in the correct quadrant. However, learning was apparent from the measurements of latency, which showed a consistent reduction in the average time taken for animals to reach the platform. This reduction was statistically significant for several of the later trials in both the 9 hour and 24 hour groups, as well as the fourth trial in the 3 hour group. Importantly, the pattern of latency reduction over the first four trials was very similar between all groups, which suggested that the process of long term memory storage was taking place in the 3 hour group animals, but that it was less advanced than the 9 hour and 24 hour groups. As mentioned above, work by O'Malley *et al.* **(O'Malley *et al.*, 2000)** suggests that animals in the 3 hour group would go on to consolidate the memory for platform location, although this is not proven.

Because the behavioural paradigm used is quite complex, involving spatial cues, swimming activity and a certain amount of stress, it was also deemed important to have an active control group in addition to completely naïve animals. This would allow the identification of changes specifically related to the task of locating the platform, rather than other aspects of exposure to the learning environment. This 'swim-only' control was matched to the 9 hour group in swimming duration, but never experienced the occurrence of a platform in the pool. Quadrant test data was not collected for this group, but it would have been instructive to determine the swimming behaviour of these animals in some way, as they would be predicted to have no preference for any particular quadrant. With reference to the above discussion, this group would differ in that they would not learn any of the components of a strategy for finding a platform, swimming to a particular goal, location, or with any expectation of escape except that dependent upon the investigator at the end of the predetermined swim time.

Use of a non-spatial learning control group would have provided useful information regarding these different aspects of the water maze strategy. A visible platform control would allow morphological investigation of the effects of the goal-driven behaviour of swimming to the platform, but a concern is that this would not be the same as swimming to an unseen platform. This possible problem could be circumvented by the use of a control in which the platform location was randomly changed from trial to trial. This control group would thus have the experience of swimming in a goal-

oriented manner and searching for a hidden platform, but would not be able to reliably predict the spatial location of the platform from experience of prior training trials. Therefore, these two controls together could possibly be used to determine the effects of these different components of searching strategy on the morphology of the dentate gyrus.

## Do synaptic population changes occur after water maze training?

In chicks, numerical density and the size of dendritic spine synapses has been shown to alter in different brain regions at different time-points after one trial passive avoidance learning **(Doubell and Stewart, 1993; Hunter and Stewart, 1993)**. In rats, both passive avoidance and water maze learning have been shown to influence the density of dendritic spine profiles **(O'Malley et al., 1998; O'Malley et al., 2000)**. The synapse density measurements in this thesis indicate that there were changes to the $N_V$ of NAS synapses in each group. However, only the value of the 9 hour group is significantly different, being greatly increased compared to all other groups. The lack of any significant increase in synapse density of the swim only group indicates the likelihood that the morphological changes are specifically associated with learning to find the submerged platform.

The mean synaptic density of the 3 hour group was very similar to naïve animals, but there was no significant retention of the memory by these animals. The lack of significant synapse density change in the 24 hour group meant that there was no simple correlation between an increase in the number of training trials and an increase in $N_V$. More training after the 9 hour time-point did not result in a greater $N_V$ in the 24 hour group, or even a sustained value similar to that of the 9 hour group. This latter point suggests that an important factor in the occurrence of morphological changes was the duration of, and/or time after the start of, training. Animals in the 24 hour group would presumably have experienced an increase in $N_V$ and a decrease in PSD area after nine hours, because they received similar training in the water maze.

However, these changes are no longer evident 15 hours later at the 24 hour timepoint, and this would lead to the suggestion that remodelling of synaptic circuits has occurred and been completed in the 24 hour group. As such, the morphological parameters are very similar to naïve animals, but may have subtle differences that are not apparent in

the parameters investigated in this study. An example of such changes is demonstrated by the changes in intersynaptic distance observed 6 days after training (**Rusakov *et al.*, 1997**). The data in this thesis also suggests that the change at 9 hours reflects part of the remodelling process involved in changes to these 'second order' parameters. The increased synapse density could be achieved by *de novo* axospinous synapse formation, or the splitting of perforated axospinous synapses. These possibilities are shown diagrammatically in Figure 45.

The density measurements for non-perforated axospinous synapses are consistent both between left and right hippocampi, and also between individuals within each group, indicating a degree of robustness in the data. Linear measurements of the neuropil thickness indicated a significant difference between animals that were perfused at different times of the year, but the data is similarly robust between hemisphere and for animals in the same group within each set of perfusions. If these two sets of data are examined independently, the values of each group and the statistical analysis indicate a similar result. This validates using the correction factor derived from the neuropil thickness measurements to combine the data. It also indicates that the statistically significant, transient morphological changes observed in the 9 hour group are robust. This data agrees with other published work, using both behavioural (**O'Malley *et al.*, 1998; O'Malley *et al.*, 2000; Sojka *et al.*, 1995**) and electrophysiological approaches (**Engert and Bonhoeffer, 1999; Geinisman *et al.*, 1991**) which indicate morphological changes occur after learning and learning-like paradigms.

The conclusion that synaptic density changes were transient was supported by calculations of the synapse to neuron ratio for each group. Stereological calculations of granule cell density for each group did not show any significant difference between groups or hemispheres, and individual values were comparable. Learning has been shown to play a role in enhancing the survival of newly generated dentate granule cells, and a recent study has indicated a role of neurogenesis in eyeblink trace conditioning, whereby reductions in the number of newly generated neurons was associated with a reduction in the percentage of conditioned responses. This was specific to the neurogenesis because no reduction was seen in animals similarly treated to prevent neurogenesis but given delay conditioning, a learning paradigm that does not require the animal to associate stimuli that are separated in time, and is not dependent upon the
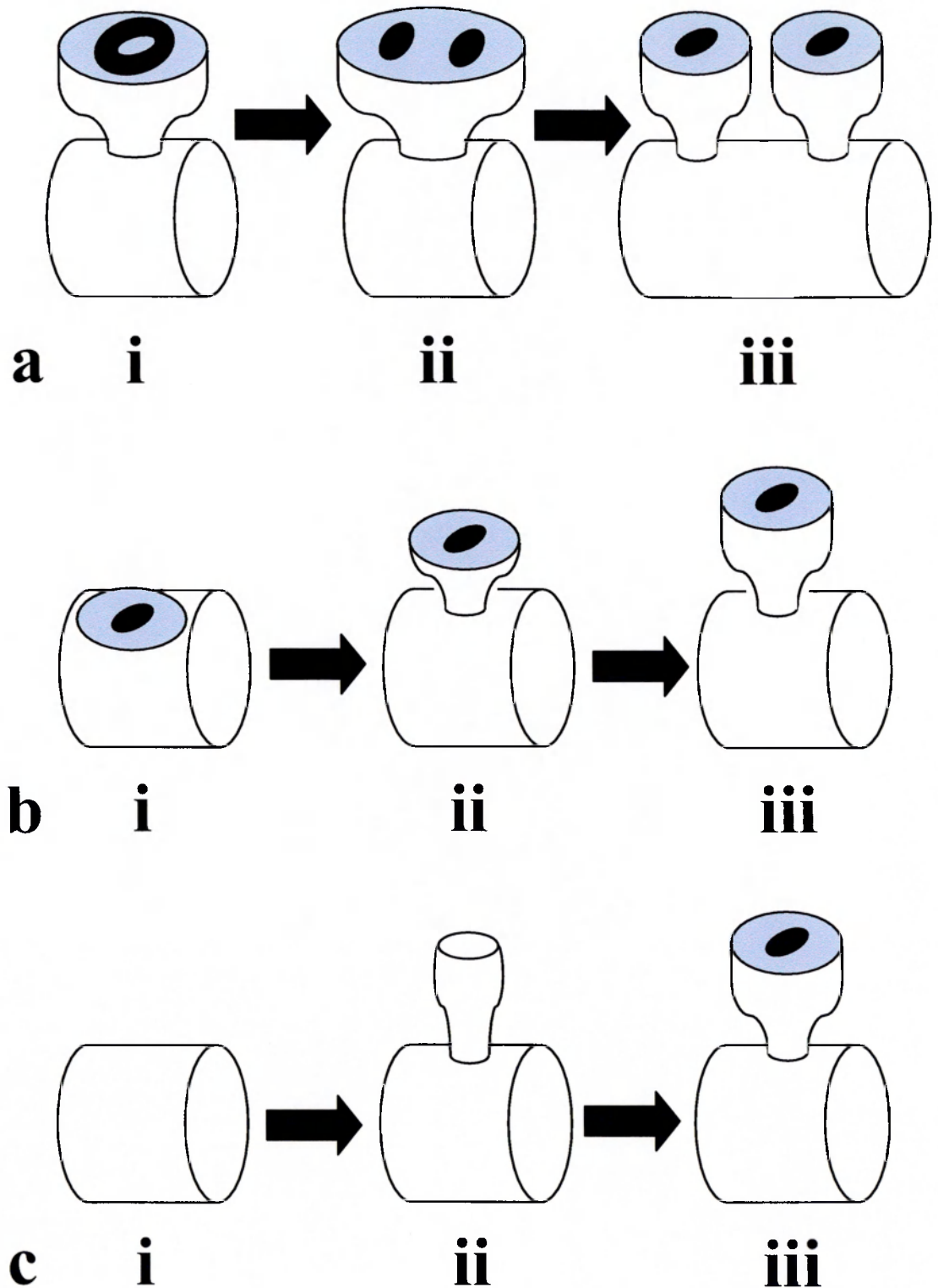
Figure 45 - Morphological mechanisms of synapse remodelling – a) large spines grow
(i), become perforated (ii), and then split into two new small spine synapses (iii). b)
axodendritic synapses (i) are pushed out from their dendritic location (ii) to form
axospinous synapses (iii). c) non synaptic dendrites (i) produce new filopodial
outgrowth (ii) which then take shape as spines and form synapses (iii). Adapted from
Carlin, 1983 and Jones, 1995.

hippocampus **(Shors *et al.*, 2001)**. These studies indicated that the newly generated cells are involved in the learning process, and theoretically would also be involved in other hippocampal-dependent tasks, such as the water maze.

As was the case for neuropil thickness, linear measurements of the cell blade thickness were significantly different between the animals that were perfused at different times of the year. Normalisation of the cell density data by the use of a calibration factor derived from these cell blade thickness measurements did not result in any changes to the significance of the differences between the groups (and in fact made the data more homogenous). Because no differences in granule cell density was observed in any of the groups examined in this thesis, the effects of any ongoing neurogenesis would appear to be minimal in terms of altering synapse to neuron ratios and the other morphological parameters examined.

Differences in the size of the hippocampal cellular and dendritic layers between animals perfused one year apart could result from several sources. The two groups of animals were perfused with two different types of fixative, the first designed to favour preservation of antigenicity and the second to preserve primarily ultrastructure (see Appendix A). Although the processing of samples for morphological analysis was conducted in a similar manner, this difference in the initial fixation by perfusion may have introduced a variable that affected morphological parameters. An additional factor could be a difference between the age of the animals, although this was controlled for and estimated to be as similar as possible between groups.

The synapse to neuron ratio in the 9 hour group is significantly greater than in any other group. These other groups do not differ from each other significantly, indicating that synapse number increases at 9 hours in connection with memory for the location of the platform. Increases in CA1 synapse number have previously been claimed to be correlated with faster water maze learning by animals exposed to an enriched environment **(Moser *et al.*, 1994)**. However, the light microscopy technique used by that study is less suitable to study dendritic spines, because not all of these structures are large enough to be visualised at this resolution. Also, the presence of some spines may be masked by the dendrite, and it was assumed that all spines contain one synapse, which is now known to be an incorrect assumption **(Stewart and Popov, paper in preparation)**.

Unbiased stereological techniques coupled with electron microscopy have been used previously to estimate the density of dendritic spines in the dentate gyrus after water maze learning, and indicate a significant increase 6 hours after training (**O'Malley et al., 2000**). Quantitative differences between studies may have arisen because the study by O'Malley et al. analysed the occurrence of dendritic spine profiles, whereas the results of this thesis are based on the analysis of morphological structures associated with synapses; the PSD, synaptic cleft and presynaptic vesicle cloud. The results here permit a more meaningful comparison between different experimental groups by enabling calculation of synapse to neuron ratios, which can be used as a normalised measure of the synaptic input onto the middle molecular layer of dentate granule cell dendrites.

The total number of synaptic contacts onto CA1 pyramidal cells of naïve adult rats has been calculated to lie in the region of 30,000 excitatory inputs (**Megías et al., 2001**). The total dendritic length of CA1 cells is typically about 13,000 μm, a value that is approximately three times that of dentate granule cells. This is typically around 4,000 μm, of which 30% is contributed by the middle molecular layer (**Claiborne et al., 1990; Ishizuka et al., 1995**). Although such data has not yet been published with regard to dentate granule cells, if a similarity in the density of dendritic spines between the two cell types is assumed, the above data can be used to approximate the number of excitatory synapses onto the middle molecular layer to be in the region of 2,770 inputs. This number is similar to the number of contacts per cell that can be derived from the synapse to neuron ratio of animals in the naïve control group.

The synapse to neuron ratio is a fractional value based on the comparison of two densities calculated separately. This is not the same as calculations of the number of synapses per neuron, which would require information about the volume of the various parts of the hippocampus. The application of the additional stereological techniques necessary for the acquisition of such information would be methodologically incompatible with the techniques used. However, although synapse to neuron ratio is not as powerful as data concerning total synapse number, it does provide a good indicator of the degree of overall synaptic connections in the middle molecular layer.

As observed for synapse density, the differences between synapse to neuron ratios indicate that the number of synaptic inputs transiently increases nine hours after training commences, but this significant increase does not occur in swimming animals which are not trained to find the platform. Swimming in the water maze may trigger some aspects of learning, because the maze could be considered an enriched environment compared to the home cage of an animal, and indeed slight differences are seen in the swim only control compared to naïve control. However, whereas synapse density shows an increase, synapse to neuron ratio shows a decrease, indicating that the swimming experience does not appear to contribute to the learning-induced changes in synapse number.

## Do spine morphology changes occur after water maze training?

Dendritic spines exhibit a high degree of heterogeneity. Larger synapses present on larger spines will have greater numbers of ion channels in the cell membrane and more ionotropic neurotransmitter receptors at synaptic sites **(Takumi *et al.*, 1999)**, as well as a greater number of presynaptic release sites. In turn, this will mean that larger synapses have a greater effect upon the postsynaptic cell. Synaptic size is therefore an important variable when considering the summation of inputs by neurons, because it is related to their functional capacity. Because learning and memory storage is believed to involve changes to synaptic strength, this is likely to result in changes to the size of a synapse.

## Synapse size

Mean synaptic height is a stereologically derived value that is directly related to the size of synapses, and provides a useful representation of their relative size. Mean synaptic height is significantly reduced in the 9 hour group compared to naïve controls, whereas this is not the case for the swim only group animals, which show a much smaller decrease. Synapses in the 3 hour group show a slight decrease in mean height, but this is not significantly different to any other group, being half way between the changes seen in the 9 hour group and both control groups. The 24 hour group value is very similar to both controls, showing a slight increase in synapse size. These results suggest that mean height transiently decreases with training, which is most evident 9 hours after training, with values subsequently returning to, or even overshooting, naïve

levels. Therefore the transient increase in synapses is coupled with a simultaneous transient decrease in their average size. This increase in the presence of smaller synapses in the overall population is consistent with the formation of new connections that have not yet matured into larger mushroom or perforated types, as mentioned above.

Calculations of $S_N$ provide a direct measure of the average area of PSD per synapse. A significant reduction is seen 9 hours after training compared to naïve control, indicating that the average size of synaptic transmission zones is reduced. No such reduction in $S_N$ is observed in the 3 hour group or the swim only group, consistent with a lack of long term learning in both groups. However, there are also no significant changes in the 24 hour group, indicating that the time after training is also important, and suggests that the change in the average PSD area of synapses is also transient. As with synapse size, the smaller average synapse PSD area observed in the 9 hour group is consistent with a greater number of smaller synapses present in the total population. These may well be new synapses in the early stages of maturation, as proposed in Figure 45.

Average synapse PSD area may also be greatly affected by synapses becoming perforated, as the conversion of non-perforated to perforated synapses probably involves larger dendritic spines. This would mean that the larger NAS synapses would have to be classified as PAS synapses, and so the NAS group would contain less large synapses with large synaptic areas. If small synapses are also being generated at this time, NAS synapse numbers would not greatly change, but the population would consist of more small synapses. The occurrence of perforated synapses is greater after LTP **(Geinisman, 1993; Itarat and Jones, 1993)**, which suggests the possibility that this process may also occur after learning. Such a change in the population could have been investigated by examining the distribution of synapse sizes in the NAS group. This would involve comparison of the average of synaptic PSD profile length in digital images, and investigation of the variability and distribution of PSD sizes. Although this method may be subject to stereological bias, and ideally 3-dimensional reconstruction would be preferable, it would have given some indication of the occurrence of such changes in the synapse population.

The area of PSD per unit volume of tissue, $S_V$, was also calculated, and provides an intriguing result. None of the mean values for the trained groups differ significantly

from the naïve control, suggesting that there is no change in the overall area of postsynaptic density contacting the dentate granule cells. However, when differences between the groups are examined, there is a significant difference between the 3 hour group compared to the 9 hour group, and the 3 hour group compared to the 24 hour group. This suggests that training is having an effect on $S_V$ by increasing the size of total excitatory input onto dentate granule cells. The initial decrease seen in the 3 hour group suggests that there is also a counteracting effect that appears to be time-dependent.

This is also demonstrated by the PSD area to neuron ratio, which suggests that swimming alone causes a reduction in this ratio. Neither the 3 hour group nor the swim only group learnt the water maze task, and their statistical difference from the 24 hour group, which did learn the task, suggests that there is a disparity between swimming in the pool environment and learning the water maze task in terms of PSD area to neuron ratio. There is a trend towards a greater total area of PSD ($S_V$) in the 9 and 24 hour groups, suggesting that an increase in contact zone area is connected with increased synaptic efficacy as a result of learning, and that this is counteracting some reducing effect on the ratio that is time-dependent and occurs in the swim-only controls.

Could there be a connection between synapse density ($N_V$) and synapse area ($S_N$) such that a constant total average area of apposition zone ($S_V$) is maintained despite morphological changes? This conclusion is reached regarding the total synapse population after LTP **(Desmond and Levy, 1988)**, although these significant changes were observed in the concave (i.e. perforated) synapse population. Statistically, the similarity in the $S_V$ to neuron ratio for each group suggests that this could be the case, but graphically there is evidence for slight changes and larger error values for the 3 hour and 24 hour groups, suggesting that some changes are occurring. Other studies in samples from rats and humans have shown that $S_V$ is reduced only in aged or Alzheimer's disease cases **(Bertoni-Freddari *et al.*, 1990; Bertoni-Freddari *et al.*, 1986)**, but this does not directly relate to changes during learning, and the accuracy of such data are questionable as unbiased stereological techniques were not used.

It is apparent that the initial stages of learning, prior to long term memory formation involve a small reduction in the average number and average size of non-perforated synapses, as shown by data from the 3 hour group. The average PSD size of the

synaptic population ($S_N$) is similar to naïve values, albeit more variable, suggesting that individual synapses maintain the size of postsynaptic specialisation involved in neurotransmission, implying the same level of function. This is reflected in the slight reduction of total potential synaptic input, which is the sum of the PSD area of all synapses. A reduced synapse to neuron ratio could be explained by the elimination of synapses **(Ehlers, 2000; Turigiano and Nelson, 2000)**. Synapses show very rapid actin-based motility, and their structure can be rapidly destabilised and disassembled after stimulation with glutamate **(Halpain, 2000)**. It may also be due to the conversion of NAS synapses into perforated axospinous or axodendritic synapses (see Figure 45).

The increased variability of $S_N$ suggests that both processes may be occurring, especially as $S_V$ does not change significantly, but they are insufficient to produce retention of the memory three hours after training. This possibility could have been investigated statistically by examining differences in the degree of variance amongst the groups, to investigate if there was more diversity in the sizes of the synaptic population in the 3 hour group. Although measurements from 3-dimensional reconstructions would have been ideal, differences may be detectable from the variance amongst the samples from each animal, and possibly the variance within each set of measurements for each animal may have helped to determine if the synaptic population was more diverse in the 3 hour group.

Conversely, nine hours after training, animals show significantly increased memory for the location of the hidden platform. These animals have significantly increased NAS synapse density (and synapse to neuron ratio), but significantly decreased average size of synapses (mean height) and average PSD area per synapse ($S_N$). Because neurogenesis and new axonal connections are not likely to occur at this time-point after learning, the new connections must be formed with the existing population of perforant path axons that project from the entorhinal cortex. The constancy of $S_V$ implies that as well as new synapse formation, some shrinkage and/or elimination of synapses from the NAS synapse population may also occur. Because individual neurons cannot be traced over time, it is not possible to determine whether any such new connections arise between previously unconnected entorhinal axons and granule cell dendrites.

Some strengthening of existing connections is conceivable, as they may be relevant to the new memory, and this may involve the formation of new connections in addition to

the modification of the existing ones. However, the increase in the diversity of connections would be important for the formation of new associations by the hippocampus. If new associations are to be made by the animal and stored as memory, it is clear that novel connections may need to be made between previously unconnected cells. The presence of branched spines and multiple synapse boutons are good indicators of increased diversity of connections **(Geinisman *et al.*, 2001; Harris, 1999)**, because their presence shows that individual axons are contacting several postsynaptic target cells, which increases the heterogeneity of excitatory inputs onto postsynaptic cells. Unfortunately this can only be completely assessed by the 3-dimensional reconstruction of serial sections which was beyond the scope of the present project.

Interestingly, the overall potential excitatory input in the 9 hour group, as measured by $S_V$ to neuron ratio, is similar to that of naïve animals. This poses the question of whether the dentate granule cells control their total (maximum) excitatory input. Such control may possibly serve a neuroprotective role, in much the same way as dendritic spines have been proposed to be neuroprotective **(Segal, 1995)**, by limiting the flow of $Ca^{2+}$ into the cell. Because the hippocampus is involved in associative memory formation, a larger number of smaller and more diverse inputs may summate to produce a greater effect than larger inputs from the same source, which may be less numerous.

For the formation of an associative memory, the increased number of connections may be particularly useful for the detection of synchronous activity. More connections facilitate a greater number of convergent inputs onto the same postsynaptic neuron arising from different cells, and this is particularly relevant if the presynaptic cells arise from different functional brain areas and subserve different aspects of sensory processing. This may be important for learning and the associative changes envisioned to occur under the Hebbian learning rule **(Bi and Poo, 2001; Turigiano and Nelson, 2000; Weinberger, 1995)**, and is likely to occur in the dentate gyrus because of the diverse nature of the cortical inputs that contribute to the sensory information transmitted by the perforant path (see introduction).

Because Hebbian synaptic modifications would favour biochemical $Ca^{2+}$-mediated signalling by way of synchronous activity and NMDA receptor activation, synapses

activated in this way would be preferentially enlarged and would thus exert more of a postsynaptic effect. This mechanism would seem likely for at least some of the strategy components of the water maze task, but other aspects of this learning not sensitive to NMDA receptor blockade may also involve $Ca^{2+}$, possibly via G-protein or voltage activated calcium channels. Use of a non-spatial random platform pretrained animal followed by pharmacological NMDA receptor blockade during spatial training may be able to distinguish between these two mechanisms in terms of effects on morphological parameters.

The results of the swim only control provide strong support for the view that learning is specifically involved in the induction of morphological changes. Despite swimming in a comparable manner to the 9 hour group, the lack of learning is paralleled by a lack of any significant morphological changes. Only slight reductions in the synapse to neuron ratio, mean height, $S_N$ and $S_V$ are seen compared to naïve animals. There was a reduction in the $S_V$ to neuron ratio, but this was not significant and also contrasts with the result of the 9 hour group. However, in the 24 hour group, the number, size and PSD area of the synapses are all comparable to naïve animals. The measures indicating the total synaptic input ($S_V$ and $S_V$ to neuron ratio) are only slightly increased, despite even greater memory retention. One argument against this conclusion is the possibility that the swim-only control does not learn any strategy related to escaping from the water, and that is why there is no change in the morphology of the synapses. However, at least some learning concerning the pool and the environment must occur, which can be considered as a different, even an enriched environment compared to the home cage, and exposure to such an environment has been reported to increase synapse density **(Moser et al., 1994)**.

The data indicates that the morphological changes are transient, which would seem to be consistent with evidence in humans that suggest memories do not permanently reside in the hippocampus but move into the cortex for long term storage **(Milner et al., 1998; Nadel and Bohbot, 2001; Squire, 1992)**. This has also become synonymous with a link between short-lasting memories that are then sequentially followed by long-term memories. However, other research suggests that such a mechanism of memory consolidation may be oversimplified. Activity in the amygdala appears to be well correlated with memory for highly emotive stimuli **(Cahill et al., 1996; Hahmann et al., 1999)**, and several different brain regions are involved in the formation of different

memory types, indicating that such tasks are not solely the domain of the hippocampus (Izquierdo *et al.*, 1998; Packard *et al.*, 1989; Packard and White, 1991).

The hippocampus has been reported to be unnecessary for visual stimulus associations (Murray *et al.*, 1993), but is important for spatial mapping (Pearce *et al.*, 1998). The conflicting findings of certain reports suggest the possibility that several memory systems operate in parallel, e.g. hippocampal and cortical, but at different speeds (Nadel and Bohbot, 2001). This suggests that short- and long-term memory formation are not necessarily sequential, which is supported by evidence that injection of certain drugs will block short-term memory but not long-term consolidation (Izquierdo *et al.*, 1998).

Evidence from studies of amnesic patients also argues for a more complex system. Retrograde amnesia with a temporal gradient, such that more remote memories are recalled better, argues against that the hippocampus has a temporary involvement in memory. However, such gradients vary according to the locus and extent of brain injury, and also the memory to be recalled. In some cases, complete (non-graded) retrograde amnesia (a lack of memory for events irrespective of how long ago they occurred) in patients with MTL damage suggested that the hippocampus is a site for memory storage, or at least is required for successful recall (Carew and Sutton, 2001; Nadel and Bohbot, 2001; Sacchetti *et al.*, 2001). Lesion studies have shown evidence for impairment of prior, supposedly consolidated learning (Cho *et al.*, 1993; Reidel *et al.*, 1999; Zola-Morgan and Squire, 1990). However, it is difficult to distinguish between a lack of storage and an inability to recall, as both produce the same effect. In human subjects, patients with MTL damage were considered not to recall the same level of details as controls, prompting the suggestion of multiple memory traces (Nadel and Moscovitch, 1997).

Memory retrieval may occur by way of an index stored in the hippocampus, which pieces together the memory from remote cortical stores. If this is so, then retrieval will reactivate an old memory, triggering a new encoding, and some evidence for this exists (Nadel and Bohbot, 2001). This possibility was investigated in a recent paper using fear conditioning and injection of the protein synthesis inhibitor anisomycin into the amygdala, and has raised questions regarding the permanence of seemingly consolidated memories (Nader *et al.*, 2000). Animals trained to associate a tone with

an electric footshock were given a reminder 14 days after training, shortly followed by anisomycin injection into the lateral and basal nuclei of the amygdala. Upon subsequent testing, animals did not freeze in response to the tone, indicating that the associative memory had been lost. Such a loss of memory was not seen in anisomycin-treated animals that did not receive a reminder prior to injection. It would therefore seem that reactivation of a fear memory stored in the amygdala reactivates the storage process, replacing the old with the new. A similar disruption pattern is also seen if the hippocampus is lesioned, rather than anisomycin injection into the amygdala; reminders just prior to surgery return a hippocampal-independent consolidated memory to a fragile, hippocampal-dependent form **(Nadel and Bohbot, 2001).**

## Mechanisms of change

Could reactivation of a memory, and the associated re-encoding, occur in the hippocampus during learning of the water maze task? This would seem possible, and has implications for the results of this thesis. Successive training trials in the water maze would become a reactivation of the learning that occurred in the very first trial, and would render the memory fragile. Each trial may therefore activate protein synthesis, and suggests that multiple waves of synaptic morphological change ensue upon each learning event. This is consistent with the multiple trace theory, either in the same set of neurons, or a subtly different set (but still involving the hippocampus). Contextual processing by the hippocampus has been shown to occur **(Good and Honey, 1991; Maren and Holt, 2000; Wincour, 1997)**, and may be an explanation for the renewed dependence of retrieved memories upon the hippocampus. Indeed, protein synthesis after memory reactivation may be behaviourally relevant, because it would permit modification of the memory representation by novel or relevant stimuli, enabling animals to adapt to changes in their natural environment, i.e. new contexts.

Morris water maze training requires several trials before a learning response can be observed, and it is difficult to determine at what stage memory for the location of the platform is formed. Unlike one trial passive avoidance or fear conditioning, there are several sequential events involved in the formation of water maze memory. The first trial, the last trial or the gradual incremental information supplied by all trials may be the dominant factor in producing the synaptic modifications that result in memory. However, because the four trials that make up one training session are relatively close

together, each training session could be considered as one single learning event with respect to other sessions. The wave of protein synthesis generated by such a training session is taken to be maximal between 3 and 6 hours later, as is the case in the hippocampus after inhibitory avoidance learning mentioned above (**Bernabeu et al., 1997; Bourtchouladze et al., 1998**). If each training session in the water maze is considered as one event, sequential sessions may therefore initiate multiple phases of protein synthesis, and render the memory vulnerable to disruption by anisomycin. However, because of the similarity of training in each water maze session, the memory will be reinforced, despite the proposed protein synthesis-induced increase in the fragility of the memory.

Previous water maze experiments indicated that synaptic remodelling involving clustering of synapses has occurred in CA1 (but not dentate gyrus) 6 days after water maze training (**Rusakov et al., 1997**). O'Malley et al. have shown that a transient increase in spine profiles takes place in the dentate gyrus 6 hours, but not 1 hour or 72 hours post-training (**O'Malley et al., 2000**). The data in this thesis further defines the boundaries of the time period during which morphological changes take place after water maze training, indicating that changes commence later than three hours after the initiation of training, and appear to be completed in the dentate gyrus 24 hours after the start of training. Disruption of long term memory formation by injection of anisomycin indicates that protein synthesis is required both initially and 4 hours after contextual fear conditioning (**Bourtchouladze et al., 1998**). It would be interesting to examine whether such inhibitors prevented the synaptic changes seen here 9 hours post-training. Given the work in rodents (**Bourtchouladze et al., 1998; Quevedo et al., 1999**), and chicks (**Sojka et al., 1995**), this would seem highly likely. It would also be beneficial to determine if the morphological changes are blocked by NMDA receptor antagonism, and whether pre-training would result in the recovery of these changes or not.

Similarly, increases in cAMP and phosphorylated CREB are seen shortly after training in an inhibitory avoidance task, and again between 3 and 6 hours after training, and manipulations of the cAMP-CREB pathway interfere with memory formation at these times (**Bernabeu et al., 1997**). Evidence indicates that polysialation of the neural cell adhesion molecule at similar time-points is necessary for passive avoidance learning (**Doyle et al., 1992**) and water maze learning (**Arami et al., 1996**). The polysialation of these structural molecules promotes conditions favourable for morphological plasticity,

141

and this process is governed by NMDA receptor activation (**Schuster** *et al.*, **1998**). The activation of such receptors has effects on the actin cytoskeleton *in vitro* (**Fischer** *et al.*, **2000**), and controls the localisation and transcription of mRNA for a cytoskeleton-binding protein (**Lyford** *et al.*, **1995; Steward** *et al.*, **1998**) and for CaMK II (**Scheetz** *et al.*, **2000**). Therefore, long term memory formation may require structural changes to the actin cytoskeleton, and the involvement of molecules that regulate the adherence of pre- and post-synaptic membranes, conditions that favour morphological restructuring.

Because both avoidance learning in rats and water maze learning require hippocampal activation and protein synthesis, and the time course of morphological changes is reasonably similar, the time course and sensitivity to inhibition of protein synthesis is also likely to be comparable. Therefore, any notable morphological restructuring of synapses would conceivably not commence until at least protein synthesis is fully underway, at least one, and probably three hours after training, as demonstrated after one trial passive avoidance (**O'Malley** *et al.*, **1998**) and spatial water maze learning (**O'Malley** *et al.*, **2000**). This conclusion is supported by the results of the 3 hour group, which show little or no alterations to the synaptic morphology of animals analysed three hours after the end of their single water maze training session. This is longer than the timecourse for changes observed *in vitro*, where experiments suggest that morphological changes can be seen after 1 hour following LTP induction in hippocampal slice cultures (**Engert and Bonhoeffer, 1999**). However, it is not clear if active synapses are formed at this stage or just filopodial extensions, nor if such changes are as rapid in the adult hippocampus *in vivo*, as the developing brain may be more inherently capable of dynamic change.

Animals in the 9 hour group were given three training sessions, the first two of which may have initiated maximal protein synthesis activity and could have provided the necessary molecules for morphological changes. A 6 hour group given two training sessions three hours apart would have indicated if morphological changes are initiated six or nine hours after learning, and would have allowed a direct comparison between this study and that of O'Malley *et al.* (**O'Malley** *et al.*, **2000**) to determine if the spaced nature of the training and the increased number of training trials given to the 9 hour group influenced the degree of morphological change. Thus, although it is not clear to

what extent the amount of training influences the amount of morphological change, what is clear is that task learning and morphological changes are related.

The results from animals in the 24 hour group present something of a paradox, because although they received five training sessions, they do not show any significant morphological differences to control groups. There are two possible explanations for these results. The fifth training session was conducted three hours prior to analysis, and so the presumed initiation of protein synthesis will not play any role in changing morphology for exactly the same reasons as the 3 hour group. The fourth training session was conducted 15 hours prior to analysis, and one explanation for the lack of significant morphological changes may be that the processes of morphological restructuring apparent in the 9 hour group have been completed 15 hours after the fourth training session in the 24 hour group. A 12 hour group would be useful in determining the end of the morphological restructuring phase, and would also prevent consolidation changes that are proposed to occur during sleep (Louie and Wilson, 2001), but the issue of increased training trials would have to be resolved in case continued training induced continuous protein synthesis, and hence a sustained alteration to morphology.

An alternative and more plausible explanation is that the important event in the learning process is the first session (or even the first trial), which will initiate the processes that produce increases in synapse density and the reorganisation of synaptic connections. Subsequent sessions do not necessarily promote more synaptic reorganisation, because the important changes in connections will have been initiated by the first training session. Instead, because the learning environment is unchanged, they would add to and reinforce the initial learning experience, strengthening the old and newly formed connections that are involved in the memory representation of platform location. Furthermore, the water maze task is unlike fear conditioning, and animals would learn about the task over time and alter their swimming, rather than show stereotypical freezing behaviour in response to the inescapable shock that accompanies the tone. It is unclear if the waves of protein synthesis would summate in some way, as there is presumably some limit to the rate of transcription and translation (number of ribosomes, etc.). It is also unclear if each wave of synthesis would be the same as the first. If less is added to the memories formed in the water maze upon each subsequent trial, would this reactivation be sufficient to activate protein synthesis at all? In fear

conditioning, reactivation appears to be just as effective, and have a similar timecourse as initial learning, because injection of anisomycin into the amygdala 6 hours after the reminder does not cause a loss of the reactivated memory **(Nader *et al.*, 2000)**. This may also be true for components of fear conditioning memory in the hippocampus **(Nadel and Bohbot, 2001)**, but it may not be the case for water maze learning.

Can the time-course of events be supported by the dynamics of protein synthesis mechanisms? The initiation of CREB-dependent protein synthesis involves calcium signalling, which will signal to the nucleus in a matter of seconds or minutes **(Berridge, 1998)**. Subsequent synthesis may take place in the order of minutes to hours, and may involve more than one set of genes, as is the case for immediate-early genes such as *Cre*. Another delaying factor is the transport of vesicle-bound components by microtubules, which has been proposed to occur at speeds of up to 300 μm per hour **(Schuman, 1999)**. This indicates that at least one hour is required for such transport. Targeted transport of mRNAs such as *Arc* will need some time to reach the required dendrites, as is shown by the accumulation of the mRNA after 2 hours **(Steward *et al.*, 1998)**.

Experiments using *in situ* hybridisation have shown that *Arc* expression is limited to the cell body until at least 1 hour after electrical stimulation, and Arc protein levels are elevated after 4 hours **(Lyford *et al.*, 1995)**. Local protein synthesis may be able to overcome these transport delays by "on-the-spot" synthesis, allowing faster (and more specific) alterations to synapses, as shown by increases in dendritic CaMK II levels 30 minutes after LTP induction **(Schuman, 1999)**. However, whether other mRNAs localised to dendrites encode structural molecules is currently unknown. The requirement for protein synthesis shortly after learning may occur locally, and this could produce functional tags **(Frey and Morris, 1997)** and/or molecules that regulate particular genes. These would then have to be transported to the nucleus so that the next wave of protein synthesis can be activated, which is suggested by the prevention of long term memories by the application of anisomycin 4 hours after learning **(Bourtchouladze *et al.*, 1998)**. This evidence lends support to the idea that the delay to the morphological changes (which accompany long term memory formation) is caused by the process of protein synthesis (and transport), a necessary requirement for long term memory formation.

## Other effects

The initial exposure to the novel environment of the water maze, and the forced nature of the task, mean that it is stressful for the animals. Such increased stress levels cause an elevation of stress hormone concentrations in the bloodstream, one of which is corticosterone. Corticosterone levels are increased after water maze training (Sandi *et al.*, 1997), but they may not be as high as after stressful procedures such as electric shock, restraint, or exposure to a predator (Park *et al.*, 2001; Plata-Salamán *et al.*, 2000). Long term stress and administration of corticosteroids have effects on memory, but this depends on the type of memory. Both low and high levels of corticosterone are detrimental to memory formation, whereas intermediate levels are beneficial (Diamond *et al.*, 1999; Lupien and McEwen, 1997; McEwen, 1999; Sandi *et al.*, 1997). Repeated training will increase the familiarity of the animals to the environment, which may reduce stress caused by swimming. However, because of the complex effects of stress hormones, such a change could be either good or bad for memory, and this may depend on how stress influences the capacity for plasticity at synapses (Kim and Yoon, 1998). One drawback of the experiments was the lack of a visible platform control, which may have also provided a useful control for the stress experienced by the animals. Animals placed into the water maze with a visible platform have an immediate and easily identifiable goal that the animal can directly see and swim towards. This may therefore have reduced stress to the animal caused by the extended time spent swimming in the water with no apparent possibility of escape.

Acute stress has effects on AMPA and NMDA receptor binding in area CA3, as well as a negative effect on AMPA receptor binding in CA1 and the dentate gyrus (Krugers *et al.*, 1993; Tocco *et al.*, 1991). Long term stress has been shown to cause dendritic atrophy in CA3 cells (Magariños and McEwen, 1995), and this may also have an effect on synapse density. However, it is difficult to determine the specific effects of water maze-related stress on dendritic spine morphology from the results of this thesis. Stress hormones are likely to have been raised by the first training trial, and the measurement of corticosterone levels would have allowed clarification and quantitation of the stress produced by water maze training, and the likely effect on learning-induced morphological changes. This would also have been useful in determining whether the stress experienced was indeed transitory and decreased with familiarity to the water maze, an idea that is supported by a reduction in peak corticosterone levels upon sequential days of restraint stress (Magariños and McEwen, 1995). Acute stress may

have an effect on the size and population dynamics of synapses, but these parameters may be more strongly influenced by morphological changes triggered by learning.

Work by Davies, Cordero, Sandi and Stewart shows that there is a significant reduction in $N_V$ with stress which is reversed in animals also trained in the water maze (**Davies et al., 2001**). This indicates that the effects of stress and learning counteract each other, and the results of this thesis could be interpreted as supporting this view. Whether stress levels decline or are maintained with time, the two groups that are most likely to suffer stress (swim only and 3 hour) show a slight decrease in synapse to neuron ratio, making the difference between them and the 9 hour group even greater than naïve animals.

$S_V$ and $S_V$ to neuron ratio also indicate that stress may reduce total excitatory input, as seen in the swim only and 3 hour groups. At the later time-points (9 and 24 hour groups), training may be counteracting this effect, as suggested by the significant difference between the 24 hour group and both of the groups experiencing more stress (swim only and 3 hour groups). As well as measuring corticosterone levels for the groups used here, it would be important to determine whether the swim only animals had similar levels of stress to the 9 hour group. Additional swim only controls for the 3 hour and 24 hour groups would also help in the understanding of this effect.

## Do receptor population changes occur after water maze training?

Initial exposure to the novel environment of the water maze may change the pattern of activity in the hippocampus, and would result in the formation of new place cell fields for that environment. Although difficult to measure directly, this can be inferred from changes to existing place cell field representations that occur when the cues in a familiar visual environment are changed or removed (**Best et al., 2001; O'Keefe and Dostrovsky, 1971; Wilson and McNaughton, 1993**). Initially, changes must be rapid, but also persistent, so that new information is quickly stored and incorporated into the neuronal representation. Short term mechanisms involve changes in vesicle release and ion channel sensitivity and conductance, as well as enzymatic events like the phosphorylation of CaMK II, although these phenomena only persist for a matter of minutes. However, less rapid events may subsequently ensue, such as modification to

the function, and possibly number, of CaMK II molecules present at a synapse (**Cho *et al.*, 1998; Silva *et al.*, 1992a**).

AMPA receptors are believed to occur in sub-synaptic organelles within the dendritic spine head, forming a stored pool of receptors separate from those present in the synaptic PSD (**Ehlers, 2000**). These receptors are believed to cycle between the synaptic membrane and sub-synaptic sites such as the early endosome in a regulated fashion. Changes to the electrical activity at a synapse are readily modifiable by the removal of AMPA receptors, which occurs as a desensitisation response following AMPA receptor activation, and this process targets the receptors for degradation (**Lüscher and Frerking, 2001**). Conversely, the activation of NMDA receptors causes the insertion of AMPA receptors into a synapse (**Lu *et al.*, 2001; Shi *et al.*, 1999**). This also targets receptors out of the degradation pathway and into a recycling pathway that inserts them back into the synapse. Although this evidence was accumulated from *in vitro* experiments, it is likely that synaptic strength could be dynamically controlled by the same or similar mechanisms in the intact brain.

Silent synapses are so-called because they do not convey information under normal patterns of stimulation. However, LTP protocols can transform these synapses into functional ones that do convey information, and this is proposed to be due to the insertion of AMPA receptors (**Isaac *et al.*, 1995; Liao *et al.*, 1995**). Such a process also occurs during the maturation of synapses, which are thought to initially consist of only NMDA receptors (**Liao *et al.*, 1999; Petralia *et al.*, 1999**). However, unlike AMPA receptors, NMDA receptor numbers at synapses are much more stable and are not thought to be regulated by activity in this way (**Lüscher and Frerking, 2001**).

The activation of NMDA receptors is required for the formation of long term memories, but not short term memories or memory recall after water maze training (**Steele and Morris, 1999**). Because these receptors require coincident pre- and post-synaptic activity to operate, they have been proposed to be important for the formation of associations. As well as generating EPSP's (excitatory post synaptic potentials), they also conduct $Ca^{2+}$ ions. This intracellular messenger has effects on CaMK II, kinases and phosphatases, all of which play a considerable role in synaptic plasticity.
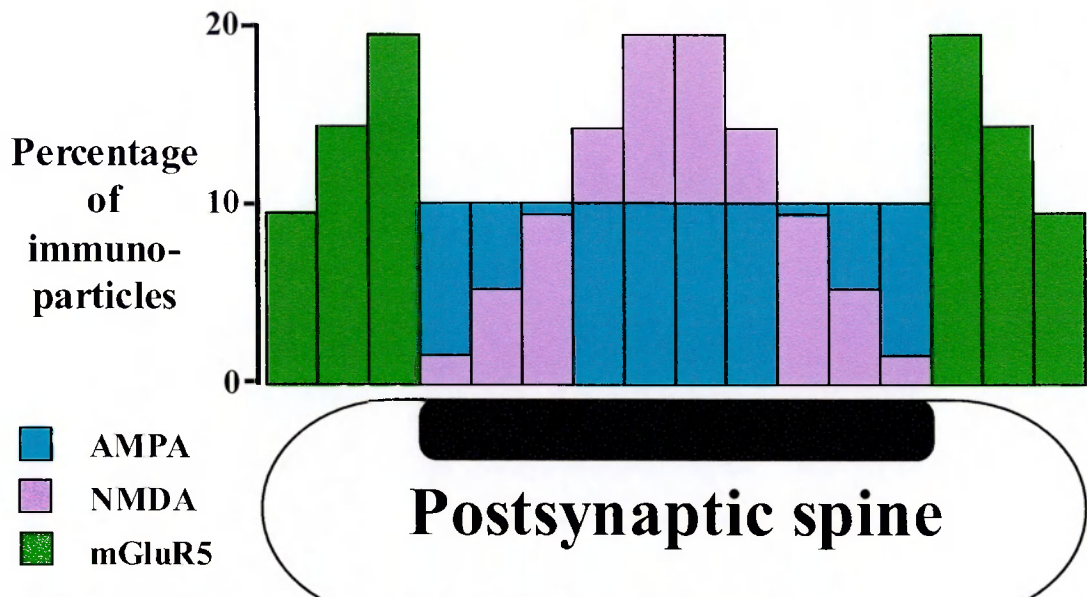
Figure 46 - The spatial localisation of receptor types at glutamatergic synapses. The percentage of immunoparticles (coloured bars) found at specific cross-sectional locations are shown in relation to the representative post-synaptic bouton beneath them. The PSD is represented by the thick black bar. Adapted from Somogyi *et al.*, 1998, and Khazaria and Weinberg, 1997.

Changes to the number of receptors present at a synapse may have an important role in the early modification of synapses that are part of learning, and can be investigated with immunogold electron microscopy. Both AMPA and NMDA type glutamate receptors are present at synapses of hippocampal dentate granule cell dendritic spines **(Nusser, 2000; Somogyi *et al.*, 1998; Takumi *et al.*, 1999)**, but where AMPA receptors are evenly distributed throughout the PSD of excitatory synapses, NMDA receptors are more commonly found in the centre of the PSD **(Kharazia and Weinberg, 1997; Somogyi *et al.*, 1998)**. This is shown diagrammatically in Figure 46. AMPA receptor numbers are likely to be proportional to synapse area, and given the changes in average synapse area observed from the morphological data, it was predicted that differences in AMPA labelling may be observed between the groups. Incidentally, because the morphological data indicated no significant hemispheric differences, the decision to limit labelling experiments to just tissue samples taken from the right hemispheres was not considered problematic.

An antibody to the NR1 subunit was chosen because this is highly expressed in the hippocampus, and is probably present in all compositional variants of the NMDA receptor **(Monyer *et al.*, 1992; Petralia *et al.*, 1994)**. However, it is not clear if such a distinction exists for AMPA-type receptors **(Baude *et al.*, 1995; Nusser *et al.*, 1998; Petralia and Wenthold, 1992)**, and so three different antibodies were used to label all AMPA receptor subunits. Kainate receptor subunits were not included in the analysis because they are mainly expressed by interneurons or CA3 mossy fibre synapses **(Frerking *et al.*, 1998; Mulle *et al.*, 2000)**. For these experiments, the only antibodies available were those raised in the same species, and so individual single labelling experiments for each category of receptor were performed. Double labelling experiments were not attempted because no suitable blocking agent was available to prevent false-positive detection. Because AMPA and NMDA receptors are known to be co-localised to glutamatergic synapses, a meaningful interpretation of the presence of glutamatergic receptors at their synapses from the individual labelling experiments was possible.

The percentage of labelled synapses present in a defined area was examined for sections in each group. Experiments indicate that LTP results in AMPA receptor insertion at functioning and/or silent synapses **(Mainen *et al.*, 1998)**, and the trafficking and recycling systems reported for these receptors appear suitable for a role in the control of synaptic efficacy **(Lüscher and Frerking, 2001)**. Although these *in vitro* experiments have investigated synapses in slices taken from young animals, it does not rule out the possibility of similar changes in adult synapses. Results of AMPA receptor labelling suggest a transient increase which peaks between the 3 and 9 hour groups, and then declines. This trend suggests that the early stages of memory formation involve changes to AMPA receptor numbers, but this must be treated with caution because none of the differences were significant. In fact, this apparent lack of change in AMPA receptors is in agreement with work indicating that it such changes are only important for LTP, and not for spatial learning **(Zamanillo *et al.*, 1999)**. The small changes may be the result of inherent variability, rather than the effect of training, and analysis is made more difficult by the low levels of labelling. Statistics of the immunolabelling experiments are such that only negative results were obtained, and so firm conclusions cannot be made. The statistical analysis indicates that the percentage of synapses labelled for glutamate receptors does not change, but such an acceptance of the null hypothesis (no difference) may be subject to statistical error. Particularly, given the

small sample size, it is difficult to ensure that type II (β) statistical errors have not been made, but this would require the determination of the statistical 'power' prior to the experiment.

The acquisition of AMPA receptors has also been proposed to be involved in the maturation of synapses **(Petralia *et al.*, 1999; Pickard *et al.*, 2000)**. This involves morphological changes in dendritic spine synapses from thin and stubby types to the larger mushroom spines (see Figures 13 and 45). Because AMPA receptors are evenly spread throughout the PSD of synapses **(Somogyi *et al.*, 1998)**, increases in synapses size may be an indication of increases in AMPA receptor number **(Nusser *et al.*, 1998)**, as a result of maturation or changes in efficacy (plasticity). The involvement of AMPA receptors in short term memory is also supported by work involving the application of NMDA receptor antagonists during a spatial task, which block the formation of long term memories, but leave working memory intact **(Steele and Morris, 1999)**. However, NMDA receptors are thought to play the principal role in LTP and long term memory formation due to their capability for co-incidence detection and the resulting calcium-mediated biochemical signalling events **(Bliss and Collingridge, 1993; Tsien *et al.*, 1996)**.

The percentage of synapses labelled for NMDA receptors was greatest in the naïve group. Particularly large decreases were seen in the 3 hour and 24 hour group, but less so in the 9 hour group, which was comparable to the naïve group. The similarity between the 3 hour group and the 24 hour group is interesting, because there is a clear difference between the memory demonstrated by these two groups. However, there is no significant difference between any of the groups in terms of the percentage of NMDA receptor-labelled synapses. When the two sets of data are combined to give an AMPA labelling to NMDA labelling ratio, the 3 hour and the 24 hour group values are larger than the 9 hour group and the naïve control group. These differences are not statistically significant, and may be strongly influenced by the reduced NMDA labelling seen in the 3 hour and 24 hour groups. The differences may well be due to the large variability in the data, which could result from the threshold of detection being close to zero. This may be especially true for the NMDA receptor labelling, which was sparse when compared to published data from our laboratory **(Fabian-Fine *et al.*, 2000)**.

Antigen preservation may have been lacking in the tissue samples, as post-embedding labelling of single sections has been reported to label up to 50% of synapses, although even for serial sections through synapses, gold is only present at up to 70% of synapses **(Takumi et al., 1999)**. Care was taken to optimise all immunolabelling reactions, but a possible explanation for the discrepancy may be the necessity for storage and transportation of samples in liquid nitrogen, as we have found that a lower level of immunoreactivity is associated with storage of samples prior to freeze substitution.

The number of gold particles present at individual synapses is indicative of the number of receptor subunits that have been labelled, and so changes to the number of gold particles per labelled synapse reflect changes in the number of receptors. For AMPA subunits, labelling shows the greatest increase in the 3 hour group, suggesting the presence of more receptors. For NMDA subunits, slight increases are observed in both the 3 hour and the 24 hour group. However, because none of these differences were significant, the data suggests that there was no substantial difference in the presence of antigens between groups for either receptor type. The ratio of AMPA to NMDA gold particles per synapse is similar in each group except the 3 hour group, which has a greater value. This may suggest that there is a change in the relative proportions of AMPA and NMDA receptors three hours after learning, but the differences are not statistically significant.

The low level of labelling may confound analysis, because comparisons must be made between sets of data that are likely to be a small portion of the total antigens present. This is especially evident from the NMDA labelling, where the standard error of the naïve group was not calculable because synaptic profiles were only labelled by one gold particle. Data from published work indicates that for freeze-substituted material, typical labelling numbers range from one to ten gold particles per synapse, and that higher numbers are also possible **(Racca et al., 2000)**.

Neither of these measures takes into account the size of the synapses in the sample, which may be important when assessing the presence of receptors, as smaller synapses are likely to have fewer receptors available for labelling. However, the total length of PSD is directly proportional to $S_V$, and the morphological data indicates that this value is not significantly different between groups (see Figure 34). This led to the conclusion that the amount of PSD exposed to antibodies will be similar for each group in each

experiment. This was verified by measuring NAS synapse $S_V$ for several sets of immunolabelled synapses using the same methods described for the morphological analysis (see Equation 9). Because there was a similar amount of synaptic PSD available for labelling in each group, differences between groups could be mainly attributed to different numbers of antigens (i.e. receptors), each of which had an equal chance of being labelled.

Calculations of the number of gold particles per μm of the total length of PSD present in NAS synapses enable the comparison of receptor numbers in each group. For AMPA receptor labelling, the greatest increase was seen in the 3 hour group, suggesting an effect of short term memory formation on AMPA receptor numbers. This result would be predicted from *in vitro* studies examining silent synapses and synaptic plasticity **(Lüscher and Frerking, 2001)**, but because none of the changes are significantly different, this interpretation must be treated with caution. This is because the labelling counts in each category of synapse may be affected by the morphological changes that occur to the synapses, particularly if macular synapses enlarge and develop a perforated PSD.

Conversely, reductions are observed in the number of gold particles per μm of PSD in sections labelled for NMDA receptors in the 3 and 24 hour groups. Again, these differences are not significant, and so the results are similarly inconclusive. Indeed, NMDA receptors are proposed to be more stable than AMPA receptors, and so changes would not be predicted. The ratio of AMPA to NMDA gold per μm PSD is greater in the 3 hour and 24 hour groups when compared to naïve and 9 hour groups, which suggests that the balance between AMPA and NMDA receptors is not maintained at these time-points. However, these differences are not significant, and so it cannot be concluded that certain training protocols differentially affect the presence of ionotropic glutamate receptors.

Because single sections are stereologically biased towards counting larger objects **(Howard and Reed, 1998)**, larger synapses with a larger PSD are more likely to be sampled. Sections through large synapses will not necessarily pass through the centre of the PSD, whereas if smaller synapses are present they are more likely to be cut though their centre. Experiments suggest that AMPA receptors are evenly distributed throughout the PSD of excitatory synapses, whereas NMDA receptors are more

commonly found in the centre (Figure 46). Therefore, although morphology will theoretically not influence AMPA receptors, sections may be biased with respect to NMDA receptor antigens because of their spatially central localisation within synapses. These morphological differences in the synapses may in part explain why there are differences in NDMA receptor labelling between groups, but the low number of labelled synapses is also a confounding issue. Immunogold labelling of serial sections would be beneficial in this regard, because it would enable the geometry of these receptors to be taken into consideration.

The number of gold particles per μm of labelled NAS synapse PSD reflects the number of receptors present at labelled synapses. This can be used to examine the labelled synapses in particular for any changes produced after learning because it reflects how many receptors are present in a given portion of PSD (i.e. receptor density). Data indicated that the differences between groups were small and not significant, and again suggested that there were no great changes to the number or density of AMPA receptors after learning. Some changes were apparent in NMDA receptor labelling, especially in the 24 hour group. These differences were also not significant overall, and the standard error of the 24 hour group value was very large. This variability may have been caused by the low levels of labelling, which resulted in only a few labelled synapses being available for analysis. The ratio of AMPA to NMDA gold particles per μm of labelled synapse indicated no significant differences between any of the groups, suggesting that labelled synapses were not expressing more or less of either receptor type as a result of learning.

The $S_V$ of the labelled population of NAS synapses was calculated to examine whether there was any difference in the area of the labelled synapses between groups. AMPA receptor labelling indicated some increases, the greatest of which was at 3 hours. This would indicate that the area of synapses containing AMPA receptors was larger in the 3 hour group, suggesting the presence of more receptors, or more synapses that contained AMPA receptors, but neither this nor any of the other differences were significant. This argues against a short term increase in the presence of AMPA receptors at synapses after learning, which contradicts the situation *in vitro* (**Lüscher and Frerking, 2001**), but agrees with work concerning behavioural learning (**Zamanillo *et al.*, 1999**). The changes to the area of synapses labelled for NMDA receptors suggests that decreases occur in the 3 and 24 hour groups. Although this could be explained by

a reduction in the number of NMDA receptors, or NMDA receptor-containing synapses, the changes are not significantly different, and they argue against increased or decreased numbers of receptors. The ratio of AMPA to NMDA $S_V$ suggests that changes in receptors are occurring, but the lack of replicates and the high variability result in no significant differences. Again, the data is inconclusive because of the low level of labelling.

The values for the average PSD area ($S_N$) of synapses in each group (Figure 36) can be used to calculate the density ($N_V$) of labelled synapses, because $S_N$ is independent of any particular reference volume. Ideally, the density should be calculated by the disector technique to eliminate any bias (due to sampling, shrinkage etc.), but this would require immunolabelling of serial sections. With this aside, calculations indicate that the density of labelled synapses does not follow the pattern of morphological changes, either for AMPA or NMDA receptor labelling. The density of labelled AMPA receptors are increased in density above naïve control levels in the 9 hour group, but also in the 3 hour group. This suggests the possibility of an increase in synapses expressing AMPA receptors, despite no increase in synapse density. This may indicate the insertion of receptors at synapses in the 3 hour group, but this is inconclusive because none of the differences are significant.

For NMDA receptors, the $N_V$ of labelled synapses is increased in the 9 hour group, as may be expected from the presence of more, presumably new, synapses. Conversely, labelled synapse $N_V$ is reduced in both the 3 and 24 hour groups, but because none of these differences are significant, this may be a result of the low labelling or the stereological aspects of sampling with single sections mentioned above. The ratio of AMPA to NMDA $N_V$ is greater in both the 3 and 24 hour groups, but the differences are not significant. Therefore, despite the fact that the ratio takes into account the changes in both AMPA and NMDA receptors, this suggests that there are no significant changes to the relative labelling of ionotropic glutamate receptor types.

As mentioned above, it is interesting that similar changes are observed in several of the measures of NMDA labelling parameters in both the 3 hour and 24 hour groups, despite different training and levels of recall. It is also puzzling that similar changes were not seen in the 9 hour group, even though this group had an intermediate amount of training and showed recall. Although none of the changes between groups were

significant, the interaction between groups for the NMDA $N_V$ data was close to significance (p = 0.083). Although Tukey's post-hoc test indicated no significant differences, comparisons of 3 hour group vs. 9 hour group and 9 hour group vs. 24 hour group were significant when analysed by the LSD post-hoc test. This test does not take into consideration the repetition of comparisons within the ANOVA design, but acknowledging this caveat, it does suggest that some changes may be present, and warrant further investigation.

## Are the different analyses linked?

Results for the percentage of labelled synapses and the numerical density of labelled synapses suggest that there may be a transient increase in the labelling of AMPA receptors around three hours after training. Although this would agree with theories indicating that synaptic plasticity involves the insertion of AMPA receptors, the statistical analysis refutes the theory because these changes are not statistically significant. If AMPA receptors were to be inserted, this would also be predicted to increase the size of synaptic PSD, because these receptors are evenly distributed throughout excitatory synapses and are correlated with synapse size **(Takumi et al., 1999)**. However, the morphological analysis indicates that there is no change in PSD area per synapse in the 3 hour group, which also contradicts AMPA receptor insertion.

The generation of LTP uses very precise patterns of stimulation, a situation which may not occur during learning, where inputs may activate cells in different ways. Because different synapses may be more or less activated, depending upon the stimulus, it is possible that increases and decreases in synaptic strength may be simultaneously occurring in different synaptic populations. The sampling procedures applied in these experiments are unable to distinguish changes in the activation state of analysed synapses, because unlike LTP, where most synapses are similarly activated, the input of sensory information is not homogenous. If positive and negative modulation of synapses does occur simultaneously, any net changes will be averaged out across the whole population, and so may remain undetected. However, values of the standard deviation may give a clue to the occurrence of this situation. Simultaneous increased and decreased synapse sizes will produce greater variation in the data, and is indicated by the larger error values for several of the morphological and immunological results in the 3 hour group. As discussed above, such variation could have been investigated

statistically to answer this question concerning the heterogeneity of synapse parameters.

Changes to NMDA receptor labelling were not significant, but small reductions in the percentage of labelled synapses, their surface area and their density seen in the 3 hour group does not agree with the idea that NMDA receptor numbers are stable. However, it does agree with the small reductions in morphological parameters such as synapse to neuron ratio, mean height and total synaptic area. Changes would be expected in the 9 hour group, where there is an increased density of smaller, presumably new connections. NMDA receptors may well be fundamental to the presence of synaptic contacts, as suggested by imaging studies of neurons during stimulation. The NMDA receptor-associated protein PSD-95 was fluorescently tagged, and shown to be dynamically regulated in parallel with morphological changes to dendritic spines **(Marrs et al., 2001)**. Also, because existing synapses can increase and decrease their fluorescence, the number of NMDA receptors could also fluctuate as a function of their size. However, the labelling results for NMDA receptors do not agree with this, showing no increase despite the morphological changes.

The morphological data indicates a significant increase in the density and synapse to neuron ratio in the 9 hour group. It might be expected that this would produce similar increases in the percentage or density of AMPA labelled synapses, but although increases are present, they are not significantly different from their respective naïve group values. One explanation for this could be the generation of new synapses, which may be silent because they have not matured and started to express AMPA receptors, and so would not be labelled. Another explanation fits in with the theory of AMPA receptor insertion and recycling, which would predict that after the initial learning and insertion of the task, the AMPA receptors would be removed again after a certain time. This is certainly possible, as different levels of activity drive the insertion or removal of AMPA receptors **(Halpain, 2000; Lüscher and Frerking, 2001)**. Metaplasticity may therefore be involved in controlling the AMPA receptor content at synapses. Synapses newly formed by associational activity would be highly activated by the novelty of the learning, facilitating increases in synaptic efficacy and AMPA receptor content, whereas subsequent familiarity with a task may result in less activation and favour reductions in efficacy (AMPA receptor numbers decrease). It is interesting to note that

LTP increases the size of synapses and the occurrence of perforated synapses, both of which possess larger PSD areas, and may therefore also contain more AMPA receptors.

With regard to data from the 24 hour group, NMDA receptor labelling is similar to that seen in the 3 hour group, and also has unexpected reductions in several of the analysed parameters. However, although these changes are not what would be predicted from the slight increases seen in the morphological data, statistical analysis indicates that both the morphological and immunological data are unchanged from their respective naïve controls, and are therefore in agreement. The AMPA receptor labelling also suggests little or no change, and none of the differences are significant, which again agrees with the morphological parameters.

## Conclusions

The work in this thesis confirms and extends existing studies concerning the effects of learning and memory storage on neuronal morphology. Interpretation of the results suggest that learning in the Morris water maze, an associative spatial task that relies on distal visual environmental cues, initiates cellular processes that modify synaptic connections. This study has examined the most common type of synapse that forms the majority of connections in the rat hippocampus, excitatory asymmetric non-perforated axospinous synapses.

The changes involve a significant increase in the density, and the synapse to neuron ratio, of these synapses nine hours after the start of a training and testing protocol that displays long term memory for the learning task. At the same time, in the same population of synapses, the average synapse is significantly reduced in size and synaptic contact area. Similar changes were not observed in naïve animals, or animals that experienced the same learning environment and swam in the pool for a similar duration of time, but did not learn to associate visual cues and locate a hidden platform. There are several possible sources from which new synapses could be generated, some of which involve other categories of synapses. However, because these types are much larger and also much less common, greater sampling and 3-dimensional reconstruction from serial sections would be beneficial for their analysis.

This increase in smaller synapses was not seen at an earlier time-point three hours after the start of a similar training and testing protocol, where a slight decrease in synapse numbers and total synapse area was found instead. Memory recall was not significantly increased at this time-point, although the training data and other work suggest that long term memory would have formed. I suggest that this was an insufficient time for the memory to consolidate, a process that has been shown to involve protein synthesis between three and six hours after learning (**Bernabeu et al., 1997; Bourtchouladze et al., 1998**). The products of protein synthesis may be involved in structural modifications to synapses, and because these may not be underway after three hours, morphological changes would also not be expected. However, smaller changes to the density, total area, size and synapse to neuron ratio at this time-point suggest that some amount of morphological change may be occurring, a possibility that is supported by confocal imaging of structural plasticity in cultured

hippocampal neurons (**Engert and Bonhoeffer, 1999; Fischer *et al.*, 2000; Matus, 2000**).

The significant morphological changes were also not seen twenty-four hours after the start of a third training protocol, despite evidence for robust long term recall of memory for the water maze. This indicates that the increased number of smaller synapses observed nine hours after training is a transient phenomenon which is complete 24 hours after learning, with synapse size and number having similar values to naïve animals, despite a greater number of training trials. Previous work indicates that synaptic reorganisation occurs after learning (**Rusakov *et al.*, 1997**), and gives credence to the idea that new associations formed by new synaptic connections are important in the formation of new memories.

The transient nature of the changes may perhaps indicate that memories do not remain in the hippocampus. However, evidence suggests that certain memories are hippocampus-dependent, particularly certain aspects such as context, and reactivation of a memory may require re-encoding via the hippocampus. The transient changes observed may therefore indicate a reorganisation of relevant inputs, a restructuring of access to extra-hippocampal storage locations, or even a change in the associations within the hippocampus in order to store some components of the memory (**McGaugh, 2000; Nadel and Bohbot, 2001; Nadel and Land, 2000**).

Immunogold labelling for neurotransmitter receptor types known to be present at excitatory synapses revealed the presence of both AMPA and NMDA receptors. Because only a fraction of receptor antigen sites remain intact after processing for electron microscopy, the labelling may be limited by the minimum number of receptors that can be detected. The labelling of AMPA receptors appeared to increase three hours after the start of training, as indicated by increases in the percentage, density and surface area of labelled synapses. However, none of the differences were significant for any of the examined parameters, suggesting that the changes may be affected by variation due to low sample size and low tissue immunoreactivity. The changes did not parallel the morphological alterations seen in each group, suggesting that AMPA receptors numbers changed after learning, but because the differences were not significant this conclusion must be treated with caution.

This is also the case because tissue from the swim only control animals was not available for immunogold labelling, meaning that changes to receptors could not be specifically attributed to an effect of learning. As was the case for AMPA receptors, the labelling of NMDA receptors was also low in these experiments when compared to published levels of immunogold labelling **(Nusser, 2000; Racca et al., 2000)**. Surprisingly, reductions in NMDA labelling were seen despite morphological stability, whereas minimal changes were observed at the time of greatest morphological change. Because the labelling differences were not significant, this could indicate that the morphology and receptor content of synapses were regulated separately. However, it is difficult to determine whether the morphological changes influence the results and analysis of the immunolabelling.

A sequence of events can be envisaged whereby a rat swims in the water maze for the first time, assimilating information about the environment. When it finds, or is guided to, the hidden platform, information about the location of the platform in relation to other objects in the room is added to the rat's cognitive map. This will involve the formation of place cell fields for the pool, including a representation of the platform location. Coincidence detection by NMDA receptors is likely to occur in the hippocampus. The influx of $Ca^{2+}$ through the NMDA receptor channel will activate regulatory enzymes, such as CaMK II, as well as affecting the presence of AMPA receptors at synapses **(Lu et al., 2001)**. The data in this thesis suggests that such activity does not cause the significant up-regulation of AMPA receptors, or changes to NMDA receptor numbers at synapses in response to spatial learning. However, the paucity of immunolabelling may mean that such changes are simply beyond the resolution of the methods as used in this thesis.

The influx of $Ca^{2+}$ also activates biochemical signalling cascades that eventually trigger the transcription of nuclear genes and the translation of mRNA into new proteins, both in the nucleus and locally in neuronal dendrites. These proteins are assisted by other biochemical cascades that allow, and increase, the structural motility of dendritic spines. This results in an increase in the number of predominantly smaller connections, and these changes appear to peak around nine hours after the learning event. Changes in synaptic morphology indicate that there are more synapses, some of which may be forming new connections relevant to the new memory. During development, as axons reach their target muscles and ramify, many more potential synaptic connections are

formed than are needed. The unwanted synapses are eliminated in an activity-dependent manner, such that the connections with the strongest or most appropriate activity are promoted in preference to other connections, which are removed **(Alberts et al., 1989)**. Hence it is conceivable that hippocampal synapses may compete with each other to be involved in the new memory, in a similar way to the formation of motor neuron synapses. Although this situation is sufficient to produce long term recall of the memory for platform location, the changes to synaptic morphology are not persistent, the increased density of synapses declining with time.

After twenty four hours, the density and morphological characteristics of the average synapse are similar to naïve animals that have not learnt the task, but although neither receptor nor morphological changes are apparent, long term recall of the memory is still possible. However, the increase in PSD $S_V$ and differences in immunogold labelling in the 24 hour group suggest that at least some synapses retain at least some of the morphological changes that are occurring. This is supported by the analysis of intersynaptic distances, which suggest morphological restructuring after twenty four hours **(Rusakov et al., 1997)**. Therefore, some of the new synapses may survive, whilst others are eliminated, as synapse numbers reduce at 24 hours.

The formation of new synaptic connections may persist, representing new associations that add to the neuronal representation of the memory. It is likely that these new connections facilitate subsequent association of stimuli relevant to the water maze, rather than being the long term location of the stored memory (a role associated with the cerebral cortex). However, the hippocampus may also store some components of the memory, such as context and relevance, as memories are not as detailed and precise when recalled in the absence of the hippocampus, as discussed above **(Frankland et al., 2001; Nadel and Bohbot, 2001)**. Storage of memory in cortical areas may involve REM sleep **(Louie and Wilson, 2001)**, and this may be one of many additional memory mechanisms that store memories in a different way, at a different rate, encoding subtly different aspects.

## Suggestions for future work

A considerable amount of research is conducted into the functioning of hippocampal CA1 pyramidal neurons and their synapses. They receive a variety of inputs, not only from CA3 cell Schaffer collaterals, but also directly from the entorhinal cortex, and it would be interesting to see if the pattern of synaptic morphological changes also occurs at these synapses. Examination of CA3 synapses would also be useful in this regard, as this may indicate whether morphological changes are a general mechanism involved in memory formation. The middle molecular layer of the dentate gyrus receives its primary innervation from the medial branch of the perforant path. It would be useful to know whether similar morphological changes occur in the inner and outer parts of the molecular layer, where afferent inputs from other areas dominate. This may indicate if they play similar or different roles in memory formation, and would also enable a comparison of synapses onto distal and proximal dendrites, which may have different roles in information processing.

Determination of the mechanisms involved in generating morphological changes would benefit from analysis of the variability between individual dendritic spine synapses. Information concerning the frequency of thin, stubby and mushroom types would facilitate analysis of the maturation state of axospinous synapses, although categorisation may need to rely on measures of bouton volume, surface area and spine neck length. Such analysis would require complete 3-dimensional reconstruction of serially sectioned synapses, preferably contained within sample volumes encompassing several $\mu m^3$ each. These sample volumes would benefit from stereological methodology, i.e. systematically random acquisition and the application of a 3-dimensional counting frame, in a similar way to the application of the optical disector technique in confocal microscopy **(Fiala and Harris, 2001; Howard and Reed, 1998)**.

Because at least four serial sections were used in this thesis for disector counting, partial reconstructions of synapses could be produced, some of which are shown in Figure 47. As mentioned above, full reconstructions would enable a more thorough analysis of the individual properties of different synaptic types, and this would be particularly suited for analysing perforated axospinous and axodendritic types. Attempts were made to apply the disector method to these synapse types, but because of their large size and lower abundance (typically ten times less than NAS synapses),

162
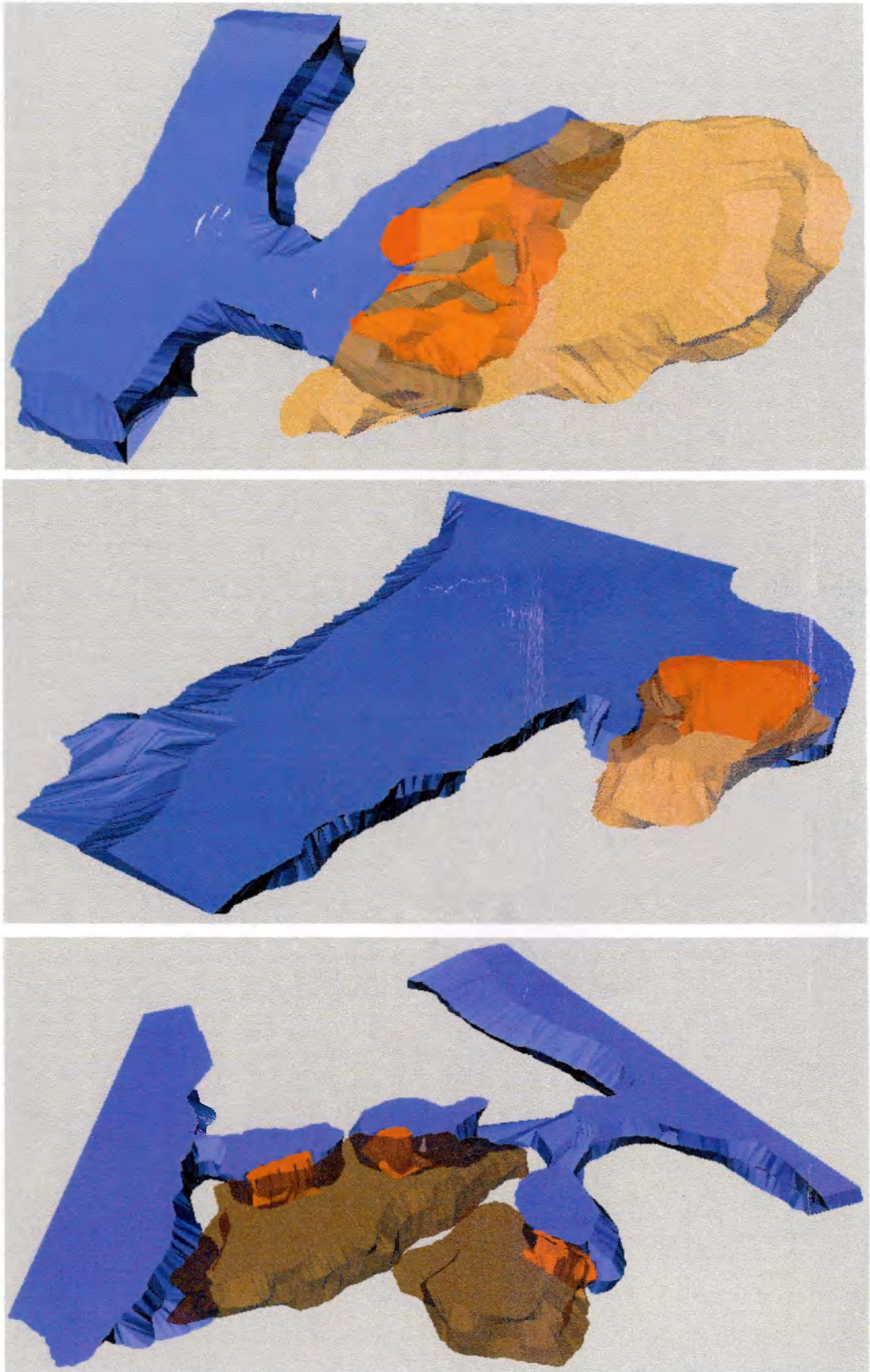
Figure 47 - Partial reconstructions of a perforated axospinous synapse (top), a non-perforated axodendritic synapse (middle) and a multiple synapse bouton containing one branched-neck spine (bottom). Dendrites are shown in blue, PSD in red, axons in orange.

163

the differences between estimates from individual animals could not be sufficiently reduced. Information about the frequency and morphological parameters of different synapses would mean that the whole population of synapses could be considered, which may provide evidence of interactions or correlations between these categories, as suggested by Figure 45.

Reconstructions may also allow the analysis of multiple synapse boutons, structures proposed to be involved in morphological restructuring, and would be able to provide measures of 'second order' morphological changes that are difficult to assess using standard sections. The term 'second order' is used to define information such as the distance between neighbouring objects, and their spatial orientation and arrangement with respect to one another (Mayhew, 1999). This may be an important factor for axospinous synapses, as their proximity to axons and their occurrence on dendrites may be important in the pattern of neuronal activity. The absence of any markers for the level of functional activity at individual synapses also makes correlations between structure and function difficult, but immunological detection of the Arc gene and protein, and chemical detection of postsynaptic calcium levels, may be useful in this regard because they identify activated synapses.

Concerning stereological methodology, the application of the Cavalieri method would allow the estimation of hippocampal volume, an important parameter if total synapse (or neuron) numbers are to be calculated. These would be preferable to other measures because they are independent of ratios or sample volumes. The use of sections obtained randomly with respect to their 3-dimensional orientation would also be beneficial, as this would ensure no stereological bias occurred in subsequent analysis **(Howard and Reed, 1998)**. The application of these techniques would require a different method of hippocampal dissection, which would require a further group of animals to be trained, but this would also allow several other factors to be examined.

The hippocampus is particularly rich in glucocorticoid receptors **(Chao et al., 1989)**, and CA3 dendrites are detrimentally affected by corticosterone **(Magariños and McEwen, 1995)**, suggesting that the stress caused by exposure to the water maze may have an effect on synaptic morphology **(de Quervain et al., 1998; McEwen, 1999)**. Measurement of corticosterone levels in each animal would enable quantification of the levels of stress caused by water maze training, as well as if these levels change in

164

sequential training trials. Stress levels in the swim only group would also be quantifiable, as this may be different in this group, especially considering that they do not have goal-orientated swimming sessions. Swim only controls matched to animals in the 3 hour and 24 hour groups would enable comparisons with the specific learning of platform location in these groups to be made, although stress levels would also need to be taken into consideration.

Another important factor is the amount of training given to animals in each group. Because different numbers of training trials were administered to different groups in the present study, this confuses the precise temporal localisation of learning with respect to the morphological changes. Although the hippocampus is involved in the formation of long term memories, other memory systems are thought to encode aspects of the memory, possibly in addition to the hippocampus **(Nadel and Bohbot, 2001; Nadel and Land, 2000)**. Correlations between end of morphological changes and the role of the hippocampus in the memory are therefore difficult to assess. The start of the learning process is also not well defined, as it is unclear whether learning takes place as a summation of experience over trials and sessions, or whether subsequent training merely modifies, or 'reconsolidates', the memory laid down by the initial learning experience. It is difficult to determine whether multiple traces are used to store the memory; particularly, whether each trial is treated as a different context, or event − perhaps this is why such large differences are observed in the whole population of synapses.

Reactivation and 'reconsolidation' of memory involves protein synthesis **(Nader et al., 2000)**, and 'weak' and 'strong' training events have different effects in terms of the time windows sensitive to protein synthesis inhibitors **(Bourtchouladze et al., 1998)**, but it is not known if this also occurs during sequential water maze training trials. This means that correlations between the start of morphological changes and the start of learning are also difficult to assess, as successive training trials may activate successive waves of protein synthesis and morphological change. The use of the same water maze training protocol (i.e. the same number of training trials) for different groups of animals would clarify this issue, enabling a direct comparison between the duration after training and morphology with respect to the formation and retention of a long term memory. The application of protein synthesis inhibitors at various time-points in these groups would be predicted to cause amnesia for the learning task, and could be used to

test whether this would also inhibit the morphological changes observed. As discussed above, the use of additional non-spatial and/or randomly hidden platform controls would enable the different aspects of the learning strategy to be investigated, and further timepoints would clarify issues concerning the 'time-window' of morphological changes and the effect of more training trials and the intensity of training.

Repetition of the experiment would also allow more samples to be prepared for immunological investigation, particularly from swim only control groups. This would also enable the preparation of samples by methods that are reported to preserve both ultrastructure and antigenicity, such as Durcupan embedment or an osmium-free Epon method (**Phend et al., 1995**). Indeed, if these methods successfully preserve both aspects of the tissue, simultaneous analysis of structural morphology and the presence of molecular components in the same synapses would be possible. One technique that may prove useful is the quantitative analysis of immunogold labelling (**Lucocq, 1992**). Immunolabelling of serial sections increases the percentage of labelled synapses, and would also enable the spatial localisation of molecules, such as neurotransmitter receptors, with respect to the 3-dimensional shape of the synapse that they are present in.

If antibodies could be obtained that allowed simultaneous labelling of AMPA and NMDA receptors, correlations between receptor numbers, synapse morphology and learning could be investigated. Labelling comparisons between different AMPA and NMDA receptor subunits may also be beneficial in understanding the changes induced by learning, as the composition of receptors can be changed by activity (**Heynen et al., 2000; Philpot et al., 2001; Snyder et al., 2001**). Statistical power calculations would also prove beneficial.

Other aspects of hippocampal function that warrant investigation are the role and potential changes to interneuron inputs onto the principal cells, which could be assessed by labelling receptors found only at these synapses, such as the $GABA_A$ receptor alpha-2 subunit (**Simbürger et al., 2001**). Acetylcholine and other neurotransmitters have a strong modulatory effect on hippocampal activity, and may have important effects that govern the overall formation of long term memory. Sleep is also involved in long term memory formation, and the 'night' phase of the 24 hour cycle should be investigated to determine the effects of sleep on morphological changes.

# References

Abraham, W. C. and Bear, M. F., 1996: Metaplasticity: the plasticity of synaptic plasticity. *Trends in Neurosciences* **19 (4)** 126-130.

Akirav, I., Sandi, C. and Richter-Levin, G., 2001: Differential activation of hippocampus and amygdala following spatial learning under stress. *European Journal of Neuroscience* **14 (4)** 719-25.

Alberts, B., Bray, D., Lewis, J., Raff, M., Roberts, K. and Watson, J. D., 1989: *Molecular biology of the cell*. Garland Publishing, Inc.: New York.

Alkon, D. L., Nelson, T. J., Zhao, W. and Cavallaro, S., 1998: Time domains of neuronal Ca2+ signalling and associative memory: steps through a calexcitin, ryanodine receptor, K+ channel cascade. *Trends in Neurosciences* **21 (12)** 529-537.

Allison, D. W., Gelfand, V. I., Spector, I. and Graig, A. M., 1998: Role of actin in anchoring postsynaptic receptors in cultured hippocampal neurons: differential attachment of NMDA versus AMPA receptors. *Journal of Neuroscience* **18 (7)** 2423-2436.

Amaral, D. G. and Witter, M. P., 1989: The three dimensional organisation of the hippocampal formation: a review of anatomical data. *Neuroscience* **31 (3)** 571-591.

Andersen, P., Bliss, T. V. P. and Skrede, K. K., 1971: Lamellar organisation of hippocampal excitatory pathways. *Experimental Brain Research* **13 (2)** 222-238.

Anwyl, R., 1999: Metabotropic glutamate receptors: electrophysiological properties and role in plasticity. *Brain Research Reviews* **29 (1)** 83-120.

Arami, S., Jucker, M., Schachner, M. and Welzl, H., 1996: The effect of continuous intraventricular infusion of L1 and NCAM antibodies on spatial learning in rats. *Behavioural Brain Research* **81 (1-2)** 81-87.

Bach, M. E., Hawkins, R. D., Osman, M., Kandel, E. R. and Mayford, M., 1995: Impairment of spatial but not contextual memory in CaMKII mutant mice with a selective loss of hippocampal LTP in the range of the theta frequency. *Cell* **81 (6)** 905-915.

Bailey, C. H. and Kandel, E. R., 1993: Structural changes accompanying memory storage. *Annual Reviews in Physiology* **55** 397-426.

Baimbridge, K. G., Celio, M. R. and Rogers, J. H., 1992: Calcium-binding proteins in the nervous system. *Trends in Neurosciences* **15 (8)** 303-308.

Bajjalieh, S. M., 1999: Synaptic vesicle docking and fusion. *Current Opinion in Neurobiology* **9 (3)** 321-328.

Bannerman, D. M., Good, M. A., Butcher, S. P., Ramsay, M. and Morris, R. G. M., 1995: Distinct components of spatial learning revealed by prior training and NMDA receptor blockade. *Nature* **378 (6553)** 182-186.

Barrionuevo, G., Schottler, F. and Lynch, G., 1980: The effects of repetitive low frequency stimulation on control and "potentiated" synaptic responses in the hippocampus. *Life Sciences* **27 (24)** 2385-2391.

Bartesaghi, R., Gessi, T. and Migliore, M., 1995: Input-output relations in the entorhinal-hippocampal-entorhinal loop: entorhinal cortex and dentate gyrus. *Hippocampus* **5 (5)** 440-451.

Baude, A., Nusser, Z., Molnár, E., McIlhinney, R. A. J. and Somogyi, P., 1995: High-resolution immunogold localisation of AMPA type glutamate receptor subunits at synaptic and non-synaptic sites in rat hippocampus. *Neuroscience* **69 (4)** 1031-1055.

Bear, M. F. and Abraham, W. C., 1996: Long-term depression in hippocampus. *Annual Reviews in Neuroscience* **19** 437-462.

Becker, C. G., Artola, A., Gerardy-Schahn, R., Becker, T., Welzl, H. and Schachner, M., 1996: The polysialic acid modification of the neural cell adhesion molecule is involved in spatial learning and hippocampal long term potentiation. *Journal of Neuroscience Research* **45 (2)** 143-152.

Ben-Ari, Y., Khazipov, R., Leinekugel, X., Caillard, O. and Gaiarsa, J.-L., 1997: GABA A, NMDA and AMPA receptors; a developmentally regulated 'ménage à trois'. *Trends in Neurosciences* **20 (11)** 523-529.

Benes, F. M. and Lange, N., 2001: Two-dimensional versus three-dimensional cell counting: a practical perspective. *Trends in Neurosciences* **24 (1)** 11-17.

Bernabeu, R., Bevilaqua, L., Ardenghi, P., Bromberg, E., Schmitz, P., Bianchin, M., Izquierdo, I. and Medina, J. H., 1997: Involvement of hippocampal cAMP/cAMP-dependent protein kinase signalling pathways in a late memory consolidation phase of aversively motivated learning in rats. *Proceedings of the National Academy of Sciences U.S.A.* **94 (13)** 7041-7046.

Berridge, M. J., 1998: Neuronal calcium signalling. *Neuron* **21 (1)** 13-26.

Bertoni-Freddari, C., Fattoretti, P., Casoli, T., Meier-Ruge, W. and Ulrich, J., 1990: Morphological adaptive response of the synaptic junctional zones in the human dentate gyrus during ageing and Alzheimer's disease. *Brain Research* **517 (1-2)** 69-75.

Bertoni-Freddari, C., Giuli, C., Pieri, C. and Paci, D., 1986: Quantitative investigation of the morphological plasticity of synaptic junctions in rat dentate gyrus during ageing. *Brain Research* **366 (1-2)** 187-92.

Best, P. J., White, A. M. and Minai, A., 2001: Spatial processing in the brain: the activity of hippocampal place cells. *Annual Reviews in Neuroscience* **24** 459-486.

Betz, W. J. and Bewick, G. S., 1993: Optical monitoring of transmitter release and synaptic vesicle recycling at the frog neuromuscular junction. *Journal of Physiology* **460** 287-309.

Bi, G.-Q. and Poo, M.-M., 2001: Synaptic modification by correlated activity: Hebb's postulate revisited. *Annual Reviews in Neuroscience* **24** 139-166.

Blichenberg, A., Schwanke, B., Rehbein, M., Garner, C. C., Richter, D. and Kindler, S., 1999: Identification of a cis-acting dendritic targeting element in MAP2 mRNAs. *Journal of Neuroscience* **19 (20)** 8818-8829.

Bliss, T. V. P. and Collingridge, G. L., 1993: A synaptic model of memory: long-term potentiation in the hippocampus. *Nature* **361 (6407)** 31-39.

Bliss, T. V. P. and Lømo, T., 1973: Long-lasting potentiation of synaptic transmission in the dentate area of the anaesthetized rabbit following stimulation of the perforant path. *Journal of Physiology* **232 (2)** 331-356.

Bortolotto, Z. A., Fitzjohn, S. M. and Collingridge, G. L., 1999: Roles of metabotropic glutamate receptors in LTP and LTD in the hippocampus. *Current Opinion in Neurobiology* **9 (3)** 299-304.

Bourtchouladze, R., Abel, T., Berman, N., Gordon, R., Lapidus, K. and Kandel, E. R., 1998: Different training procedures recruit either one or two critical periods for contextual memory consolidation, each of which requires protein synthesis and PKA. *Learning and Memory* **5 (4-5)** 365-374.

Bradley, P. and Horn, G., 1979: Neuronal plasticity in the chick brain: morphological effects of visual experience on neurones in hyperstriatum accessorium. *Brain Research* **162 (1)** 148-153.

Brakeman, P. R., Lanahan, A. A., O'Brien, R., Roche, K., Barnes, C. A., Huganir, R. L. and Worley, P. F., 1997: Homer: a protein that selectively binds metabotropic glutamate receptors. *Nature* **386 (6622)** 284-288.

Brown, M. W. and Aggleton, J. P., 2001: Recognition memory: what are the roles of the perirhinal cortex and hippocampus? *Nature Reviews Neuroscience* **2 (1)** 51-61.

Brown, M. W. and Horn, G., 1979: Neuronal plasticity in the chick brain: electrophysiological effects of visual experience on hyperstriatal neurones. *Brain Research* **162 (1)** 142-147.

Brun, V. H., Ytterbø, K., Morris, R. G. M., Moser, M.-B. and Moser, E. I., 2001: Retrograde amnesia for spatial memory induced by NMDA receptor-mediated long-term potentiation. *Journal of Neuroscience* **21 (1)** 356-362.

Buchs, P.-A. and Muller, D., 1996: Induction of long-term potentiation is associated with major ultrastructural changes of activated synapses. *Proceedings of the National Academy of Sciences U.S.A.* **93 (15)** 8040-8045.

Burette, F., Jay, T. M. and Laroche, S., 1997: Reversal of LTP in the hippocampal afferent fibre system to the prefrontal cortex in vivo with low-frequency patterns of stimulation that do not produce LTD. *Journal of Neurophysiology* **78 (2)** 1155-1160.

Burgess, N., Becker, S., King, J. A. and O'Keefe, J., 2001: Memory for events and their spatial context: models and experiments. *Philosophical Transactions of the Royal Society of London Series B* **356 (1413)** 1493-1503.

Cahill, L., Haier, R. J., Fallon, J., Alkire, M. T., Tang, C., Keator, D., Wu, J. and McGaugh, J. L., 1996: Amygdala activity at encoding correlated with long-term, free recall of emotional information. *Proceedings of the National Academy of Sciences U.S.A.* **93 (15)** 8016-8021.

Caramanos, Z. and Shapiro, M. L., 1994: Spatial memory and N-methyl-D-aspartate receptor antagonists APV and MK801: memory impairments depend on familiarity with the environment, drug dose, and training duration. *Behavioural Neuroscience* **108 (1)** 30-43.

Carew, T. J. and Sutton, M. A., 2001: Molecular stepping stones in memory consolidation. *Nature Neuroscience* **4 (8)** 769-771.

Carlin, R. K. and Siekevitz, P., 1983: Plasticity in the central nervous system: Do synapses divide? *Proceedings of the National Academy of Sciences U.S.A.* **80 (11)** 3517-3521.

Carroll, R. C., Lissin, D. V., von Zastrow, M., Nicoll, R. A. and Malenka, R. C., 1999: Rapid redistribution of glutamate receptors contributes to long-term depression in hippocampal cultures. *Nature Neuroscience* **2 (5)** 454-460.

Castro-Alamancos, M. A., Donoghue, J. P. and Connors, B. W., 1995: Different forms of synaptic plasticity in somatosensory and motor areas of the neocortex. *Journal of Neuroscience* **15 (7 pt 2)** 5324-5333.

Chao, H. M., Choo, P. H. and McEwen, B. S., 1989: Glucocorticoid and mineralocorticoid receptor mRNA expression in rat brain. *Neuroendocrinology* **50 (4)** 365-371.

Cho, Y. H., Giese, K. P., Tanila, H., Silva, A. J. and Eichenbaum, H., 1998: Abnormal hippocampal spatial representations in αCaMKII T286A and CREBαδ - mice. *Science* **279 (5352)** 867-869.

Cho, Y. H., Beracochea, D. and Jaffard, R., 1993: Extended temporal gradient for the retrograde and anterograde amnesia produced by ibotenate entorhinal cortex lesions in mice. *Journal of Neuroscience* **13 (4)** 1759-1766.

Claiborne, B. J., Amaral, D. G. and Cowan, W. M., 1990: Quantitative, three-dimensional analysis of granule cell dendrites in the rat dentate gyrus. *Journal of Comparative Neurology* **302 (2)** 206-219.

Coggeshall, R. E. and Lekan, H. A., 1996: Methods for determining numbers of cells and synapses: A case for more uniform standards of review. *Journal of Comparative Neurology* **364 (1)** 6-15.

Collingridge, G. L., Kehl, S. J. and McLennan, H., 1983: Excitatory amino acids in synaptic transmission in the Schaffer collateral-commissural pathway of the rat hippocampus. *Journal of Physiology* **334** 33-46.

Coq, J.-O., 1999: Tactile impoverishment and sensorimotor restriction deteriorate the forepaw cutaneous map in the primary somatosensory cortex of adult rats. *Experimental Brain Research* **129 (4)** 518-531.

Craig, A. M., 1998: Activity and synaptic receptor targeting: the long view. *Neuron* **21 (2)** 459-462.

Craig, A. M., Blackstone, C. D., Huganir, R. L. and Banker, G., 1994: Selective clustering of glutamate and γ-aminobutyric acid receptors opposite terminals releasing the corresponding neurotransmitters. *Proceedings of the National Academy of Sciences U.S.A.* **91 (26)** 12373-12377.

Davies, H. A., Cordero, M. I., Sandi, C. and Stewart, M. G., 2001: Alterations in CA3 synaptic morphometry in rat hippocampus after exposure to a chronic stress paradigm. *Society for Neuroscience Abstracts* **Volume 27**, Program number 532.8.

De Groot, D. M. G., 1988: Comparison of methods for the estimation of the thickness of ultrathin tissue sections. *Journal of Microscopy* **151 (1)** 23-42.

de Quervain, D. J.-F., Roozendaal, B. and McGaugh, J. L., 1998: Stress and glucocorticoids impair retrieval of long-term spatial memory. *Nature* **394 (6695)** 787-790.

Desmond, N. L. and Levy, W. B., 1986a: Changes in the numerical density of synaptic contacts with long-term potentiation in the hippocampal dentate gyrus. *Journal of Comparative Neurology* **253 (4)** 466-475.

Desmond, N. L. and Levy, W. B., 1986b: Changes in the postsynaptic density with long-term potentiation in the dentate gyrus. *Journal of Comparative Neurology* **253 (4)** 476-482.

Desmond, N. L. and Levy, W. B., 1988: Synaptic interface surface area increases with long-term potentiation in the hippocampal dentate gyrus. *Brain Research* **453 (1-2)** 308-14.

Diamond, D. M., Park, C. R., Heman, K. L. and Rose, G. M., 1999: Exposing rats to a predator impairs spatial working memory in the radial arm water maze. *Hippocampus* **9 (5)** 542-552.

Dong, H., O'Brien, R. J., Fung, E. T., Lanahan, A. A., Worley, P. F. and Huganir, R. L., 1997: GRIP: a synaptic PDZ domain-containing protein that interacts with AMPA receptors. *Nature* **386 (6622)** 279-284.

Doubell, T. P. and Stewart, M. G., 1993: Short-term changes in the numerical density of synapses in the intermediate and medial hyperstriatum ventrale following one-trial passive avoidance training in the chick. *Journal of Neuroscience* **13 (5)** 2230-6.

Doyère, V., Rédini-Del Negro, C., Dutrieux, G., Le Floch, G., Davis, S. and Laroche, S., 1995: Potentiation or depression of synaptic efficacy in the dentate gyrus is determined by the relationship between the conditioned and unconditioned stimulus in a classical conditioning paradigm in rats. *Behavioural Brain Research* **70 (1)** 15-29.

Doyère, V., Srebro, B. and Laroche, S., 1997: Heterosynaptic LTD and depotentiation in the medial perforant path of the dentate gyrus in the freely moving rat. *Journal of Neurophysiology* **77 (2)** 571-578.

Doyle, E., Nolan, P. M., Bell, R. and Regan, C. M., 1992: Intraventricular infusions of anti-neural cell adhesion molecules in a discrete posttraining period impair consolidation of a passive avoidance response in the rat. *Journal of Neurochemistry* **59 (4)** 1570-1573.

Dudek, S. M. and Bear, M. F., 1993: Bidirectional long-term modification of synaptic effectiveness in the adult and immature hippocampus. *Journal of Neuroscience* **13 (7)** 2910-2918.

Dunaevsky, A., Tashiro, A., Majewska, A., Mason, C. and Yuste, R., 1999: Developmental regulation of spine motility in the mammalian central nervous system. *Proceedings of the National Academy of Sciences U.S.A.* **96 (23)** 13438-13443.

Edelman, G. D. and Jones, F. S., 1998: Gene regulation of cell adhesion: a key step in neural morphogenesis. *Brain Research Reviews* **26 (2-3)** 337-352.

Ehlers, M. D., 2000: Reinsertion or degradation of AMPA receptors determined by activity-dependent endocytotic sorting. *Neuron* **28 (2)** 511-525.

Eldridge, L. L., Knowlton, B. J., Furmanski, C. S., Bookheimer, S. Y. and Engel, S. A., 2000: Remembering episodes: a selective role for the hippocampus during retrieval. *Nature Neuroscience* **3 (11)** 1149-1152.

Engert, F. and Bonhoeffer, T., 1999: Dendritic spine changes associated with hippocampal long-term synaptic plasticity. *Nature* **399 (6731)** 66-70.

Fabian-Fine, R., Volknandt, W., Fine, A. and Stewart, M. G., 2000: Age-dependent pre- and postsynaptic distribution of AMPA receptors a synapses in CA3 stratum radiatum of hippocampal slice cultures compared with intact brain. *European Journal of Neuroscience* **12 (10)** 3687-3700.

Fahy, F. L., Riches, I. P. and Brown, M. W., 1993: Neuronal activity related to visual recognition memory: long-term memory and the encoding of recency and familiarity information in the primate anterior and medial inferior temporal and rhinal cortex. *Experimental Brain Research* **96 (3)** 457-472.

Faneslow, M. S., 1998: Pavlovian conditioning, negative feedback, and blocking: mechanisms that regulate association formation. *Neuron* **20 (3)** 625-627.

Fiala, J. C. and Harris, K. M., 2001: Extending unbiased stereology of brain ultrastructure to three-dimensional volumes. *Journal of the American Medical Informatics Association* **8 (1)** 1-16.

Fields, R. D. and Itoh, K., 1996: Neural cell adhesion molecules in activity-dependent development and synaptic plasticity. *Trends in Neurosciences* **19 (11)** 473-480.

Finnerty, G. T. and Connors, B. W., 2000: Sensory deprivation without competition yields modest alterations of short-term synaptic dynamics. *Proceedings of the National Academy of Sciences U.S.A.* **97 (23)** 12864-12868.

Fischer, M., Kaech, S., Knutti, D. and Matus, A., 1998: Rapid actin-based plasticity in dendritic spines. *Neuron* **20 (5)** 847-854.

Fischer, M., Kaech, S., Wagner, U., Brinkhaus, H. and Matus, A., 2000: Glutamate receptors regulate actin-based plasticity in dendritic spines. *Nature Neuroscience* **3 (9)** 887-894.

Fisher, S. A., Fischer, T. M. and Carew, T. J., 1997: Multiple overlapping processes underlying short term synaptic enhancement. *Trends in Neurosciences* **20 (4)** 170-177.

Foster, D. J., Morris, R. G. M. and Dayan, P., 2000: A model of hippocampally dependent navigation, using the temporal difference learning rule. *Hippocampus* **10 (1)** 1-16.

Frankland, P. W., O'Brien, C., Ohno, M., Kirkwood, A. and Silva, A. J., 2001: alpha-CaMKII-dependent plasticity in the cortex is required for permanent memory. *Nature* **411 (6835)** 309-313.

Frerking, M., Malenka, R. C. and Nicoll, R. A., 1998: Synaptic activation of kainate receptors on hippocampal interneurons. *Nature Neuroscience* **1 (6)** 479-486.

Freund, T. F. and Buzsaki, G., 1996: Interneurons of the hippocampus. *Hippocampus* **6 (4)** 347-470.

Frey, U. and Morris, R. G. M., 1997: Synaptic tagging and long-term potentiation. *Nature* **385 (6616)** 533-536.

Fuster, J. M., 1997: Network memory. *Trends in Neurosciences* **20 (10)** 451-459.

Geinisman, Y., 1993: Perforated axospinous synapses with multiple, completely partitioned transmission zones: probable structural intermediates in synaptic plasticity. *Hippocampus* **3 (4)** 417-434.

Geinisman, Y., Berry, R. W., Disterhoft, J. F., Power, J. M. and Van der Zee, E. A., 2001: Associative learning elicits the formation of multiple-synapse boutons. *Journal of Neuroscience* **21 (5)** 5568-5573.

Geinisman, Y., deToledo-Morrell, L. and Morrell, F., 1991: Induction of long-term potentiation is associated with an increase in the number of axospinous synapses with segmented postsynaptic densities. *Brain Research* **566 (1-2)** 77-88.

Geinisman, Y., deToledo-Morrell, L., Morrell, F., Persina, I. S. and Beatty, M. A., 1996: Synapse restructuring associated with the maintenance phase of hippocampal long-term potentiation. *Journal of Comparative Neurology* **368 (3)** 413-423.

Geinisman, Y., Disterhoft, J. F., Gundersen, H. J. G., McEchron, M. D., Persina, I. S., Power, J. M., van der Zee, E. A. and West, M. J., 2000: Remodelling of hippocampal synapses after hippocampus-dependent associative learning. *Journal of Comparative Neurology* **417 (1)** 49-59.

Geppert, M. and Südhof, T. C., 1998: RAB3 and synaptotagmin: the yin and yang of synaptic membrane fusion. *Annual Reviews in Neuroscience* **21** 75-95.

Gomperts, S. N., Carroll, R., Malenka, R. C. and Nicoll, R. A., 2000: Distinct roles for ionotropic and metabotropic glutamate receptors in the maturation of excitatory synapses. *Journal of Neuroscience* **20 (6)** 2229-2237.

Good, M. and Honey, R. C., 1991: Conditioning and contextual memory retrieval in hippocampal rats. *Behavioural Neuroscience* **105 (4)** 499-509.

Guena, S., 2000: Appreciating the difference between design-based and model-based sampling strategies in quantitative morphology of the nervous system. *Journal of Comparative Neurology* **427 (3)** 333-339.

Guthrie, P. B., Segal, M. and Kater, S. B., 1991: Independent regulation of calcium revealed by imaging dendritic spines. *Nature* **354 (6348)** 76-80.

Guzowski, J. F., McNaughton, B. L., Barnes, C. A. and Worley, P. F., 1999: Environment-specific expression of the immediate-early gene Arc in hippocampal neuronal ensembles. *Nature Neuroscience* **2 (12)** 1120-1124.

Guzowski, J. F., Lyford, G. L., Stevenson, G. D., Houston, F. P., McGaugh, J. L., Worley, P. F. and Barnes, C. A., 2000: Inhibition of activity-dependent arc protein expression in the rat hippocampus impairs the maintenance of long-term potentiation and the consolidation of long-term memory. *Journal of Neuroscience* **20 (11)** 3993-4001.

Halpain, S., 2000: Actin and the agile spine: how and why do dendritic spines dance? *Trends in Neurosciences* **23 (4)** 141-146.

Hamann, S. B., Ely, T. D., Grafton, S. T. and Kilts, C. D., 1999: Amygdala activity related to enhanced memory for pleasant and aversive stimuli. *Nature Neuroscience* **2 (3)** 289-293.

Hardingham, G. E., Arnold, F. J. L. and Bading, H., 2001: Nuclear calcium signalling controls CREB-mediated gene expression triggered by synaptic activity. *Nature Neuroscience* **4 (3)** 261-267.

Harris, K. M., 1999: Structure, development, and plasticity of dendritic spines. *Current Opinion in Neurobiology* **9 (3)** 343-348.

Harris, K. M. and Kater, S. B., 1994: Dendritic spines: cellular specializations imparting both stability and flexibility to synaptic function. *Annual Reviews in Neuroscience* **17** 341-371.

Hebb, D. O., 1949: *The Organisation of Behaviour: a Neuropsychological Theory.* Wiley: New York, NY.

Helmchen, F., Svoboda, K., Denk, W. and Tank, D. W., 1999: In vivo dendritic calcium dynamics in deep layer cortical pyramidal neurons. *Nature Neuroscience* **2** **(11)** 989-996.

Heynen, A. J., Abraham, W. C. and Bear, M. F., 1996: Bidirectional modification of CA1 synapses in the adult hippocampus in vivo. *Nature* **381** **(6578)** 163-166.

Heynen, A. J., Quinlan, E. M., Bae, D. C. and Bear, M. F., 2000: Bidirectional, activity-dependent regulation of glutamate receptors in the adult hippocampus *in vivo*. *Neuron* **28** **(2)** 527-536.

Hollmann, M. and Heinemann, S., 1994: Cloned glutamate receptors. *Annual Reviews in Neuroscience* **17** 31-108.

Holst, B. D., Vanderklish, P. W., Krushel, L. A., Zhou, W., Langdon, R. B., McWhirter, J. R., Edelman, G. M. and Crossin, K. L., 1998: Allosteric modulation of AMPA-type glutamate receptors increases activity of the promoter for the neural cell adhesion molecule, N-CAM. *Proceedings of the National Academy of Sciences U.S.A.* **95 (5)** 2597-2602.

Horn, G., Nicol, A. U. and Brown, M. W., 2001: Tracking memory's trace. *Proceedings of the National Academy of Sciences U.S.A.* **98 (9)** 5282-5287.

Howard, C. V. and Reed, M. G., 1998: *Unbiased Stereology.* BIOS Scientific Publishers: 9 Newtec Place, Magdalen Road, Oxford OX4 1RE, U.K.

Hubel, D. H. and Wiesel, T. N., 1968: Receptive fields and functional architecture of monkey striate cortex. *Journal of Physiology* **195 (1)** 215-243.

Hunter, A. and Stewart, M. G., 1993: Long-term increases in the numerical density of synapses in the chick lobus parolfactorius after passive avoidance training. *Brain Research* **605 (2)** 251-5.

Impey, S., Mark, M., Villacres, E. C., Poser, S., Chavkin, C. and Storm, D. R., 1996: Induction of CRE-mediated gene expression by stimuli that generate long lasting LTP in area CA1 of the hippocampus. *Neuron* **16 (5)** 973-982.

Impey, S., Smith, D. M., Obrietan, K., Donahue, R., Wade, C. and Storm, D. R., 1998: Stimulation of cAMP response element (CRE)-mediated transcription during contextual learning. *Nature Neuroscience* **1 (7)** 595-601.

Insausti, R., Herrero, M. T. and Witter, M. P., 1997: Entorhinal cortex of the rat: cytoarchitectonic subdivisions and the origin and distribution of cortical efferents. *Hippocampus* **7 (2)** 146-183.

Isaac, J. T. R., Nicoll, R. A. and Malenka, R. C., 1995: Evidence for silent synapses: implications for the expression of LTP. *Neuron* **15 (2)** 427-434.

Ishizuka, N., Cowan, W. M. and Amaral, D. G., 1995: A quantitative analysis of the dendritic organisation of pyramidal cells ion the rat hippocampus. *Journal of Comparative Neurology* **362 (1)** 17-45.

Itarat, W. and Jones, D. G., 1993: Morphological characteristics of perforated synapses in the latter stages of synaptogenesis in rat neocortex: stereological and three-dimensional approaches. *Journal of Neurocytology* **22 (9)** 753-764.

Izquierdo, I., Barros, D. M., Mello e Souza, T., de Souza, M. M., Izquierdo, L. A. and Medina, J. H., 1998: Mechanisms for memory types differ. *Nature* **393 (6686)** 635-636.

Jenkins, W. M., Merzenich, M. M., Ochs, M. T., Allard, T. and Guic-Robles, E., 1990: Functional reorganization of primary somatosensory cortex in adult owl monkeys after behaviorally controlled tactile stimulation. *Journal of Neurophysiology* **63 (1)** 82-104.

Johnston, D., Hoffman, D. A., Colbert, C. M.. and Magee, J. C., 1999: Regulation of back-propagating action potentials in hippocampal neurons. *Current Opinion in Neurobiology* **9 (3)** 288-292.

Jones, D. G. and Harris, R. J., 1995: An analysis of contemporary morphological concepts of synaptic remodelling in the CNS: perforated synapses revisited. *Reviews in the Neurosciences* **6 (3)** 177-219.

Jones, M. W., Errington, M. L., French, P. J., Fine, A., Bliss, T. V. P., Garel, S., Charnay, P., Bozon, B., Laroche, S. and Davis, S., 2001: A requirement for the immediate early gene *Zif268* in the expression of late LTP and long-term memories. *Nature Neuroscience* **4 (3)** 289-296.

Jones, T. A., Klintsova, A. Y., Kilman, V. L., Sirevaag, A. M. and Greenough, W. T., 1997: Induction of multiple synapses by experience in the visual cortex of adult rats. *Neurobiology of Learning and Memory* **68 (1)** 13-20.

Kaas, J. H., Merzenich, M. M. and Killackey, H. P., 1983: The reorganization of somatosensory cortex following peripheral nerve damage in adult and developing mammals. *Annual Reviews in Neuroscience* **6** 325-56.

Kacharmina, J. E., Job, C., Crino, P. and Eberwine, J., 2000: Stimulation of glutamate receptor protein synthesis and membrane insertion within isolated neuronal dendrites. *Proceedings of the National Academy of Sciences U.S.A.* **97 (21)** 11545-11550.

Kaech, S., Ludin, B. and Matus, A., 1996: Cytoskeletal plasticity in cells expressing neuronal microtubule-associated proteins. *Neuron* **17 (6)** 1189-1199.

Kelly, P. T., McGuinness, T. L. and Greengard, P., 1984: Evidence that the major postsynaptic density protein is a component of a Ca2+/calmodulin-dependent protein kinase. *Proceedings of the National Academy of Sciences U.S.A.* **81 (3)** 945-949.

Kennedy, M. B., 1998: Signal transduction molecules at the glutamatergic postsynaptic membrane. *Brain Research Reviews* **26 (2-3)** 243-257.

Kennedy, M. B., Bennett, M. K. and Erondu, N. E., 1983: Biochemical and immunochemical evidence that the "major postsynaptic density protein" is a subunit of a calmodulin-dependent protein kinase. *Proceedings of the National Academy of Sciences U.S.A.* **80 (23)** 7357-7361.

Kentros, C., Hargreaves, E., Hawkins, R. D., Kandel, E. R., Shapiro, M. and Muller, R. V., 1998: Abolition of long-term stability of new hippocampal place cell maps by NMDA receptor blockade. *Science* **280 (5372)** 2121-2126.

Kerr, D. S. and Abraham, W. C., 1993: Comparison of associative and non-associative conditioning procedures in the induction of LTD in CA1 of the hippocampus. *Synapse* **14 (4)** 305-313.

Kerr, D. S. and Abraham, W. C., 1996: LTD: many means to how many ends? *Hippocampus* **6 (1)** 30-34.

Kharazia, V. N. and Weinberg, R. J., 1997: Tangential synaptic distribution of NMDA and AMPA receptors in rat neocortex. *Neuroscience Letters* **238 (1-2)** 41-44.

Kim, J. J. and Yoon, K. S., 1998: Stress: metaplastic effects in the hippocampus. *Trends in Neurosciences* **21 (12)** 505-509.

Kirkwood, A. and Bear, M. F., 1994: Hebbian synapses in visual cortex. *Journal of Neuroscience* **14 (3 pt 2)** 1634-1645.

Kleschevnikov, A. M. and Routtenberg, A., 2001: PKC activation rescues LTP from NMDA receptor blockade. *Hippocampus* **11 (2)** 168-175.

Koester, H. J. and Sakmann, B., 1998: Calcium dynamics in single spines during coincident pre- and postsynaptic activity depend on relative timing of back-propagating action potentials and subthreshold excitatory postsynaptic potentials. *Proceedings of the National Academy of Sciences U.S.A.* **95 (16)** 9596-9601.

Korkotian, E. and Segal, M., 1999: Release of calcium from stores alters the morphology of dendritic spines in cultured hippocampal neurons. *Proceedings of the National Academy of Sciences U.S.A.* **96 (21)** 12068-12073.

Kornau, H.-K., Schenker, L. T., Kennedy, M. B. and Seeburg, P. H., 1995: Domain interaction between NMDA receptor subunits and the postsynaptic density protein PSD-95. *Science* **269 (5231)** 1737-1740.

Krugers, H. J., Koolhaas, J. M. and Korf, J., 1993: A single stress-experience alters glutamate receptor-binding in rat hippocampal CA3 area. *Neuroscience Letters* **154 (1-2)** 73-77.

Larson, J., Wong, D. and Lynch, G., 1986: Patterned stimulation at the theta frequency is optimal for the induction of hippocampal long-term potentiation. *Brain Research* **368 (2)** 347-350.

Lechner, H. A. and Byrne, J. H., 1998: New perspectives on Classical conditioning: a synthesis of Hebbian and non-Hebbian mechanisms. *Neuron* **20 (3)** 355-358.

LeMasson, G., Marder, E. and Abbott, L. F., 1993: Activity-dependent regulation of conductances in model neurones. *Science* **259 (5103)** 1915-1917.

Lendvai, B., Stern, E. A., Chen, B. and Svoboda, K., 2000: Experience-dependent plasticity of dendritic spines in the developing rat barrel cortex in vitro. *Nature* **404 (6780)** 876-881.

Li, S., Anwyl, R. and Rowan, M. J., 2000: A persistent reduction in short-term facilitation accompanies long-term potentiation in the CA1 area in the intact hippocampus. *Neuroscience* **100 (2)** 213-220.

Liao, D., Hessler, N. A. and Manilow, R., 1995: Activation of postsynaptically silent synapses during pairing-induced LTP in CA1 region of hippocampal slice. *Nature* **375 (6530)** 400-404.

Liao, D., Zhang, X., O'Brien, R., Ehlers, M. D. and Huganir, R. L., 1999: Regulation of morphological postsynaptic silent synapses in developing hippocampal neurons. *Nature Neuroscience* **2 (1)** 37-43.

Lieberman, D. N. and Mody, I., 1999: Casein kinase II regulates NMDA channel function in hippocampal neurons. *Nature Neuroscience* **2 (2)** 125-132.

Lisberger, S. G., 1998: Cerebellar LTD: a molecular mechanism of behavioural learning? *Cell* **92 (6)** 701-704.

Lisman, J., 1989: A mechanism for the Hebb and the anti-Hebb processes underlying learning and memory. *Proceedings of the National Academy of Sciences U.S.A.* **86 (23)** 9574-9578.

Lisman, J., 1994: The CaM kinase II hypothesis for the storage of synaptic memory. *Trends in Neurosciences* **17 (10)** 406-412.

Lisman, J. E. and Harris, K. M., 1993: Quantal analysis and synaptic anatomy - integrating two views of hippocampal plasticity. *Trends in Neurosciences* **16 (4)** 141-147.

Lissen, D. V., Gomperts, S. N., Carroll, R. C., Christine, C. W., Kalman, D., Kitamura, M., Hardy, S., Nicoll, R. A., Malenka, R. C. and von Zastrow, M., 1998: Activity differentially regulates the surface expression of synaptic AMPA and NMDA glutamate receptors. *Proceedings of the National Academy of Sciences U.S.A.* **95 (12)** 7097-7102.

Liu, D., Bei, D., Parmar, H. and Matus, A., 2000: Activity-regulated, cytoskeleton-associated protein (Arc) is essential for visceral endoderm organization during early embryogenesis. *Mechanisms of Development* **92 (2)** 207-215.

Lorente de No, R., 1934: Studies on the structure of the cerebral cortex. II Continuation of the study of the ammonic system. *Journal of Psychol. Neurol.* **46** 113-177.

Louie, K. and Wilson, M. A., 2001: Temporally structured replay of awake hippocampal ensemble activity during rapid eye movement sleep. *Neuron* **29 (1)** 145-156.

Lu, W.-Y., Man, H.-Y., Ju, W., Trimble, W. S., MacDonald, J. F. and Wang, Y. T., 2001: Activation of synaptic NMDA receptors induces membrane insertion of new AMPA receptors and LTP in cultured hippocampal neurons. *Neuron* **29 (1)** 243-254.

Lucocq, J., 1992: Quantitation of gold labelling and estimation of labelling efficiency with a stereological counting method. *Journal of Histochemistry and Cytochemistry* **40 (12)** 1929-1936.

Lupien, S. J. and McEwen, B. S., 1997: The acute effects of corticosteroids on cognition: integration of animal and human model studies. *Brain Research Reviews* **24 (1)** 1-27.

Lüscher, C. and Frerking, M., 2001: Restless AMPA receptors: implications for synaptic transmission and plasticity. *Trends in Neurosciences* **24 (11)** 665-670.

Lüthi, A., Laurent, J.-P., Figurov, A., Muller, D. and Schachner, M., 1994: Hippocampal long term potentiation and neural cell adhesion molecules L1 and NCAM. *Nature* **372 (6508)** 777-779.

Lyford, G. L., Yamagata, K., Kaufmann, W. E., Barnes, C. A., Sanders, L. K., Copeland, N. G., Gilbert, D. J., Jenkins, N. A., Lanahan, A. A. and Worley, P. F., 1995: *Arc*, a growth factor and activity-regulated gene, encodes a novel cytoskeleton-associated protein that is enriched in neuronal dendrites. *Neuron* **14 (2)** 433-445.

Lynch, G. S., Dunwiddie, T. and Grybkoff, V., 1977: Heterosynaptic depression: A postsynaptic correlate of long-term potentiation. *Nature* **266 (5604)** 737-739.

Lynch, G., Larson, J., Kelso, S., Barrionuevo, G. and Schottler, F., 1983: Intracellular injections of EGTA block induction of hippocampal long- term potentiation. *Nature* **305 (5936)** 719-721.

Magariños, A. M. and McEwen, B. S., 1995: Stress-induced atrophy of apical dendrites of hippocampal CA3c neurons: involvement of glucocorticoid secretion and excitatory amino acid receptors. *Neuroscience* **69 (1)** 89-98.

Mainen, Z. F., Jia, Z., Roder, J. and Manilow, R., 1998: Use-dependent AMPA receptor block in mice lacking GluR2 suggests postsynaptic site for LTP expression. *Nature Neuroscience* **1 (7)** 579-586.

Majewska, A., Brown, E., Ross, J. and Yuste, R., 2000: Mechanisms of calcium decay kinetics in hippocampal spines: role of spine calcium pumps and calcium diffusion through the spine neck in biochemical compartmentalization. *Journal of Neuroscience* **20 (5)** 1722-1734.

Malenka, R. C., 1994: Synaptic plasticity in the hippocampus: LTP and LTD. *Cell* **78 (4)** 535-538.

Maletic-Savatic, M., Malinow, R. and Svoboda, K., 1999: Rapid dendritic morphogenesis in CA1 hippocampal dendrites induced by synaptic activity. *Science* **283 (5409)** 1923-1927.

Manahan-Vaughan, D., Braunewell, K.-H. and Reymann, K. G., 1998: Subtype-specific involvement of metabotropic glutamate receptors in two forms of long term potentiation in the dentate gyrus of freely moving rats. *Neuroscience* **86 (3)** 709-721.

Maren, S. and Holt, W., 2000: The hippocampus and contextual memory retrieval in Pavlovian conditioning. *Behavioural Brain Research* **110 (1-2)** 97-108.

Markram, H. and Tsodyks, M., 1996: Redistribution of synaptic efficacy between neocortical pyramidal neurons. *Nature* **382 (6594)** 807-810.

Marrs, G. S., Green, S. H. and Dailey, M. E., 2001: Rapid formation and remodelling of postsynaptic densities in developing dendrites. *Nature Neuroscience* **4 (10)** 1006-1013.

Martin, K. C., Barad, M. and Kandel, E. R., 2000a: Local protein synthesis and its role in synapse-specific plasticity. *Current Opinion in Neurobiology* **10 (5)** 587-592.

Martin, K. C., Casadio, A., Zhu, H., E, Y., Rose, J. C., Chen, M., Bailey, C. H. and Kandel, E. R., 1997: Synapse-specific, long term facilitation of Aplysia sensory to motor synapses: a function for local protein synthesis in memory storage. *Cell* **91 (7)** 927-938.

Martin, S. J., Grimwood, P. D. and Morris, R. G. M., 2000b: Synaptic plasticity and memory: an evaluation of the hypothesis. *Annual Reviews in Neuroscience* **23** 649-711.

Mattson, M. P., LaFerla, F. M., Chan, S. L., Leissring, M. A., Shepel, P. N. and Geiger, J. D., 2000: Calcium signalling in the ER: its role in neuronal plasticity and neurodegenerative disorders. *Trends in Neurosciences* **23 (5)** 222-229.

Matus, A., 1999: Postsynaptic actin and neuronal plasticity. *Current Opinion in Neurobiology* **9 (5)** 561-565.

Matus, A., 2000: Actin-based plasticity in dendritic spines. *Science* **290 (5492)** 754-758.

Mauk, M. D., Garcia, K. S., Medina, J. F. and Steele, P. M., 1998: Does cerebellar LTD mediate motor learning? Toward a resolution without a smoking gun. *Neuron* **20 (3)** 359-362.

Mayhew, T. M., 1996: How to count synapses unbiasedly and efficiently at the ultrastructural level: proposal for a standard sampling and counting protocol. *Journal of Neurocytology* **25 (12)** 793-804.

Mayhew, T. M., 1999: Second-order stereology and ultrastructural examination of the spatial arrangements of tissue compartments within glomeruli of normal and diabetic kidneys. *Journal of Microscopy* **195 (2)** 87-95.

McEwen, B. S., 1999: Stress and hippocampal plasticity. *Annual Reviews in Neuroscience* 22 105-122.

Megías, M., Emri, Z., Freund, T. F. and Gulyás, A. I., 2001: Total number and distribution of inhibitory and excitatory synapses on hippocampal CA1 pyramidal cells. *Neuroscience* 102 (3) 527-540.

Merzenich, M. M., Kaas, J. H., Wall, J. Nelson, R. J., Sur, M. and Felleman, D., 1983: Topographic reorganization of somatosensory cortical areas 3b and 1 in adult monkeys following restricted deafferentation. *Neuroscience* 8 (1) 33-55.

Milner, B., Squire, L. R. and Kandel, E. R., 1998: Cognitive neuroscience and the study of memory. *Neuron* 20 (3) 445-468.

Mishkin, M., Suzuki, W. A., Gadian, D. G. and Vargha-Khadem, F., 1998: Hierarchical organisation of cognitive memory. *Philosophical Transactions of the Royal Society of London Series B* 352 (1360) 1461-1467.

Monyer, H., Sprengel, R., Schoepfer, R., Herb, A., Higuchi, M., Lomeli, H., Burnashev, N., Sakmann, B. and Seeburg, P. H., 1992: Heteromeric NMDA receptors: molecular and functional distinction of subtypes. *Science* 256 (5060) 1217-1221.

Morris, R., 1984: Developments of a water-maze procedure for studying spatial learning in the rat. *Journal of Neuroscience Methods* 11 (1) 47-60.

Morris, R. G. M., Garrud, P., Rawlins, J. N. P. and O'Keefe, J., 1982: Place navigation impaired in rats with hippocampal lesions. *Nature* 297 (5868) 681-683.

Morris, R. G., Anderson, E., Lynch, G. S. and Baudry, M., 1986: Selective impairment of learning and blockade of long-term potentiation by an N-methyl-D-aspartate receptor antagonist, AP5. *Nature* 319 (6056) 774-776.

Moser, E., Moser, M.-B. and Andersen, P., 1993: Spatial learning impairment parallels the magnitude of dorsal hippocampal lesions, but is hardly present following ventral lesions. *Journal of Neuroscience* 13 (9) 3916-3925.

Moser, E. I. and Moser, M.-B., 1999: Is learning blocked by saturation of synaptic weights in the hippocampus? *Neuroscience and Biobehavioural Reviews* 23 (5) 661-672.

Moser, M.-B., Moser, E., Forrest, E., Andersen, P. and Morris, R. G. M., 1995: Spatial learning with a minislab in the dorsal hippocampus. *Proceedings of the National Academy of Sciences U.S.A.* 92 (21) 9697-9701.

Moser, M.-B., Trommald, M. and Andersen, P., 1994: An increase in dendritic spine density on hippocampal CA1 pyramidal cells following spatial learning in adult rats suggests the formation of new synapses. *Proceedings of the National Academy of Sciences U.S.A.* 91 (26) 12673-12675.

Mulkey, R. M., Endo, S., Shenolikar, S. and Malenka, R.C., 1994: Involvement of a calcineurin/inhibitor-1 phosphatase cascade in hippocampal long-term depression. *Nature* 369 (6480) 486-488.

Mulle, C., Sailer, A., Swanson, G. T., Brana, C., O'Gorman, S., Bettler, B. and Heinemann, S. F., 2000: Subunit composition of kainate receptors in hippocampal interneurons. *Neuron* **28 (2)** 475-484.

Muller, D., Wang, C., Skibo, G., Toni, N., Cremer, H., Calaora, V., Rougon, G. and Kiss, J. Z., 1996: PSA-NCAM is required for activity-induced synaptic plasticity. *Neuron* **17 (3)** 413-422.

Müller, W. and Connor, J. A., 1991: Dendritic spines as individual neuronal compartments for synaptic Ca2+ responses. *Nature* **354 (6348)** 73-76.

Murphy, G. G. and Glanzman, D. L., 1997: Mediation of classical conditioning in *Aplysia californica* by long term potentiation of sensorimotor synapses. *Science* **278 (5337)** 467-471.

Murray, E. A., Gaffan, D. and Mishkin, M., 1993: Neural substrates of visual stimulus-stimulus association in rhesus monkeys. . *Journal of Neuroscience* **13 (10)** 4549-4561.

Nadel, L. and Moscovitch, M., 1997: Memory consolidation, retrograde amnesia and the hippocampal complex. *Current Opinion in Neurobiology* **7 (2)** 217-227.

Nadel, L. and Bohbot, V., 2001: Consolidation of memory. *Hippocampus* **11 (1)** 56-60.

Nadel, L. and Land, C., 2000: Memory traces revisited. *Nature Reviews Neuroscience* **1 (3)** 209-219.

Nader, K., Schafe, G. E. and Le Doux, J. E., 2000: Fear memories require protein synthesis in the amygdala for reconsolidation after retrieval. *Nature* **406 (6797)** 722-726.

Neher, E., 1998: Vesicle pools and Ca2+ microdomains: new tools for understanding their roles in neurotransmitter release. *Neuron* **20 (3)** 389-399.

Neuhoff, H., Roeper, J. and Schweizer, M., 1999: Activity-dependent formation of perforated synapses in cultured hippocampal neurons. *European Journal of Neuroscience* **11 (12)** 4241-4250.

Nolte, J., 1993: *The Human Brain. An introduction to its functional anatomy.* Mosby-Year Book Inc.: 11830 Westline Industrial Drive, St. Louis, Missouri 63146.

Nusser, Z., 2000: AMPA and NMDA receptors: similarities and differences in their synaptic distribution. *Current Opinion in Neurobiology* **10 (3)** 337-341.

Nusser, Z., Lujan, R., Laube, G., Roberts, J. D. B., Molnar, E. and Somogyi, P., 1998: Cell type and pathway dependence of synaptic AMPA receptor number and variability in the hippocampus. *Neuron* **21 (3)** 545-559.

O'Brien, R. J., Kamboj, S., Ehlers, M. D., Rosen, K. R., Fischbach, G. D. and Huganir, R. L., 1998: Activity-dependent modulation of synaptic AMPA receptor accumulation. *Neuron* **21 (5)** 1067-1078.

O'Keefe, J. and Dostrovsky, J., 1971: The hippocampus as a spatial map. Preliminary evidence from unit activity in the freely-moving rat. *Brain Research* **34 (1)** 171-175.

Okuno, H., Tokuyama, W., Li, Y.-X., Hashimoto, T. and Miyashita, Y., 1999: Quantitative evaluation of neurotrophin and *trk* mRNA expression in visual and limbic areas along the occipito-temporo-hippocampal pathway in adult Macaque monkeys. *Journal of Comparative Neurology* **408 (3)** 378-398.

O'Malley, A., O'Connell, C. and Regan, C. M., 1998: Ultrastructural analysis reveals avoidance conditioning to induce a transient increase in hippocampal dentate spine density in the 6 hour post-training period of consolidation. *Neuroscience* **87 (3)** 607-613.

O'Malley, A., O'Connell, C. and Regan, C. M., 2000: Transient spine density increases in the mid-molecular layer of hippocampal dentate gyrus accompany consolidation of a spatial learning task in the rodent. *Neuroscience* **99 (2)** 229-232.

Otani, S. and Connor, J. A., 1995: Long-term depression of naive synapses in adult hippocampus induced by asynchronous synaptic activity. *Journal of Neurophysiology* **73 (6)** 2596-2601.

Packard, M. G., Hirsh, R. and White, N. M., 1989: Differential effects of fornix and caudate nucleus lesions on two radial maze tasks: evidence for multiple memory systems. *Journal of Neuroscience* **9 (5)** 1465-72.

Packard, M. G. and White, N. M., 1991: Dissociation of hippocampus and caudate nucleus memory systems by posttraining intracerebral injection of dopamine agonists. *Behavioural Neuroscience* **105 (2)** 295-306.

Paolillo, M., Feliciello, A., Porcellini, A., Garbi, C., Bifulco, M., Schinelli, S., Ventra, C., Stabile, E., Ricciardelli, G., Schettini, G. and Avvedimento, E. V., 1999: The type and the localisation of cAMP-dependent protein kinase regulate transmission of cAMP signals to the nucleus in cortical and cerebellar granule cells. *Journal of Biological Chemistry* **274 (10)** 6546-6552.

Park, C. R., Campbell, A. M., Wilbanks, A. L., Smith, T. P., Fleshner, M. and Diamond, D. M., 2001: U-shaped function between endogenous corticosterone and spatial memory impairments in stressed rats. *Society for Neuroscience Abstracts* **Volume 27**, Program Number 532.10.

Patel, S. N., Rose, S. P. R. and Stewart, M. G., 1988: Training induced dendritic spine density changes are specifically related to memory formation processes in the chick, *Gallus domesticus. Brain Research* **463 (1)** 168-173.

Paxinos, G. and Watson, C., 1998: *The rat brain in stereotaxic coordinates.* 4th Edition Academic Press:

Pearce, J. M., Roberts, A. D. L. and Good, M., 1998: Hippocampal lesions disrupt navigation based on cognitive maps but not heading vectors. *Nature* **396 (6706)** 75-77.

Persohn, E., Pollerberg, E. and Schachner, M., 1989: Immunoelectron-microscopic localization of the 180kD component of the neural cell adhesion molecule NCAM in postsynaptic membranes. *Journal of Comparative Neurology* **288** (1) 92-100.

Peters, A., Palay, S. L. and Webster, H de F., 1991: *The Fine Structure of the Nervous System: the cells and their processes.* Harper & Row: London.

Petralia, R. S., Esteban, J. A., Wang, Y.-X., Partridge, J. G., Zhao, H.-M., Wenthold, R. J. and Manilow, R., 1999: Selective acquisition of AMPA receptors over postnatal development suggests a molecular basis for silent synapses. *Nature Neuroscience* **2** (1) 31-36.

Petralia, R. S., Wang, Y.-X. and Wenthold, R. J., 1994: The NMDA receptor subunits NR2A and NR2B show histological and ultrastructural localisation patterns similar to those of NR1. *Journal of Neuroscience* **14** (10) 6102-6120.

Petralia, R. S. and Wenthold, R. J., 1992: Light and electron immunocytochemical localisation of AMPA-selective glutamate receptors in the rat brain. *Journal of Comparative Neurology* **318** (3) 329-354.

Phend, K. D., Rustioni, A. and Weinberg, R. J., 1995: An osmium-free method of epon embedment that preserves both ultrastructure and antigenicity for post-embedding immunocytochemistry. *Journal of Histochemistry and Cytochemistry* **43** (3) 283-292.

Philpot, B. D., Sekhar, A. K., Shouval, H. Z. and Bear, M. F., 2001: Visual experience and deprivation bidirectionally modify the composition and function of NMDA receptors in visual cortex. *Neuron* **29** (1) 157-169.

Pickard, L., Noël, J., Henley, J. M., Collingridge, G. L. and Molnar, E., 2000: Developmental changes in synaptic AMPA and NMDA receptor distribution and AMPA receptor subunit composition in living hippocampal neurons. *Journal of Neuroscience* **20** (21) 7922-7931.

Plata-Salamán, C. R., Ilyin, S. E., Turrin, N. P., Gayle, D., Flynn, M. C., Bedard, T., Merali, Z. and Anisman, H., 2000: Neither acute nor chronic exposure to a naturalistic (predator) stressor influences the interleukin-1β system, tumour necrosis factor-α, transforming growth factor-βb1, and neuropeptide mRNAs in specific brain regions. *Brain Research Bulletin* **51** (2) 187-193.

Poldrack, R. A. and Gabrieli, J. D. E., 1998: Memory and the brain: what's right and what's left? *Cell* **93** (7) 1091-1093.

Price, N. E. and Mumby, M. C., 1999: Brain protein serine/threonine phosphatases. *Current Opinion in Neurobiology* **9** (3) 336-342.

Quevedo, J., Vianna, M. R., Roesler, R., de-Paris, F., Izquierdo, I. and Rose, S. P., 1999: Two time windows of anisomycin-induced amnesia for inhibitory avoidance training in rats: protection from amnesia by pretraining but not pre-exposure to the task apparatus. *Learning and Memory* **6** (6) 600-607.

Racca, C., Stephenson, F. A., Streit, P., Roberts, J. D. B. and Somogyi, P., 2000: NMDA receptor content of synapses in stratum radiatum of the hippocampal CA1 area. *Journal of Neuroscience* **20 (7)** 2512-2522.

Rao, A. and Craig, A. M., 1997: Activity regulates the synaptic localization of the NMDA receptor in hippocampal neurons. *Neuron* **19 (4)** 801-812.

Raymond, L. A., Blackstone, C. D. and Huganir, R. L., 1993: Phosphorylation of amino acid neurotransmitter receptors in synaptic plasticity. *Trends in Neurosciences* **16 (4)** 147-153.

Richter-Levin, G., Canevari, L. and Bliss, T. V. P., 1998: Spatial training and high-frequency stimulation engage a common pathway to enhance glutamate release in the hippocampus. *Learning and Memory* **4 (6)** 445-450.

Riedel, G., 1996: Function of metabotropic glutamate receptors in learning and memory. *Trends in Neurosciences* **19 (6)** 219-224.

Riedel, G., Micheau, J., Lam, A. G., Roloff, E., Martin, S. J., Bridge, H., Hoz, L., Poeschel, B., McCulloch, J. and Morris, R. G., 1999: Reversible neural inactivation reveals hippocampal participation in several memory processes. *Nature Neuroscience* **2 (10)** 898-905.

Rose, G. J. and Call, S. J., 1992: Evidence for the role of dendritic spines in the temporal filtering properties of neurons: The decoding problem and beyond. *Proceedings of the National Academy of Sciences U.S.A.* **89 (20)** 9662-9665.

Rose, G. M. and Dunwiddie, T. V., 1986: Induction of hippocampal long-term potentiation using physiologically patterned stimulation. *Neuroscience Letters* **69 (3)** 244-248.

Rotenberg, A., Mayford, M., Hawkins, R. D., Kandel, E. R. and Muller, R. U., 1996: Mice expressing activated CaMK II lack low frequency LTP and do not form stable place cells in the CA1 region of the hippocampus. *Cell* **87 (7)** 1351-1361.

Rusakov, D. A., Davies, H. A., Harrison, E., Diana, G., Richter-Levin, G., Bliss, T. V. P. and Stewart, M. G., 1997: Ultrastructural synaptic correlates of spatial learning in rat hippocampus. *Neuroscience* **80 (1)** 69-77.

Rusakov, D. A., Stewart, M. G. and Korogod, S. M., 1996: Branching of active dendritic spines as a mechanism for controlling synaptic efficacy. *Neuroscience* **75 (1)** 315-323.

Rutishauser, U. and Landmesser, L., 1996: Polysialic acid in the vertebrate nervous system: a promoter of plasticity in cell-cell interactions. *Trends in Neurosciences* **19 (10)** 422-427.

Ryugo, D. K., Ryugo, R. and Killackay, H. P., 1975: Changes in pyramidal cell density consequent to vibrissae removal in the newborn rat. *Brain Research* **96 (1)** 82-87.

Sacchetti, B., Lorenzini, C. A., Baldi, E., Bucherelli, C., Roberto, M., Tassoni, G. and Brunelli, M., 2001: Long-lasting hippocampal potentiation and contextual memory consolidation. *European Journal of Neuroscience* **13 (12)** 2291-2298.

Sakimura, K., Kutsuwada, T., Ito, I., Manabe, T., Takayama, C., Etsuko, K., Yagi, T., Aizawa, S., Inoue, Y., Sugiyama, H. and Mishina, M., 1995: Reduced hippocampal LTP and spatial learning in mice lacking NMDA receptor ε1 subunit. *Nature* **373 (6510)** 151-155.

Sandi, C., Loscertales, M. and Guaza, C., 1997: Experience-dependent facilitating effect of corticosterone on spatial memory formation in the water maze. *European Journal of Neuroscience* **9 (4)** 637-642.

Sans, N., Petralia, R. S., Wang, Y.-X., Blahos II, J., Hell, J. W. and Wenthold, R. J., 2000: A developmental change in NMDA receptor-associated proteins at hippocampal synapses. *Journal of Neuroscience* **20 (3)** 1260-1271.

Saucier, D. and Cain, D. P., 1995: Spatial learning without NMDA receptor-dependent long-term potentiation. *Nature* **378 (6553)** 186-189.

Scannevin, R. H. and Huganir, R. L., 2000: Postsynaptic organisation and regulation of excitatory synapses. *Nature Reviews Neuroscience* **1 (2)** 133-141.

Scheetz, A. J., Nairn, A. C. and Constantine-Paton, M., 2000: NMDA receptor-mediated control of protein synthesis at developing synapses. *Nature Neuroscience* **3 (3)** 211-216.

Schmid, R.-S., Graff, R. D., Schaller, M. D., Chen, S., Schachner, M., Hemperly, J. J. and Maness, P. F., 1999: NCAM stimulates the Ras-MAPK pathway and CREB phosphorylation in neuronal cells. *Journal of Neurobiology* **38 (4)** 542-558.

Schuman, E. M., 1997: Synapse specificity and long-term information storage. *Neuron* **18 (3)** 339-342.

Schuman, E. M., 1999: mRNA trafficking and local protein synthesis at the synapse. *Neuron* **23 (4)** 645-648.

Schuster, T., Krug, M., Hassan, H. and Schachner, M., 1998: Increase in proportion of hippocampal spine synapses expressing neural cell adhesion molecule NCAM180 following long term potentiation. *Journal of Neurobiology* **37 (3)** 359-372.

Segal, M., 1995: Dendritic spines for neuroprotection: a hypothesis. *Trends in Neurosciences* **18 (11)** 468-71.

Segal, M., 2001: Rapid plasticity of dendritic spine: hints to possible functions? *Progress in Neurobiology* **63 (1)** 61-70.

Serafini, T., 1999: Finding a partner in a crowd: neuronal diversity and synaptogenesis. *Cell* **98 (2)** 133-136.

Shepherd, G. M. and Erulkar, S. D., 1997: Centenary of the synapse: from Sherrington to the molecular biology of the synapse and beyond. *Trends in Neurosciences* **20 (9)** 385-392.

Sherrington, C. S., 1897: *A Text Book of Physiology, Part III: The Central Nervous System.* 7<sup>th</sup> Edition, Foster, M. ed. Macmillan: London.

Shi, S.-H., Hayashi, Y., Petralia, R. S., Zaman, S. H., Wenthold, R. J., Svoboda, K. and Manilow, R., 1999: Rapid spine delivery and redistribution of AMPA receptors after synaptic NMDA receptor activation. *Science* **284 (5421)** 1811-1816.

Shors, T. J., Miesegaes, G., Beylin, A., Zhao, M., Rydel, T. and Gould, E., 2001: Neurogenesis in the adult is involved in the formation of trace memories. *Nature* **410 (6826)** 372-375.

Silva, A. J., Giese, K. P., Fedorov, N. B., Frankland, P. W. and Kogan, J. H., 1998a: Molecular, cellular and neuroanatomical substrates of place learning. *Neurobiology of Learning and Memory* **70 (1-2)** 44-61.

Silva, A. J., Kogan, J. H., Frankland, P. W. and Kida, S., 1998b: CREB and memory. *Annual Reviews in Neuroscience* **21** 127-148.

Silva, A. J., Paylor, R., Wehner, J. M. and Tonegawa, S., 1992a: Impaired spatial learning in alpha-calcium-calmodulin kinase II mutant mice. *Science* **257 (5067)** 206-211.

Silva, A. J., Stevens, C. F., Tonegawa, S. and Wang, Y., 1992b: Deficient hippocampal long-term potentiation in alpha-calcium-calmodulin kinase II mutant mice. *Science* **257 (5067)** 201-206.

Simbürger, E., Plaschke, M., Fritschy, J.-M. and Nitsch, R., 2001: Localisation of two major GABA A receptor subunits in the dentate gyrus of the rat and cell type-specific up-regulation following entorhinal cortex lesion. *Neuroscience* **102 (4)** 789-803.

Singer, W., 1999: Time as coding space? *Current Opinion in Neurobiology* **9 (2)** 189-194.

Skelton, R. W., Scarth, A. S., Wilkie, D. M., Miller, J. J. and Phillips, A. G., 1987: Long-term increases in dentate granule cell responsivity accompany operant conditioning. *Journal of Neuroscience* **7 (10)** 3081-3087.

Skibo, G. G., Davies, H. A., Rusakov, D. A., Stewart, M. G. and Schachner, M., 1998: Increased immunogold labelling of neural cell adhesion molecule isoforms in synaptic active zones of the chick striatum 5-6 hours after one-trial passive avoidance training. *Neuroscience* **82 (1)** 1-5.

Snyder, E. M., Philpot, B. D., Huber, K. M., Dong, X., Fallon, J. R. and Bear, M. F., 2001: Internalization of ionotropic glutamate receptors in response to mGluR activation. *Nature Neuroscience* **4 (11)** 1079-1085.

Sojka, M., Davies, H. A., Harrison, E. and Stewart, M. G., 1995: Long-term increases in synaptic density in chick CNS after passive avoidance training are blocked by an inhibitor of protein synthesis. *Brain Research* **684 (2)** 209-14.

Somogyi, P., Tamás, G., Lujan, R. and Buhl, E. H., 1998: Salient features of synaptic organisation in the cerebral cortex. *Brain Research Reviews* **26 (2-3)** 113-135.

Sorra, K. E., Fiala, J. C. and Harris, K. M., 1998: Critical assessment of the involvement of perforations, spinules and spine branching in hippocampal synapse formation. *Journal of Comparative Neurology* **398 (2)** 225-240.

Sorra, K. E. and Harris, K. M., 1998: Stability in synapse number and size at 2 hr after long term potentiation in hippocampal area CA1. *Journal of Neuroscience* **18 (2)** 658-671.

Spacek, J. and Harris, K. M., 1997: Three-dimensional organisation of smooth endoplasmic reticulum in hippocampal CA1 dendrites and dendritic spines of the immature and mature rat. *Journal of Neuroscience* **17 (1)** 190-203.

Squire, L. R. and Zola-Morgan, S., 1991: The medial temporal lobe memory system. *Science* **253 (5026)** 1380-1385.

Stanley, E. F., 1997: The calcium channel and the organisation of the presynaptic transmitter release face. *Trends in Neurosciences* **20 (9)** 404-409.

Squire, L. R., 1992: Memory and the hippocampus: a synthesis from findings with rats, monkeys and humans. *Psychology Reviews* **99 (2)** 195-231.

Stanton, P. K. and Sejnowski, T. J. 1989: Associative long-term depression in the hippocampus induced by hebbian covariance. *Nature* **339 (6221)** 215-218.

Stanton, P. K., 1996: LTD, LTP, and the sliding threshold for long-term synaptic plasticity. *Hippocampus* **6 (1)** 35-42.

Steele, R. J. and Morris, R. G. M., 1999: Delay-dependent impairment of a matching-to-place task with chronic and intrahippocampal infusion of the NMDA-antagonist D-AP5. *Hippocampus* **9 (2)** 118-136.

Steele, R. J., Stewart, M. G. and Rose, S. P. R., 1995: Increases in NMDA receptor binding are specifically related to memory for a passive avoidance task in the chick: a quantitative autoradiographic study. *Brain Research* **674 (2)** 352-356.

Sterio, D. C., 1984: The unbiased estimation of number and sizes of arbitrary particles using the disector. *Journal of Microscopy* **134 (2)** 127-136.

Stevens, C. F., 1996: Spatial learning and memory: the beginning of a dream. *Cell* **87 (7)** 1147-1148.

Steward, O., 1997: mRNA localisation in neurons: a multipurpose mechanism? *Neuron* **18 (1)** 9-12.

Steward, O., Wallace, C. S., Lyford, G. L. and Worley, P. F., 1998: Synaptic activation causes the mRNA for the IEG *Arc* to localise selectively near activated postsynaptic sites on dendrites. *Neuron* **21 (4)** 741-751.

Stewart, M. G., Harrison, E., Rusakov, D. A., Richter-Levin, G. and Maroun, M., 2000: Re-structuring of synapses 24 hours after induction of long-term potentiation in the dentate gyrus of the rat hippocampus *in vivo*. *Neuroscience* **100 (2)** 221-227.

Südhof, T. C., 1995: The synaptic vesicle cycle: a cascade of protein-protein interactions. *Nature* **375 (6533)** 645-653.

Suzuki, W. A. and Amaral, D. G., 1994: Topographic organisation of the reciprocal connections between the monkey entorhinal cortex and the perirhinal and parahippocampal corticies. *Journal of Neuroscience* **14 (3)** 1856-1877.

Suzuki, W. A., 1999: The long and the short of it: memory signals in the medial temporal lobe. *Neuron* **24 (2)** 295-298.

Takechi, H., Eilers, J. and Konnerth, A., 1998: A new class of synaptic response involving calcium release in dendritic spines. *Nature* **396 (6713)** 757-760.

Takumi, Y., Ramirez-Leon, V., Laake, P., Rinvik, E. and Ottersen, O. P., 1999: Different modes of expression of AMPA and NMDA receptors in hippocampal synapses. *Nature Neuroscience* **2 (7)** 618-624.

Tang, L., Hung, C. P. and Schuman, E. M., 1998: A role for the cadherin family of cell adhesion molecules in hippocampal long-term potentiation. *Neuron* **20 (6)** 1165-1175.

Tang, Y.-P., Shimizu, E., Dube, G. R., Rampon, C., Kerchner, G. A., Zhuo, M., Liu, G. and Tsien, J. Z., 1999: Genetic enhancement of learning and memory in mice. *Nature* **401 (6748)** 63-69.

Taube, J. S., 1995: Place cells recorded in the parasubiculum of freely moving rats. *Hippocampus* **5 (6)** 569-583.

Thiels, E., Xiaping, X., Yeckel, M. F., Barrionuevo, G. and Berger, T. W., 1996: NMDA receptor-dependent LTD in different subfields of hippocampus in vivo and in vitro. *Hippocampus* **6 (1)** 43-51.

Thompson, A. M., 2000: Facilitation, augmentation and potentiation at central synapses. *Trends in Neurosciences* **23 (7)** 305-312.

Tocco, G., Shors, T. J., Baudry, M. and Thompson, R. F., 1991: Selective increase in AMPA binding to the AMPA/quisqualate receptor in the hippocampus in response to acute stress. *Brain Research* **559 (1)** 168-171.

Tompa, P. and Friedrich, P., 1998: Synaptic metaplasticity and the local charge effect in postsynaptic densities. *Trends in Neurosciences* **21 (3)** 97-102.

Toni, N., Buchs, P.-A., Nikonenko, I., Bron, C. R. and Muller, D., 1999: LTP promotes formation of multiple spine synapses between a single axon terminal and a dendrite. *Nature* **402 (6760)** 421-425.

Tovar, K. R. and Westbrook, G. L., 1999: The incorporation of NMDA receptors with a distinct subunit composition at nascent hippocampal synapses *in vitro*. *Journal of Neuroscience* **19 (10)** 4180-4188.

Trommald, M., Hulleberg, G. and Andersen, P., 1996: Long-term potentiation is associated with new excitatory spine synapses on rat dentate granule cells. *Learning & Memory* **3 (2-3)** 218-228.

Tsien, J. Z., Huerta, P. and Tonegawa, S., 1996: The essential role of hippocampal CA1 NMDA receptor-dependent synaptic plasticity in spatial memory. *Cell* **87 (7)** 1327-1338.

Tully, T., 1998: Toward a molecular biology of memory: the light's coming on! *Nature Neuroscience* **1 (7)** 543-545.

Turigiano, G. G. and Nelson, S. B., 2000: Hebb and homeostasis in neuronal plasticity. *Current Opinion in Neurobiology* **10 (3)** 358-364.

Turrigiano, G. G., Leslie, K. R., Desai, N. S., Rutherford, L. C. and Nelson, S. B., 1998: Activity-dependent scaling of quantal amplitude in neocortical neurons. *Nature* **391 (6670)** 892-896.

Underwood, E. E., 1970: *Quantitative Stereology*. Addison-Wesley Publishing Company: Reading, Massachusetts, U.S.A.

van Rossum, D. and Hanisch, U.-K., 1999: Cytoskeletal dynamics in dendritic spines: direct modulation by glutamate receptors? *Trends in Neurosciences* **22 (7)** 290-295.

Vann, S. D., Brown, M. W., Erichsen, J. T. and Aggleton, J. P., 2000: Fos imaging reveals differential patterns of hippocampal and parahippocampal subfield activation in rats in response to different spatial memory tests. *Journal of Neuroscience* **20 (7)** 2711-2718.

von Bonin, G. and Bailey, P., 1947: *The neocortex of* Macaca mulatta. Urbana, IL: University of Illinois.

Walsh, F. S. and Doherty, P., 1997: Neural cell adhesion molecules of the immunoglobulin superfamily: role in axon growth and guidance. *Annual Reviews in Cellular and Developmental Biology* **13** 425-456.

Weeks, A. C. W., Ivanco, T. L., LeBoutillier, J. C., Racine, R. J. and Petit, T. L., 1998: The degree of potentiation is associated with synaptic number during the maintenance of long-term potentiation in the rat dentate gyrus. *Brain Research* **798 (1-2)** 211-216.

Weinberger, N. M. (1995) Retuning the brain by fear conditioning. In: *The Cognitive Neurosciences*, pp. 1071-1089. Ed. M. S. Gazzaniga. The M.I.T. Press: Cambridge, Massachusetts.

Wells, D. G., Richter, J. D. and Fallon, J. R., 2000: Molecular mechanisms for activity-regulated protein synthesis in the synapto-dendritic compartment. *Current Opinion in Neurobiology* **10 (1)** 132-137.

West, M. J., 1999: Stereological methods for estimating the total number of neurons and synapses: issues of precision and bias. *Trends in Neurosciences* **22 (2)** 51-61.

West, M. J., 2001: 2-D versus 3-D counting - a debate. *Trends in Neurosciences* **24 (7)** 374-375.

Wiesel, T. N. and Hubel, D. H., 1965: Comparison of the effects of unilateral and bilateral eye closure on cortical unit responses in kittens. *Journal of Neurophysiology* **28 (6)** 1029-40.

Willingham, D. B., 1997: Systems of memory in the human brain. *Neuron* **18 (1)** 5-8.

Wilson, M. A. and McNaughton, B. L., 1993: Dynamics of the hippocampal ensemble code for space. *Science* **261 (5124)** 1055-1058.

Wincour, G., McDonald, R. M. and Moscovitch, M., 2001: Anterograde and retrograde amnesia in rats with large hippocampal lesions. *Hippocampus* **11 (1)** 18-26.

Winson, J., 1978: Loss of hippocampal theta rhythm results in spatial memory deficit in the rat. *Science* **201 (4351)** 160-163.

Wincour, G., 1997: Hippocampal lesions after conditioning to conditional and contextual stimuli. *Behavioural Brain Research* **88 (2)** 219-229.

Witter, M. P., 1993: Organization of the entorhinal-hippocampal system: a review of current anatomical data. *Hippocampus* **3 (Special issue)** 33-44.

Witter, M. P., Naber, P. A., van Haeften, T., Machielsen, W. C. M., Rombouts, S. A. R. B., Barkhof, F., Scheltens, P., Lopes da Silva, F. H., 2000: Cortico-hippocampal communication by way of parallel parahippocampal-subicular pathways. *Hippocampus* **10 (4)** 398-410.

Wong, S. T., J., A., Figueroa, X. A., Pineda, V. V., Schaefer, M. L., Chavkin, C. C., Muglia, L. J. and Storm, D. R., 1999: Calcium-stimulated adenylyl cyclase activity is critical for hippocampus-dependent long-term memory and late phase LTP. *Neuron* **23 (4)** 787-798.

Wu, G.-Y., Deisseroth, K. and Tsien, R. W., 2001: Spaced stimuli stabilize MAPK pathway activation and its effects on dendritic morphology. *Nature Neuroscience* **4 (2)** 151-158.

Wyszynski, M., Kharazia, V., Shanghvi, R., Rao, A., Beggs, A. H., Craig, A. M. Weinberg, R. and Sheng, M., 1998: Differential regional expression and ultrastructural localisation of alpha-actinin-2, a putative NMDA receptor-anchoring protein, in rat brain. *Journal of Neuroscience* **18 (4)** 1383-1392.

Yakel, J. L., 1997: Calcineurin regulation of synaptic function: from ion channels to transmitter release and gene transcription. *Trends in Pharmacological Sciences* **18 (4)** 124-134.

Yang, Y., Bauer, C., Strasser, G., Wollman, R., Julien, J. P. and Fuchs, E., 1999: Integrators of the cytoskeleton that stabilise microtubules. *Cell* **98 (2)** 229-238.

Yuste, R., Majewska, A. and Holthoff, K., 2000: From form to function: calcium compartmentalization in dendritic spines. *Nature Neuroscience* **3 (7)** 653-659.

Zamanillo, D., Sprengel, R., Hvalby, Ø., Jensen, V., Burnashev, N., Rozov, A., Kaiser, K. M. M., Köster, H. J., Borchardt, T., Worley, P., Lübke, J., Frotscher, M., Kelly, P. H., Sommer, B., Andersen, P., Seeburg, P. H. and Sakmann, B., 1999: Importance of AMPA receptors for hippocampal synaptic plasticity but not for spatial learning. *Science* **284 (5421)** 1805-1811.

Zhang, W. and Benson, D. L., 2000: Development and molecular organisation of dendritic spines and their synapses. *Hippocampus* **10 (5)** 512-526.

Zhu, X. O., McCabe, B. J., Aggleton, J. P. and Brown, M. W., 1997: Differential activation of the rat hippocampus and perirhinal cortex by novel visual stimuli and a novel environment. *Neuroscience Letters* **229 (2)** 141-143.

Ziff, E. B., 1997: Enlightening the postsynaptic density. *Neuron* **19 (6)** 1163-1174.

Zigmond, M. J., Bloom, F. E., Roberts, J. L. and Squire, L. R., 1999: *Fundamental Neuroscience.* Academic Press: New York.

Zola-Morgan, S. M. and Squire, L. R., 1990: The primate hippocampal formation: evidence for a time-limited role in memory storage. *Science* **250 (4978)** 288-290.

# __Appendix A__

## Perfusion solution recipes

Normal saline solution – 0.9% NaCl
- Add 9g NaCl to 1 litre of $ddH_2O$

Phosphate buffer 0.2M - pH 7.4
- Dissolve 23.28g of $Na_2HPO_4$ and 4.97g of $NaH_2PO_4.H_2O$ in 1 litre $ddH_2O$
- Adjust pH with dilute HCl or NaOH

Fixative for ultrastructure preservation by Epon processing

2% Paraformaldehyde and 2% Glutaraldehyde in 0.1M Phosphate buffer at pH 7.4

To be made up immediately prior to use:
- Heat 350ml $ddH_2O$ to not more than +60°C and add 20g of Paraformaldehyde powder
- Add up to 5ml of 1M NaOH solution (1 NaOH pellet per ml of $ddH_20$)
- Allow to cool
- Add 80ml electron microscopy-grade vacuum distilled Glutaraldehyde (25% solution)
- Add $ddH_2O$ to make volume 500ml
- Add 500ml 0.2M Phosphate buffer (pH 7.4)
- Filter before use

Fixative for immunoreactivity preservation by Lowicryl processing

4% Paraformaldehyde and 0.05% Glutaraldehyde with 0.2% Picric acid in 0.1M Phosphate buffer at pH 7.4

To be made up immediately prior to use:
- Heat 350ml $ddH_2O$ to not more than +60°C and add 40g of Paraformaldehyde powder
- Add up to 5ml of 1M NaOH solution (1 NaOH pellet per ml of $ddH_20$)
- Allow to cool
- Add 2ml electron microscopy-grade vacuum distilled Glutaraldehyde (25% solution)
- Add 2ml Picric acid
- Add $ddH_2O$ to make volume 500ml
- Add 500ml 0.2M Phosphate buffer (pH 7.4)
- Filter before use

## Resin recipes

Epon resin was mixed as required using the following recipe:
- Warm components, measuring cylinder and mixing bottle in the oven
- Combine 20ml Agar100/Epon812, 16ml DDSA and 8ml MNA
- Carefully mix for 20 minutes, preventing any air bubbles
- Add 1.3ml BDMA initiator
- Carefully mix for 20 more minutes

Lowicryl HM20 resin was mixed as required using the following recipe:
- Combine 2.98g (ml) Crosslinker D and 17.02g (ml) Monomer E
- Add 0.1g Initiator C and allow to dissolve
- Remove oxygen from solution by bubbling through with nitrogen gas

## Epon embedding protocol

- Wash fixed and dissected samples in 0.1M phosphate buffer (pH 7.4) three times for 10 minutes each at r.t. (room temperature).
- Leave in 1% Osmium Tetroxide in 0.1M phosphate buffer (pH 7.4) for 1 hour at r.t.
- Wash in 0.1M phosphate buffer (pH 7.4) once for 10 minutes at r.t.

Samples were dehydrated in a Lynx autoprocessor at +20°C using the following protocol:

| | | |
|---|---|---|
| 1) | 30% Acetone | 10 minutes |
| 2) | 50% Acetone | 20 minutes |
| 3) | 70% Acetone | 20 minutes |
| 4) | 90% Acetone | 20 minutes |
| 5) | 100% Acetone | 20 minutes |
| 6) | 100% Acetone | 20 minutes |
| 7) | 100% Acetone purified by molecular sieve | 3 hours |
| 8) | 50:50 Epon:Acetone purified by molecular sieve | 3 hours |
| 9) | 60:40 Epon:Acetone purified by molecular sieve | 3 hours |
| 10) | 70:30 Epon:Acetone purified by molecular sieve | 3 hours |
| 11) | 80:20 Epon:Acetone purified by molecular sieve | 16 hours |
| 12) | Fresh Epon | 6 hours |

Constant agitation was applied at all times. Samples were then embedded using fresh Epon into individually labelled polythene capsule moulds and polymerised at +60°C in an oven for at least 24 hours.

## Lowicryl embedding protocol

Fixed and dissected samples were soaked in 0.125M triethanolamine hydrochloride in 0.1M phosphate buffer (pH 7.4). for 30-60 minutes at r.t.

Fixed and dissected samples were soaked in the following series of cryoprotectant solutions:
- 0.125M triethanolamine hydrochloride in 0.1M phosphate buffer (pH 7.4) for 30-60 minutes at r.t.
- 10% analar glycerol in 0.1M phosphate buffer for 20-60 minutes at r.t.
- 20% analar glycerol in 0.1M phosphate buffer for 30-60 minutes at r.t.
- 30% analar glycerol in 0.1M phosphate buffer for 60 minutes at r.t.

Samples were impact frozen onto liquid nitrogen-cooled copper mirrors using a Reichert MM80E impact freezer.

Samples were then transferred into a Leica AFS, freeze substituted and embedded using the following protocol:
- 0.5% Uranyl Acetate in alanar methanol                    at -85°C for 24 hours

- Fresh analar methanol      at -85°C for 1 hour
- Fresh analar methanol      at -85°C for 1 hour
- Fresh analar methanol      at -85°C for 22 hours
- Fresh analar methanol      at -50°C for 22 hours
- 1:1 Lowicryl HM20 resin : analar methanol      at -50°C for 1 hour
- 2:1 Lowicryl HM20 resin : analar methanol      at -50°C for 1 hour
- Lowicryl HM20 resin      at -50°C for 1 hour
- Lowicryl HM20 resin      at -50°C for 22 hours
- Lowicryl HM20 resin      at -50°C for 1 hour
- Transfer into flat moulds and fill with fresh Lowicryl HM20 resin (at ⁻50°C)
- Polymerise under 360nm wavelength ultraviolet light      at -50°C for 48 hours

The temperature was then raised to +20°C. All solutions were pre-cooled before being applied to the tissue samples.
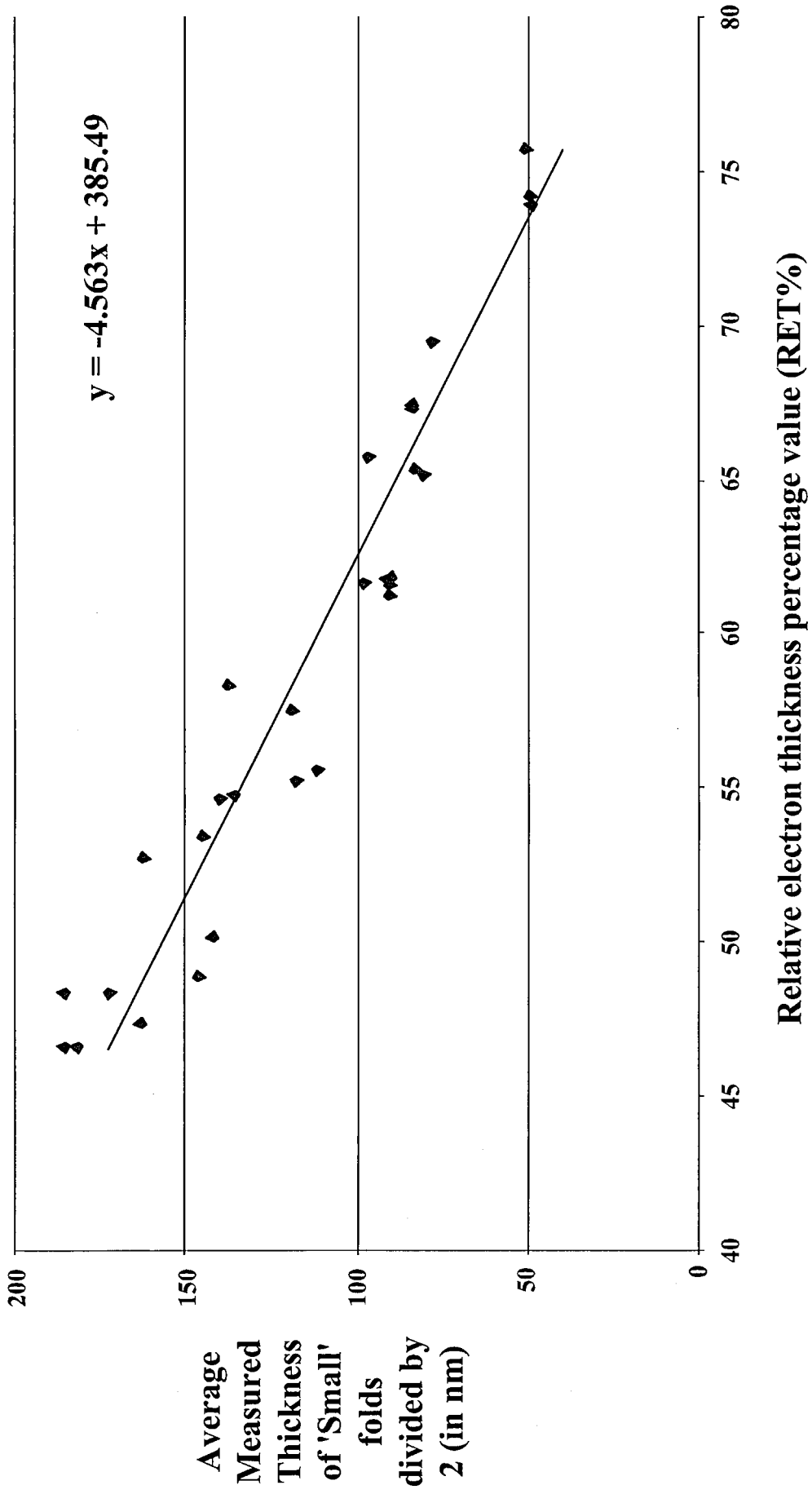
Figure 48 - RET% calibration curve used for Epon thickness estimation, showing the equation of the curve.

# Appendix B

## Antibodies

All the primary antibodies used for immunogold labelling were of affinity purified polyclonal type and available from commercial sources:

Anti-glutamate receptor 1 – raised in rabbit.
  Supplied by Chemicon International, catalogue number AB1504.
  This antibody was raised to part of the carboxy-terminus sequence of the rat GluR1 peptide (SHSSGMPLGATGL) and is not cross-reactive with other AMPA receptor subunits (GluR2, 3 or 4).

Anti-glutamate receptor 2 & 3 – raised in rabbit.
  Supplied by Chemicon International, catalogue number AB1506.
  This antibody was raised to part of the carboxy-terminus sequence of the rat GluR2 peptide (EGYNVYGIESVKI). It recognises GluR2 & 3 but not GluR1 or 4.

Anti-glutamate receptor 4 – raised in rabbit.
  Supplied by Chemicon International, catalogue number AB1508.
  This antibody was raised to part of the carboxy-terminus sequence of the rat GluR4 peptide (RQSSGLAVIASDLP) and is not cross-reactive with other AMPA receptor subunits (GluR1, 2 or 3).

Anti-NMDAR1 – raised in rabbit.
  Supplied by Chemicon International, catalogue number AB1516.
  This antibody was raised to a synthetic peptide corresponding to the carboxy-terminus of the rat subunit (LQNQKDTVLPRRAIEREEGQLQLCSRHRES). It is selective for splice variants NR1-1a, NR1-1b, NR1-2a and NR1-2b, but is not cross-reactive with other glutamate receptor subunits.

15nm gold conjugated to anti-rabbit IgG – raised in goat.
  Supplied by British Biocell International, catalogue number EM.GAR15.

## Method for immunogold labelling

The final immunogold labelling protocol was performed as follows:

1) Non-specific blocking step in PBSA – 30 minute incubation at r.t. (room temperature).
2) Primary antibody cocktail for AMPA receptors GluR1, GluR2&3, GluR4. All diluted 1:20 (5µg/ml) in PBSA – incubation at +4°C for 16 hours.
OR
  Primary antibody for NMDA receptor NR1. Diluted 1:80 (1.25µg/ml) in PBSA – incubation at +4°C for 63 hours.
3) Wash 3 times in PBSA for 5 minutes per wash at r.t.
4) Secondary antibody 15nm gold goat anti-rabbit IgG. Diluted 1:100 (0.185µg/ml) in PBSA – 1 hour incubation at r.t.
5) Wash 3 times in PBSA for 5 minutes per wash at r.t.

6) Gold label fixed in place with 2% glutaraldehyde in ddH$_2$O - 2 minute incubation at r.t.
7) Wash 3 times in PBSA for 5 minutes per wash at r.t.
8) Wash 3 times in ddH$_2$O for 5 minutes per wash at r.t.

Sections were then contrast stained with Uranyl Acetate for 30 minutes at +20$^\circ$C and Lead Citrate for 7 minutes at +20$^\circ$C using an LKB ultrastainer.


## Immunogold labelling buffer recipe

PBS (phosphate buffered saline) pH 8.2 was made according to the following recipe:

- Add 148mg Na$_2$HPO$_4$, 43mg KH$_2$PO$_4$ and 720mg NaCl to 100ml ddH$_2$O
- Adjust pH with dilute HCl or NaOH


PBSA – PBS with 0.5% Bovine Serum Albumin (BSA)

- Add 5mg of BSA for each millilitre of PBS